NEURONAL PLASTICITY AND NEUROMODULATION IN DEVELOPMENT AND DEVELOPMENTAL DISORDERS

EDITED BY: Volker Mall and Jean-Pierre Sao-Ming Lin

PUBLISHED IN: Frontiers in Neurology and Frontiers in Pediatrics

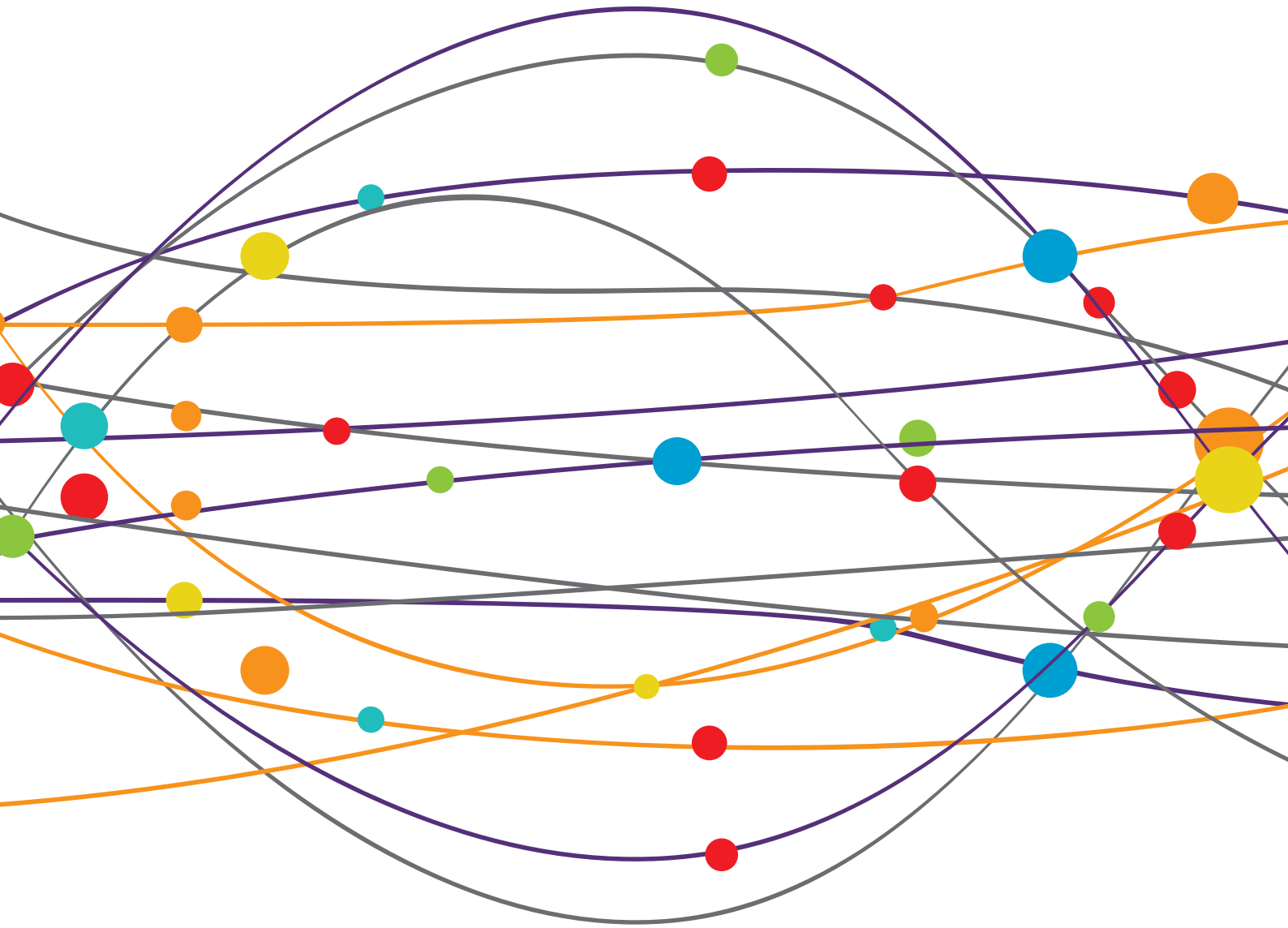

frontiers Research Topics

frontiers

Frontiers eBook Copyright Statement

The copyright in the text of individual articles in this eBook is the property of their respective authors or their respective institutions or funders. The copyright in graphics and images within each article may be subject to copyright of other parties. In both cases this is subject to a license granted to Frontiers.

The compilation of articles constituting this eBook is the property of Frontiers.

Each article within this eBook, and the eBook itself, are published under the most recent version of the Creative Commons CC-BY licence. The version current at the date of publication of this eBook is CC-BY 4.0. If the CC-BY licence is updated, the licence granted by Frontiers is automatically updated to the new version.

When exercising any right under the CC-BY licence, Frontiers must be attributed as the original publisher of the article or eBook, as applicable.

Authors have the responsibility of ensuring that any graphics or other materials which are the property of others may be included in the CC-BY licence, but this should be checked before relying on the CC-BY licence to reproduce those materials. Any copyright notices relating to those materials must be complied with.

Copyright and source acknowledgement notices may not be removed and must be displayed in any copy, derivative work or partial copy which includes the elements in question.

All copyright, and all rights therein, are protected by national and international copyright laws. The above represents a summary only. For further information please read Frontiers' Conditions for Website Use and Copyright Statement, and the applicable CC-BY licence.

ISSN 1664-8714
ISBN 978-2-88976-360-3
DOI 10.3389/978-2-88976-360-3

About Frontiers

Frontiers is more than just an open-access publisher of scholarly articles: it is a pioneering approach to the world of academia, radically improving the way scholarly research is managed. The grand vision of Frontiers is a world where all people have an equal opportunity to seek, share and generate knowledge. Frontiers provides immediate and permanent online open access to all its publications, but this alone is not enough to realize our grand goals.

Frontiers Journal Series

The Frontiers Journal Series is a multi-tier and interdisciplinary set of open-access, online journals, promising a paradigm shift from the current review, selection and dissemination processes in academic publishing. All Frontiers journals are driven by researchers for researchers; therefore, they constitute a service to the scholarly community. At the same time, the Frontiers Journal Series operates on a revolutionary invention, the tiered publishing system, initially addressing specific communities of scholars, and gradually climbing up to broader public understanding, thus serving the interests of the lay society, too.

Dedication to Quality

Each Frontiers article is a landmark of the highest quality, thanks to genuinely collaborative interactions between authors and review editors, who include some of the world's best academicians. Research must be certified by peers before entering a stream of knowledge that may eventually reach the public - and shape society; therefore, Frontiers only applies the most rigorous and unbiased reviews.
Frontiers revolutionizes research publishing by freely delivering the most outstanding research, evaluated with no bias from both the academic and social point of view. By applying the most advanced information technologies, Frontiers is catapulting scholarly publishing into a new generation.

What are Frontiers Research Topics?

Frontiers Research Topics are very popular trademarks of the Frontiers Journals Series: they are collections of at least ten articles, all centered on a particular subject. With their unique mix of varied contributions from Original Research to Review Articles, Frontiers Research Topics unify the most influential researchers, the latest key findings and historical advances in a hot research area! Find out more on how to host your own Frontiers Research Topic or contribute to one as an author by contacting the Frontiers Editorial Office: frontiersin.org/about/contact

NEURONAL PLASTICITY AND NEUROMODULATION IN DEVELOPMENT AND DEVELOPMENTAL DISORDERS

Topic Editors:
Volker Mall, Technical University of Munich, Germany
Jean-Pierre Sao-Ming Lin, Guy's and St Thomas' NHS Foundation Trust, United Kingdom

Citation: Mall, V., Lin, J.-P. S.-M., eds. (2022). Neuronal Plasticity and Neuromodulation in Development and Developmental Disorders. Lausanne: Frontiers Media SA. doi: 10.3389/978-2-88976-360-3

Table of Contents

frontiers | Frontiers in Neurology

EDITORIAL
published: 23 May 2022
doi: 10.3389/fneur.2022.912046

Editorial: Neuronal Plasticity and Neuromodulation in Development and Developmental Disorders

Jean-Pierre Lin [1,2]*

[1] Children's Neurosciences Evelina London Children's Hospital, Guy's and St Thomas' NHS Foundation Trust, London, United Kingdom, [2] Faculty of Life Sciences and Medicine, Department of Women and Children's Health, School of Life Course and Population Sciences, King's College London, London, United Kingdom

Keywords: neuromodulation, developmental neurobiology, neuroplasticity, childhood, neurology

Editorial on the Research Topic

Neuronal Plasticity and Neuromodulation in Development and Developmental Disorders

The growth and function of the developing brain are a triumph of hope over expectation against impossible natural odds. Development and pathophysiology compete with each other to achieve rewarding functions and the seemingly endlessly adaptable nervous system is edited and pruned accordingly within windows of neuroplasticity which open and close according to genetic rules and neuro-environmental experiences leading to adaptive complexity, vulnerability and disruption (1). Unsurprisingly, every experience, thought, action and reaction have a *neuromodulating* effect on the developing and developed nervous system. Robust systems survive to become stronger and more adaptive.

As we move from syndromic diagnoses composed of symptoms and signs to fundamentally molecular diagnostic formulations, it is clear that old divisions of neurology into disorders brain, spinal cord and neuromuscular functions dissolve into more basic units of cellular functional behavior and systems neuromodulation.

Diagnosis, the process of discovering the nature of a problem or illness through examination, imaging, neurophysiological, biochemical and genetic testing and prognosis, our understanding of the likely future outcome or course of a diagnosis, will always lag behind this curve of new discoveries and understanding of developing, disordered, brain function.

Neuromodulation seeks to describe and understand dynamic, self-adapting, functional and dysfunctional systems for which dynamic solutions are required.

Clinicians, like philosophers are capable of teaching and defending doctrines, which in theoretical and practical terms obstruct clinical progress. The "fallacy of misplaced concreteness" was coined by the philosopher Alfred North Whitehead. One commits the fallacy of misplaced concreteness when one mistakes an abstract belief, opinion, or concept about the way things are for a physical or "concrete" reality: "There is an error; but it is merely the accidental error of mistaking the abstract for the concrete." *"Science and the Modern World," Alfred North Whitehead (1925/1953).*

In pediatric neurology the attribution of motor dysfunction to disturbances of the corticospinal tract known as the "upper motorneuron" syndrome has long dominated clinical thinking. However in this volume on neuroplasticity, the efficacy of Constraint-Induced Movement Therapy (CIMT) and Bimanual training is reportedly "independent of CST connectivity pattern," contrary to the study hypothesis of the investigators. Furthermore, "children with an ipsilateral CST lesion, previously thought to be maladaptive, have the capacity to improve as well as children with a contralateral or bilateral CST lesions following intensive CIMT or Bimanual training," thus overturning a long-held *"misplaced concreteness."* It is regrettable that this work may take decades to reach undergraduate and junior clinical education and training on the grounds that it is "too specialized" or only applies to pediatrics. But I remember

OPEN ACCESS

Edited and reviewed by:
Jo Madeleine Wilmshurst, University of Cape Town, South Africa

***Correspondence:**
Jean-Pierre Lin
jeanpierrelin@icloud.com

Specialty section:
This article was submitted to Pediatric Neurology, a section of the journal Frontiers in Neurology

Received: *03 April 2022*
Accepted: *12 April 2022*
Published: *23 May 2022*

Citation:
Lin J-P (2022) Editorial: Neuronal Plasticity and Neuromodulation in Development and Developmental Disorders. Front. Neurol. 13:912046. doi: 10.3389/fneur.2022.912046

well failing to understand how the upper motor neurone concept alone explained the phenomenology of adult and childhood strokes. Accordingly, and perhaps unsurprisingly the authors report in their concluding remarks that disordered sensorimotor integration may play a significant role in motor dysfunction and this is backed up by reports of greater responses to CIMT in children with poor sensory function (Friel et al.).

Opportunistic study is often required to inform our conceptual understanding of neurodevelopmental processes but require specific clinical conditions such as those which obtained in the measurement of age-related lateralization of cerebral inhibition i.e., "Go" and "No-Go" inhibition which was measured in children undergoing continuous subdural electrocorticography (ECoG) recordings for epilepsy surgery localization. This revealed a predominantly right-sided inhibition in the inferior frontal gyrus (IFG) associated with theta (4–8 Hz) and high-gamma (HG) (70–200 Hz) power spectra, thus giving us an opportunistically-derived developmental insight into such inhibitory functions (Kuo et al.).

At the opposite end of the spectrum, mathematical modeling of chronic deep brain stimulation (DBS)-dependency i.e., susceptibility to *status dystonicus* following abrupt withdrawal of continuous DBS neuromodulation for intractable dystonia, is revealed as highly dependent on the "neuroplastic nature of a disorder" or an individual. This could help modeling predicted responses to DBS withdrawal. This model predicts that insertion and withdrawal of DBS in individuals with *"high plasticity"* has little observable effect whereas DBS withdrawal in conditions of "*low plasticity"* such as in chronic Parkinsonism or dystonia may result in status dystonicus (Trenado et al.).

Whereas the success of therapeutic interventions dominate all medical literature, defining the client population, instruments of intervention, definition and measurement of the successful outcome are the subject of endless debate about the value of case-report, cohort or randomized-control trial in supporting decision trees and guidelines. Often this begins by defining what we know and how we have come to such an understanding, first through the use of readily available diagnostic tools, then more complex, systems-based neurophysiological tools, followed by expert opinions, then inevitably, by clinical-neurophysiological ***supervised machine-learning*** algorithms that can shed light on how different dynamic systems respond to interventions such as DBS, allowing case-specific predictions of outcome. This might also be referred to as "*precision medicine*" that can identify a range of outcomes for individual clinical cases beyond the conventional statistical box and whisker plot of significant differences (McClelland and Lin).

Novel therapies also known as new ways of thinking about old problems are urgently needed and must be relevant to our understanding of neuroplasticity and neuromodulation.

Novel therapies include cognitive training strategies such as Cognitive Orientation to daily Occupational Performance (CO-OP) in childhood hyperkinetic movement disorders may be a more effective and low-cost means of achieving patient-selected functional goals and could be applied in health services worldwide, including resource-poor countries. CO-OP appears superior to repetitive practicing, especially preferable to practicing something in a way which is unhelpful (Gimeno et al.).

Another novel therapy could include "sub-threshold stimuli" such as "stochastic resonance (SR) sub-threshold mechanical noise stimulation" using sub-threshold vibrotactile noise stimulation of the wrist via a specialized wrist-watch. This may improve manual dexterity test scores in developmental coordination disorder (DCD). If repeatable and translatable to everyday life the smart watch of the future may deliver sub-threshold stimuli leading to motor improvements applicable to other motor disorders e.g., following neurological injuries or simply with motor decline of the elderly. Ultimately, we may all want one of these subthreshold stimulus systems!

Neuromodulation in its widest sense has no boundaries and consequently applications are potentially limitless and not necessarily costly.

The evolving concepts and tools elucidating neuroplasticity and neuromodulation, strongly support the case for further funding and training in the exciting fields of neuroplasticity, neuromodulation and neuro-rehabilitation.

AUTHOR CONTRIBUTIONS

The author confirms being the sole contributor of this work and has approved it for publication.

ACKNOWLEDGMENTS

The author would like to thank his co-editor Professor Volker Mall in his editorial contributions and all the contributors to this Research Topic.

REFERENCES

1. Ismail FY, Fatemi A, Johnston MV. Cerebral plasticity: Windows of opportunity in the developing brain. *Eur J Paediatr Neurol.* (2017) 21:23–48. doi: 10.1016/j.ejpn.2016.07.007

Conflict of Interest: The author declares that the research was conducted in the absence of any commercial or financial relationships that could be construed as a potential conflict of interest.

Publisher's Note: All claims expressed in this article are solely those of the authors and do not necessarily represent those of their affiliated organizations, or those of the publisher, the editors and the reviewers. Any product that may be evaluated in this article, or claim that may be made by its manufacturer, is not guaranteed or endorsed by the publisher.

Copyright © 2022 Lin. This is an open-access article distributed under the terms of the Creative Commons Attribution License (CC BY). The use, distribution or reproduction in other forums is permitted, provided the original author(s) and the copyright owner(s) are credited and that the original publication in this journal is cited, in accordance with accepted academic practice. No use, distribution or reproduction is permitted which does not comply with these terms.

frontiers in Pediatrics

ORIGINAL RESEARCH
published: 21 January 2021
doi: 10.3389/fped.2020.600337

Cognitive Strategy Training in Childhood-Onset Movement Disorders: Replication Across Therapists

Hortensia Gimeno[1,2*], *Helene J. Polatajko*[3], *Jean-Pierre Lin*[1], *Victoria Cornelius*[4] and *Richard G. Brown*[2,5]

[1] Complex Motor Disorders Service, Paediatric Neurosciences, Evelina London Children's Hospital, Guy's & St Thomas' NHS Foundation Trust, London, United Kingdom, [2] Department of Psychology, King's College London, Institute of Psychiatry, Psychology and Neuroscience, London, United Kingdom, [3] Department of Occupational Science and Occupational Therapy, University of Toronto, Toronto, ON, Canada, [4] Imperial Clinical Trials Unit, Imperial College London, School of Public Health, London, United Kingdom, [5] South London and Maudsley NHS Foundation Trust, London, United Kingdom

OPEN ACCESS

Edited by:
Jo Madeleine Wilmshurst, University of Cape Town, South Africa

Reviewed by:
Wang-Tso Lee, National Taiwan University Hospital, Taiwan
Juan Dario Ortigoza-Escobar, Pediatric Research Hospital Sant Joan de Déu, Spain

***Correspondence:**
Hortensia Gimeno
hortensia.gimeno@gstt.nhs.uk; hortensia.gimeno@kcl.ac.uk

Specialty section:
This article was submitted to Pediatric Neurology, a section of the journal Frontiers in Pediatrics

Received: *29 August 2020*
Accepted: *24 November 2020*
Published: *21 January 2021*

Citation:
Gimeno H, Polatajko HJ, Lin J-P, Cornelius V and Brown RG (2021) Cognitive Strategy Training in Childhood-Onset Movement Disorders: Replication Across Therapists. Front. Pediatr. 8:600337. doi: 10.3389/fped.2020.600337

Objective: To explore preliminary effectiveness of the Cognitive Orientation to daily Occupational Performance (CO-OP) Approach in improving outcomes in childhood-onset hyperkinetic movement disorders (HMDs) including dyskinetic cerebral palsy following deep brain stimulation (DBS) across UK clinical occupational therapists.

Methods: Randomized, multiple-baseline, Single Case Experimental Design N-of-1 trial with replications across participants. Five self-selected goals were identified: three goals were worked on during CO-OP and two goals were left untreated and used to assess skills transfer. Participants were between 6 and 21 years and had received DBS surgery with baseline Manual Ability Classification System (MACS) levels I–IV. Participants were randomized to typical or extended baseline (2 vs. 6 weeks), followed by 10 weekly individual CO-OP sessions. The primary outcome was functional performance measured by the Performance Quality Rating Scale-Individualized (PQRS-I), assessed before, during, and following treatment. Outcome assessors were blinded to baseline allocation, session number, and assessment time. A non-overlapping index, Tau-*U*, was used to measure effect size.

Results: Of the 12 participants recruited, 10 commenced and completed treatment. In total, 63% of trained goals improved with effect sizes 0.66–1.00 ("moderate" to "large" effect), seen for all children in at least one goal. Skills transfer was found in 37% of the untrained goals in six participants.

Conclusions: Cognitive strategy use improved participant-selected functional goals in childhood-onset HMD, more than just practice during baseline. Preliminary effectiveness is shown when the intervention is delivered in clinical practice by different therapists in routine clinical settings.

Keywords: single case experimental design, dystonia, cerebral palsy, rehabilitation, participation

INTRODUCTION

In children and young people with a hyperkinetic movement disorder (HMD) including dyskinetic cerebral palsy (CP) surgical treatments such as deep brain stimulation (DBS) can be effective in reducing severity of motor impairments (e.g., dystonia) (1, 2). However, children can be left with persistent functional problems in outperforming everyday tasks that are important to them and their families (3).

A recent systematic review of interventions for CP indicated strong evidence that surgical interventions, such as intrathecal baclofen infusion pump or selective dorsal rhizotomy, and medical interventions, such as botulinum toxin injections, reduce tone in children with spastic CP (4). However, it is the combination of these interventions with adjunct rehabilitation such as strength training or occupational therapy that yield effective results in improving motor and/or functional outcomes. However, there is scant evidence to guide rehabilitation practice following interventions such as DBS in children and young people (4) and only a few small studies in adult-onset dystonia (5, 6). Even in specialist centers, number of cases are relatively small, and the heterogeneity of these disorders in terms of etiology, motor severity, and non-motor factors make the planning and implementation of large scale randomized controlled trials (RCTs) challenging.

Nevertheless, rehabilitation approaches are available but, to date, lack robust evidence for their feasibility and efficacy. We have recently reported a proof-of-concept efficacy study (7) of the Cognitive Orientation to daily Occupational Performance (CO-OP) (8) used with children and young people with HMD and DBS in place. CO-OP is an individualized, client-centered approach that uses personalized strategies to achieve client-chosen functional goals. The results provided preliminary evidence to support the feasibility, acceptability, and potential efficacy, evaluated using single-case experimental design replications (7). In that study, treatment was delivered by a single experienced occupational therapist in a specialist pediatric movement disorder service. It is important to explore if these findings can be replicated in routine settings and implemented by local therapists.

Therapist effects, including training and experience, can be a fundamental variable in studies investigating any rehabilitation intervention effectiveness (9–11). Single-case experimental design methodology provides the opportunity, with limited numbers, to simultaneously investigate treatment efficacy and therapist effects (12, 13).

This study aimed to explore whether the results from a previous single-case experimental design proof-of-concept (efficacy) study (7, 14) could be replicated by other therapists (adherence to protocol) based in non-specialized services (effectiveness) (15). Further, the study sought to assess the impact of practice by using an extended baseline with repeated assessment of participant-selected goals prior to commencing treatment.

METHODS

The study evaluated the CO-OP approach, as an adjunct to DBS, delivered by non-specialist occupational therapists with a range of clinical experience, to children and young people with HMD. The full trial protocol is available (15) and was implemented with minor changes. Single-case experimental design methodology followed the Single Case Reporting Guideline in Behavioral Interventions (SCRIBE) (12).

Research Question

Does the CO-OP approach improve outcomes for children and young people with HMD on participant-selected goals when undertaken in a non-specialized clinical setting?

Standard Protocol Approvals, Registrations, and Patient Consents

Ethical approval was obtained by the NHS Health Research Authority (Oxford A Research Ethics Committee, 14/SC/1159). The trial was registered (ISRCTN57997252). Written informed consent was obtained from all parents and from participants over 12 years of age. Assent was obtained from younger children. Written permission was obtained in all cases.

Design

This study used a randomized, multiple-baseline, N-of-1 design with replications across six therapists (N-of-1 with five replications) in 12 children and young people (N-of-1 trial with 11 replications) (NB: number achieved was N-of-1 with 9 replications across participants).

A consecutive series of multiple baseline N-of-1 trials was completed using concealed randomization to allocate length of baseline (2 vs. 6 weeks). The extended baseline permitted an examination of whether repeated baselining (practicing the goals without CO-OP input) and DBS only has an impact on skill improvement.

Sample Size

In an N-of-1 design with replications across participants, sample (series) size is not based on the power to test group effects using inferential statistics. Instead, each separate trial examines change over time within an individual, thus allowing us to determine whether treatment is effective for each individual using predefined quantitative and qualitative criteria. In N-of-1 studies, the number of replications (participants recruited) chosen after the first case is often based on pragmatic grounds related to the known heterogeneity of the clinical sample. The number of measurements within each time period is also based on pragmatic factors such as length of treatment and the likely variability in outcome. It is recommended that an initial N-of-1 trial plus three replications are necessary as a minimum to explore efficacy of an intervention but five replications is better (16). Similarly, it is recommended that at least three assessment points are measured as a baseline before the intervention is introduced (16) but preferably five (17). A sample size of 10 was judged to be sufficient to provide information on

whether the intervention produced meaningful clinical change for individuals, to examine the direction of "average treatment effect" across individuals, and to provide estimates of the within- and between-subject variability of outcomes in this population. This sample size will also allow us to obtain information on ease of recruitment and adherence to protocol that might inform any future clinical trial. As standard in N-of-1 trial, this number of participants will allow for statistical analysis of effect size of the intervention relative to baseline.

Participants

The study included children and young people with HMD who had previously undergone DBS (or where surgery was scheduled) at the complex motor disorders service (CMDS) database at Evelina London Children's Hospital, UK, that met the inclusion criteria from information in their medical records ($n = 27$). The 10 patients that had participated in the previous study were not eligible. Full inclusion criteria for the study has been reported elsewhere (7): (a) diagnosis of pediatric HMD other than neurodegenerative conditions; (b) sufficient receptive and expressive communication ability to follow simple instructions and engagement with treatment; (c) age 6 to 21 years; (d) Manual Abilities Classification System (MACS) levels I–IV; (e) emerging skills in self-care; (f) ability to mobilize independently; (g) cognitive ability of 6 years of age or IQ above 70; and (h) DBS electrodes *in situ* and without signs of infection.

Twelve participants were recruited and admitted to the study sequentially. Further information about eligibility criteria and recruitment procedure are outlined in the study protocol (14, 15). **Figure 1** describes the recruitment process and randomization to two arms and reasons for exclusion. Details of the participants are provided in **Table 1**.

Therapists

The Evelina Children's Hospital is a tertiary treatment center providing advanced interventions for children with complex motor disorders. Children are referred from across the UK. For this trial, 19 therapists were initially contacted in centers close to the homes of the 27 potential participants, and 3 additional therapists were approached via special interest group networks. Seven agreed to take part in the study prior to enrolment of the first participant, with six eventually matched to one or more patient participants. Details of the therapists are provided in **Supplementary Information 1**.

Intervention Description

CO-OP intervention comprised 10 treatment sessions of up to 1 h each, delivered weekly at the participant's home. The frequency of intervention sessions was negotiated between the treating therapist and the participant and family. All therapists had attended CO-OP training workshops (2–3 days) led by CO-OP Academy certified instructors. Ongoing clinical supervision was provided by investigator HG. For more information, please see study protocols (14, 15).

Primary Outcome

Performance change in self (participant)-selected goals was measured using the Performance Quality Rating Scale—individualized (PQRS-i) (7). This is a 10-point observational scale, with 1 representing "cannot do the task at all" and 10 representing "does task very well." The PQRS-i does not penalize the child or young person for how the task is performed or whether dystonia is present or not. PQRS-i is a scale based on observation of the behavior (behavior defined as the task at hand). The child is asked to perform the chosen goals, in their natural environment (i.e., their home), using utensils and materials familiar to them. Performance was videoed by the primary investigator. Performance scores were obtained by rating video recordings of all baselines and post-intervention sessions and a sample of eighteen 5-min randomly selected video segments of the intervention sessions. The videos were randomly presented in a non-chronological order and rated by a trained independent, blinded PQRS-i rater. For more information about how the performance clips for intervention were selected, please refer to the study protocol (14).

Assessments of outcomes were completed several times at each study phase (baseline, during treatment, and end of treatment). Five task-based goals were self-identified by each participant with the aid of the Canadian Occupational Performance Measure (COPM) (18) (data not reported here). Three of the goals were addressed in the CO-OP intervention (trained goals) and two, which were not addressed in the sessions with the therapist, were used to assess generalization and transfer (untrained goals). The participants chose which goals they wished to work on in therapy.

Analysis

Outcomes and significance of change were analyzed and evaluated using a set of complementary approaches following SCRIBE guidelines. Improvement is also summarized for the group in terms of number of goals improved.

Visual Analysis

Changes in means, levels, trends, variability, latency, and consistency were evaluated using visual graph analysis (19–21). PQRS-i data were graphed with separate data points in each phase (baseline, intervention, and post-intervention).

Quantitative Statistical Analysis of Performance Change Between Baseline and Post-intervention

Serial dependency at baseline was firstly calculated using auto-correlation (AC) so that the most appropriate analysis approach could be chosen, which were (i) differences in individual means and 95% confidence interval for overall change pre- and post-*t*-test; (ii) regression, initially fitting a naïve linear regression model using ordinary least squares (OLS) for reference only (22, 23); and (iii) effect size calculated using non-overlapping index of the Kendall's Tau for non-overlap with baseline trend control (Tau-*U*) (24) taking into consideration baseline AC in the calculation. Effect size is considered "large" ("very effective intervention") when Tau-*U* is $\geq$0.93, "moderate" ("effective intervention") for values 0.66 to 0.92, and "weak" when values are $\leq$0.65.

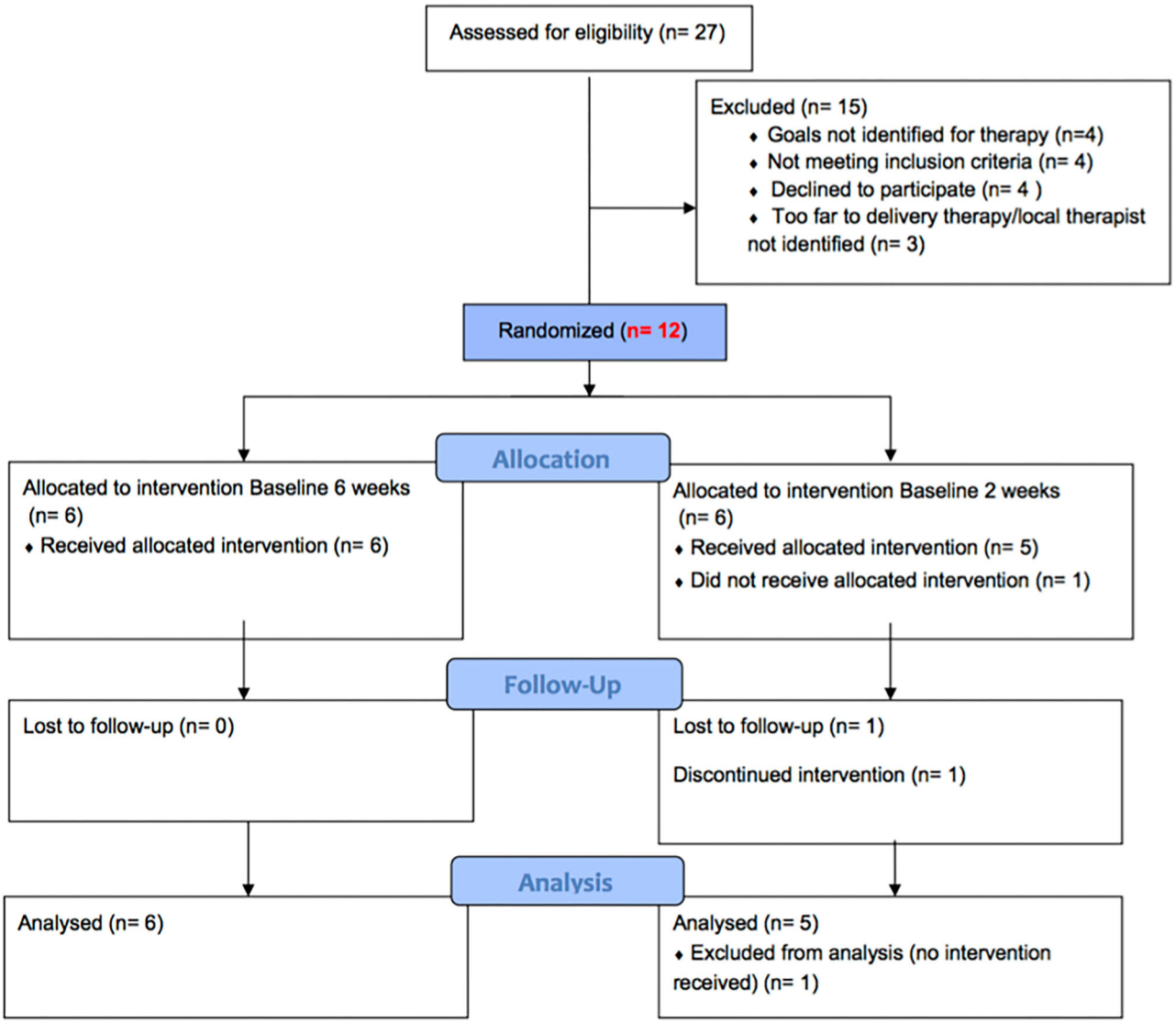

FIGURE 1 | Recruitment diagram shows the total number of participants approached.

Clinically Significant Change Between Baseline and Post-intervention

A change of at least 2 points on the PQRS-i was used to indicate clinical significance in order to match other similar scales such as the COPM (18). Differences between mean scores from pre- and post- were calculated for each individual for each goal.

Quantitative statistical analysis of performance change between CO-OP and treatment as usual (DBS and practice of the goals): Changes in performance across the extended baseline (6 weeks with at least 18 data points) was specifically evaluated. Differences between individual goal means and 95% confidence interval for change of first session and sixth session of baseline (*t*-test) were calculated for those participants randomized to 6 weeks baseline length.

Analysis of Results in Relation to Therapist-Related Fidelity to Treatment

Fidelity to treatment was evaluated by reviewing randomly selected video-recorded treatment sessions by a CO-OP expert external to the study team using the CO-OP Academy fidelity checklist (25). The randomly selected treatment session per therapist was evaluated fully by the external expert. Therapist factors (training and years of experience) and the fidelity to treatment were explored for their possible impact on clinical outcome.

Adherence to CO-OP Protocol

Fidelity to treatment was evaluated by reviewing randomly selected video-recorded treatment sessions by a CO-OP expert external to the study team using the CO-OP Academy fidelity

TABLE 1 | Participant demographic and clinical characteristics ($N = 12$).

Child	Therapist	Age	Gender	Randomization group	Diagnosis	Etiology	Phenotype	DBS duration	GMFCS	MACS
1	1	11 y 8 m	Female	2 weeks	Dyskinetic CP	Acquired (secondary to Kernicterus)	Dystonia	6 m	II	IV
2	2	16 y 11 m	Female	2 weeks	Dyskinetic CP secondary to maternal ruptured uterus	Acquired (secondary)	Dystonia and choreoathetosis	4 y	III	IV
3*	Dropped out	19 y 4 m	Female	6 weeks	Early onset generalized dystonia. DYT-TOR1A (DYT-1)	Inherited (Primary)	Dystonia	2 y 6 m	III	II
4	3	8 y 6 m	Female	6 weeks	Stroke	Acquired (secondary)	Dystonia	6 m	II	II
5	4	19 y 10 m	Female	2 weeks	Childhood-onset progressive dystonia. KMT2B (DYT28)	Inherited (Primary)	Dystonia	9 m	II	III
6	5	16 y 7 m	Male	2 weeks	Dyskinetic CP	Acquired (secondary to HIE)	Dystonia and choreoathetosis	6 m	II	II
7**	Not eligible	14 y	Female	6 weeks	Dopa Responsive Dystonia	Inherited (Primary)	Dystonia	–	III	II
8	4	9 y 8 m	Female	6 weeks	Myoclonus dystonia. DYT-SGCE (DYT-11)	Inherited (Primary)	Dystonia and myoclonus	2 m	I	II
9	6	9 y 3 m	Male	6 weeks	GA-1	Acquired (secondary)	Dystonia and chorea	3 y	III	IV
10	4	18 y 11 m	Male	2 weeks	Stroke	Acquired (secondary)	Dystonia	6 m	II	II
11	4	17 y 4 m	Male	2 weeks	Dyskinetic CP secondary to maternal placental abruption	Acquired (secondary)	Dystonia and chorea	15 m	II	II
12	4	15 y 9 m	Female	6 weeks	Dyskinetic CP	Acquired (secondary to HIE)	Dystonia and myoclonus	4 y 6 m	I	II

Child number reflects the order of recruitment.

**Case 3 withdrew for personal reasons after baseline.*

***Case 7 was no longer eligible for the study at the start of baseline assessment.*

DBS, Deep Brain Stimulation; GMFCS, Gross Motor Function Classification System; MACS, Manual Ability Classification System; CP, Cerebral Palsy; HIE, Hypoxic Ischemic Encephalopathy; GA, Glutaric Aciduria type 1; y, year; m, month.

Table 1 *shows demographic characteristics for all cases recruited to this study with cases organized firstly by those allocated to 2 weeks baseline followed by the participants allocated for 6 weeks baseline. Child number reflects the order of recruitment. Diagnosis, etiology, and phenotype are provided as well as DBS duration, DBS, and MACS levels.*

checklist (25). The randomly selected treatment session per therapist was evaluated fully by the external expert.

RESULTS

The participants (eight female, four male) ranged in age from 8 years and 6 months to 19 years and 10 months, with a range of primary diagnoses, etiologies, and clinical phenotypes (**Table 1**). Duration since DBS ranged from 6 months to 4 years 6 months. Of the 12 participants, 1 was excluded before functional assessments and intervention commenced as scheduled surgery was canceled, and one withdrew following baseline assessment. Of the remainder, all completed the planned 10 CO-OP sessions. For completeness, details of all 12 participants are provided in the results tables. A summary of statistical and clinical significance is represented in **Table 2** and more detail is shown in **Table 3** with statistical parameters and results.

Outcome

Visual Analysis

Results of participant 1 are presented graphically with trained and untrained goals in **Figure 2**. The graph shows changes following intervention in all trained goals though mild in one of the three and significant in the other two goals. **Figure 2** also shows transfer to untrained goals in one of the two goals chosen to measure this construct. The graphs for the remaining replication cases (including the case that did not proceed to intervention) are provided in **Figures 3–12**.

Quantitative Analysis of Performance Changes

Statistical differences between means in baseline and post-intervention supported the visual inspections and indicated that all participants achieved a significant improvement on at least one trained goal, with 63% (19/30) of goals improving across participants at post-test (**Tables 2**, **3**). Two participants improved on all of their trained goals, five improved on two goals, and three improved on a single goal. For the untrained goals, 7 of the 10 participants receiving CO-OP improved on at least one of the untrained goals, with 37% (7/19) of goals improving overall. Two participants showed deterioration in one of the two selected untrained goals.

Baseline trend (i.e., auto-correlation) was found in six goals and therefore the use of Tau-*U* correction for baseline trend was used. Using this index, all participants achieved improvement

TABLE 2 | Summary of outcomes (mean change, effect size, clinical significance) with three separate analyses of the individual goals per participant.

Child	Trained goals	*t*-test difference in means	Effect size (Tau-*U*)	CSC	Untrained goals	*t*-test difference in means	Effect size (Tau-*U*)	CSC
1	G1: Putting T-shirt	No change	Weak	Improved	G4: Eating with a spoon |	Improved	Moderate	Improved
	G2: Drinking from open cup	Improved	Moderate	Improved	G5: Applying lip balm	No change	Weak	No change
	G3: Pouring water	Improved	Strong	Improved				
2	G1: Drinking	No change	Weak	No change	G4: Eating crisps	Worse	Deteriorates mod	Worse
	G2: Brushing teeth	Improved	Strong	Improved	G5: Doing buttons	No change	Weak	No change
	G3: Pouring water	Improved	Moderate	Improved				
4	G1: Doing zips	Improved	Moderate	Improved	G4: Opening a snack	No change	Weak	Improved
	G2: Doing buttons	No change	Weak	Improved	G5: Putting socks on	Worse	Deteriorates mod	Worse
	G3: Putting shoes on	No change	Weak	No change				
5	G1: Applying mascara	Improved	Moderate	Improved	G4. Applying lipstick	Improved	Moderate	No change
	G2: Making a ham sandwich	Improved	Strong	Improved	G5: Brushing teeth	No change	Weak	No change
	G3: Carrying a cup of tea	Improved	Moderate	Improved				
6	G1: Buttering and cutting bread	Improved	Strong	Improved	G4. Writing signature on small window in paper	Improved	Moderate	Improved
	G2: Cooking in oven and taking out dish	No change	Weak	No change	G5: Cutting an apple	Improved	Strong	Improved
	G3: Cooking pasta	Improved	Moderate	Improved				
8	G1: Drinking without spilling	No change	Weak	No change	G4. Pouring water	No change	Weak	Improved
	G2: Handwriting	Improved	Moderate	Improved	G5: Carrying water	No change	Weak	Improved
	G3: Stirring food	Improved	Strong	Improved				
9	G1: Eating with a spoon	No change	Weak	Improved	G4. Brushing teeth	Improved	Moderate	No change
	G2: Drinking without spilling	Improved	Moderate	Improved	G5: Putting a t-shirt on	No change	Weak	No change
	G3: Riding a bike	No change	Weak	No change				
10	G1: Carrying a cup of tea	No change	Weak	No change	G4. Putting sheet on plastic folder	No change	Weak	No change
	G2: Cutting fingernails	Improved	Strong	Improved	G5: Opening tin of tomatoes	Improved	Moderate	Improved
	G3: Doing shoelaces	Improved	Strong	Improved				
11	G1: Cutting bread	Improved	Strong	Improved	G4. Leg elevation exercise	No change	Weak	No change
	G2: Putting socks on	Improved	Strong	Improved	G5: not set			
	G3: External rotation hip exercise	Improved	Strong	Improved				
12	G1: Applying mascara	Improved	Strong	Improved	G4. Carrying water	Improved	Strong	Improved
	G2: Drinking from a glass	No change	Weak	No change	G5: Eating with a spoon	No change	Weak	No change
	G3: Eating with knife and fork	No change	Weak	No change				

G, Goal; CSC, clinically significance change; NT, Not tested.

in at least one goal with moderate or large effect size. A "large" effect ($\geq$0.93) ("very effective intervention") was obtained in 80% of children post-intervention. In total, the effect size was "large" for 37% of trained goals overall post-treatment. For other trained goals, "moderate" effects (0.66 to 0.92) ("effective intervention") were obtained in 70% of children and for 27% of trained goals overall at post-intervention. "Weak" effects ($\leq$0.65) were seen in 11 goals (37%) overall across eight children at post-intervention. No negative effects (deterioration) were observed for trained goals.

For untrained goals, "large" or "moderate" effect was seen in 37% of goals (7/19) overall in six children post-treatment, and "weak" effects in 53%. Deterioration with "moderate" negative effects were seen in two goals for two different children. **Supplementary Information 2** summarizes results for effect size using non-overlapping index, Tau-*U*.

Clinically Significant Change

All participants showed a positive change of at least two PQRS-i points (based on the difference between the phase means) on at least one goal, at the end of treatment (**Tables 2**, **3**). Post-intervention, 6 out of the 10 participants showed clinically significant improvement on two of their trained goals and two children improved on all trained goals. For untrained goals, six children showed significant transfer on at least one goal at post-intervention.

TABLE 3 | Results including statistical at-test analysis and changes in slope with negative *T*-test indicating improvement in change pre-post scores whilst positive *t*-test scores indicate negative trend.

Child number (goal)		Weeks	Baseline	Post Rx	Post	Trend	*T*-test post-pre-		Slope beta (p)
	AC	Length	Mean (SD)	Mean (SD)	PQRS 2p change		Mean shift (95% CI)	*P*	
TRAINED GOALS									
1 (1)	1.80	2	3.17 (2.40)	5.33 (0.52)	Yes	↑	−2.17 (−4.68, 0.35)	0.078	−0.454 (0.103)
1 (2)	Constant	2	1.0 (0.00)	2.00 (0.89)	No	None	−1.00 (−1.94, −0.06)	0.041	0.187 (0.314)
1 (3)	Constant	2	1.0 (0.00)	5.00 (1.79)	Yes	↑	−4.00 (−5.88, −2.12)	0.003	0.553 (0.001)
2 (1)	2.429	2	2.00 (1.26)	1.60 (0.89)	No	None	0.40 (−1.08, 1.88)	0.56	−0.077 (0.676)
2 (2)	2.177	2	4.00 (1.15)	6.00 (0.00)	Yes	None	−2.00 (−3.84, −0.16)	0.041	0.339 (0.156)
2 (3)	0.934	2	2.17 (0.75)	4.67 (1.86)	Yes	↑	−2.50 (−4.46, −0.54)	0.020	0.612 (0.015)
5 (1)	1.989	2	4.86 (1.07)	7.17 (1.17)	Yes	↑	−2.31 (−3.70, −0.92)	0.004	0.605 (0.0005)
5 (2)	2.252	2	2.33 (0.52)	5.50 (0.55)	Yes	↑	−3.17 (−3.85, −2.48)	<0.001	0.446 (0.029)
5 (3)	1.480	2	4.00 (1.00)	6.83 (2.14)	Yes	↑	−2.83 (−5.09, −0.58)	0.021	0.434 (0.039)
6 (1)	3.000	2	2.67 (1.15)	6.83 (1.17)	Yes	↑	−4.17 (−6.41, −1.92)	0.006	0.676 (0.006
6 (2)	0.0000	2	9.50 (0.71)	9.50 (0.84)	No	None	0 (−2.53, −2.53)	1	0.260 (0.350)
6 (3)	3.000	2	4.33 (1.53)	7.50 (2.43)	Yes	↑	−3.17 (−6.38, 0.05)	0.053	0.330 (0.155)
10 (1)	2.853	2	9.0 (0.63)	9.00 (1.67)	No	None	0 (−1.76, 1.76)	1	0.000 (1.000)
10 (2)	2.449	2	1.33 (0.52)	9.67 (0.52)	Yes	↑	−8.33 (−9.00, −7.67)	<0.001	0.625 (0.000)
10 (3)	2.498	2	1.17 (0.41)	10.00 (0.00)	Yes	↑	−8.33 (−9.26, −8.40)	<0.001	0.888 (0.000)
11 (1)	1.504	2	3.0 (0.63)	6.67 (2.25)	Yes	↑	−3.67 (−6.02, −1.31)	0.009	0.382 (0.021)
11 (2)	2.578	2	6.0 (1.67)	10.00 (0.00)	Yes	↑	−4.00 (−5.76, −2.24)	0.002	0.873 (0.000)
11 (3)	2.547	2	1.14 (0.38)	5.00 (0.00)	Yes	↑	−3.86 (−4.21, −3.51)	<0.001	0.873 (0.000)
3 (1)	1.697	6	4.81 (1.21)	No Rx		None	Dropped out		
3 (2)	2.379	6	6.76 (0.89)	No Rx		None	Dropped out		
3 (3)	1.216	6	5.29 (2.10)	No Rx		None	Dropped out		
4 (1)	2.120	6	1.06 (0.24)	7.00 (4.65)	Yes	↑	−5.94 (−10.82, −1.06)	0.026	0.626 (0.0000)
4 (2)	1.005	6	2.12 (1.58)	4.60 (3.36)	Yes	↑	−2.48 (−6.60, 1.63)	0.176	0.431 (0.019)
4 (3)	Constant	6	1.0 (0.00)	2.80 (3.49)	No		−1.80 (−6.14, 2.54)	0.313	0.262 (0.141)
8 (1)	2.226	6	4.25 (2.02)	4.33 (3.87)	No	None	−0.08 (−3.63, 3.46)	0.956	0.191 (0.296)
8 (2)	2.018	6	4.05 (1.27)	6.83 (0.75)	Yes	↑	−2.78 (−3.68, −1.88)	<0.001	0.585 (0.001)
8 (3)	1.901	6	3.44 (2.55)	9.00 (2.00)	Yes	↑	−5.56 (−7.10, −4.02)	<0.001	0.669 (0.000)
9 (1)	1.875	6	4.61 (1.85)	5.75 (1.16)	No	None	−1.14 (−2.39, 0.11)	0.072	0.139 (0.337)
9 (2)	1.686	6	1.94 (1.39)	4.50 (1.05)	Yes	↑	−2.56 (−3.74, −1.37)	<0.001	0.564 (0.001)
9 (3)	Constant	6	1.0 (0.00)	1.00 (0.00)	No	None	−4.00 (−6.51, −1.49)	0.009	0.210 (0.188)
12 (1)	1.981	6	3.0 (1.93)	10.00 (0.00)	Yes	↑	−7.00 (−8.07, −5.93)	<0.001	0.837 (0.000)
12 (2)	1.404	6	1.94 (1.89)	1.67 (0.58)	No	None	0.28 (−0.94, 1.50)	0.628	0.194 (0.232)
12 (3)	2.263	6	4.06 (2.43)	3.00 (1.00)	No	↓	1.06 (−0.89, 3.01)	0.243	0.299 (0.046)
			Baseline	**Post Rx**	**Post**	**Trend**	***T*-test pre–post**		**Slope beta (p)**
	AC		**Mean (SD)**	**Mean (SD)**	**2p**		**Mean shift (95% CI)**	***P***	
UNTRAINED GOALS									
1 (4)	1.258	2	5.00 (1.94)	8.50 (1.05)	Yes	↑	−3.50 (−5.11, −1.89)	<0.001	0.733 (0.001)
1 (5)	1.361	2	2.50 (1.64)	3.50 (1.05)	No	None	−1.00 (−2.81, 0.82)	0.242	0.369 (0.237)
2 (4)	2.394	2	4.00 (1.67)	2.17 (0.41)	No	↓	1.83 (0.08, 3.58)	0.043	−0.636 (0.026)
2 (5)	Constant	2	1.0 (0.00)	1.0 (0.00)	No	None	−0.90 (−9.14, 7.34)	0.664	Constant
5 (4)	2.107	2	2.83 (0.75)	4.71 (0.95)	No	↑	−1.88 (−2.92, −0.84)	0.002	0.762 (0.002)
5 (5)	1.654	2	4.67 (1.03)	5.60 (0.55)	No	None	−0.93 (−2.06, 0.20)	0.093	0.516 (0.104)
6 (4)	3.400	2	4.00 (1.83)	7.50 (2.35)	Yes	↑	−3.50 (−6.57, −0.43)	0.031	0.663 (0.037)
6 (5)	3.000	2	2.67 (0.58)	7.17 (1.83)	Yes	↑	−4.50 (−6.47, −2.53)	0.001	0.836 (0.005)
10 (4)	2.842	2	7.17 (1.47)	8.33 (1.86)	No	None	−1.17 (−3.34, 1.01)	0.258	0.356 (0.256)
10 (5)	1.249	2	6.33 (1.51)	8.67 (0.52)	Yes	↑	−2.33 (−3.91, −0.75)	0.011	0.750 (0.005)

(Continued)

TABLE 3 | Continued

			Baseline	Post Rx	Post	Trend	*T*-test pre–post		Slope beta (p)
	AC		Mean (SD)	Mean (SD)	2p		Mean shift (95% CI)	*P*	
11 (4)	1.586	2	4.29 (1.50)	5.00 (1.41)	No	None	−0.71 (−2.41, 0.98)	0.377	0.253 (0.377)
11 (5)	Not set	2	N/A	N/A	N/A	N/A	N/A	N/A	N/A
3 (4)	1.780	6	2.38 (2.66)	No Rx		None	Dropped out		
3 (5)	1.987	6	3.43 (1.55)	No Rx		None	Dropped out		
4 (4)	2.304	6	5.25 (4.43)	8.25 (3.06)	Yes	↑	−3.00 (−6.24, 0.24)	0.067	−0.343 (0.101)
4 (5)	1.887	6	7.54 (1.76)	4.25 (2.50)	No	↓	3.29 (−0.45, 7.03)	0.071	−0.609 (0.009)
8 (4)	1.853	6	5.44 (2.20)	8.00 (3.16)	Yes	↑	−2.56 (−5.88, 0.77)	0.111	0.426 (0.038)
8 (5)	1.749	6	6.43 (3.74)	8.67 (3.27)	Yes	None	−2.23 (−5.74, 1.28)	0.183	0.248 (0.194)
9 (4)	1.903	6	2.11 (0.68)	4.00 (1.26)	No	↑	−1.89 (−3.21, −0.57)	0.013	0.710 (0.000)
9 (5)	0.732	6	5.06 (1.80)	6.00 (2.00)	No	None	−0.94 (−3.07, 1.82)	0.335	0.225 (0.289)
12 (4)	0.960	6	1.41 (1.00)	6.33 (1.53)	Yes	↑	−4.92 (−8.39, −1.46)	0.024	0.865 (0.000)
12 (5)	0.726	6	3.88 (2.12)	3.33 (0.58)	No	None	0.39 (−0.77, 1.87)	0.386	−0.102 (0.667)

AC, Auto-correlation; SD, Standard Deviation; CSC, Clinically Significance Change; CI, Confidence Interval; NT, non-tested; ↑, Ascendant; ↓, Descendent.
Table 3 *shows three separate analysis of the individual goals per participant. Negative T-test indicates improvement in change pre–post scores whilst positive t-test scores indicates negative trend.*

Quantitative Statistical Analysis of Performance Change Between DBS+CO-OP and DBS+Extended Baseline/Practice of the Goals)

Differences between means in extended baseline using *t*-test supported the visual inspections and indicated that DBS and practice alone did not offer improvement in the majority of goals (see **Supplementary Information 3**). There was, however, significant improvement in 4 out of the 25 goals for four out of five participants during extended baseline/practice. Significant deterioration was also noted for two participants for a total of three goals during extended baseline/practice.

Analysis of Results in Relation to Therapist-Related Fidelity to Treatment

The six treating therapists varied in years of experience from recently qualified to 20 years (see **Supplementary Information 1**). Two out of the six therapists achieved <50% on fidelity checklist with the lowest scores on two of the key elements of the CO-OP approach, Guided Discovery and collaborative Dynamic Performance Analysis (DPA). The two participants treated by the therapists with the lowest fidelity score achieved improvement in goals, but the majority of overall change was measured during the baseline phase with limited improvement over the course of therapy.

DATA AVAILABILITY

Access to de-identified participant data may be requested by contacting the first author.

DISCUSSION

This is the second of two studies exploring the use of the CO-OP approach with childhood-onset HMD post-DBS. The first was set up as a proof of concept and preliminary efficacy (i.e., can the intervention be implemented?). The present study was set up as preliminary evaluation of effectiveness (i.e., can it be delivered in every day practice?) and reports the results in performance improvement when the intervention is delivered by local occupational therapists not specialized in HMD and with only basic training in the CO-OP approach based in centers across the UK. Together, the two studies provide evidence that CO-OP is a feasible and acceptable intervention for children and young people with HMD following DBS, with the potential to produce clinically meaningful improvement.

The results obtained in the present study are promising on two grounds: Firstly, although treatment fidelity was variable, CO-OP can be delivered by occupational therapists independent of their years of training and with a relative low-intensity training course, which makes this approach feasible in the context of clinical practice for further formal evaluation. Secondly, replicability has been demonstrated across multiple therapists, in a substantial number of children and young people with heterogeneous presentations of HMD and DBS duration. The total number of successful replications ($n = 10$) reported here and in combination with those reported previously (N-of-1 plus 8 replications) exceeds the three to five replications recommended in single-case experimental design, increasing confidence in the results. In this study, all eligible participants in the CMDS database were approached and all who consented were recruited to the study, reducing the risk of bias selection.

As in the first N-of-1 series with eight replications (7), skill improvement following CO-OP was seen in all children and young people, independently of their baseline characteristics and with a broad range of goals as outlined in **Table 2**. The majority (19/30) of goals addressed in therapy improved during the CO-OP intervention (63% goals improved compared to 75% of goals in the first study). This indicates slightly lower goal improvement rates than in the previous series completed by a therapist experienced in movement disorders and CO-OP. This is in line with reported literature indicating that effectiveness studies closer to the "real-world" setting often show lower improvement

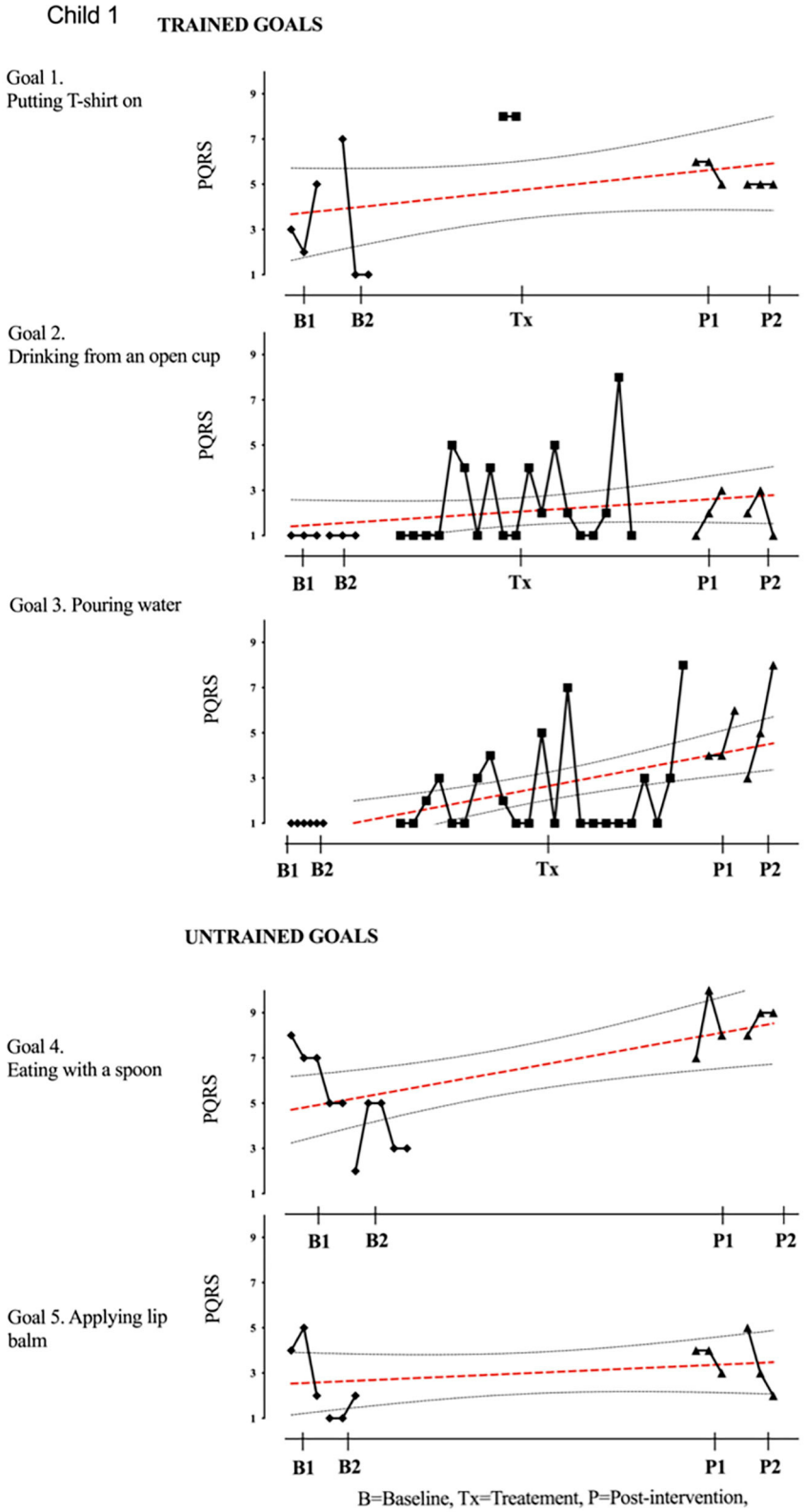

FIGURE 2 | Participant 1, PQRS-i scores (y-axis) for GI-5 for each trial phase (x-axis). For participant 1, the graph indicates a significant improvement in goals 2–4 with stable baseline on goals 2 and 3 (drinking from an open cup and pouring water) and change in slope observed during the treatment session. Even though improved, variability of performance was observed at the post-intervention phase. The visual data provides evidence on means, levels, trends, variability, latency, and consistency across the different phases of the study for each participant and for each individual goal. Also shown is the OLS regression line and 95% confidence range.

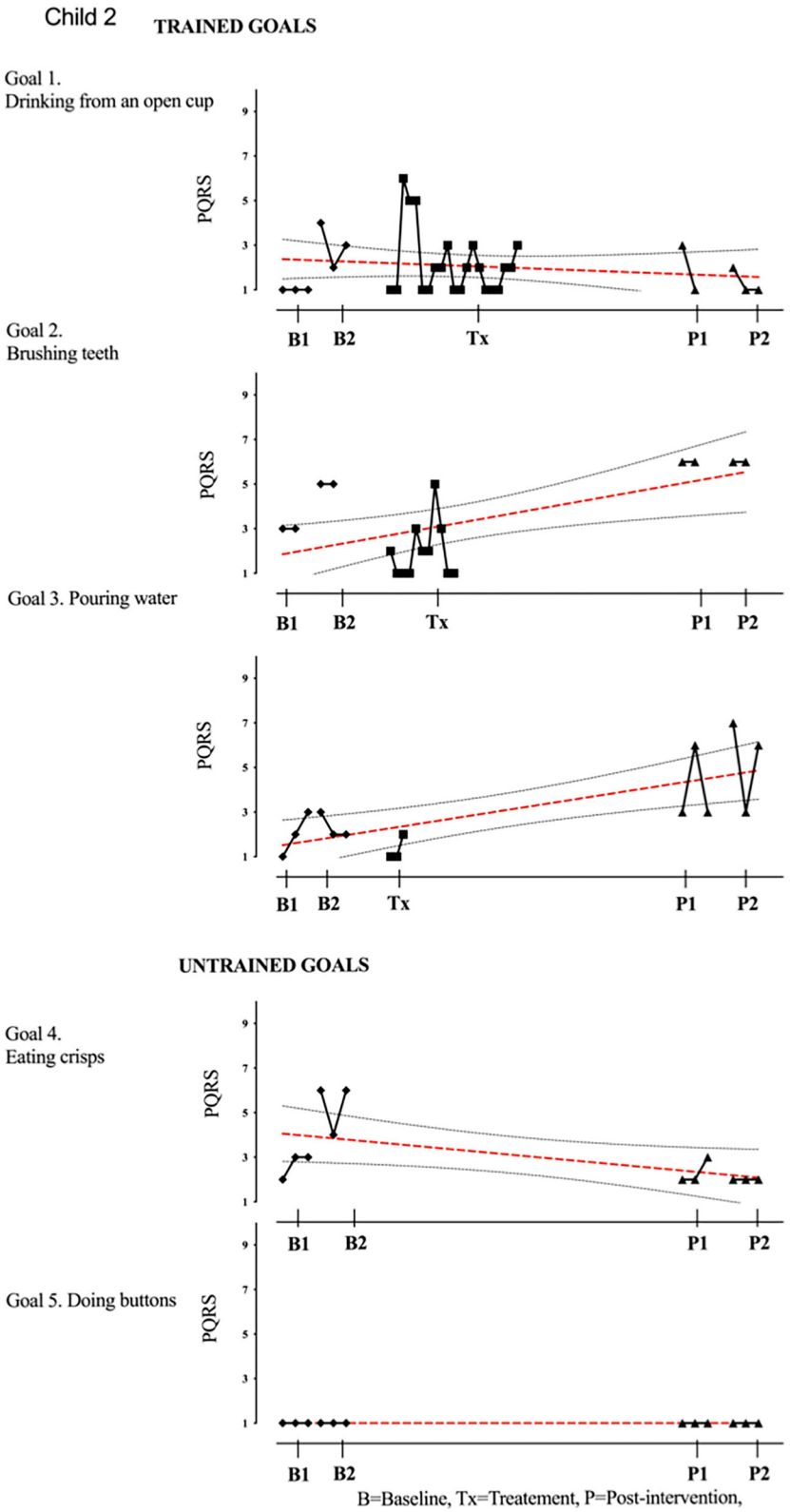

FIGURE 3 | Child 2 PQRS-i scores (y-axis) for GI-5 for each trial phase (x-axis). **Supplementary Information 3**. Child 2. Results with OLS regression line superimposed.

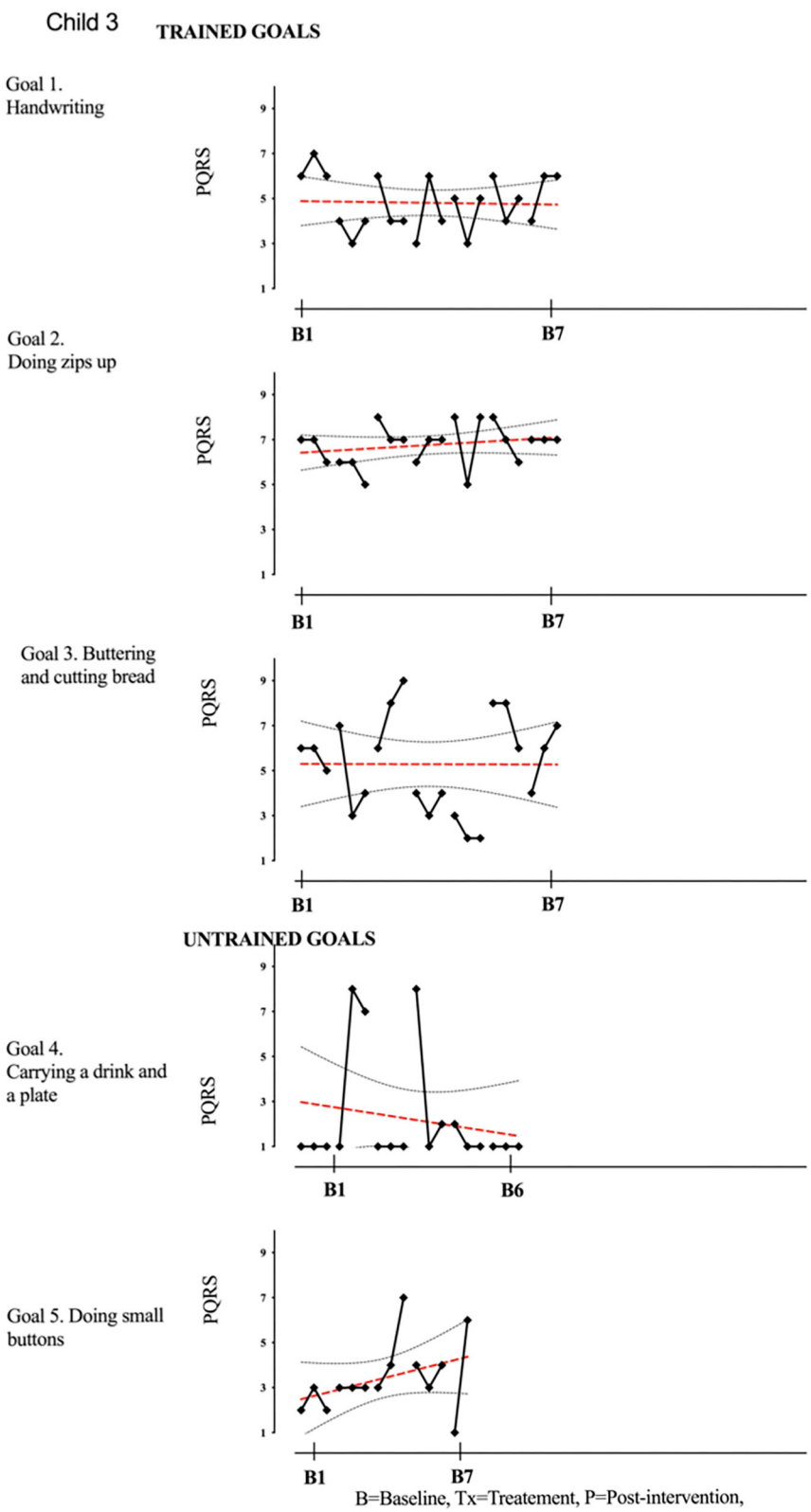

FIGURE 4 | Child 3 PQRS-i scores (y-axis) for GI-5 for each trial phase (x-axis). Results with OLS regression line superimposed.

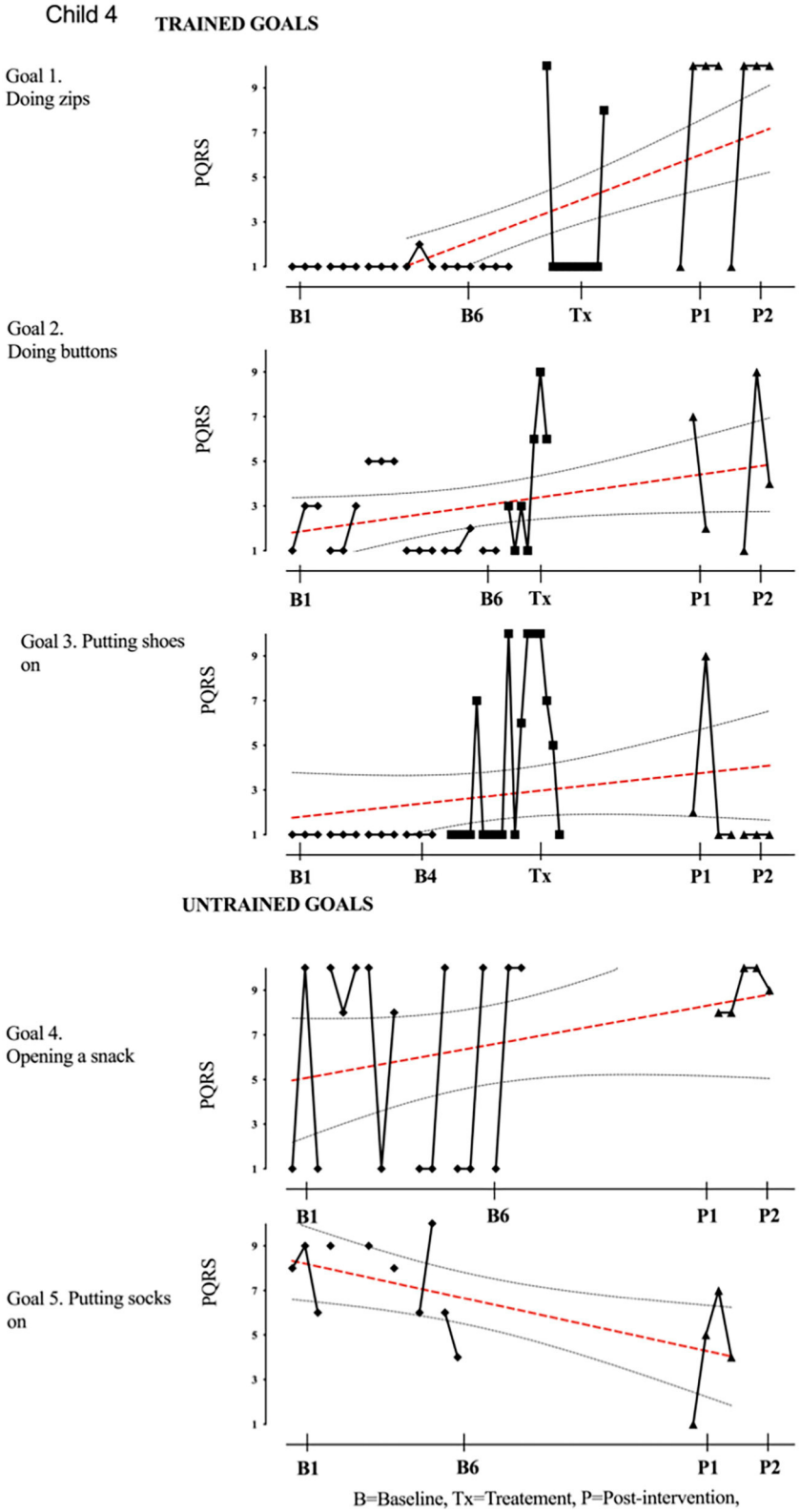

FIGURE 5 | Child 4 PQRS-i scores (y-axis) for GI-5 for each trial phase (x-axis). Results with OLS regression line superimposed.

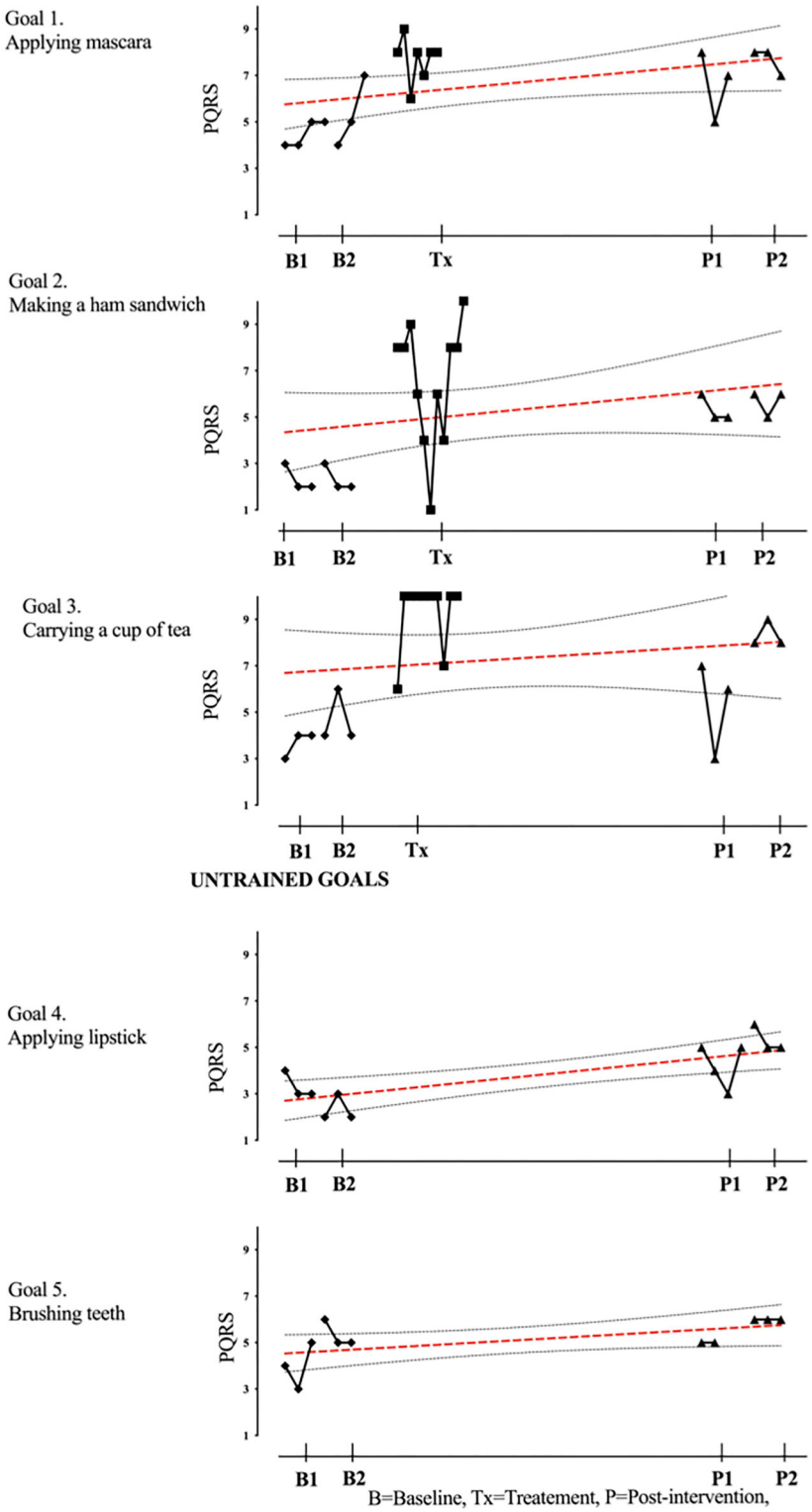

FIGURE 6 | Child 5 PQRS-i scores (y-axis) for GI-5 for each trial phase (x-axis). Results with OLS regression line superimposed.

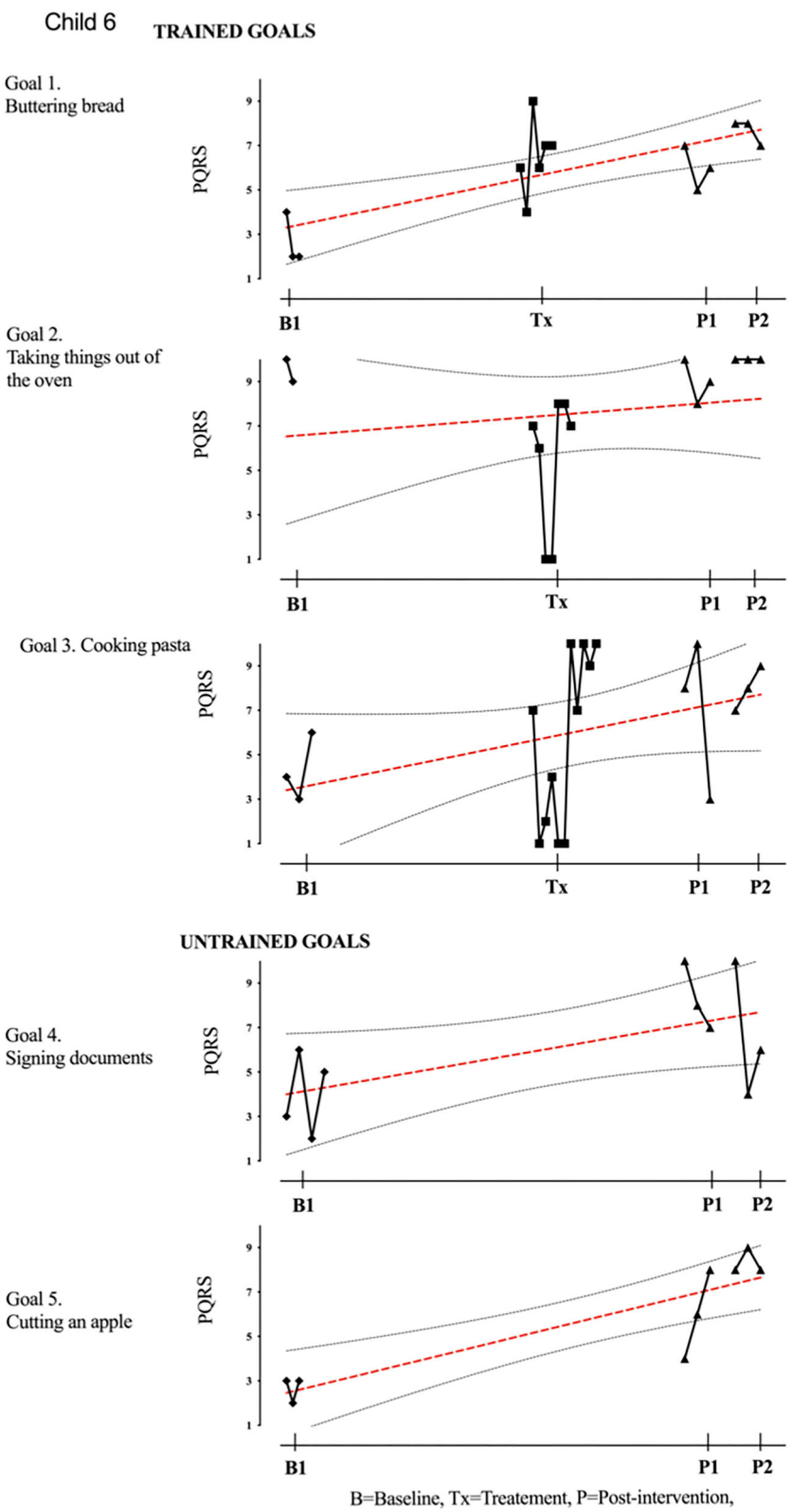

FIGURE 7 | Child 6 PQRS-i scores (y-axis) for GI-5 for each trial phase (x-axis). Results with OLS regression line superimposed.

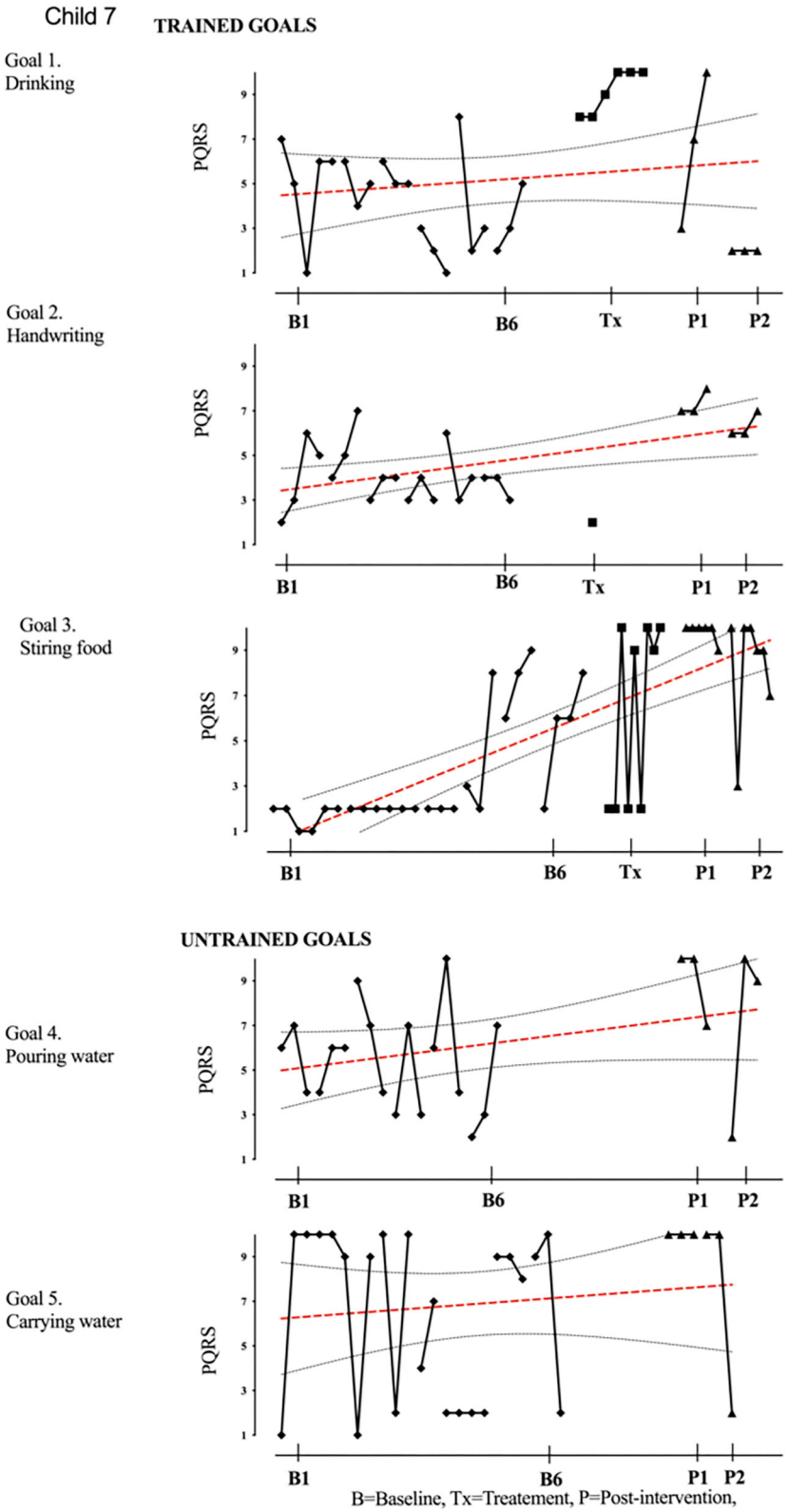

FIGURE 8 | Child 7 PQRS-i scores (y-axis) for GI-5 for each trial phase (x-axis). Results with OLS regression line superimposed.

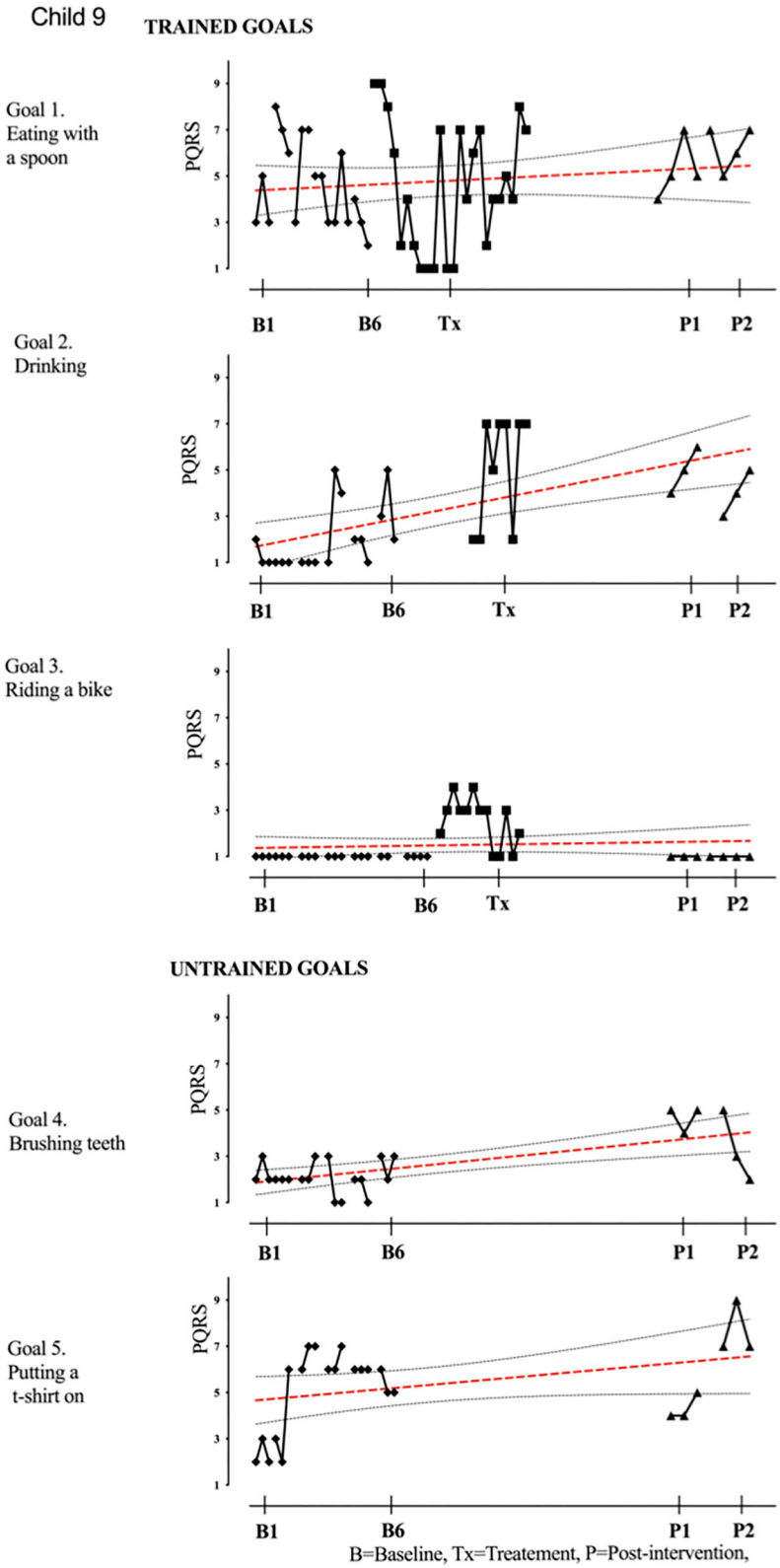

FIGURE 9 | Child 9 PQRS-i scores (y-axis) for GI-5 for each trial phase (x-axis). Results with OLS regression line superimposed.

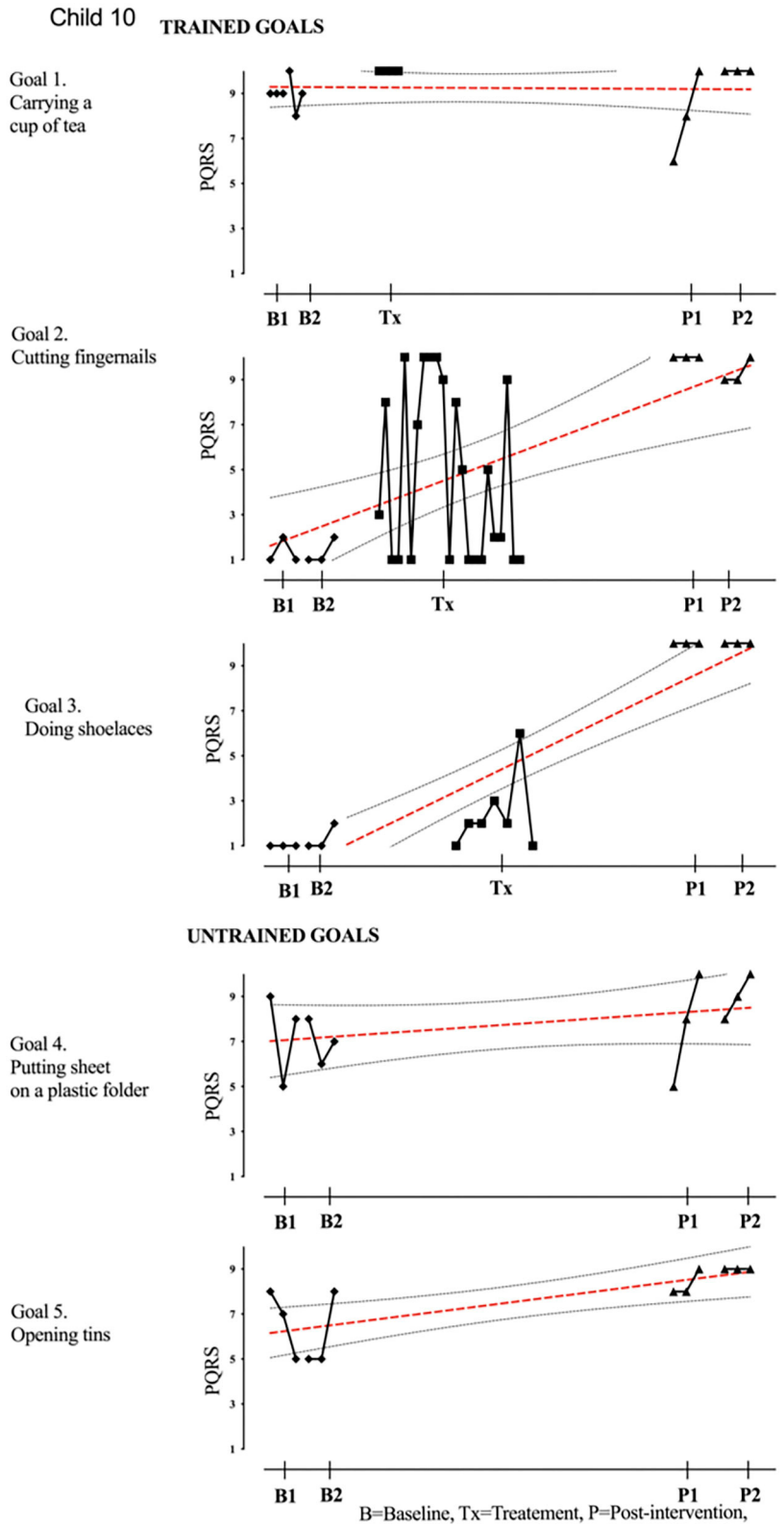

FIGURE 10 | Child 10 PQRS-i scores (y-axis) for GI-5 for each trial phase (x-axis). Results with OLS regression line superimposed.

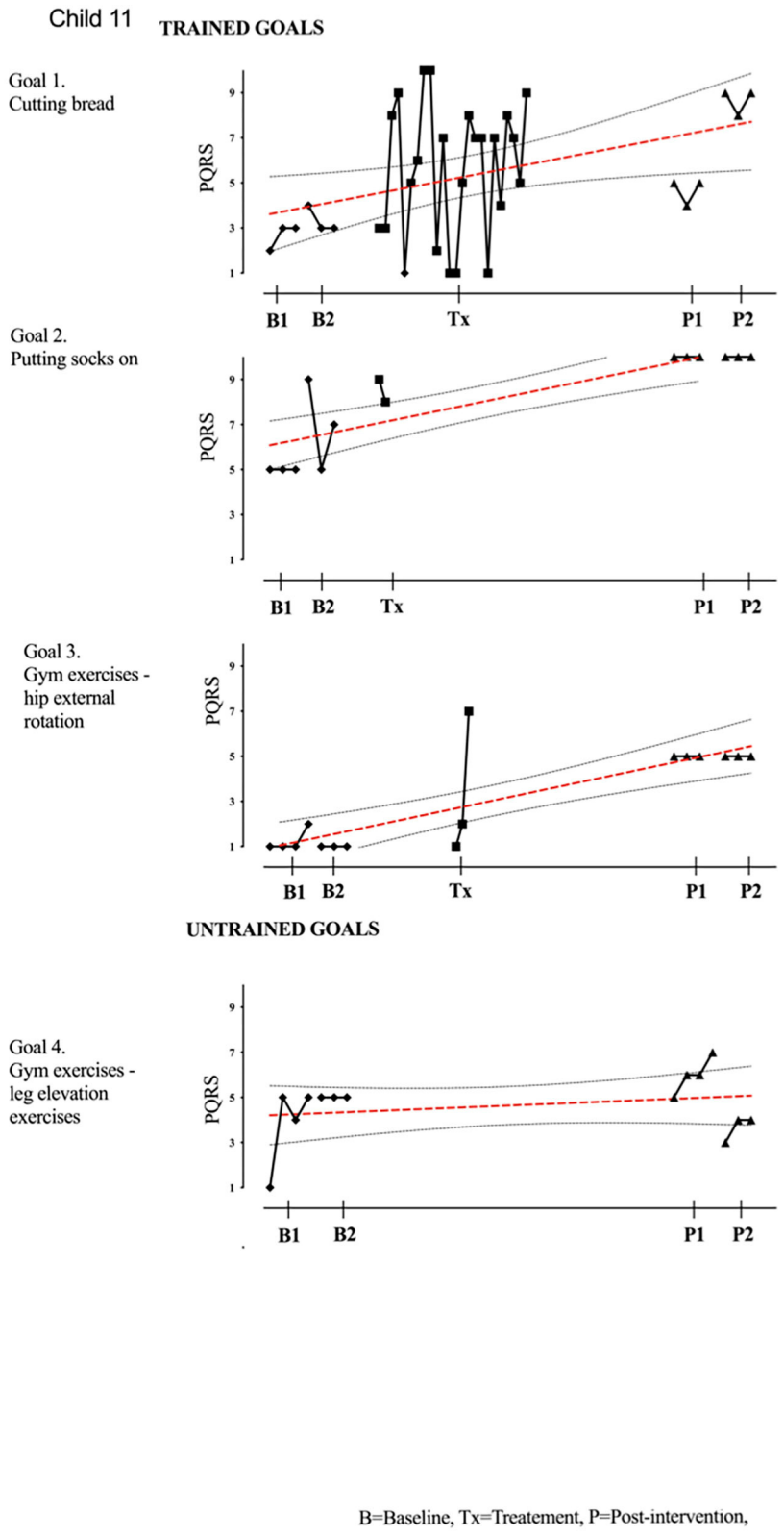

FIGURE 11 | Child 11 PQRS-i scores (y-axis) for GI-5 for each trial phase (x-axis). Results with OLS regression line superimposed.

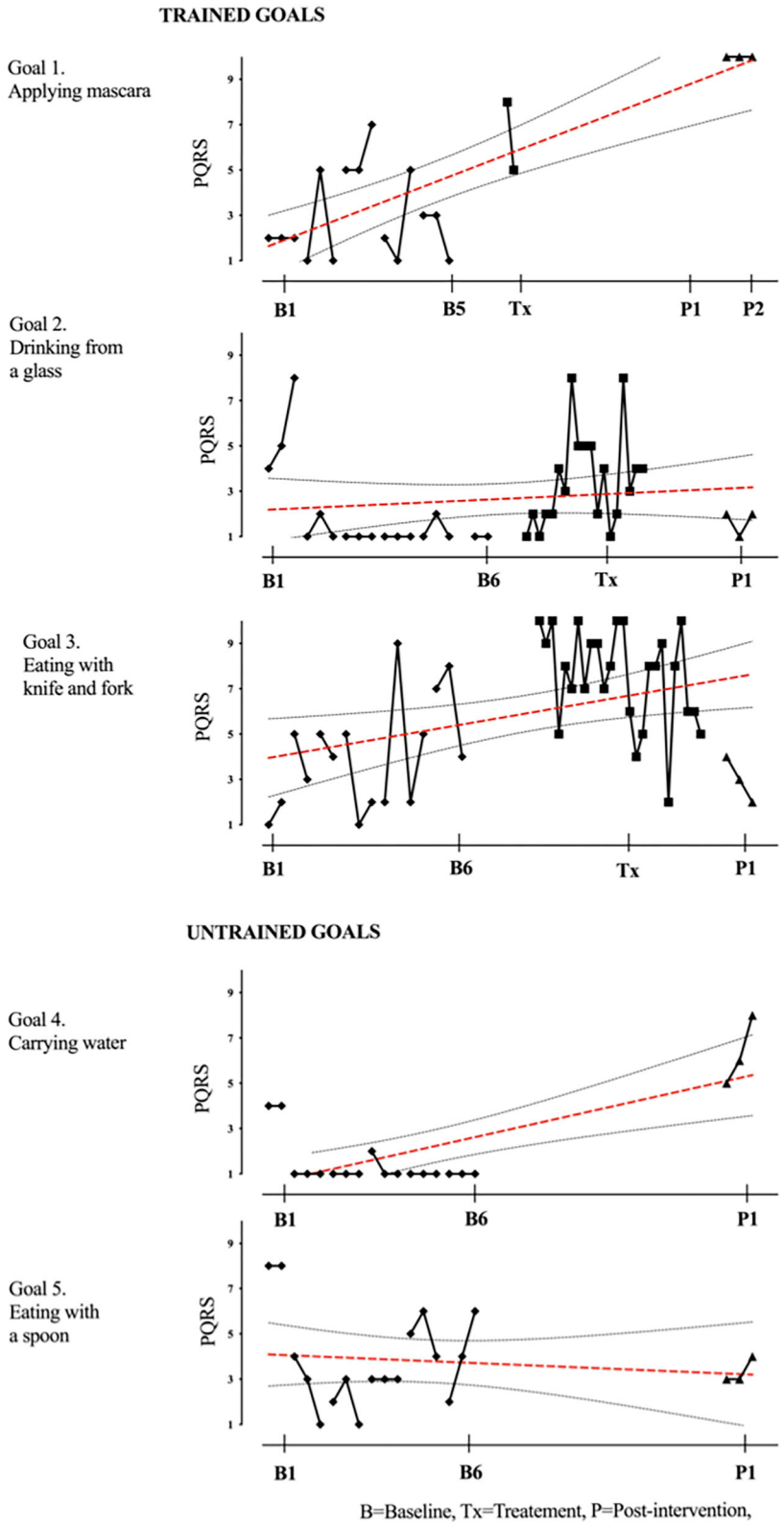

FIGURE 12 | Child 12 PQRS-i scores (y-axis) for GI-5 for each trial phase (x-axis). Results with OLS regression line superimposed.

rates than in efficacy studies taking place in specialist centers (26). However, the results indicate that useful results are still possible with a relative brief therapy intervention (<10 h per participant) and low training requirements, as well as for therapists with no prior experience in HMD.

Results suggest that meaningful functional improvement is possible in children with a range of etiologies and clinical presentations in childhood-onset HMD. Half of the group achieved at least two out of the three goals worked in therapy. The participants achieving only one goal included one participant with childhood stroke, a participant with CP, and one participant with a metabolic disorder.

While robust positive change was observed on at least one trained goal by all participants, some goals showed no change. Of those children who improved on only one goal, the unimproved goals worked on were doing buttons and putting shoes on for the child with stroke (participant 4), toothbrushing and drinking for child with metabolic disorder (participant 9), eating with knife and fork, and applying mascara for child with CP (participant 12). Possible explanations for the lack of improvement could relate to the difficulty of the selected goal in relation the participants' motor impairment, the fidelity of treatment, or the expertise of the therapist. Although challenging, similar goals successfully improved in other participants with the same characteristics, suggesting that the goal itself may not be the limiting factor or the clinical characteristics. Therapist effects may have been important in some of the cases that showed limited clinical gains. Fidelity to treatment was rated <50% for case 4 (38%) and case 9 (49%) who both improved on only a single goal. Therefore, wider improvement might have been hindered by the diluted delivered version of the CO-OP intervention. It may well be that outcome relates to a combination of the difficulty in the chosen goal itself and the therapists' difficulty to apply the CO-OP approach to these more challenging goals. Future trials may require greater investment in training and supervision.

Although improvement on trained goals is an important outcome, the real potential of this treatment lies in its generalizability and transferability, enabling improving performance beyond the treatment sessions, thereby broadening the reach of the CO-OP approach. In the present study skill transfer was observed in seven of the untrained goals, across five participants. This is similar to the previous single-therapist HMD single-case experimental design (7) and in adults with stroke (27). Even if evidence for the generalizability of transfer is somewhat limited, the potential is demonstrated and warrants further work to enhance this crucial outcome.

Finally, the present study permitted an assessment of the impact of repeated practice on the goals with DBS *in situ* prior to the systematic application of the CO-OP approach. Improvement during extended baseline (DBS and practice) (**Supplementary Information 3**) was noted for 4 of 25 goals in four out of the five children randomly allocated to extended baseline. In such cases, it was hard to disentangle the effects of practice and neuromodulation with DBS. However, given that only some of the goals improved in the extended period ($n = 4$, 16%), it is more likely due to practice effects than DBS. In the remainder, who showed stable baseline performance, improvement could be more confidently attributed to the CO-OP approach.

As with any study, there are limitations that warrant mentioning. All of the participants in this study had DBS *in situ*, raising the possibility that DBS-related factors may moderate the outcome of CO-OP. The careful design of both, this and the former proof-of-concept study (7), allowed for manipulation of DBS length of neuromodulation as a variable. Those with neuromodulation in place for longer than 1 year, when most of the change has taken place, particularly in inherited genetic dystonias, showed improvement when the CO-OP intervention started and not necessarily on the baseline period. Secondly, the extended baseline used in this study allowed for close monitoring of change happening within a 6 week period with no therapy intervention, showing much less change on the goals set by the participants. Finally, and most importantly, given that neuromodulation is a global management approach, improvement would be expected to be seen across any goals (trained or untrained) the young person performs. This was not the case in either of the studies performed in the short study periods within these studies, indicating that transfer and indeed goal acquisition are most likely due to the effect of the CO-OP approach. However, goal attainments after DBS in genetic and acquired childhood onset dystonia disorders have been reported without CO-OP at 1–2 years post-DBS implant (28). Without DBS intervention, dystonia worsens (29) along with fixed deformities (30) irrespective of the cause and conventional surgical and medical approaches failed to address the needs of children with HMD (31). DBS neuromodulation is a global management approach to reducing dystonia, chorea, myoclonus, and tremor, often in children with little or no pre-existing motor repertoire in whom dystonia reduction does not equate with spontaneous acquisition of skills after DBS intervention, even with conventional practice and repetition of desired motor skill. For the networked efficacy of DBS, motor and sensory pathways must be intact (32). In addition, cognitive function appears preserved or even enhanced following DBS in isolated-genetic (33), and in addition to cognitive stability, perceptual reasoning may be increased after DBS in acquired (34) dystonias, respectively, supporting the place of cognitive strategies to boost goal acquisition and transfer of skills to untrained goals with CO-OP approach after DBS.

It is therefore postulated that DBS accelerates or facilitates the efficacy of CO-OP by reducing dystonia and also by modifying the underlying cerebral plasticity. Since, as a guide, it may take up to 2 years for the full benefits of DBS to manifest in isolated genetic dystonias and longer in acquired dystonias, applying methods that enhance the overall speed of goal attainment through a cognitive problem-solving approach is clearly urgently required in childhood when the windows of plasticity are limited (35).

In conclusion, the presented results are promising for a number of reasons. This trial is the first attempt to systematically evaluate the potential effectiveness of a rehabilitation intervention for children and young people with HMD across therapists. Although further testing of efficacy and

effectiveness through large-scale trials is required, the present study shows that CO-OP is a feasible and acceptable approach to rehabilitation following DBS for children and young people with HMD and that changes are overall significant for client-chosen goals, including in children with dyskinetic CP, for whom DBS or any other current management modality does not currently provide enough functional changes.

As described, fidelity to treatment was variable and sometimes sub-optimal, indicating the importance of training and supervision in future trials. The limited transfer achieved to untrained goals also warrants further investigation in relation to delivery of the intervention, dosage (timing, frequency, and duration), and any modifications that might be required to achieve transfer to goals not addressed in therapy for this population. Finally, the promising results from using CO-OP with HMD and DBS warrant further investigation of the CO-OP approach in dystonia, which offers a treatment option for a wider number of potential patients. Further, the results from this study and the previous study indicate that practice alone does not provide improvement in self-selected goals. This suggest that simple goal-oriented approaches recommended by experts in dystonia might not be sufficient without the more cognitive problem-solving element inherent in CO-OP. Future research comparing CO-OP with other goal-oriented approaches would be valuable.

DATA AVAILABILITY STATEMENT

The raw data supporting the conclusions of this article will be made available by the authors, without undue reservation.

ETHICS STATEMENT

The studies involving human participants were reviewed and approved by Oxford A Research Ethics Committee, 14/SC/1159. Written informed consent to participate in this study was provided by the participants' legal guardian/next of kin.

AUTHOR CONTRIBUTIONS

HG completed all statistical analysis. This was supervised by VC, senior trial statistician. HG: research study, conception, organization, execution, manuscript preparation, and writing of the first draft. HP, J-PL, VC, and RB: research study, conception, manuscript preparation, and review and critique. All authors contributed to the article and approved the submitted version.

FUNDING

HG was funded by a National Institute for Health Research (NIHR/HEE Clinical Doctoral Research Fellowship, CDRF-2013-04-039). This paper represents independent research partly funded by the National Institute for Health Research (NIHR) (HG) and the NIHR Biomedical Research Center at South London and Maudsley NHS Foundation Trust and King's College London (RB). The views expressed are those of the author(s) and not necessarily those of the NHS, the NIHR, or the Department of Health. J-PL has received grants from the Guy's and St Thomas' Charity G060708 to set up the Complex Motor Disorders Service Multidisciplinary Team for Deep Brain Stimulation and Intrathecal Baclofen Service, the Dystonia Society UK Grant 01/2011 and 07/2013, and Action Medical Research GN2097.

ACKNOWLEDGMENTS

We would like to thank the children, young people, and their families that participated in the study. We would also like to thank the occupational therapists who delivered the intervention.

SUPPLEMENTARY MATERIAL

The Supplementary Material for this article can be found online at: https://www.frontiersin.org/articles/10.3389/fped.2020.600337/full#supplementary-material

REFERENCES

1. Moro E, LeReun C, Krauss JK, Albanese A, Lin JP, Walleser Autiero S, et al. Efficacy of pallidal stimulation in isolated dystonia: a systematic review and meta-analysis. *Eur J Neurol.* (2017) 24:552–60. doi: 10.1111/ene.13255
2. Koy A, Hellmich M, Pauls KA, Marks W, Lin JP, Fricke O, et al. Effects of deep brain stimulation in dyskinetic cerebral palsy: a meta-analysis. *Mov Disord.* (2013) 28:647–54. doi: 10.1002/mds.25339
3. Gimeno H, Chard G, Selway R, A K, Lin JP. Functional outcomes using the assessment of motor and process skills following deep brain stimulation. *Dev Med Child Neurol.* (2016) 58(Suppl. 1):2–18. doi: 10.1111/dmcn.12997
4. Novak I, Morgan C, Fahey M, Finch-Edmondson M, Galea C, Hines A, et al. State of the evidence traffic lights 2019: systematic review of interventions for preventing and treating children with cerebral palsy. *Curr Neurol Neurosci Rep.* (2020) 20:3. doi: 10.1007/s11910-020-1022-z
5. van den Dool J, Visser B, Koelman JH, Engelbert RH, Tijssen MA. Long-term specialized physical therapy in cervical dystonia: outcomes of a randomized controlled trial. *Arch Phys Med Rehabil.* (2019) 100:1417–25. doi: 10.1016/j.apmr.2019.01.013
6. de Pauw J, van der Velden K, Meirte J, van Daele U, Truijen S, Cras P, et al. The effectiveness of physiotherapy for cervical dystonia: a systematic literature review. *J Neurol.* (2014) 261:1857–65. doi: 10.1007/s00415-013-7220-8
7. Gimeno H, Brown RG, Lin JP, Cornelius V, Polatajko HJ. Cognitive approach to rehabilitation in children with hyperkinetic movement disorders post-DBS. *Neurology.* (2019) 92:e1212–24. doi: 10.1212/WNL.0000000000007092
8. Polatajko H, Mandich A. *Enabling Occupation in Children: The Cognitive Orientation to Daily Occupational Performance (CO-OP) Approach*. Ottawa, ON: CAOT Publications (2004).
9. Okiishi JC, Lambert MJ, Eggett D, Nielsen L, Dayton DD, Vermeersch DA. An analysis of therapist treatment effects: toward providing feedback to individual therapists on their clients' psychotherapy outcome. *J Clin Psychol.* (2006) 62:1157–72. doi: 10.1002/jclp.20272
10. Mason L, Grey N, Veale D. My therapist is a student? The impact of therapist experience and client severity on cognitive behavioural therapy outcomes for people with anxiety disorders. *Behav Cogn Psychother.* (2016) 44:193–202. doi: 10.1017/S1352465815000065
11. King G. The role of the therapist in therapeutic change: how knowledge from mental health can inform pediatric rehabilitation. *Phys*

Occup Ther Pediatr. (2017) 37:121–38. doi: 10.1080/01942638.2016.1185508
12. Tate RL, Perdices M, Rosenkoetter U, McDonald S, Togher L, Shadish W, et al. The single-case reporting guideline in behavioural interventions (SCRIBE) 2016: explanation and elaboration. *Arch Sci Psychol.* (2016) 4:10–31. doi: 10.1037/arc0000027
13. Barlow D, Nock M, Hersen M. *Beyond the Individual: Direct, Systematic, and Clinical Replication Procedures.* 3rd ed. Boston, MA: Pearsons Education, Inc. (2009).
14. Gimeno H, Polatajko HJ, Cornelius V, Lin JP, Brown RG. Protocol for N-of-1 trials proof of concept for rehabilitation of childhood-onset dystonia: study 1: protocole des essais de validation a effectif unique pour la readaptation de la dystonie debutant dans l'enfance: Etude 1. *Can J Occup Ther.* (2018) 85:242–54. doi: 10.1177/0008417417707532
15. Gimeno H, Polatajko HJ, Cornelius V, Lin JP, Brown RG. Protocol for N-of-1 trials with replications across therapists for childhood-onset dystonia rehabilitation: study 2: protocole des essais a effectif unique avec repetitions par differents ergotherapeutes pour la readaptation de la dystonie debutant dans l'enfance: Etude 2. *Can J Occup Ther.* (2018) 85:255–60. doi: 10.1177/0008417417707734
16. Barlow D, Nock M, Hersen M. *Single Case Experimental Designs. Strategies for Studying Behavior Change.* 3rd ed. Boston, MA: Pearson (2009).
17. Kratochwill TR, Hitchcock JH, Horner RH, Levin JR, Odom SL, Rindskopf DM, et al. Single-case intervention research design standards. *Remed Special Educ.* (2012) 34:26–38. doi: 10.1177/0741932512452794
18. Law M, Baptiste S, McColl MA, Opzoomer A, Polatajko H, Pollock N. *Canadian Occupational Performance Measure.* 5th ed. Ottawa, ON: CAOT Publications ACE (2014).
19. Kratochwill TR, Levin JR. Enhancing the scientific credibility of single-case intervention research: randomization to the rescue. *Psychol Methods.* (2010) 15:124–44. doi: 10.1037/a0017736
20. Nourbakhsh R, Ottenbacher KJ. The statistical analysis of single-subject data: a comparative examination. *Phys Ther.* (1994) 74:768–76. doi: 10.1093/ptj/74.8.768
21. Kazdin AE. *Single-Case Research Designs: Methods for Clinical and Applied Settings.* 2nd ed. New York, NY: Oxford University Press, Inc (2011).
22. Swaminathan H, Rogers HJ, Horner RH, Sugai G, Smolkowski K. Regression models and effect size measures for single case designs. *Neuropsychol Rehabil.* (2014) 24:554–71. doi: 10.1080/09602011.2014.887586
23. Maggin DM, Swaminathan H, Rogers HJ, O'Keeffe BV, Sugai G, Horner RH. A generalized least squares regression approach for computing effect sizes in single-case research: application examples. *J Sch Psychol.* (2011) 49:301–21. doi: 10.1016/j.jsp.2011.03.004
24. Parker RI, Vannest KJ, Davis JL, Sauber SB. Combining nonoverlap and trend for single-case research: Tau-U. *Behav Ther.* (2011) 42:284–99. doi: 10.1016/j.beth.2010.08.006
25. McEwen S, Polatajko H, Wolf T, Baum C, Executive C-OA. *CO-OP Fidelity Checklist*. (2015). Available online at: http://www.ot.utoronto.ca/coop/research/coop_research/fidelity.html (accessed July 20, 2020).
26. Singal AG, Higgins PD, Waljee AK. A primer on effectiveness and efficacy trials. *Clin Transl Gastroenterol.* (2014) 5:e45. doi: 10.1038/ctg.2013.13
27. McEwen SE, Polatajko HJ, Huijbregts MP, Ryan JD. Exploring a cognitive-based treatment approach to improve motor-based skill performance in chronic stroke: results of three single case experiments. *Brain Inj.* (2009) 23:1041–53. doi: 10.3109/02699050903421107
28. Gimeno H, Tustin K, Lumsden D, Ashkan K, Selway R, Lin JP. Evaluation of functional goal outcomes using the canadian occupational performance measure (COPM) following deep brain stimulation (DBS) in childhood dystonia. *Eur J Paediatr Neurol.* (2014) 18:308–16. doi: 10.1016/j.ejpn.2013.12.010
29. Lin JP, Lumsden DE, Gimeno H, Kaminska M. The impact and prognosis for dystonia in childhood including dystonic cerebral palsy: a clinical and demographic tertiary cohort study. *J Neurol Neurosurg Psychiatry.* (2014) 85:1239–44. doi: 10.1136/jnnp-2013-307041
30. Lumsden DE, Gimeno H, Tustin K, Kaminska M, Lin JP. Interventional studies in childhood dystonia do not address the concerns of children and their carers. *Eur J Paediatr Neurol.* (2015) 19:327–36. doi: 10.1016/j.ejpn.2015.01.003
31. Lumsden DE, Gimeno H, Elze M, Tustin K, Kaminska M, Lin JP. Progression to musculoskeletal deformity in childhood dystonia. *Eur J Paediatr Neurol.* (2016) 20:339–45. doi: 10.1016/j.ejpn.2016.02.006
32. McClelland VM, Fialho D, Flexney-Briscoe D, Holder GE, Elze MC, Gimeno H, et al. Somatosensory evoked potentials and central motor conduction times in children with dystonia and their correlation with outcomes from deep brain stimulation of the globus pallidus internus. *Clin Neurophysiol.* (2018) 129:473–86. doi: 10.1016/j.clinph.2017.11.017
33. Owen T, Gimeno H, Selway R, Lin JP. Cognitive function in children with primary dystonia before and after deep brain stimulation. *Eur J Paediatr Neurol.* (2015) 19:48–55. doi: 10.1016/j.ejpn.2014.09.004
34. Owen T, Adegboye D, Gimeno H, Selway R, Lin JP. Stable cognitive functioning with improved perceptual reasoning in children with dyskinetic cerebral palsy and other secondary dystonias after deep brain stimulation. *Eur J Paediatr Neurol.* (2017) 21:193–201. doi: 10.1016/j.ejpn.2016.10.003
35. Ismail FY, Fatemi A, Johnston MV. Cerebral plasticity: windows of opportunity in the developing brain. *Eur J Paediatr Neurol.* (2017) 21:23–48. doi: 10.1016/j.ejpn.2016.07.007

Conflict of Interest: J-PL has received unrestricted educational support for instructional courses and consultancy fees from Medtronic Ltd.

The remaining authors declare that the research was conducted in the absence of any commercial or financial relationships that could be construed as a potential conflict of interest.

Copyright © 2021 Gimeno, Polatajko, Lin, Cornelius and Brown. This is an open-access article distributed under the terms of the Creative Commons Attribution License (CC BY). The use, distribution or reproduction in other forums is permitted, provided the original author(s) and the copyright owner(s) are credited and that the original publication in this journal is cited, in accordance with accepted academic practice. No use, distribution or reproduction is permitted which does not comply with these terms.

frontiers in Neurology

ORIGINAL RESEARCH
published: 30 March 2021
doi: 10.3389/fneur.2021.626608

Influence of Stochastic Resonance on Manual Dexterity in Children With Developmental Coordination Disorder: A Double-Blind Interventional Study

Satoshi Nobusako[1,2]*, *Michihiro Osumi*[1,2], *Atsushi Matsuo*[1,2], *Emi Furukawa*[1,3], *Takaki Maeda*[4], *Sotaro Shimada*[5], *Akio Nakai*[6] and *Shu Morioka*[1,2]

[1] Neurorehabilitation Research Center, Kio University, Kitakatsuragi-gun, Japan, [2] Graduate School of Health Science, Kio University, Kitakatsuragi-gun, Japan, [3] Faculty of Nursing, University of Hyogo, Akashi, Japan, [4] Department of Neuropsychiatry, Keio University School of Medicine, Tokyo, Japan, [5] Department of Electronics and Bioinformatics School of Science and Technology, Meiji University, Kawasaki, Japan, [6] Graduate School of Clinical Education & The Center for the Study of Child Development, Institute for Education, Mukogawa Women's University, Nishinomiya, Japan

OPEN ACCESS

Edited by:
Jean-Pierre Sao-Ming Lin, Guy's and St Thomas' NHS Foundation Trust, United Kingdom

Reviewed by:
Tai-Heng Chen, Kaohsiung Medical University, Taiwan
Francesca Felicia Operto, University of Salerno, Italy

***Correspondence:**
Satoshi Nobusako
s.nobusako@kio.ac.jp

Specialty section:
This article was submitted to Pediatric Neurology, a section of the journal Frontiers in Neurology

Received: 12 January 2021
Accepted: 08 March 2021
Published: 30 March 2021

Citation:
Nobusako S, Osumi M, Matsuo A, Furukawa E, Maeda T, Shimada S, Nakai A and Morioka S (2021) Influence of Stochastic Resonance on Manual Dexterity in Children With Developmental Coordination Disorder: A Double-Blind Interventional Study. Front. Neurol. 12:626608. doi: 10.3389/fneur.2021.626608

Background: There is increasing evidence that the stochastic resonance (SR) phenomenon provided by subthreshold mechanical noise stimulation improves the sensory-motor system. However, the effect of SR on children with developmental coordination disorder (DCD) is unclear. The purpose of this study was to assess whether SR activated by subthreshold vibrotactile noise stimulation of the wrist influences manual dexterity in children with DCD.

Methods: A double-blind interventional study was conducted. Participants were 30 children (age: 9.3 ± 1.44 years, range 6–11 years; 27 male, three female; 25 right-handed, five left-handed) meeting DCD diagnostic criteria in DSM-5. The manual dexterity test was administered the day before SR intervention (baseline-data). SR was elicited using subthreshold vibrotactile noise stimulation at 60% of the vibrotactile threshold measured at the wrist. SR was delivered two times and the manual dexterity test was administered during each SR stimulation block (SR-on condition) and after each SR stimulation block (SR-off), for a total of four measurements. Target outcomes were the component score, the standard score, and the percentile score of the manual dexterity test.

Results: The manual dexterity test scores in the SR-on condition were significantly improved compared to scores at the baseline and in the SR-off condition ($p < 0.001$).

Conclusions: The present study showed that subthreshold noise stimulation eliciting SR significantly improved manual dexterity outcomes in children with DCD during stimulation but not after stimulation. Future studies will need to investigate the carry-over effects of SR stimulation.

Keywords: children, developmental coordination disorder, double-blind study, manual dexterity, stochastic resonance, subthreshold vibrotactile noise stimulation

INTRODUCTION

Developmental coordination disorder (DCD) is characterized by clumsiness in fine (hand writing and shoelace tying) and gross (playing sport and getting dressed) motor skills and affects ∼5–6% of school-aged children, making it the most common childhood movement disorder (1, 2). DCD in children not only affects daily life performance, but also has psychological implications such as reduced self-esteem and increased risk of anxiety and depression (3–5). In 50–70% of children with DCD, motor difficulties persist through adolescence and adulthood (1, 2). Therefore, motor difficulties are an important concern and the development of effective intervention is an urgent issue.

Subthreshold mechanical noise stimulation to the body is known to improve the sensory-motor system. This improvement is related to the stochastic resonance (SR) phenomenon, also known as "noise benefit," that can occur in various sensory and motor systems (6). For example, SR has been shown to improve tactile sensitivity (7, 8). In addition, previous studies have demonstrated improvements in balance, walking, and hand movements due to SR elicited by vibrotactile noise stimulation (9–11). These kinds of improvements were observed not only in healthy participants but also in patients with diabetes, stroke, and Parkinson's disease, and in children with cerebral palsy (7–10, 12, 13).

One case study reported the effect of SR on a child with DCD (14). This study showed that the manual dexterity test score during SR was significantly improved compared to the score obtained without SR, suggesting that stimulation eliciting SR could be effective for children with DCD. However, the study was a case study and further investigation is needed to address the possible effect of SR on clumsiness in children with DCD. In this study we addressed the influence of SR on manual dexterity in children with DCD. We used a block design with / without SR in a double-blind intervention study, with both children and evaluators blinded to the SR condition.

MATERIALS AND METHODS

Participants

Children were enrolled in regular classes at public primary schools in Osaka, Japan, and were recruited from the pool of children who were requested physical assessment and physical therapy due to clumsiness by their teachers or parents. Participants met the four DCD diagnostic criteria (A–D) in the Diagnostic and statistical manual of mental disorders 5th edition (DSM-5) (1): (A) Less than the 16th percentile in the Movement Assessment Battery for Children-2nd Edition (M-ABC2); (B) Less than the cut-off point of the Japanese version of the Developmental Coordination Disorder Questionnaire (DCDQ) (15), (C) Onset of symptoms early in development, and (D) No diagnosis of a general medical condition (e.g., cerebral palsy, hemiplegia, and muscular dystrophy), visual impairment, or intellectual disability (1). Eligibility was assessed by combining interviews to parents and the results of regular assessments provided by the school's doctor. Based on these four criteria, 30 children with DCD were selected (mean age ± standard deviation (SD): 9.3 ± 1.44 years; age range: 6–11 years; 27 male, three female; 25 right-handed, five left-handed). Although it was not an exclusion criterion, none of the children who participated in this study had a diagnosis of other developmental disorders (e.g., autism spectrum disorder, attention deficit hyperactivity disorder, and learning disorder). **Table 1** shows the information of participated children collected the day before the SR intervention in this study (**Table 1**).

The experimental procedures were approved by the ethics committee of the Graduate School and Faculty of Health Sciences at Kio University (approval number: R1-22). There were no potential risks for study participants. No personal identification information was collected. Children and their parents and caregivers were given detailed explanation of the study and parents/caregivers provided written informed consent for participation of their children in the study and for publication of the study results. The experimental procedures were compliant with the ethical standards of the 1964 Declaration of Helsinki regarding the treatment of human participants in research.

Procedures

Figure 1 shows the experimental protocol. The study was a double-blind intervention study with block design. Experiments were conducted in the prescribed rooms at each primary school and were organized in two separate sessions in two subsequent days per each participant. On the first day, the M-ABC2 and other measurements (DCDQ, the Social Communication Questionnaire: SCQ, the Attention-Deficit Hyperactivity Disorder-Rating Scale: ADHD-RS, and the Depression Self-Rating Scale for Children: DSRS-C) were taken as the baseline-data. On the 2nd day, SR was delivered two times and the manual dexterity tests were administered during each SR stimulation block (SR-on condition) and after each SR stimulation block (SR-off), for a total of four measurements. To mitigate possible learning effects in the manual dexterity test, the participants were divided into two groups (A and B) according to their order of enrollment. Fifteen children (those with odd progressive number) were administered the manual dexterity test in the following order: SR-on, SR-off, SR-on, and SR-off conditions (Group A; age: 9.3 ± 1.39 years; range: 7–11 years; 13 male, two female; 12 right-handed, three left-handed). The remaining 15 children (those with even progressive numbers) were administered the manual dexterity test in the following order: SR-off, SR-on, SR-off, and SR-on conditions (Group B; age: 9.3 ± 1.48 years; range: 6–11 years; 14 male, one female; 13 right-handed, two left-handed). Participants and evaluators performing the manual dexterity test were blinded about the group participants were assigned to and were not aware of the SR-on and SR-off conditions. There were no significant differences in age ($Z = -0.064$, $p = 0.967$), sex [$\chi 2 = 0.370$, $\chi 2_{(0.95)} = 3.841$, $p = 0.543$], or preferred hand [$\chi 2 = 0.240$, $\chi 2_{(0.95)} = 3.841$, $p = 0.624$] between Group A and Group B.

TABLE 1 | Results of tests conducted on the day before the current study (Baseline-data).

No.	Group	Age (years)	Sex	Preferred hand	M-ABC2												DCDQ				SCQ	ADHD-RS (%)	DSRS-C
					MD Component score	MD Standard score	MD Percentile score	A&C Component score	A&C Standard score	A&C Percentile score	Balance Component score	Balance Standard score	Balance Percentile score	Total Component score	Total Standard score	Total Percentile score	Control during movement	Fine motor and handwriting	General coordination	Total score			
1	A	11	M	R	12	3	1	7	2	0.5	12	3	1	31	2	0.5	8	4	5	17	15	89	5
2	B	10	M	R	21	6	9	13	6	9	28	9	37	62	6	9	24	8	21	53	6	50	7
3	A	7	M	L	15	4	2	8	2	0.5	13	4	2	36	2	0.5	8	6	5	19	19	95	9
4	B	10	M	R	17	5	5	17	9	37	22	6	9	56	5	5	11	7	9	27	26	93	10
5	A	10	M	R	16	5	5	17	9	37	22	6	9	56	5	5	10	9	10	29	20	91	13
6	B	8	M	R	19	6	9	14	7	16	29	9	37	62	6	9	20	7	19	46	4	80	8
7	A	9	M	R	16	5	5	16	8	25	28	9	37	60	6	9	18	8	20	46	5	75	10
8	B	10	M	R	32	11	63	12	5	5	16	5	5	60	6	9	14	8	7	29	9	87	3
9	A	8	M	R	18	5	5	10	4	2	16	5	5	44	4	2	11	7	11	29	10	25	8
10	B	11	M	R	19	6	9	10	4	2	11	3	1	40	3	1	17	12	12	41	14	80	3
11	A	11	M	R	19	6	9	10	4	2	11	3	1	40	3	1	18	8	15	41	9	50	6
12	B	7	M	R	24	8	25	8	2	0.5	25	8	25	57	6	9	9	16	13	38	5	50	9
13	A	10	M	R	26	9	37	10	4	2	25	8	25	61	6	9	12	11	7	30	17	97	16
14	B	8	M	L	21	6	9	11	5	5	30	9	37	62	6	9	15	8	8	31	25	99	13
15	A	9	M	L	19	6	9	13	4	2	29	9	37	61	6	9	18	9	9	36	22	97	15
16	B	10	M	R	27	9	37	14	7	16	20	6	9	61	6	9	16	11	14	41	9	50	3
17	A	8	F	R	14	4	2	7	2	0.5	10	2	0.5	31	2	0.5	11	11	11	33	1	50	3
18	B	9	M	R	21	6	9	11	5	5	15	5	5	47	4	2	15	7	16	38	4	89	5
19	A	8	M	R	21	6	9	11	5	5	15	5	5	47	4	2	12	8	15	35	6	91	7
20	B	11	M	R	21	6	9	12	5	5	25	8	25	58	6	9	13	16	13	42	9	50	12
21	A	11	F	R	6	2	0.5	9	3	1	9	2	0.5	24	1	0.1	10	12	11	33	4	94	7
22	B	6	M	L	10	3	1	19	10	50	19	6	9	48	4	2	13	6	7	26	2	95	1
23	A	7	M	L	10	3	1	19	10	50	19	6	9	48	4	2	12	4	7	23	10	98	4
24	B	10	M	R	20	6	9	15	8	25	27	8	25	62	6	9	18	12	15	45	2	25	8
25	A	9	M	R	20	6	9	18	9	37	22	6	9	60	6	9	20	17	14	51	1	50	8
26	B	8	M	R	19	6	9	8	2	0.5	28	9	37	55	5	5	12	4	8	24	16	80	4
27	A	11	M	R	20	6	9	11	3	1	10	2	0.5	41	3	1	13	14	10	37	7	98	22
28	B	10	F	R	7	2	0.5	10	4	2	9	2	0.5	26	1	0.1	8	7	11	26	16	92	10
29	A	10	M	R	14	4	2	12	5	5	23	7	16	49	4	2	18	8	9	35	1	80	7
30	B	11	M	R	19	6	9	14	7	16	29	9	37	62	6	9	21	9	11	41	4	84	6
Mean		9.3	M,	R,	18.1	5.5	10.6	12.2	5.3	12.2	19.9	6.0	15.2	50.2	4.5	5.0	14.2	9.1	11.4	34.7	9.9	76.1	8.1
SD		1.4	$n = 27$	$n = 25$	5.5	2.0	13.2	3.4	2.5	15.2	7.0	2.4	14.1	11.7	1.6	3.7	4.2	3.4	4.1	8.9	7.3	22.3	4.5
Range		6–11	F,	L,	6–32	2–11	1–63	7–19	2–10	1–50	9–30	2–9	1–37	24–62	1–6	0.1–9	8–24	4–17	5–21	17–53	1–26	25–99	1–22
Skewness		−0.47	$n = 3$	$n = 5$	−0.07	0.51	2.57	0.45	0.39	1.32	−0.14	−0.25	0.55	−0.76	−0.68	0.02	0.39	0.69	0.57	0.04	0.67	−0.90	1.03
Kurtosis		−0.78			0.74	1.14	7.99	−0.64	−0.92	0.72	−1.44	−1.22	−1.35	−0.51	−0.72	−1.92	−0.62	0.09	−0.09	−0.49	−0.53	−0.35	1.75

No., Reception number. The odd number of reception numbers was divided into Group A, and the even number was divided into Group B. M, Male; F, Female; R, Right; L, Left; M-ABC2, the Movement Assessment Battery for Children-2nd Edition; MD, Manual Dexterity; A&C, Aiming & Catching; DCDQ, the Developmental Coordination Disorder Questionnaire; SCQ, the Social Communication Questionnaire; ADHD-RS, the Attention-Deficit Hyperactivity Disorder-Rating Scale; DSRS-C, the Depression Self-Rating Scale for Children; SD, Standard Deviation.

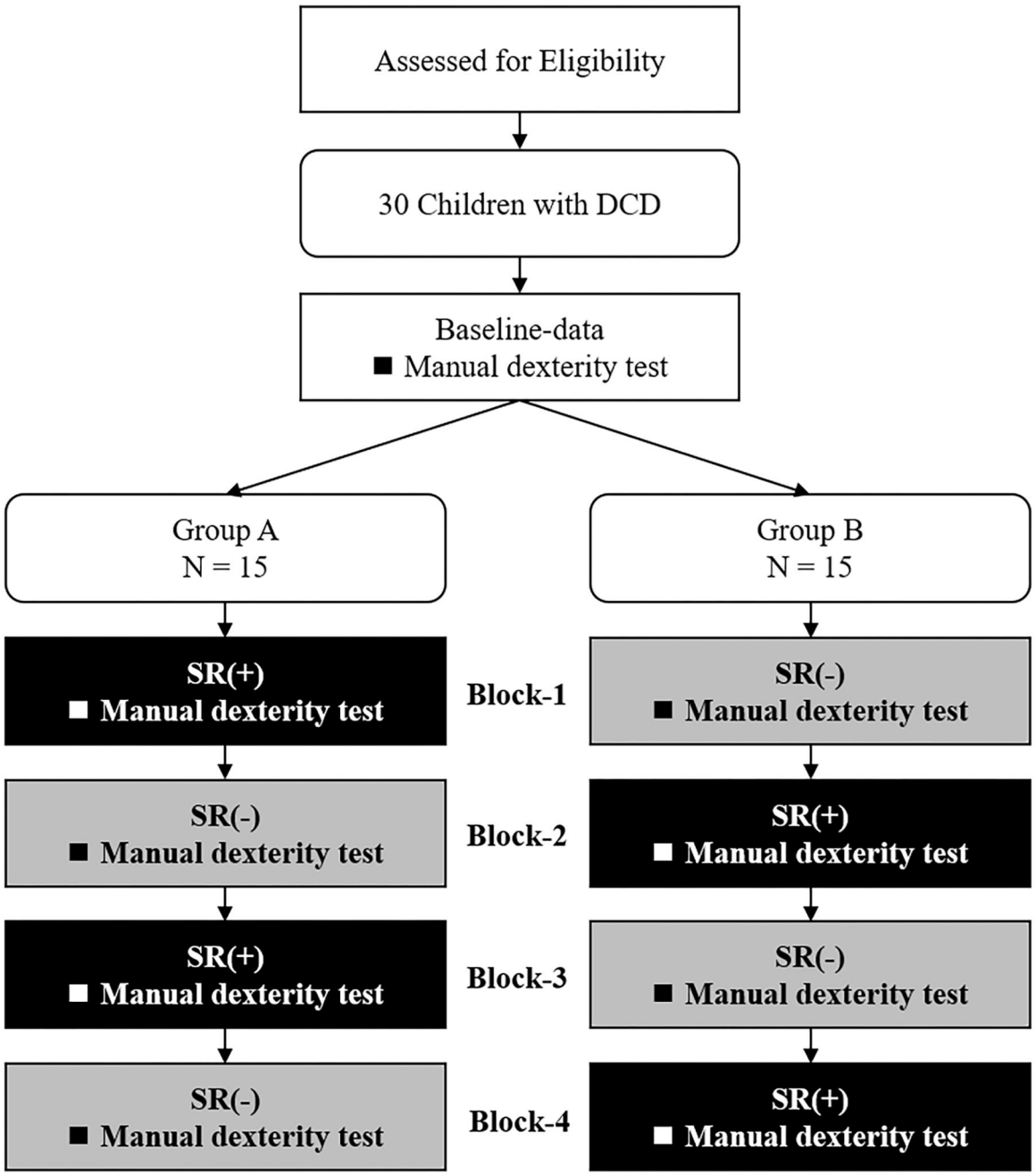

FIGURE 1 | Current experimental protocol. DCD, developmental coordination disorder; SR(+), stochastic resonance-on condition; SR(-), stochastic resonance-off condition.

Stochastic Resonance Intervention: Subthreshold Vibrotactile Noise Stimulation

To elicit SR, subthreshold vibrotactile noise stimulation was applied using four compact devices (length: 10 mm; width: 18 mm; height: 2 mm; Vibration Actuator Sprinter α; Nidec Seimitsu, Nagano, Japan) attached to the volar and dorsal areas of children's right and left wrists using contact tape (i.e., two devices on the right wrist and two devices on the left wrist). The resonance frequency of the device was 170 ± 10 Hz (average ± SD). Low-pass filters at 500 Hz were used as per previous studies (7, 8, 10, 11, 14, 16, 17). A digital amplifier (FX Audio D802; North Flat Japan, Osaka, Japan) was used to output the white noise signals needed to elicit SR through the vibrotactile actuators. Consistent with previous studies (7, 8, 10, 11, 14, 16, 17), we attached the device to the wrist to minimize manual

TABLE 2 | Comparisons of baseline data between Groups A and B.

Group		Age (years)	Sex	Preferred hand	M-ABC2				DCDQ				SCQ	ADHD-RS	DSRS-C
					Manual dexterity	Aiming and catching	Balance	Total	Control during movement	Fine motor and handwriting	General coordination	Total			
A	Mean	9.3	M, $n = 13$ F, $n = 2$	R, $n = 12$ L, $n = 3$	7.0	11.4	10.5	3.5	13.3	9.1	10.6	32.9	9.8	78.7	9.3
	SD	1.39			8.65	16.32	12.29	3.50	3.89	3.40	3.95	8.88	6.97	22.65	4.96
B	Mean	9.3	M, $n = 14$ F, $n = 1$	R, $n = 13$ L, $n = 2$	14.2	12.9	19.9	6.4	15.1	9.2	12.3	36.5	10.1	73.6	6.8
	SD	1.48			15.72	14.01	14.32	3.39	4.28	3.39	4.11	8.50	7.52	21.69	3.49
	P-value	0.967	0.543	0.624	0.067	0.267	0.074	0.050	0.250	0.918	0.283	0.283	0.967	0.345	0.129

The M-ABC2 and ADHD-RS scores are percentile score.

ADHD-RS, Attention-Deficit Hyperactivity Disorder-Rating Scale; DCDQ, Developmental Coordination Disorder Questionnaire; DSRS-C, Depression Self-Rating Scale for Children; F, Female; L, Left; M, Male; M-ABC2, Movement Assessment Battery for Children-2nd Edition; R, Right; SCQ, Social Communication Questionnaire; SD, Standard Deviation.

interruption while affecting the tactile sensation of the fingers. The intensity of the vibrotactile noise was set to 60% of the vibrotactile threshold at the beginning of the test—a level shown to be optimum to elicit SR in sensory systems (7, 8, 10, 11, 14, 16, 17). The sensory thresholds for vibrotactile noise were measured immediately before each of the four measurement blocks, irrespective of whether it was an SR-on or SR-off condition. The vibrotactile noise device remained attached throughout testing and it was turned on and off at the beginning and at the end of each block to implement the SR-on/SR-off conditions. Control over the SR-on/SR-off condition was given to an experimenter different than the one who administered the manual dexterity test. Children were blinded to the condition as they could not feel the subthreshold noise stimuli and were not informed about the SR-on/SR-off conditions.

Outcome: Manual Dexterity Test

The manual dexterity test of the M-ABC2 is a standardized, age-adjusted test to evaluate the DCD diagnostic criterion A of DSM-5 (18). This test has good test-retest reliability (minimum value at any age is 0.75), good inter-rater reliability (0.70), and good concurrent validity (18). This test has three age bands: 3–6 years (age band 1), 7–10 years (age band 2), and 11–16 years (age band 3). In the current study, each child received three subtests that were appropriate for his/her age band. Children in the age band 1 (3–6 years) were evaluated by the posting coins test, threading beads test, and drawing trail I test. The age band 1 test was performed by 0 participants in Group A and 1 participant in Group B. Children in the age band 2 (7–10 years) were evaluated by the placing pegs test, threading lace test, and drawing trail II test. The age band 2 test was administered to 11 participants in Group A and 11 participants in Group B. Children in the age band 3 (11–16 years) were evaluated by the turning pegs test, triangle with nuts and bolts test, and drawing trail III test. The age band 3 test was completed by four participants in Group A and three participants in Group B. The manual dexterity test was conducted twice in each block, with a total of 8 tests for each child throughout the experiment. The component score, standard score, and percentile score were then calculated from the obtained raw scores. An increase in the component score, standard score, and percentile score suggest an improvement in manual dexterity. The manual dexterity test was administered by a specifically trained, certified physical therapist who was blinded to the SR-on and SR-off conditions.

Statistical Analysis

The baseline data (age, sex, preferred hand, and M-ABC2, DCDQ, SCQ, ADHD-RS, and DSRS-C scores) were compared statistically between Groups A and B. Sex and preferred hand were compared between Groups A and B using the chi-square test for independence. According to the Shapiro-Wilk test, age, all percentile scores of M-ABC2, the control during movement of DCDQ, SCQ, and ADHD-RS scores were not normally distributed, so they were compared between Groups A and B using the Mann-Whitney U test. The DCDQ fine motor and handwriting, general coordination, and total scores, as well as the DSRS-C score, were normally distributed according to the

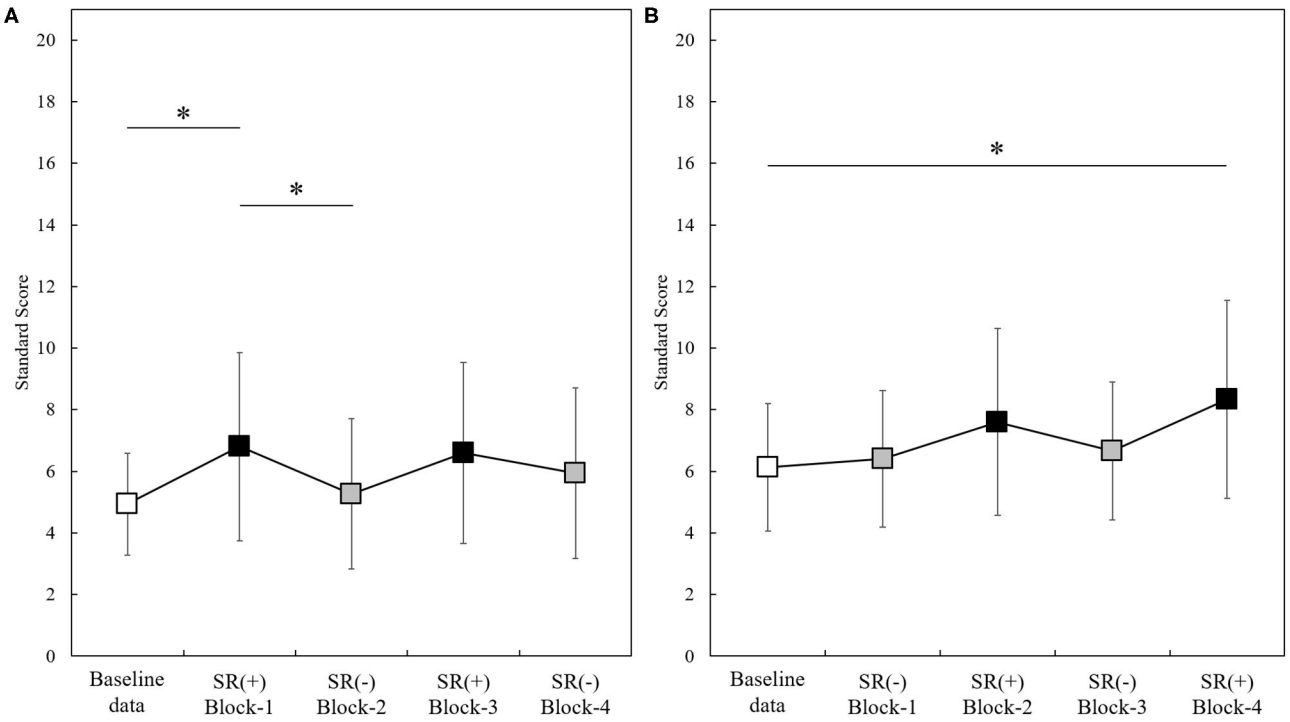

FIGURE 2 | Standard scores measured through the experiment in the two groups (Group A, $N = 15$; Group B, $N = 15$). Baseline-data (white squares); SR(+): SR-on condition (black squares); SR(-): SR-off condition (gray squares). *$p < 0.05$. Panel **(A)**: Standard scores (mean ± standard deviation) in Group A ($N = 15$). Panel **(B)**: Standard scores (mean ± standard deviation) in Group B ($N = 15$).

Shapiro-Wilk test, and were compared between Groups A and B using an independent samples *t*-test.

The results of the manual dexterity test scores (component score, standard score, and percentile score) measured throughout the experiment (baseline-data, Block-1,−2,−3,−4) were compared in each of the two groups (Group A, $N = 15$; Group B, $N = 15$). The Shapiro-Wilk test showed that Group A component scores and standard scores and Group B component scores were normally distributed. Repeated measures one-way analysis of variance (ANOVA) was used to analyze these scores measured throughout the experiment (baseline-data, Block-1,−2,−3,−4). Multiple comparisons in *post-hoc* analyses were performed using paired *t*-tests. Group A percentile scores and Group B standard scores and percentile scores measured throughout the experiment (baseline-data, Block-1,−2,−3,−4) were compared using the Friedman test because those data were not normally distributed as shown by the Shapiro-Wilk test, and the Wilcoxon signed-rank test was used for multiple comparisons in *post-hoc* analyses.

The results of the manual dexterity test (component score, standard score, and percentile score) were compared considering the baseline-data, SR-on condition (scores averaged over the two blocks), and SR-off condition (scores averaged over the two blocks) in the whole group ($N = 30$). Since component scores were normally distributed as shown by the Shapiro-Wilk test, they were compared using repeated measures one-way ANOVA and *post-hoc* multiple comparisons were performed using paired *t*-tests. The standard scores and percentile scores were not normally distributed as shown by the Shapiro-Wilk test, they were compared using the Friedman test and *post-hoc* multiple comparisons were performed using the Wilcoxon signed-rank test.

The significance level was set at $\alpha = 0.05$ for all statistical analyses, and the Bonferroni correction was used to adjust for multiple comparisons in *post-hoc* analyses. The effect size was calculated. All statistical analyses were performed using SPSS, version 24 (SPSS, Chicago, IL, USA).

RESULTS

Table 2 shows the results of the comparisons of baseline data between Groups A and B. There were no differences in age ($Z = -0.064$, $p = 0.967$), sex [$\chi^2 = 0.370$, $\chi^2_{(0.95)} = 3.841$, $p = 0.543$], and preferred hand [$\chi^2 = 0.240$, $\chi^2_{(0.95)} = 3.841$, $p = 0.624$] between Groups A and B. There were no differences in the M-ABC2 scores between Groups A and B (Manual dexterity: $Z = -1.952$, $p = 0.067$; Aiming and catching: $Z = -1.154$, $p = 0.267$; Balance: $Z = -1.809$, $p = 0.074$; Total: $Z = -2.045$, $p = 0.050$), but they tended to be slightly higher in Group B. There were no differences in the scores for DCDQ (Control during movement: $Z = -1.188$, $p = 0.250$; Fine motor and handwriting: $t = -0.104$, $p = 0.918$; General coordination: $t = -1.095$, $p = 0.283$; Total: $t = -1.096$, $p = 0.283$), SCQ ($Z = -0.062$, $p = 0.967$), ADHD-RS

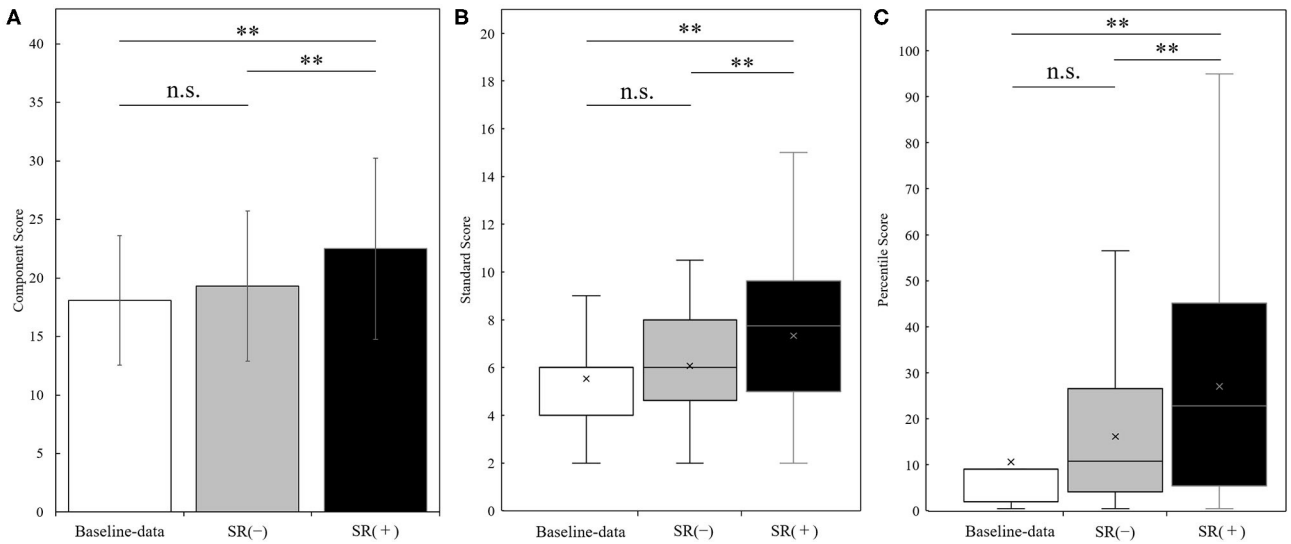

FIGURE 3 | Results of the manual dexterity test (panel **A**: component score; panel **B**: standard score; panel **C**: percentile score) measured at the baseline-data, in the SR-off conditions (SR(-)), and the SR-on conditions (SR(+)) ($N = 30$). Results of the manual dexterity test (Panel **A**: component score, mean ± standard deviation; panel **B**: standard score, boxplot; panel **C**: percentile score, boxplot) in the baseline-data (white bars), the SR-off conditions (SR(-), gray bars), and the SR-on conditions (SR(+), black bars). $^{**}p < 0.001$; n.s. = not significant.

($Z = -0.983$, $p = 0.345$), and DSRS-C ($t = 1.563$, $p = 0.129$) between Groups A and B.

All participants ($N = 30$) completed the current experimental protocol.

Statistical analysis showed that the changes in component scores observed in Group A and B throughout the experiment were statistically significant [Group A: $F_{(4, 56)} = 8.156$, $p < 0.001$; Group B: $F_{(4, 56)} = 8.575$, $p < 0.001$]. *Post-hoc* analysis showed that the component scores of Group A in Block-1 (SR-on condition) and Block-3 (SR-on condition) were significantly higher than in the baseline-data and Block-2 (SR-off condition) (Block-1 vs. baseline-data, $p = 0.023$; Block-1 vs. Block-2, $p = 0.003$; Block-3 vs. baseline-data, $p = 0.038$; Block-3 vs. Block-2, $p = 0.027$; all with after Bonferroni correction). In Group B, the component scores in Block-2 (SR-on condition) were significantly higher than the baseline-data ($p = 0.008$; after Bonferroni correction), and the component scores measured in Block-4 (SR-on condition) were significantly higher than the those measured at the baseline-data and in Block-1 (SR-off condition)(Block-4 vs. baseline-data, $p = 0.001$; Block-4 vs. Block-1, $p = 0.036$; after Bonferroni correction).

Figure 2 shows the change standard scores for Group A ($N = 15$) and Group B ($N = 15$) throughout the experiment (baseline-data,−1,−2,−3,−4). The change in standard scores in Group A and B observed throughout the experiment (baseline-data, Block-1,−2,−3,−4) were statistically significant [Group A: $F_{(4,56)} = 7.204$, $p < 0.001$; Group B: $p < 0.001$]. *Post-hoc* analysis showed that the standard scores measured in Group A in Block-1 (SR-on condition) were significantly higher than those at the baseline-data and those in Block-2 (SR-off condition) (Block-1 vs. baseline-data, $p = 0.040$; Block-1 vs. Block-2, $p = 0.015$; all Bonferroni-corrected) (**Figure 2A**). Standard scores measured in Group B in Block-4 (SR-on condition) were significantly higher than baseline-data ($p = 0.020$; after Bonferroni correction) (**Figure 2B**).

The change in percentile scores in Group A and B observed throughout the experiment (baseline-data, Block-1,−2,−3,−4) was significant (Group A: $p < 0.001$; Group B: $p < 0.001$). *Post-hoc* analysis showed that percentile scores measured in Group A in Block-1 (SR-on condition) were significantly higher than in Block-2 (SR-off condition) ($p = 0.048$; after Bonferroni correction), and that percentile scores measured in Group B in Block-4 (SR-on condition) were significantly higher than those from baseline-data ($p = 0.022$; after Bonferroni correction).

Figure 3 shows the results of manual dexterity test (component score, standard score, and percentile score) in the baseline-data, SR-on condition (averaged over two blocks), and SR-off condition (averaged over two blocks) in the whole sample ($N = 30$). There was a significant change in component score in the three conditions as shown by repeated measures one-way ANOVA between three conditions [$F_{(2, 58)} = 25.385$, $p < 0.001$]. *Post-hoc* analysis showed that the component score in the SR-on condition was significantly higher than in the baseline-data and SR-off conditions (SR-on vs. baseline-data, $t_{(29)} = -6.196$, $p < 0.001$, effect size (r) = 0.75; SR-on vs. SR-off, $t_{(29)} = -5.689$, $p < 0.001$, effect size (r) = 0.73; all after Bonferroni correction). No statistically significant difference in component score between baseline-data and SR-off condition was observed [$t_{(29)} = -1.892$, $p = 0.205$, after Bonferroni correction, effect size (r) = 0.33] (**Figure 3A**).

There was a significant change in standard score in the three conditions as shown by the Friedman test ($p < 0.001$). *Post-hoc* analysis showed that the standard score in the SR-on

condition was significantly higher than the standard score in the baseline-data and SR-off condition (SR-on vs. baseline-data, $z = -4.116$, $p < 0.001$, effect size (r) $= -0.75$; SR-on vs. SR-off, $z = -3.693$, $p < 0.001$, effect size (r) $= -0.67$; all after Bonferroni correction). No significant difference in standard score between baseline-data and SR-off condition was observed ($z = -1.873$, $p = 0.183$, after Bonferroni correction, effect size (r) $= -0.34$) (**Figure 3B**).

There was a significant change in percentile score in the three conditions as shown by the Friedman test ($p < 0.001$). *Post-hoc* analysis showed that the percentile score in the SR-on condition was significantly higher than the percentile score in the baseline-data and SR-off condition (SR-on vs. baseline-data, $z = -4.108$, $p < 0.001$, effect size (r) $= -0.75$; SR-on vs. SR-off, $z = -3.667$, $p < 0.001$, effect size (r) $= -0.67$; all after Bonferroni correction). No significant difference in percentile score between baseline-data and SR-off condition was observed ($z = -2.146$, $p = 0.0957$, after Bonferroni correction, effect size (r) $= -0.39$) (**Figure 3C**).

DISCUSSION

The present study showed that manual dexterity under SR-on conditions was significantly improved compared to the baseline-data and to the SR-off conditions. Analysis of test scores throughout the experiment showed that the observed improvement in manual dexterity was not an effect of learning during the experiment but was specifically generated during the SR-on condition.

Hand tactile sensation is a very important factor for accurate and quick manual dexterity (19–22). Previous studies showed that vibrotactile noise stimulation to the wrist with an intensity of 60% of the sensory threshold as used within this study improved fingertip tactility and manual dexterity in the affected limbs of patients with stroke (7, 8, 10). Therefore, the improvement in manual dexterity observed under SR-on condition in the current study may have been due to an improvement in hand tactile sensitivity that is an important component of manual dexterity.

In general, children with DCD have lower ability to effectively use tactile information for movement and have to rely more on visual information (14, 23–25). However, an earlier case study showed that the problem of visual dependence in a child with DCD may be improved as a result of SR stimulation similar to the one used in this study (14). Therefore, the significant improvement in manual dexterity observed during the SR-on condition in the current study may be due both to an increase in tactile sensitivity and a reduction in visual dependence.

In addition, sensory-motor integration is a very important function for manual dexterity in children (26, 27). A previous study showed that the application of SR to healthy young individuals significantly improved sensory-motor integration (17). In addition, one case study showed that SR intervention may improve sensory-motor integration in a child with DCD (14). Therefore, the significant improvement in manual dexterity observed in the SR-on condition may be related to possible improvement in sensory-motor integration.

The advantage of the SR intervention here presented is that children only need to wear a compact SR device and no special efforts are needed to use the device. In the current study, the SR-on and -off conditions were altered and the effects observed during the SR-on conditions were not observed under subsequent SR-off conditions, suggesting that there is no carry-over (retention) effect when switching from SR-on to SR-off. Therefore, future studies will need to investigate the possible influence of the duration of the SR stimulation on carry-over (retention) effects and understand if and under which circumstances the beneficial effects of subthreshold stimulation can be sustained after the end of stimulation. In other words, how long do children with DCD need to wear the device to see a carryover effect? What activities should they perform while they are wearing the device in order to have a carryover effect? These questions need to be clarified. In addition, vibrotactile noise stimulation is non-invasive and unconscious, and the children did not complain of any discomfort (e.g., pain) in this study. However, it is not known whether this stimulation will have a negative effect on the body when it is applied for a long period of time. Future studies are needed to investigate these possible adverse effects. These future studies should help to clarify when clinicians should consider stopping SR administration and the criteria for identifying the inefficacy of SR.

An important limitation of the study is that the children were assigned to two groups according to their order of enrollment, and although there were no significant differences in the baseline data of both groups, they were not completely equal with respect to age and sex. Therefore, in the future, randomized controlled trials should be conducted with larger sample sizes, completely matched for age and sex, and assigned to intervention and no-intervention groups. In addition, the outcome of this study used the M-ABC2, the international standard assessment battery for DCD, but future studies should also use other tools, such as the NEPSY second edition, to assess sensorimotor and visuospatial functions to verify whether manual dexterity improves in the long term.

DATA AVAILABILITY STATEMENT

The raw data supporting the conclusions of this article will be made available by the authors, without undue reservation.

ETHICS STATEMENT

The studies involving human participants were reviewed and approved by The ethics committee of the Graduate School and Faculty of Health Sciences at Kio University (approval number: R1-22). Written informed consent to participate in this study was provided by the participants' legal guardian/next of kin.

AUTHOR CONTRIBUTIONS

SN designed the study, collected and analyzed the data, and wrote the manuscript. MO provided experimental equipment and assisted in collecting data. AN provided evaluation battery and

helped with data analyses. AM, EF, TM, SS, and SM supervised the study. All authors read and approved the manuscript.

FUNDING

This work was supported by JSPS KAKENHI, Grant-in-Aid for Young Scientists (Grant Number 18K17700), JSPS KAKENHI, Grant-in-Aid for Scientific Research (C) (Grant Number 16K09981).

ACKNOWLEDGMENTS

The authors wish to acknowledge and thank the children who participated in this study and their parents and caregivers.

REFERENCES

1. American Psychiatric Association. *Diagnostic and Statistical Manual of Mental Disorders*. 5th edn. Arlington, VA: American Psychiatric Association (2013). doi: 10.1176/appi.books.9780890425596
2. Blank R, Barnett AL, Cairney J, Green D, Kirby A, Polatajko H, et al. International clinical practice recommendations on the definition, diagnosis, assessment, intervention, and psychosocial aspects of developmental coordination disorder. *Dev Med Child Neurol.* (2019) 61:242–85. doi: 10.1111/dmcn.14132
3. Lingam R, Jongmans MJ, Ellis M, Hunt LP, Golding J, Emond A. Mental health difficulties in children with developmental coordination disorder. *Pediatrics.* (2012) 129:e882–91. doi: 10.1542/peds.2011-1556
4. Cairney J, Rigoli D, Piek J. Developmental coordination disorder and internalizing problems in children: the environmental stress hypothesis elaborated. *Dev Rev.* (2013) 33:224–38. doi: 10.1016/j.dr.2013.07.002
5. Missiuna C, Cairney J, Pollock N, Campbell W, Russell DJ, Macdonald K, et al. Psychological distress in children with developmental coordination disorder and attention-deficit hyperactivity disorder. *Res Dev Disabil.* (2014) 35:1198–207. doi: 10.1016/j.ridd.2014.01.007
6. McDonnell MD, Abbott D. What is stochastic resonance? Definitions, misconceptions, debates, and its relevance to biology. *PLoS Comput Biol.* (2009) 5:e1000348. doi: 10.1371/journal.pcbi.1000348
7. Enders LR, Hur P, Johnson MJ, Seo NJ. Remote vibrotactile noise improves light touch sensation in stroke survivors'fingertips via stochastic resonance. *J Neuroeng Rehabil.* (2013) 10:105. doi: 10.1186/1743-0003-10-105
8. Lakshminarayanan K, Lauer AW, Ramakrishnan V, Webster JG, Seo NJ. Application of vibration to wrist and hand skin affects fingertip tactile sensation. *Physiol Rep*. (2015) 3:e12465. doi: 10.14814/phy2.12465
9. Priplata AA, Patritti BL, Niemi JB, Hughes R, Gravelle DC, Lipsitz LA, et al. Noise-enhanced balance control in patients with diabetes and patients with stroke. *Ann Neurol.* (2006) 59:4–12. doi: 10.1002/ana.20670
10. Seo NJ, Kosmopoulos ML, Enders LR, Hur P. Effect of remote sensory noise on hand function post stroke. *Front Hum Neurosci.* (2014) 8:934. doi: 10.3389/fnhum.2014.00934
11. Hur P, Wan YH, Seo NJ. Investigating the role of vibrotactile noise in early response to perturbation. *IEEE Trans Biomed Eng.* (2014) 61:1628–33. doi: 10.1109/TBME.2013.2294672
12. Kaut O, Brenig D, Marek M, Allert N, Wüllner U. Postural stability in Parkinson's disease patients is improved after stochastic resonance therapy. *Parkinsons Dis.* (2016) 2016:7948721. doi: 10.1155/2016/7948721
13. Zarkou A, Lee SCK, Prosser LA, Hwang S, Jeka J. Stochastic resonance stimulation improves balance in children with cerebral palsy: a case control study. *J Neuroeng Rehabil.* (2018) 15:115. doi: 10.1186/s12984-018-0467-7
14. Nobusako S, Osumi M, Matsuo A, Furukawa E, Maeda T, Shimada S, et al. Subthreshold vibrotactile noise stimulation immediately improves manual dexterity in a child with developmental coordination disorder: A single-case study. *Front Neurol.* (2019) 10:717. doi: 10.3389/fneur.2019.00717
15. Nakai A, Miyachi T, Okada R, Tani I, Nakajima S, Onishi M, et al. Evaluation of the Japanese version of the Developmental Coordination Disorder Questionnaire as a screening tool for clumsiness of Japanese children. *Res Dev Disabil.* (2011) 32:1615–22. doi: 10.1016/j.ridd.2011.02.012
16. Seo NJ, Lakshminarayanan K, Bonilha L, Lauer AW, Schmit BD. Effect of imperceptible vibratory noise applied to wrist skin on fingertip touch evoked potentials - an EEG study. *Physiol Rep.* (2015) 3:e12624. doi: 10.14814/phy2.12624
17. Nobusako S, Osumi M, Matsuo A, Fukuchi T, Nakai A, Zama T, et al. Stochastic resonance improves visuomotor temporal integration in healthy young adults. *PLoS ONE.* (2018) 13:e0209382. doi: 10.1371/journal.pone.0209382
18. Henderson SE, Sugden DA, Barnett AL. *Movement Assessment Battery for Children-2*. 2nd edn. United Kingdom: Harcourt Assessment (2007). doi: 10.1037/t55281-000
19. Johansson RS, Westling G. Roles of glabrous skin receptors and sensorimotor memory in automatic control of precision grip when lifting rougher or more slippery objects. *Exp Brain Res.* (1984) 56:550–64. doi: 10.1007/BF00237997
20. Augurelle AS, Smith AM, Lejeune T, Thonnard JL. Importance of cutaneous feedback in maintaining a secure grip during manipulation of hand-held objects. *J Neurophysiol.* (2003) 89:665–71. doi: 10.1152/jn.00249.2002
21. Monzee J, Lamarre Y, Smith AM. The effects of digital anesthesia on force control using a precision grip. *J Neurophysiol.* (2003) 89:672–83. doi: 10.1152/jn.00434.2001
22. Zatsiorsky VM, Latash ML. Prehension synergies. *Exerc Sport Sci Rev*. (2004) 32:75–80. doi: 10.1097/00003677-200404000-00007
23. Deconinck FJ, De Clercq D, Van Coster R, Ooostra A, Dewitte G, Savelsbergh GJ, et al. Sensory contributions to balance in boys with developmental coordination disorder. *Adapt Phys Activ Q.* (2008) 25:17–35. doi: 10.1123/apaq.25.1.17
24. Deconinck FJ, De Clercq D, Savelsbergh GJ, Van Coster R, Oostra A, Dewitte G, et al. Visual contribution to walking in children with Developmental Coordination Disorder. *Child Care Health Dev.* (2006) 32:711–22. doi: 10.1111/j.1365-2214.2006.00685.x
25. Biancotto M, Skabar A, Bulgheroni M, Carrozzi M, Zoia S. Neuromotor deficits in developmental coordination disorder: evidence from a reach-to-grasp task. *Res Dev Disabil.* (2011) 32:1293–300. doi: 10.1016/j.ridd.2011.02.007
26. Nobusako S, Sakai A, Tsujimoto T, Shuto T, Nishi Y, Asano D, et al. Deficits in Visuo-motor temporal integration impacts manual dexterity in probable developmental coordination disorder. *Front Neurol.* (2018) 9:114. doi: 10.3389/fneur.2018.00114
27. Nobusako S, Sakai A, Tsujimoto T, Shuto T, Nishi Y, Asano D, et al. Manual dexterity is a strong predictor of visuo-motor temporal integration in children. *Front Psychol.* (2018) 9:948. doi: 10.3389/fpsyg.2018.00948

Conflict of Interest: The authors declare that the research was conducted in the absence of any commercial or financial relationships that could be construed as a potential conflict of interest.

Copyright © 2021 Nobusako, Osumi, Matsuo, Furukawa, Maeda, Shimada, Nakai and Morioka. This is an open-access article distributed under the terms of the Creative Commons Attribution License (CC BY). The use, distribution or reproduction in other forums is permitted, provided the original author(s) and the copyright owner(s) are credited and that the original publication in this journal is cited, in accordance with accepted academic practice. No use, distribution or reproduction is permitted which does not comply with these terms.

frontiers in Neurology

CLINICAL TRIAL
published: 03 May 2021
doi: 10.3389/fneur.2021.660780

Improvements in Upper Extremity Function Following Intensive Training Are Independent of Corticospinal Tract Organization in Children With Unilateral Spastic Cerebral Palsy: A Clinical Randomized Trial

Kathleen M. Friel[1,2], *Claudio L. Ferre*[1,3], *Marina Brandao*[4], *Hsing-Ching Kuo*[3], *Karen Chin*[1,3], *Ya-Ching Hung*[5], *Maxime T. Robert*[1,2], *Veronique H. Flamand*[3], *Ana Smorenburg*[1,2], *Yannick Bleyenheuft*[6], *Jason B. Carmel*[7], *Talita Campos*[1,3] *and Andrew M. Gordon*[3]*

[1] Burke Neurological Institute, White Plains, NY, United States, [2] Weill Cornell Medicine, New York, NY, United States, [3] Teachers College, Columbia University, New York, NY, United States, [4] Universidade Federal de Minas Gerais, Belo Horizonte, Brazil, [5] Queens College, City University of New York, New York, NY, United States, [6] Université Catholique de Louvain, Brussels, Belgium, [7] Weinberg Family Cerebral Palsy Center, Columbia University Medical Center, New York, NY, United States

OPEN ACCESS

Edited by:
Volker Mall,
Technical University of Munich, Germany

Reviewed by:
Martin Staudt,
Schön Klinik, Germany
Maurizio Elia,
Oasi Research Institute (IRCCS), Italy

***Correspondence:**
Andrew M. Gordon
ag275@columbia.edu

Specialty section:
This article was submitted to Pediatric Neurology, a section of the journal Frontiers in Neurology

Received: 29 January 2021
Accepted: 06 April 2021
Published: 03 May 2021

Citation:
Friel KM, Ferre CL, Brandao M, Kuo H-C, Chin K, Hung Y-C, Robert MT, Flamand VH, Smorenburg A, Bleyenheuft Y, Carmel JB, Campos T and Gordon AM (2021) Improvements in Upper Extremity Function Following Intensive Training Are Independent of Corticospinal Tract Organization in Children With Unilateral Spastic Cerebral Palsy: A Clinical Randomized Trial. Front. Neurol. 12:660780. doi: 10.3389/fneur.2021.660780

Background/Objectives: Intensive training of the more affected upper extremity (UE) has been shown to be effective for children with unilateral spastic cerebral palsy (USCP). Two types of UE training have been particularly successful: Constraint-Induced Movement Therapy (CIMT) and Bimanual training. Reorganization of the corticospinal tract (CST) early during development often occurs in USCP. Prior studies have suggested that children with an ipsilateral CST controlling the affected UE may improve less following CIMT than children with a contralateral CST. We tested the hypothesis that improvements in UE function after intensive training depend on CST laterality.

Study Participants and Setting: Eighty-two children with USCP, age 5 years 10 months to 17 years, University laboratory setting.

Materials/Methods: Single-pulse transcranial magnetic stimulation (TMS) was used to determine each child's CST connectivity pattern. Children were stratified by age, sex, baseline hand function and CST connectivity pattern, and randomized to receive either CIMT or Bimanual training, each of which were provided in a day-camp setting (90 h). Hand function was tested before, immediately and 6 months after the intervention with the Jebsen-Taylor Test of Hand Function, the Assisting Hand Assessment, the Box and Block Test, and ABILHAND-Kids. The Canadian Occupational Performance Measure was used to track goal achievement and the Pediatric Evaluation of Disability Inventory was used to assess functioning in daily living activities at home.

Results: In contrast to our hypothesis, participants had statistically similar improvements for both CIMT and Bimanual training for all measures independent of their CST connectivity pattern (contralateral, ipsilateral, or bilateral) ($p < 0.05$ in all cases).

Conclusions/Significance: The efficacy of CIMT and Bimanual training is independent of CST connectivity pattern. Children with an ipsilateral CST, previously thought to be maladaptive, have the capacity to improve as well as children with a contralateral or bilateral CST following intensive CIMT or Bimanual training.

Clinical Trial Registration: www.ClinicalTrials.gov, identifier NCT02918890.

Keywords: hemiplegia, transcramial magnetic stimulation, Hand-Arm Bimanual Intensive Therapy (HABIT), rehabilitation, constraint-induced movement therapy (CIMT), brain reorganization, neuroplasicity, physical rehabilitation

INTRODUCTION

Unilateral spastic cerebral palsy (USCP) is characterized by sensorimotor deficits, particularly upper extremity (UE) impairments mainly on one side of the body. In the past decade, the evidence base for effective therapies has expanded considerably (1). The best available therapies for UE impairments in children with USCP involve intensive, skill-based motor training (2–7). Despite the general efficacy of these intensive interventions, there is considerable individual variability in responsiveness (8–10). The high costs and time associated with intensive therapy highlight the need for a greater understanding of neurophysiological mechanisms that may mediate functional recovery and can be targeted to optimize interventions.

One potential key determinant to how children respond to UE therapies is developmental adaptation of the motor system following early brain injury. The principal pathway for control of skilled UE movements is the corticospinal tract (CST) (11). During typical development, early bilateral projections of the CST are pruned leading to a predominantly contralateral system (12). In the context of a perinatal injury, there is often a loss of direct projections of the CST from the injured motor cortex to contralateral spinal cord motor circuits (13). Depending on the timing and size of injury, there may be an aberrant reorganization of the motor system in which the uncrossed (i.e., ipsilateral) projections from the non-lesioned hemisphere retain control of the affected hand (14). These ipsilateral connections, found in more than half of children with USCP, have been considered to be "maladaptive" (15, 16), and those who retain contralateral projections have better hand function than those who do not [e.g., (10, 17–19)]. However, there is growing evidence that ipsilateral pathways have the capacity to support substantial motor function (20, 21). The ipsilateral motor map can contain an abundance of distal UE representations and are plastic (10, 21, 22). In fact, greater relative overlap of the affected and less affected hand representation within the contralesional hemisphere has been shown to be associated with better hand function (23). This suggests that overlapping representations might be adaptively "yoked," with cortical control of the child's less affected hand supporting that of the affected hand.

Two types of training have been shown to be among the most efficacious approaches to improving UE function (1). Constraint-induced movement therapy involves restraint of the less affected UE and intensive unimanual practice with the more affected UE [e.g., (24)]. Bimanual training involves provision of tasks that necessitate or instruct use of both UE with the more affected UE generally used as an assist (25). Both approaches have been found to result in similar efficacy for most clinical outcomes [e.g., (2, 26–30)]. However, the heterogeneity in children with UCSP described above raises important questions about the relation between CST pathway reorganization and treatment outcome. Studies of CIMT have suggested that children with ipsilateral control of the affected UE show markedly reduced improvements in movement speed (16) and cortical excitability (31) compared to children with a contralateral CST, possibly due to the absence of typical interhemispheric inhibition and/or a potential hemispheric dissociation of affected hand representations in the primary motor cortex and somatosensory cortex in these children (16, 31–33). In contrast, we have shown that improvements in skill and increases in motor maps occur independently of CST laterality following bimanual training (10, 21). Thus, CST laterality (especially ipsilateral reorganization) may predict outcomes, depending on whether the training is unimanual or bimanual. Despite the growing awareness of CST laterality as a potential biomarker of recovery, its relation to CIMT and bimanual training, two approaches with high levels of evidence for improving motor function in children with USCP (1), has not been formally tested in a large-sample prospective trial.

In the present study we tested the hypothesis that improvements in UE function following either CIMT or bimanual training depend on CST laterality and type of training (unimanual vs. bimanual) in children with USCP. In particular, we predict that whereas children with a maintained contralateral CST will respond equally to CIMT and bimanual training, children with ipsilateral CST laterality will be less responsive to CIMT than bimanual training. We tested our hypothesis in a randomized clinical trial in which children were randomized to receive either 90 h of CIMT or Hand-Arm Bimanual Intensive Training (HABIT).

METHODS

All study procedures were approved by the Institutional Review Boards of Teachers College, Columbia University, where the treatments were conducted, the Burke Neurological Institute, where TMS evaluations were performed, and Weill Cornell Medicine, where magnetic resonance imaging (MRI) was performed. Children and their caregivers provided written informed assent and consent.

Participants

Demographics and clinical characteristics of participants are provided in **Table 1**. Participants were recruited from clinics in the NYC area, our Web site (http://www.tc.edu/centers/cit/), ClinicalTrials.gov (NCT02918890), and online support groups. All participants were randomized (see below) to receive Hand-Arm Bimanual Intensive Training (HABIT) or Constraint-Induced Movement Therapy (CIMT) program, delivered in a day camp model (6 h/day, 15 days). Six cohorts participated in the intervention delivered in a summer day camp setting. The inclusion criteria for were: (1) age 5.5–17 years, (2) diagnosed with USCP, (3) capable of participating in a 15 day, 6 h/day camp while separated from caregiver(s), (4) capable of following directions regarding hand use and testing, (5) capable of communicating needs, (6) mainstreamed in age-appropriate school classroom, and (7) able to lift the more affected arm 15 cm above a table surface and grasp light objects. The exclusion criteria were: (1) unwillingness to comply with instructions or other behavioral issues making delivery of an intensive therapy infeasible, (2) health problems unassociated with hemiplegia, (3) visual impairment that could interfere with participation, (4) orthopedic surgery on the more affected hand within 1 year, (5) presence of metallic objects in the body, and (6) botulinum toxin in the more affected upper extremity within the past 6 months or intended treatment within the study period, (7) seizures after the age of 2 years, (8) family history of seizure disorders, (9) current medication use to lower the seizure threshold, (10) claustrophobia, or (11) pregnancy. Sample size calculations were based on the results of the Assisting Hand Assessment (AHA) and Jebsen-Taylor Test of Hand Function (JTTHF) outcomes of a prior CIMT/HABIT RCT (2) and pilot data. The difference in effect size of improvement in hand function was estimated to be 0.35 (difference change JTTHF = 102 s, sd = 120, AHA change 7 logits, sd = 10), alpha = 0.05, beta = 0.8 and 20% potential dropout. The analysis yielded 82 children.

TABLE 1 | Included participant characteristics.

	CIMT group	HABIT group
N	40	39
Mean age in years, months (SD)	9.4 (2.10)	9,7 (3,5)
Sex		
Male	27	21
Female	13	18
Affected hemisphere		
Right	19	14
Left	21	25
Lesion type		
Middle cerebral artery	10	13
Periventricular	25	23
Malformation	2	1
Unknown	3	2
Corticospinal tract laterality		
Contralateral	7	3
Bilateral	7	6
Ipsilateral	26	30
MACS		
I	9	12
II	25	21
III	6	6
Baseline AHA, mean (SD) (95% CI), logits	56.7 (20.7) (50.1, 63.3)	55.2 (8.7) (52.4, 58.1)
Baseline JTTHF, more-affected, mean (SD) (95% CI), sec	405.1 (306.8) (306.9, 503.2)	402.5 (296.5) (306.4, 498.7)
Baseline JTTHF, less-affected, mean (SD) (95% CI), sec	56.7 (20.7) (39.1, 74.3)	63.8 (40.0) (43.8, 83.9)
Baseline COPM Perf, mean (SD) (95% CI), score	2.9 (1.1) (2.5, 3.2)	3.0 (1.4) (2.5, 3.4)
Baseline COPM Sat, mean (SD) (95% CI), score	3.1 (1.6) (2.6, 3.6)	3.3 (1.8) (2.7, 3.9)
Baseline BBT, more-affected, mean (SD) (95% CI), sec	18.2 (10.1) (15.0, 21.5)	16.6 (9.8) (13.5, 23.0)
Baseline BBT, less-affected, mean (SD) (95% CI), sec	42.9 (12.7) (29.6, 56.1)	41.1 (12.8) (28.2, 54.0)
Baseline PEDI-FS, mean (SD) (95% CI), score	63.8 (6.1) (61.9, 65.8)	63.2 (7.0) (61.0, 65.5)
Baseline PEDI-CA, mean (SD) (95% CI), score	33.8 (5.4) (32.0, 35.5)	33.2 (5.7) (31.9, 35.6)
Baseline ABILHAND-Kids, mean (SD) (95% CI), score	1.9 (1.6) (1.4, 2.4)	1.7 (1.1) (1.4, 2.1)

MACS, Manual Ability Classification System; AHA, Assisting Hand Assessment; JTTHF, Jebsen-Taylor Test of Hand Function; COPM, Canadian Occupational Performance Measure; BBT, Box and Block Test; PEDI, Pediatric Evaluation of Disability Inventory (FS, Functional skills subscale; CA, Caregiver assistance in self-care subscale).

Randomization

Before randomization, children completed all baseline outcome measures. Block randomization was implemented for each cohort of participants (8–18 children). Each cohort was stratified by age, sex, baseline hand function, and CST connectivity pattern as closely as possible, then randomized offsite using concealed allocation to receive either CIMT or HABIT.

Interventions

General Intervention Procedures

Children participated in an intensive hand training intervention using either one (CIMT) or both (HABIT) hands. Children attended for 6 h/day over 15 days (90 h). During the intervention, children were paired with a trained interventionist, with an interventionist:child ratio of at least 1:1. The interventionists included physical and occupational therapists, graduate students in kinesiology/neuroscience, speech pathology, and psychology, and undergraduates. Interventionists were supervised by experienced PT/OTs who enforced protocol fidelity, and both the interventionists and supervisors were blinded to CST connectivity patterns. Prior to the intervention, a training session was administered by the supervisors and standardized based on the established manual of procedures for CIMT and HABIT. Fidelity was reinforced by supervisors during the day camp and during daily post-camp meetings. Participants receiving CIMT and HABIT were located in separate rooms. Each room was supervised by additional experienced PTs/OTs, who modeled and ensured uniformity of treatment. Each day,

interventionists had team meetings to discuss the progress and needs of each child.

Participants worked one-on-one with their interventionist or in groups (while still paired with individual interventionists). Interventionists were matched with children prior to randomization considering the child's age, sex, and interests. Emphasis was placed on making the experience enjoyable. Activities were divided into whole and part task practice. Whole task practice involved sequencing successive movements within the context of activities (e.g., games, arts and crafts, goal training). The activities were performed continuously for at least 15–20 min. Targeted movements and spatial and temporal coordination were practiced within the context of completing the task. Part task practice (analogous to "shaping" in the psychology literature) (25, 34) involved breaking down motor skills into smaller components and reinforcement of successive approximations of the desired behavior (e.g., card turning to promote forearm supination) while increasing repetitions and progressing skill requirements. This approach also served to increase treatment intensity by requiring as many repetitions as possible over repeated 30-s intervals (typically a minimum of 5 intervals).

Task difficulty was graded by varying the spatial/temporal constraints or by providing tasks that required progressive skilled use as task performance improved. The difficulty was increased when the participant was successful on 7 of 10 repetitions. Task performance was recorded, and positive reinforcement and task- and age-specific knowledge of results were provided for encouragement (35).

Constraint-Induced Movement Therapy

CIMT was modified to be child-focused (2, 34). The restraint consisted of a cotton sling fastened to the child's trunk with the distal end enclosed to prevent using the less affected arm or hand as an assist. The sling was continuously worn throughout this intervention except when a break was requested (<0.5 h per 6 h session).

Task Selection

To engage the child in the intervention and to maintain engagement, we established a list of fine motor and manipulative gross motor activities that elicit movement behaviors of interest and included a battery of age-appropriate, unimanual functional and play activities. Interventionists selected tasks based on which train to the targeted hand impairments and the child's interest. Task difficulty was progressed as children improved by requiring greater speed, accuracy, or movement repetition.

Hand-Arm Bimanual Intensive Therapy

Task Selection

We previously identified age-appropriate fine and gross motor activities that require use of both hands (2, 25). Activities were chosen by taking into consideration the role of the more affected UE increasing in complexity from passive assist to active manipulator. While task demands were graded to allow success, children were typically asked to use the more affected UE in the same manner as that of the non-dominant limb of a typically developing child. Directions were provided to the child before the start of each task in order to avoid use of compensatory strategies. These directions specified how each hand will be used during the activity, although choice was often provided to keep the approach child-centered (e.g., use the more affected hand to roll the dice or move a board piece during a game) (2, 25).

Outcome Measures

We chose several measures of hand function to capture different aspects of manual ability. Assessments were administered by an experienced physical or occupational therapist who was blinded to the treatment allocation and CST connectivity of each child. The Assisting Hand Assessment (AHA, version 4.4) measured bimanual hand use. The Jebsen-Taylor Test of Hand Function (JTTHF) measured unimanual dexterity of the affected hand. The AHA and JTTHF were pre-determined primary outcome measures.

Several secondary outcome measures were also used. The Box and Blocks Test (BBT) measured unimanual dexterity. The Canadian Occupational Performance Measure (COPM) measured caregiver perceptions of a child's performance of functional goals, and satisfaction with how well the child can perform the goal. The ABILHAND-Kids is a parent-report of child's manual ability. The Pediatric Evaluation of Disability Inventory (PEDI) was used to measure functioning in the home environment (i.e., self-care domain). All measures were administered immediately before treatment (pre-test), within 2 days after (post-test), and 6 months after treatment (followup).

Bimanual Hand Function

AHA

The AHA is a validated test for measuring bimanual hand use in children with UE impairments. The AHA measures the use of the more affected hand in bimanual activities during a play-like testing session (36). Sessions were videotaped and scored off-site by a blinded evaluator. The AHA has excellent validity, reliability (0.97–0.99) and responsiveness to change (37). The AHA units were used for the analysis. The smallest detectable difference (SDD) for AHA is an improvement of at least 5 units (38).

Unimanual Dexterity

JTTHF

The JTTHF measures the time taken to complete six unimanual tasks, which include flipping cards, moving small objects, and lifting cans (39, 40). The total score is the amount of time taken to complete all tasks. The test was performed on both the more affected and less affected hands. The JTTHF is well-validated and has excellent reliability (40, 41).

BBT

The BBT measures how many blocks (2.5 cm^3) an individual can move from one box, over a barrier, to an adjacent box in 1 min (42). Both hands were tested. The BBT is valid and reliable for children with CP (41).

Hand Use in Daily Functioning

COPM

The COPM is a structured interview in which the individuals are asked to identify up to five functional goals (43). In this study, parents reported their child's functional goals. Parents rated how well children perform each goal (COPM-Performance), and how satisfied they were with the child's performance (COPM-Satisfaction). The same caregiver was interviewed before and after the intervention. A change of 2 or more points in each scale of COPM is considered a minimum clinically important difference (MCID) (43). The COPM has been validated for parents of children with disabilities (44).

ABILHAND-Kids

The questionnaire measures the ability of a child to perform specific 21 daily tasks which require hand use, according to the parent's perspective (45). It has been validated for children with CP over the age of 6 and it is a reliable test (45, 46).

PEDI

Caregivers were interviewed to assess children's daily functioning using the PEDI, a valid/reliable test (47) focusing on child's functioning in daily living activities at home (48). Children's functional skills (PEDI-FS) and caregiver assistance (PEDI-CA) in self-care were assessed.

Determination of CST Laterality

We determined CST laterality in two ways. (1) TMS (primary approach): We determined which hemisphere evokes muscle activation of the affected hand when TMS is applied to the primary motor cortex (M1); (2) DTI (secondary approach): We used DTI to visualize the affected CST only in children whose CST laterality could not be determined with TMS. We have shown that DTI is an accurate surrogate measure of CST laterality (49).

Transcranial Magnetic Stimulation

Single-pulse transcranial magnetic stimulation (TMS) was used to determine which hemisphere's M1 controlled movement of the child's more affected hand. We recorded EMG from the first dorsal interosseous (FDI) muscle in both hands. Skin was cleaned with rubbing alcohol and a mild abrasive (NuPrep, Weaver and Company, Aurora, CO). Electrodes were placed on the FDI muscle belly. Reference electrodes were placed on the muscle tendon, and a ground electrode was placed on the wrist styloid process. EMG was recorded with Neuroconn hardware and software (Neuroprax, Germany). The Neuroconn received a trigger input from the TMS stimulator, such that the relative timing of an EMG response to a stimulus could be measured and visualized. The EMG response to TMS is a motor evoked potential (MEP).

We identified the spot at which a single TMS pulse evoked the strongest MEP in the affected FDI muscle (the motor "hotspot"). To identify the motor hotspot, single TMS pulses were delivered to the child's scalp, starting ∼4 cm from midline above the ear. The initial TMS stimulus intensity was 50% stimulator output. If an MEP was not found, the coil position was moved in 1 cm increments to stimulate the scalp above motor cortex on both hemispheres. Stimulus intensity was increased in 2–5% increments until an MEP was found (50). We stimulated up to 80% stimulator output, because higher stimulation can be painful to participants. If we were unable to find an MEP in the motor strip, we stimulated at 80% stimulator output at 50 points across frontal and parietal cortices in one hemisphere. If no MEP was found at any of these sites, we classified that hemisphere as having no direct control of the movement of either upper extremity.

After the motor hotspot was found, the resting motor threshold (rMT) was determined. The rMT was defined as the minimum stimulus intensity needed to evoke an MEP in the affected FDI in 6 of 10 trials. Stimuli were delivered at a frequency <0.1 Hz. If an MEP was found after 6 of 10 pulses, the stimulus intensity was lowered 2% until an MEP was no longer found in 6 of 10 trials.

We then placed a circular grid over the hemisphere, centered over the hotspot, using Brainsight. The grid had a 10 cm diameter, with five concentric rings, each gridpoint placed 1 cm apart. The grid was centered over the hotspot for that hemisphere. Although there was always one maximally responsive hotspot, by stimulating each point of the grid, we captured all other responsive regions in motor cortex. We stimulated each site 1–3 times (2–3 times if a response was found) at 110% the participant's rMT. By stimulating at 110% rMT, we thoroughly searched for all motor cortex representations of the upper extremities. Responses, as described below, were sites at which a TMS stimulus evoked an MEP 50 μV or larger. As described in detail elsewhere, we calculated the ratio between the number of responses in the more affected FDI obtained from the lesioned and contralesional hemispheres (10, 51, 52). This ratio is the laterality index (LI).

Participants were categorized as having a contralateral CST connectivity pattern if the LI was between 0.9 and 1; i.e., 90–100% of the responses in the more affected hand come from the lesioned hemisphere. Participants were categorized as having an ipsilateral CST connectivity pattern if the LI was between 0 and 0.1; i.e., 0–10% of the responses in the affected hand come from the lesioned hemisphere. Participants were categorized as having a bilateral CST connectivity pattern if the LI was between 0.1 and 0.9.

Transcranial Magnetic Stimulation Analysis

The latency and peak-to-peak amplitude of each TMS pulse was measured using a suite of custom-written MATLAB (Mathworks, Waltham, MA) scripts. If the latency of the MEP was longer than 40 ms after the TMS pulse, that trial was excluded from analysis. Additionally, if high levels (>100 μV) of background EMG activity were seen before the MEP, the trial was excluded from analysis.

Magnetic Resonance Imaging

Each child received a structural MR scan (MP-RAGE, 3D, T1-weighted) and diffusion tensor imaging scan, without sedation prior to participation. The structural MRI was used to co-register TMS stimulation targets with specific brain landmarks, using a frameless stereotaxic neuronavigation system (Brainsight

Frameless, Rogue Research, Montreal, QC, Canada). For TMS localization, there is normal variability in brain topography relative to scalp landmarks. MR scans were done on a Siemens Prisma MRI Scanner (Malvern, PA) in the Citigroup Biomedical Imaging Center (CBIC). Structural scans (165 slices) were taken at a resolution of 256 × 256 px. The structural MRI was used to identify the lesion type and extent, as well as to localize the TMS coil (i.e., neuronavigation). The DTI scan was done during the same session as the structural MRI. For DTI, a 65-direction protocol was used, 75 slices per direction at a resolution of 112 × 112 px each.

Diffusion Tensor Imaging Analysis

DT images for participants whose CST laterality could not be determined with TMS due to excessively high threshold or safety reasons were imported into DTI Studio (Johns Hopkins University) software for processing and analyses. This has been shown to be a reliable surrogate for TMS in determining CST laterality (22, 49). Image series for each participant were screened for movement artifact, and slices showing artifact were removed. Since obtained images using 65 gradients and performed duplicate scans, up to 30% of slices may be removed without compromising feasibility of tract reconstruction. Using DTI Studio, we placed region of interest seeds in the affected motor cortex and cerebral peduncle, and later in the unaffected motor cortex and cerebral peduncle. We used tractography to find tracts that passed through both ROIs. We categorized each CST as present or absent. If there was a present CST on the affected side, the child was categorized as having a contralateral CST. If there was not a CST present on the affected side, and a CST present on the other side, the child was categorized as having an ipsilateral CST (49). Note that, with this approach, "bilateral" CST connectivity cannot be detected.

Statistical Analysis

This was an intention-to-treat study. If a child missed their 6 month assessment, we imputed their missing data based on the average change data for other participants in their subgroup. Statistical analyses were performed using SPSS (IBM, version 26). A treatment (CIMT, HABIT) × CST connectivity pattern (contralateral, ipsilateral, bilateral) × test session (pre-, post-, 6 month) ANOVA with repeated measures on test session was performed on all measures and Newman-Keuls *post-hoc* tests were performed where appropriate. Regression analyses were done to determine predictors of outcomes. For children with a bilateral CST, correlations were done between the LI and changes in outcome measures. Statistical significance was considered at the $p < 0.05$ level.

RESULTS

Patient Flow

Patient flow is shown in the CONSORT diagram (**Figure 1**, see legend for details). During recruitment, 212 individuals were screened. Ultimately, 83 qualified individuals agreed to participate and were randomized to CIMT or HABIT. One child was randomized to HABIT after pre-test, but chose not to participate on the first day of treatment due to social anxiety. Thus, 82 participants (41 per group) completed the treatment, although we were unable to complete TMS or DTI on 3 participants so only data of the 79 participants with CST determination were included (39 for CIMT, 40 for HABIT). All other children completed the intervention, along with pre- and immediate post-intervention assessments, but 7 children missed the 6 month follow up assessments (CIMT $n = 3$, HABIT $n = 4$) and their data points were imputed. The results were the same whether or not data for these children were included. We were unable to determine the CST connectivity pattern for 3 children. The results were the same whether or not data for these children were included as well. Lesion type was missing for 5 children who declined MRIs. These 5 children were excluded from analyses of lesion type. **Table 1** describes participant characteristics. There were no significant treatment group differences in baseline scores for any measure.

Adverse Events

Five children had adverse events. One child had a seizure 9 days after completing the immediate post-test. The event took place immediately after an overseas flight without sleep and after the child fell from bed. Two children had seizures (one suspected and one confirmed) shortly before the 6-month follow up. One child broke the more affected UE between the immediate and 6-month follow up. Six-month follow up evaluations were not conducted on these 4 participants. A fifth child fell and required stitches in the head within a month of the 6-month follow up. This child completed clinical testing for the 6-month follow up. None of the events were deemed to be study-related.

Bimanual Hand Function

Figure 2 shows the change scores for the AHA as a function of treatment and CST organization (mean scores can be seen in **Table 2**). As seen in the figure, overall there was improvement across both treatments and CST organization patterns, but there were variations within each group. There was a significant increase of 1.8 and 2.4 AHA-units for CIMT and HABIT, respectively, across test sessions {$[F_{(2, 72)} = 14.91$, $p < 0.001$, partial eta$^2 = 0.11]$, **Table 2** and **Figure 2**}. Five participants in the CIMT group and 11 in the HABIT group reached the SDD. Newman-Keuls *post-hoc* tests revealed a significant improvement between the pre-test and immediate post-test that was maintained at 6 months. There were no interactions between intervention group and test session or intervention group, CST connectivity pattern and test session ($p > 0.05$).

Unimanual Dexterity

Figure 3 shows the change scores for the JTTHF for the more affected hand as a function of treatment and CST organization (mean scores can be seen in **Table 2**). There was a 111.1 s (24%) and a 56.3 s (11%) decrease in time for CIMT and HABIT, respectively {$[F_{(2, 72)} = 44.0$ $p < 0.001$, partial eta$^2 = 0.34]$, **Table 2** and **Figure 3**}. Newman-Keuls *post-hoc* tests revealed a significant improvement between the pre-test and immediate post-test that was maintained at 6 months. There

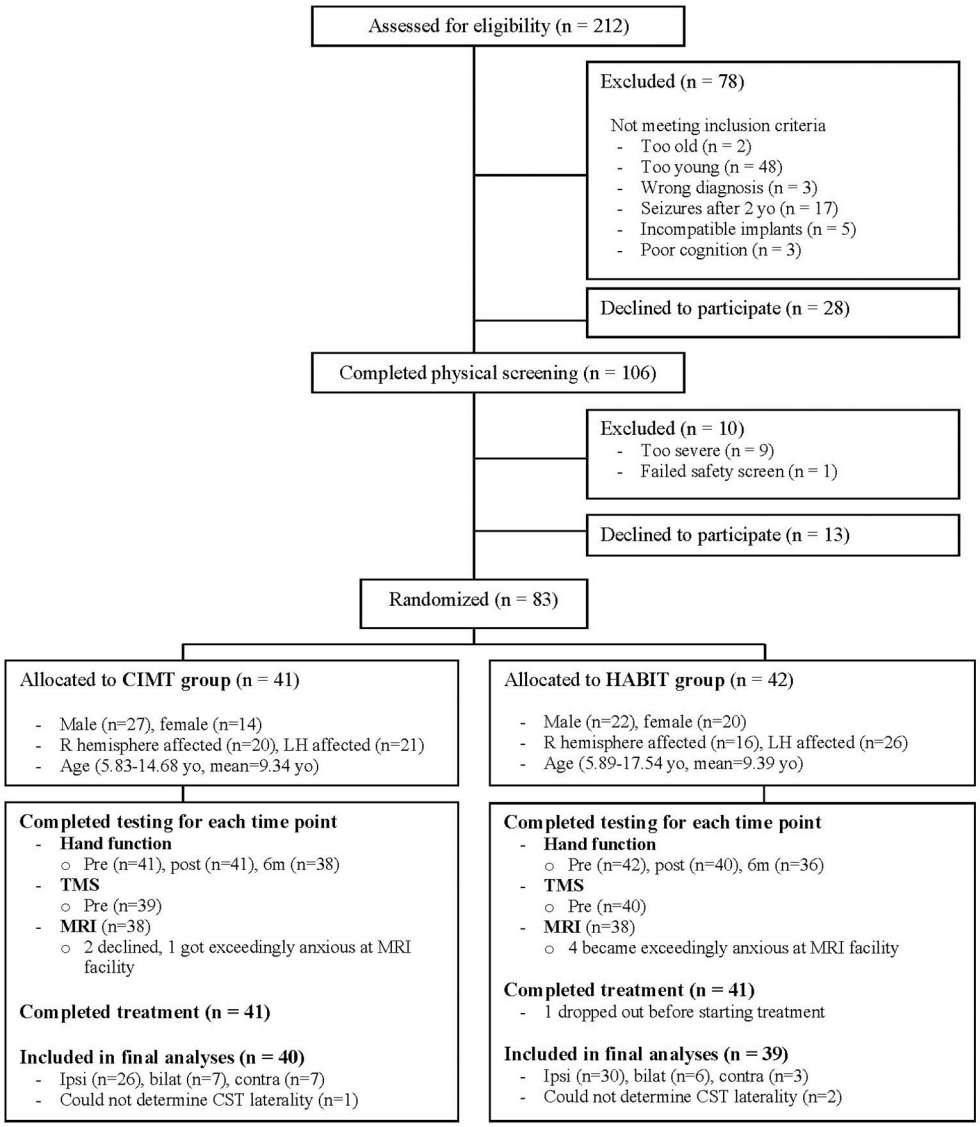

FIGURE 1 | CONSORT flow diagram showing progress through the stages of the study, including flow of participants, withdrawals, and inclusion in analyses. A total of 212 individuals were screened by phone or e-mail. Of these 78 children did not meet the study criteria and 28 declined participation. The remaining 106 children potentially met the study criteria and were invited to undergo physical screening. Ten children were excluded and 13 who qualified declined to participate. The remaining 83 children were stratified by age, sex, baseline hand function and CST connectivity pattern, and randomized to receive either CIMT or HABIT. One child in the HABIT group dropped out before starting treatment, and 41 children in each group completed the intended treatments. We were unable to complete TMS or DTI on 3 participants due to exceedingly high thresholds or safety concerns, so only data of the 79 participants with CST determination were included (39 for CIMT, 40 for HABIT).

were no interactions between intervention group and test session or intervention group, CST connectivity pattern and test session ($p > 0.05$). There was no change in the less affected hand ($p > 0.05$).

There was an increase in the Box and Blocks performed with the more affected hand for both groups (12.29 for CIMT, 10.47 for HABIT) [$F_{(2, 72)} = 50.77$, $p < 0.001$ partial eta$^2 = 0.53$] (**Table 2**). Newman-Keuls *post-hoc* tests revealed a significant improvement between the pre-test and immediate post-test that was maintained at 6 months. There were no interactions between intervention group and test session or intervention group, CST connectivity pattern and test session ($p > 0.05$). There was no change in the less affected hand ($p > 0.05$).

Hand Use in Daily Functioning

For the ABILHAND-Kids (**Table 2**) both treatments resulted in significant improvement [$F_{(2, 72)} = 1139.8$ $p < 0.001$, partial eta$^2 = 0.97$]. There were no interactions between intervention group and test session or intervention group, CST connectivity pattern and test session ($p > 0.05$).

Most goals defined in the COPM were bimanual (remaining ones were unimanual with the more affected hand). Most of the

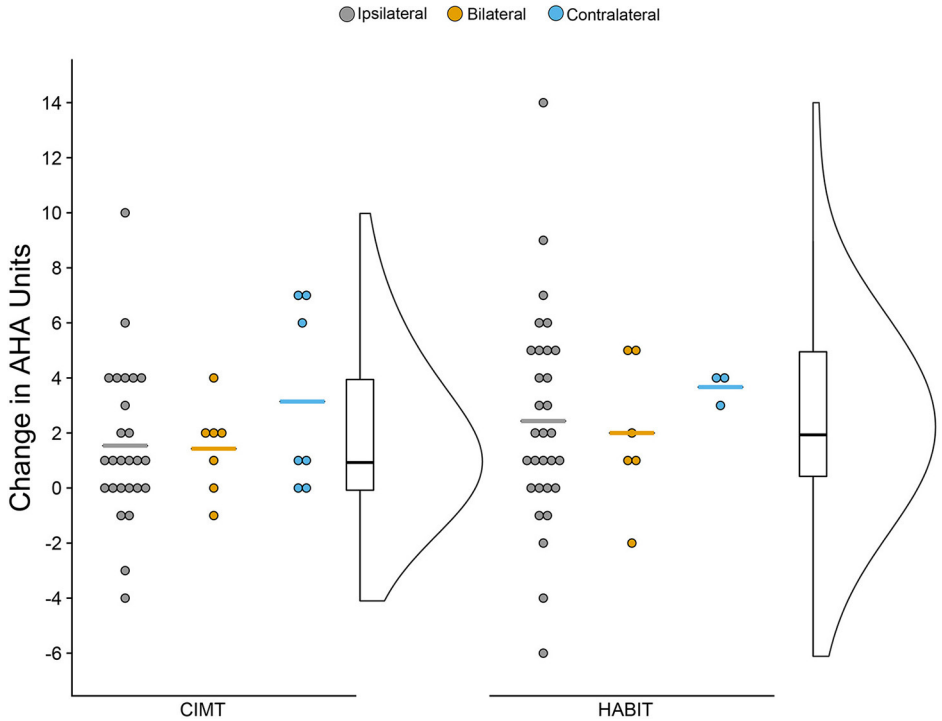

FIGURE 2 | Raincloud Plot of Changes (Pre-test to Post-test) in AHA by Therapy Group and CST Connectivity. Dots represent raw change scores for individual children (positive scores = improvements). Horizontal colored lines represent mean of CST group. Boxplots represent median and quartiles of therapy group data. Curve represents probability distribution of therapy group data.

goals comprised self-care activities (e.g., dressing, grooming, and eating), followed by play (e.g., ball activities). Both groups had significant improvements in the COPM after the intervention on performance [$F_{(2, 72)} = 89.06$, $p < 0.001$, partial eta$^2 = 0.61$] and on satisfaction [$F_{(2, 72)} = 1139.9$, $p < 0.001$, partial eta$^2 = 0.96$] (**Table 2**). Twenty-four participants in the CIMT group and 29 in the HABIT group reached the MCID of 2 or more points for COPM performance. Twenty-five participants in CIMT group and 30 in the HABIT group reached the MCID of 2 or more points for COPM satisfaction. There were no interactions between intervention group and test session or intervention group, CST connectivity pattern and test session ($p > 0.05$).

Finally, there was an overall improvement in the PEDI-Functional Skills and PEDI- Caregiver Assistance in self-care over time [$F_{(2, 72)} = 4727.9$, $p < 0.001$, partial eta$^2 = 0.99$] (**Table 2**). There were no interactions between intervention group and test session or intervention group, CST connectivity pattern and test session ($p > 0.05$).

Children With a Bilateral CST

Although the above analyses indicated that intervention efficacy was independent of CST laterality, we further examined children with a bilateral CST. We examined correlations between LI and the percent change in each outcome measure for the combined CIMT and HABIT groups (note that the groups were too small to considered by individual treatment). **Figure 4** shows correlations between LI and changes in AHA (A) and JTTHF (B). As seen in the figure, there was no significant relation between change scores and LI for the AHA ($r = -0.08$) or JTTFF ($r = 0.51$, but $r = 0.07$ when an outlier >3.5 SD from the mean change score was removed). There were no significant correlations between LI and change in any other outcome measure (BBT: $r = 0.09$, pCOPM-Performance $r = -0.23$, COPM-Satisfaction $r = 0.24$, ABILHAND: $r = -0.36$, PEDI-Caregiver Assistance: $r = -0.34$, PEDI-Functional Skills: $r = 0.14$).

Given the relatively small number of participants with purely CST connectivity, we also reanalyzed all measures considering just two groups: contralateral CST connectivity present (combining the contralateral and bilateral groups) or contralateral CST connectivity absent (ipsilateral group). There still were no interactions between CST connectivity group and treatment for any measure.

Predictors of Improvement

There were no statistically significant predictors of improvement among the many potential covariates examined. Specifically, there was no significant association between MACS level ($p > 0.1$), lesion type ($p > 0.2$), sex ($p > 0.6$), age ($p > 0.4$), side of lesion ($p > 0.4$), and baseline function ($p > 0.1$) on improvement in any outcome measure.

DISCUSSION

This is the first study, to our knowledge, to prospectively examine how CST laterality in children with USCP might

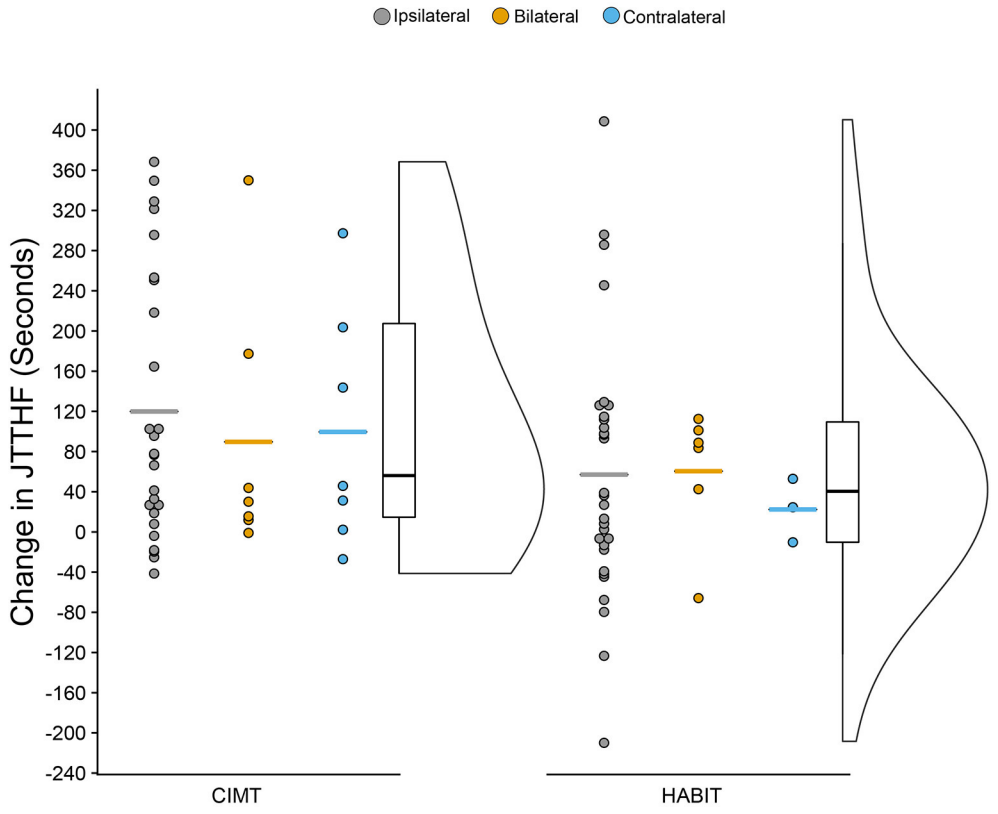

FIGURE 3 | Raincloud Plot of Changes (Pre-test to Post-test) in JTTHF by Therapy Group and CST Connectivity (positive scores = improvements).

mediate functional recovery following intensive unimanual or bimanual therapy. We found the efficacy of intensive training to be independent of CST connectivity pattern for all measures. This finding did not support our hypothesis that improvements in UE function following either CIMT or bimanual training depend on CST laterality and type of training (unimanual vs. bimanual) in children with USCP. That is, children with ipsilateral, bilateral, and contralateral CST connectivity improved equally in both CIMT and HABIT. We discuss possible reasons for these findings.

CST Connectivity Does Not Predict Treatment Efficacy

When brain injury is superimposed on development, the motor system exhibits an extraordinary capacity to adapt. In children with USCP, this flexibility is manifested as rewiring of the CST and has intricate consequences for sensorimotor function. Studies suggest CST laterality is associated with the magnitude of UE impairments (10, 17–19). Yet, the variability in UE function observed in children with USCP and the observation that an ipsilateral CST may provide a neural substrate for plasticity (21, 22) has made a precise understanding of how developmental reorganization impacts motor skills difficult. Perhaps more importantly, there has been contradictory evidence regarding the role CST laterality may play in mediating response to therapy. Studies of CIMT have proposed ipsilateral CST connectivity as a limiting factor to recovery (16, 31), although the relationship between CST connectivity and CIMT outcomes is not unequivocal (8). It should be noted that both of these studies had small sample sizes ($n = 16$ in each study). In a larger study of HABIT ($n = 33$) the results suggest children improve regardless of connectivity pattern (21). We sought to adjudicate between these differences in a larger, prospective randomized control trial.

Despite variability in outcomes, overall children with ipsilateral, contralateral, and bilateral CST connectivity patterns improved on all outcome measures for both CIMT and HABIT. Although we recruited only a small sample of children with contralateral CST connectivity, their responsiveness to CIMT and HABIT is consistent with previous studies. Combining this group with children with bilateral connectivity did not change this finding, and the strength of the contralateral projections in the bilateral CST group did not relate to the outcomes. The discrepancy in improvements following CIMT for the children with ipsilateral CST connectivity seen in our study and that of Islam et al. (8) and not in the study by Kuhnke et al. (16) potentially may be explained by several factors. First the participants in the Kuhnke et al. (16) study were considerably older, with a mean age of 17 years (range 10–30 years) compared to our study with a mean age of 9.5. Thus, it is

TABLE 2 | Outcome measures.

	Pre-test (95% CI)	Post-test (95% CI)	6 m follow-up (95% CI)
CIMT			
AHA (0–100 units)			
Ipsilateral CST	52.5 (48.5, 56.6)	54 (50.2, 57.8)	54.4 (50.3, 58.4)
Bilateral CST	62.3 (57.1, 67.5)	63.7 (57.6, 69.8)	64.1 (57.8, 70.5)
Contralateral CST	55.4 (50.4, 60.5)	58.6 (52.6, 64.5)	58.1 (52.4, 63.9)
JTTHF, more-affected (seconds)			
Ipsilateral CST	479.5 (358.5, 600.5)	354.1 (254.5, 453.7)	342.4 (233, 451.9)
Bilateral CST	265.6 (46.6, 484.6)	175.9 (−28.8, 380.7)	213.3 (13.6, 413)
Contralateral CST	323.6 (89.9, 557.3)	224 (47.4, 400.7)	266.1 (109.5, 422.7)
JTTHF, less-affected (seconds)			
Ipsilateral CST	61.7 (53.9, 69.6)	58.3 (49.8, 66.8)	53.3 (45.7, 60.8)
Bilateral CST	47.3 (38, 56.5)	47.5 (34.8, 60.1)	49.1 (41.4, 56.8)
Contralateral CST	49.4 (35.2, 63.5)	43.3 (34.4, 52.2)	46.1 (33, 59.1)
COPM Performance (0–10 rank)			
Ipsilateral CST	2.9 (2.5, 3.3)	5.7 (5, 6.4)	6 (5.3, 6.7)
Bilateral CST	3.2 (2.5, 3.9)	6.3 (5.3, 7.4)	6.6 (5.7, 7.4)
Contralateral CST	2.5 (1.2, 3.8)	4.8 (3.3, 6.4)	5.3 (4.6, 6.1)
COPM Satisfaction (0–10 rank)			
Ipsilateral CST	3.2 (2.6, 3.8)	6.4 (5.5, 7.3)	6.6 (5.9, 7.3)
Bilateral CST	3 (1.8, 4.3)	7.2 (6, 8.4)	7.3 (6.5, 8.2)
Contralateral CST	2.9 (1.9, 4)	5.7 (3.8, 7.7)	6.3 (5, 7.5)
BBT, more-affected (*n* of blocks)			
Ipsilateral CST	16.6 (12.1, 21.1)	19.2 (13.9, 24.4)	19.7 (14.6, 24.8)
Bilateral CST	21.4 (15, 27.9)	27 (20.5, 33.5)	24.7 (17.4, 31.9)
Contralateral CST	18.9 (14.7, 23.1)	25.6 (21, 30.1)	23.4 (18.7, 28)
BBT, less-affected (seconds)			
Ipsilateral CST	42.2 (36.9, 47.6)	46.6 (40.5, 52.7)	46.9 (41.5, 52.3)
Bilateral CST	44.9 (35, 54.8)	48.9 (37.6, 60.1)	50.5 (38.8, 62.3)
Contralateral CST	42.9 (38.4, 47.3)	48.1 (41.6, 54.7)	48 (44, 52)
PEDI functional skills			
Ipsilateral CST	63.4 (61.1, 65.6)	66.5 (64.7, 68.3)	67.7 (66.1, 69.3)
Bilateral CST	64.9 (58.8, 70.9)	69.1 (65.8, 72.5)	69.5 (66.3, 72.7)
Contralateral CST	64.3 (61.3, 67.2)	65.3 (62.5, 68)	66 (63.4, 68.6)
PEDI caregiver assistance			
Ipsilateral CST	33.7 (31.4, 36)	35.6 (33.8, 37.4)	37.4 (35.7, 39.1)
Bilateral CST	35 (31.4, 38.6)	35.9 (32, 39.8)	36.9 (32.3, 41.5)
Contralateral CST	33.9 (30.7, 37)	35.1 (32.3, 37.9)	35.9 (35.1, 36.6)
ABILHAND-Kids			
Ipsilateral CST	1.6 (1, 2.3)	2.3 (1.7, 3)	2.7 (2.1, 3.2)
Bilateral CST	2.2 (1, 3.4)	2.5 (1.2, 3.8)	2.8 (1.4, 4.3)
Contralateral CST	2.6 (1.8, 3.3)	2.4 (1.6, 3.1)	2.3 (1.2, 3.4)
HABIT			
AHA (0–100 units)			
Ipsilateral CST	54.8 (51.4, 58.1)	57.2 (54.1, 60.3)	56.5 (53.4, 59.5)
Bilateral CST	54.5 (48.1, 60.9)	56.5 (49.4, 63.6)	56.7 (50.5, 62.8)
Contralateral CST	61.3 (57.9, 64.8)	65 (57.9, 72.1)	66.3 (62.9, 69.8)
JTTHF, more-affected (seconds)			
Ipsilateral CST	435.7 (331.2, 540.2)	378.6 (281.3, 476)	380.2 (274.2, 486.2)
Bilateral CST	377.3 (122.4, 632.1)	316.8 (90.8, 542.8)	323.8 (152, 495.5)
Contralateral CST	121.3 (−183.9, 426.5)	98.9 (−170.5, 368.4)	146 (−152, 444)

(Continued)

TABLE 2 | Continued

	Pre-test (95% CI)	Post-test (95% CI)	6 m follow-up (95% CI)
JTTHF, less-affected (seconds)			
Ipsilateral CST	70.6 (65.6, 75.5)	64.9 (58.7, 71.1)	55.4 (50.5, 60.3)
Bilateral CST	41.5 (−23.1, 106.2)	42.6 (−13.3, 98.5)	42.1 (21.2, 63)
Contralateral CST	41.9 (12.1, 71.7)	47 (35.2, 58.8)	44.2 (12.5, 75.8)
COPM performance (0–10 rank)			
Ipsilateral CST	2.8 (2.3, 3.4)	6.4 (5.8, 7)	6.1 (5.5, 6.6)
Bilateral CST	3.6 (2.9, 4.2)	6.5 (5, 8.1)	6.5 (4.9, 8)
Contralateral CST	3.5 (3.2, 3.7)	5.9 (4.6, 7.1)	6.9 (5.5, 8.4)
COPM satisfaction (0–10 rank)			
Ipsilateral CST	3.3 (2.6, 4)	7 (6.4, 7.7)	6.5 (5.8, 7.1)
Bilateral CST	2.7 (2.1, 3.3)	6.8 (5.5, 8.1)	6.8 (5.5, 8.1)
Contralateral CST	4.4 (2.1, 6.7)	6.1 (3.7, 8.5)	7.7 (5.9, 9.5)
BBT, more-affected (*n* of blocks)			
Ipsilateral CST	16.2 (12.5, 19.9)	19.2 (15.6, 22.8)	19.3 (15.6, 23)
Bilateral CST	14 (7.9, 20.1)	18.7 (10, 27.4)	18.2 (9.5, 26.9)
Contralateral CST	26 (19.2, 32.8)	27 (20.6, 33.4)	31.3 (19.7, 42.9)
BBT, less-affected (seconds)			
Ipsilateral CST	39.9 (35.2, 44.6)	43.8 (39.8, 47.8)	46.7 (42.1, 51.3)
Bilateral CST	46.3 (36.5, 56.1)	49.2 (36.9, 61.4)	49.4 (37.5, 61.3)
Contralateral CST	43 (30.3, 55.7)	51.3 (44.7, 58)	56 (41.2, 70.8)
PEDI functional skills			
Ipsilateral CST	62.1 (59.7, 64.6)	66.5 (64.5, 68.5)	66.7 (64.7, 68.7)
Bilateral CST	68.7 (62.6, 74.7)	70.2 (66.2, 74.2)	69.6 (66.7, 72.5)
Contralateral CST	63.3 (57.6, 69)	64.7 (60.7, 68.6)	67.3 (64.3, 70.3)
PEDI caregiver assistance			
Ipsilateral CST	32.9 (31, 34.7)	35.2 (33.8, 36.7)	35.6 (34, 37.3)
Bilateral CST	36.2 (30.4, 42)	37.4 (35.2, 39.6)	38 (35.1, 41)
Contralateral CST	37.3 (26.5, 48.1)	37.3 (27.8, 46.8)	35.3 (30.6, 40)
ABILHAND-Kids			
Ipsilateral CST	1.6 (1.2, 2)	2.3 (1.9, 2.7)	2.4 (1.9, 2.8)
Bilateral CST	2.2 (1.2, 3.3)	2.7 (2.1, 3.3)	2.9 (1.7, 4.1)
Contralateral CST	2.3 (1.7, 2.8)	2.1 (1.9, 2.2)	3.3 (2.8, 3.8)

CST, cortical spinal tract laterality; AHA, Assisting Hand Assessment; JTTHF, Jebsen-Taylor Test of Hand Function; COPM, Canadian Occupational Performance Measure; BBT, Box and Block Test; PEDI, Pediatric Evaluation of Disability Inventory.

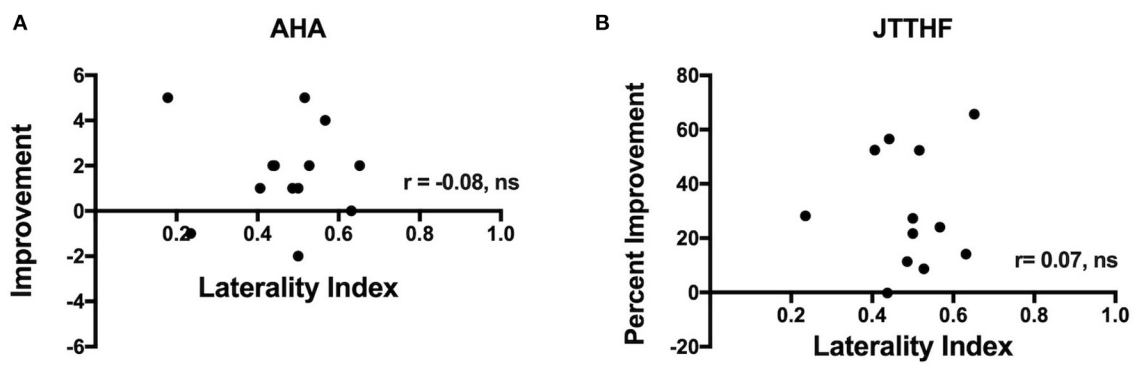

FIGURE 4 | Plots showing correlations between laterality index and improvement in **(A)** AHA and **(B)** JTTHF immediately after the intervention. Note that one JTTHF change value was >3.5 SD from the mean and was excluded from the correlation.

possible that decreased neuroplasticity or the long development of compensatory strategies and life and treatment experiences may have limited the response to treatment in some individuals or that there may be an interaction between age and CST connectivity. However, we did not find a relation between age and outcomes for any measure in the present study. Furthermore, the study by Islam et al. (8) also had an older age group (age 10–16 years) yet reported improvements in participants with ipsilateral connectivity. Thus, this may not be the primary reason for the discrepancy.

The discrepancy in findings may be due to the differing outcomes. Our study and that of Islam et al. (8) used the AHA and JTTHF to determine efficacy of assisting hand use in bimanual activities and unimanual dexterity, respectively. These measures are validated in these age groups. The Kuhnke et al. (16) study used the Wolf Motor Function Test (WMFT) to determine unimanual dexterity, which is validated for adults who had experienced a stroke. As acknowledged by the authors, this test may be appropriate for a large number of their participants who were within the adult age range, but is not validated for the younger participants in their study. The outcomes may be test-dependent, as evidenced by the lack of changes on the Melbourne Assessment reported by Islam et al. (8). Nonetheless, there is some overlap in the manual activities between the WMFT and JTTHF, so it is unclear whether the findings may be due to the differing tests.

The differences between studies could also be due to baseline severity of hand impairments. There is not agreement across studies regarding the effects of severity and outcome following intensive treatment. For example, in a small study of CIMT we found children with greater severity improved more following CIMT (24). Poorer baseline hand function predicted a best response for unimanual capacity immediately after CIMT or bimanual training (9). Similarly, Simon-Martinez et al. (53) found better improvements among children with worse bimanual hand function following combined CIMT and action observation. However, we did not find a relationship between severity and outcomes following larger studies of CIMT and HABIT (2, 4, 10). It should be noted that the lack of overlapping measures precludes us from determining severity differences between our study and that of Kuhnke et al. (16). However, an important consideration is that most studies have exclusion criteria that don't allow the children with the mildest or most severe hand function participate, and thus the relationship cannot clearly be determined across the USCP population. Given the large heterogeneity of individuals with USCP, the discrepancies in outcomes may be due to the specific sample enrolled. To our knowledge, our sample of children with ipsilateral CST connectivity participating in CIMT and bimanual training is the largest to date, and this large sample may suggest that even children with ipsilateral connectivity benefit following either CIMT or bimanual training.

Response to Treatment

Despite significant changes on the AHA for both the HABIT and CIMT groups, the majority of participants did not reach the SDD. We did not find any factors that relate to the change in AHA scores. It is possible that since 70% of our sample had participated in our prior CIMT or HABIT ($n = 23$) studies or had received varying forms of CIMT ($n = 35$) ranging from wearing a sock in usual and customary care to full programs with a cast worn 24/7 at other sites prior to participating, there may have been a ceiling effect. Analysis of the children who did and did not receive previous intensive treatment suggested similar gains, although the latter group was quite small. Interestingly, 3 of the 5 participants in the CIMT group who reached the SDD for the AHA (**Figure 2**) had a contralateral CST pattern. Thus, with a larger number of these individuals the findings might suggest they respond better on average than children with other CST connectivity patterns. Nonetheless, children with ipsilateral CST connectivity patterns also improved and were among the children who reached the SDD for CIMT, and were the most common CST subgroup reaching the SDD for HABIT.

Despite the small individual AHA changes, significant changes were found across groups for all measures. More than two-thirds of the participants across both groups exceeded the MCID for goal performance as rated by caregivers. Thus, the majority of parents perceived clinically meaningful improvements in functional goals related to hand use.

Our finding that children improve equally across CST connectivity groups in both interventions is consistent with a systematic review that concluded that the minimum threshold dose needed to elicit improvements in children with USCP is 30–40 h (54) and at least 60 h for optimal improvements (55). Although the studies reviewed did not stratify by CST connectivity, our interventions involved ∼3× the minimum dose required to elicit changes and 50% more than the recommended intensity. Moreover, our motor learning-based, task-specific training, which also included functional goal training, are aligned with the type of interventions that lead to efficacy at a lower dose than general for UE motor training (54). Animal models suggest that high intensity training can result in increases in synaptic density in M1 (56), and increase cholinergic spinal interneurons (57). However, the high dose of treatment in the present study may have contributed to the lack of treatment differences based on CST connectivity. It is conceivable that differences (especially for the ipsilateral CST group) would be observed at lower doses.

Other Neurological Predictors of Efficacy

Although CST connectivity patterns seemingly do not predict treatment outcome, there may be other brain areas that are more predictive. For example, children with greater structural, functional and connective brain damage have been shown to exhibit enhanced responses to bimanual intervention (58).

Functional connectivity of sensorimotor networks may differ depending on patterns of CST reorganization. Simon-Martinez et al. (59) found that children with a contralateral CST show increased connectivity between M1 and pre-motor cortices, whereas children with a bilateral CST show higher connectivity between M1 and somatosensory association areas. Impaired sensation (60, 61) and sensorimotor connectivity (62, 63) is related to poor motor performance. However, children with poor sensory function had larger improvements following CIMT or CIMT plus action observation (53). Thus, the integrity of the sensory tracts and whether they are maintained in the lesioned hemisphere (33, 64) may relate to functional improvements.

Furthermore, brain lesion type and resulting volumetric changes (65) and the integrity of the corpus callosum have also been shown to relate to hand function (66). It is not directly known whether integrity of these interhemispheric connections is predictive of treatment efficacy. It is likely that there are complex interactions between the integrity of various areas and treatment outcome that are beyond the scope of the present study.

Limitations

Despite being one of the largest studies comparing CIMT with bimanual training, there were not an equal number of participants with each CST connectivity pattern. Although we did have a large number of participants with ipsilateral connectivity, adding to the confidence that such connectivity is not maladaptive, we had a small number of children with purely a contralateral pattern. This may be because these children may have very mild hand function impairments in which they do not qualify or whose parents do not view the effort/potential benefit as being attractive. However, the responsiveness of these individuals across studies is not in doubt, and the findings held true even when the contralateral and bilateral groups were combined. The latter group is perhaps more complex. It is unclear whether they can be considered a homogeneous group given the laterality indices varied considerably across participants. Nonetheless, these indices did not correlate with outcomes, and further study is warranted.

The large number of participants who had received intensive therapies prior to participating in this study may have limited our gains in UE function by creating ceiling effects. Although the gains were similar whether or not children had received previous intensive therapy, the favorable response to prior therapy may have influenced the decision to participate in this study, and thus these could potentially be "best responders." The small number of first-time participants precludes us from examining whether CST connectivity predicts treatment outcomes in first-time participants.

Conclusions

The present study suggests children with ipsilateral, bilateral, and contralateral CST connectivity improved equally in both CIMT and HABIT. Thus, children with an ipsilateral CST, previously thought to be maladaptive, have the capacity to improve as well as children with a contralateral or bilateral CST following intensive CIMT or Bimanual training.

DATA AVAILABILITY STATEMENT

The raw data supporting the conclusions of this article will be made available by the authors, without undue reservation.

ETHICS STATEMENT

The studies involving human participants were reviewed and approved by Institutional Review Boards of Teachers College, Columbia University, Burke Neurological Institute and Weill Cornell Medicine. Written informed consent to participate in this study was provided by the participants' legal guardian/next of kin.

AUTHOR CONTRIBUTIONS

KF and AG conceptualized the project and oversaw its implementation. KF, AG, CF, and MB wrote the manuscript. KF, CF, KC, H-CK, VF, MR, AS, and TC performed TMS and contributed to analyses. CF, MB, Y-CH, VF, H-CK, YB, and KC contributed to clinical supervision of treatment. JC assessed neurological reports and oversaw TMS safety. All authors provided editorial input to the final manuscript.

FUNDING

The authors disclosed receipt of the following financial support for the research, authorship, and/or publication of this article: This research was supported by NIH Grants R01HD076436 and by the National Center for Advancing Translational Science of the NIH under Award Number UL1TR002384.

ACKNOWLEDGMENTS

We thank Dr. Jason Fuller, Alexandra Agins, Tiffany Chin, Antonella D'Ascanio, Shivakeshavan Ratnadurai-Giridharan, Samantha Gold, Toby Kashket, MaryClare McDonough, Katerina Newman, Sarah Sylla, Kathleen Samuelson, Brittany Zaita for assistance with TMS procedures and Bernadette Gillick for advice on administering TMS in children. We thank Lauren Tyndorf, Julie Paradis, Daniela Ebner, Melania García Estévez, and Laura Yeo for supervising some camp sessions, Katrina Long, Amanda Sarafian, Orit Herzberg-Keller, Swetha Krishnaswamy, Grace-Anne Herard, Ellen Osei, and Genni Hester for serving as evaluators, the volunteer interventionists for their help during the camp, Dr. Lisa Wagner, OT for Assisting Hand Assessment scoring and the participants and their families for their participation. A portion of this work was originally published in abstract form (67).

REFERENCES

1. Novak I, Morgan C, Fahey M, Finch-Edmondson M, Galea C, Hines A, et al. State of the evidence traffic lights 2019: systematic review of interventions for preventing and treating children with cerebral palsy. *Curr Neurol Neurosci Rep*. (2020) 20:3. doi: 10.1007/s11910-020-1022-z
2. Gordon AM, Hung YC, Brandao M, Ferre CL, Kuo HC, Friel K, et al. Bimanual training and constraint-induced movement therapy in children with hemiplegic cerebral palsy: a randomized trial. *Neurorehabil Neural Repair*. (2011) 25:692–702. doi: 10.1177/1545968311402508
3. Hung YC, Casertano L, Hillman A, Gordon AM. The effect of intensive bimanual training on coordination of the hands

in children with congenital hemiplegia. *Res Dev Disabil*. (2011) 32:2724–31. doi: 10.1016/j.ridd.2011.05.038
4. Brandão MB, Ferre C, Kuo HC, Rameckers EA, Bleyenheuft Y, Hung YC, et al. Comparison of structured skill and unstructured practice during intensive bimanual training in children with unilateral spastic cerebral palsy. *Neurorehabil Neural Repair*. (2014) 28:452–61. doi: 10.1177/1545968313516871
5. Bleyenheuft Y, Arnould C, Brandao MB, Bleyenheuft C, Gordon AM. Hand and arm bimanual intensive therapy including lower extremity (HABIT-ILE) in children with unilateral spastic cerebral palsy: a randomized trial. *Neurorehabil Neural Repair*. (2015) 29:645–57. doi: 10.1177/1545968314562109
6. Gordon AM. Impaired voluntary movement control and its rehabilitation in cerebral palsy. *Adv Exp Med Biol*. (2016) 957:291–311. doi: 10.1007/978-3-319-47313-0_16
7. Ferre CL, Gordon AM. Coaction of individual and environmental factors: a review of intensive therapy paradigms for children with unilateral spastic cerebral palsy. *Dev Med Child Neurol*. (2017) 59:1139–45. doi: 10.1111/dmcn.13497
8. Islam M, Nordstrand L, Holmström L, Kits A, Forssberg H, Eliasson A-C. Is outcome of constraint-induced movement therapy in unilateral cerebral palsy dependent on corticomotor projection pattern and brain lesion characteristics? *Dev Med Child Neurol*. (2014) 56:252–8. doi: 10.1111/dmcn.12353
9. Sakzewski L, Ziviani J, Boyd RN. Best responders after intensive upper-limb training for children with unilateral cerebral palsy. *Arch Phys Med Rehabil*. (2011) 92:578–84. doi: 10.1016/j.apmr.2010.12.003
10. Smorenburg ARP, Gordon AM, Kuo H-C, Ferre CL, Brandao M, Bleyenheuft Y, et al. Does corticospinal tract connectivity influence the response to intensive bimanual therapy in children with unilateral cerebral palsy? *Neurorehabil Neural Repair*. (2017) 31:250–60. doi: 10.1177/1545968316675427
11. Lawrence DG, Kuypers HG. The functional organization of the motor system in the monkey. I. The effects of bilateral pyramidal lesions. *Brain J Neurol*. (1968) 91:1–14. doi: 10.1093/brain/91.1.1
12. Eyre JA, Taylor JP, Villagra F, Smith M, Miller S. Evidence of activity-dependent withdrawal of corticospinal projections during human development. *Neurology*. (2001) 57:1543–54. doi: 10.1212/WNL.57.9.1543
13. Friel KM, Williams PT, Serradj N, Chakrabarty S, Martin JH. Activity-based therapies for repair of the corticospinal system injured during development. *Front Neurol*. (2014) 5:229. doi: 10.3389/fneur.2014.00229
14. Jaspers E, Byblow WD, Feys H, Wenderoth N. The corticospinal tract: a biomarker to categorize upper limb functional potential in unilateral cerebral palsy. *Front Pediatr*. (2016) 3:112. doi: 10.3389/fped.2015.00112
15. Staudt M. Reorganization after pre- and perinatal brain lesions. *J Anat*. (2010) 217:469–74. doi: 10.1111/j.1469-7580.2010.01262.x
16. Kuhnke N, Juenger H, Walther M, Berweck S, Mall V, Staudt M. Do patients with congenital hemiparesis and ipsilateral corticospinal projections respond differently to constraint-induced movement therapy? *Dev Med Child Neurol*. (2008) 50:898–903. doi: 10.1111/j.1469-8749.2008.03119.x
17. Holmström L, Vollmer B, Tedroff K, Islam M, Persson JK, Kits A, et al. Hand function in relation to brain lesions and corticomotor-projection pattern in children with unilateral cerebral palsy. *Dev Med Child Neurol*. (2010) 52:145–52. doi: 10.1111/j.1469-8749.2009.03496.x
18. Staudt M, Gerloff C, Grodd W, Holthausen H, Niemann G, Krageloh-Mann I. Reorganization in congenital hemiparesis acquired at different gestational ages. *Ann Neurol*. (2004) 56:854–63. doi: 10.1002/ana.20297
19. Feys H, Eyssen M, Jaspers E, Klingels K, Desloovere K, Molenaers G, et al. Relation between neuroradiological findings and upper limb function in hemiplegic cerebral palsy. *Eur J Paediatr Neurol*. (2010) 14:169–77. doi: 10.1016/j.ejpn.2009.01.004
20. Staudt M, Grodd W, Gerloff C, Erb M, Stitz J, Krägeloh-Mann I. Two types of ipsilateral reorganization in congenital hemiparesis: a TMS and fMRI study. *Brain J Neurol*. (2002) 125:2222–37. doi: 10.1093/brain/awf227
21. Friel KM, Kuo HC, Fuller J, Ferre CL, Brandao M, Carmel JB, et al. Skilled bimanual training drives motor cortex plasticity in children with unilateral cerebral palsy. *Neurorehabil Neural Repair*. (2016) 30:834–44. doi: 10.1177/1545968315625838
22. Bleyenheuft Y, Dricot L, Gilis N, Kuo HC, Grandin C, Bleyenheuft C, et al. Capturing neuroplastic changes after bimanual intensive rehabilitation in children with unilateral spastic cerebral palsy: a combined DTI, TMS and fMRI pilot study. *Res Dev Disabil*. (2015) 43–44:136–49. doi: 10.1016/j.ridd.2015.06.014
23. Marneweck M, Kuo HC, Smorenburg ARP, Ferre CL, Flamand VH, Gupta D, et al. The relationship between hand function and overlapping motor representations of the hands in the contralesional hemisphere in unilateral spastic cerebral palsy. *Neurorehabil Neural Repair*. (2018) 32:62–72. doi: 10.1177/1545968317745991
24. Charles JR, Wolf SL, Schneider JA, Gordon AM. Efficacy of a child-friendly form of constraint-induced movement therapy in hemiplegic cerebral palsy: a randomized control trial. *Dev Med Child Neurol*. (2006) 48:635–42. doi: 10.1017/S0012162206001356
25. Charles J, Gordon AM. Development of hand-arm bimanual intensive training (HABIT) for improving bimanual coordination in children with hemiplegic cerebral palsy. *Dev Med Child Neurol*. (2006) 48:931–6. doi: 10.1017/S0012162206002039
26. Gordon AM, Chinnan A, Gill S, Petra E, Hung YC, Charles J. Both constraint-induced movement therapy and bimanual training lead to improved performance of upper extremity function in children with hemiplegia. *Dev Med Child Neurol*. (2008) 50:957–8. doi: 10.1111/j.1469-8749.2008.03166.x
27. Sakzewski L, Ziviani J, Abbott DF, Macdonell RAL, Jackson GD, Boyd RN. Randomized trial of constraint-induced movement therapy and bimanual training on activity outcomes for children with congenital hemiplegia. *Dev Med Child Neurol*. (2011) 53:313–20. doi: 10.1111/j.1469-8749.2010.03859.x
28. Facchin P, Rosa-Rizzotto M, Visona Dalla Pozza L, Turconi AC, Pagliano E, Signorini S, et al. Multisite trial comparing the efficacy of constraint-induced movement therapy with that of bimanual intensive training in children with hemiplegic cerebral palsy: postintervention results. *Am J Phys Med Rehabil*. (2011) 90:539–53. doi: 10.1097/PHM.0b013e3182247076
29. Deppe W, Thuemmler K, Fleischer J, Berger C, Meyer S, Wiedemann B. Modified constraint-induced movement therapy versus intensive bimanual training for children with hemiplegia—a randomized controlled trial. *Clin Rehabil*. (2013) 27:909–20. doi: 10.1177/0269215513483764
30. Gelkop N, Burshtein DG, Lahav A, Brezner A, Al-Oraibi S, Ferre CL, et al. Efficacy of constraint-induced movement therapy and bimanual training in children with hemiplegic cerebral palsy in an educational setting. *Phys Occup Ther Pediatr*. (2015) 35:24–39. doi: 10.3109/01942638.2014.925027
31. Juenger H, Kuhnke N, Braun C, Ummenhofer F, Wilke M, Walther M, et al. Two types of exercise-induced neuroplasticity in congenital hemiparesis: a transcranial magnetic stimulation, functional MRI, and magnetoencephalography study. *Dev Med Child Neurol*. (2013) 55:941–51. doi: 10.1111/dmcn.12209
32. Murase N, Duque J, Mazzocchio R, Cohen LG. Influence of interhemispheric interactions on motor function in chronic stroke. *Ann Neurol*. (2004) 55:400–9. doi: 10.1002/ana.10848
33. Staudt M, Braun C, Gerloff C, Erb M, Grodd W, Krägeloh-Mann I. Developing somatosensory projections bypass periventricular brain lesions. *Neurology*. (2006) 67:522–5. doi: 10.1212/01.wnl.0000227937.49151.fd
34. Gordon AM, Charles J, Wolf SL. Methods of constraint-induced movement therapy for children with hemiplegic cerebral palsy: development of a child-friendly intervention for improving upper-extremity function. *Arch Phys Med Rehabil*. (2005) 86:837–44. doi: 10.1016/j.apmr.2004.10.008
35. Shea CH, Wright DL. Contextual dependencies: influence on response latency. *Memory*. (1995) 3:81–95. doi: 10.1080/09658219508251498
36. Krumlinde-sundholm L, Eliasson A-C. Development of the assisting hand assessment: a rasch-built measure intended for children with unilateral upper limb impairments. *Scand J Occup Ther*. (2003) 10:16–26. doi: 10.1080/11038120310004529
37. Krumlinde-Sundholm L, Holmefur M, Kottorp A, Eliasson AC. The assisting hand assessment: current evidence of validity, reliability, and responsiveness to change. *Dev Med Child Neurol*. (2007) 49:259–64. doi: 10.1111/j.1469-8749.2007.00259.x

38. Krumlinde-Sundholm L. Reporting outcomes of the assisting hand assessment: what scale should be used? *Dev Med Child Neurol*. (2012) 54:807–8. doi: 10.1111/j.1469-8749.2012.04361.x
39. Jebsen RH, Taylor N, Trieschmann RB, Trotter MJ, Howard LA. An objective and standardized test of hand function. *Arch Phys Med Rehabil*. (1969) 50:311–9.
40. Taylor N, Sand PL, Jebsen RH. Evaluation of hand function in children. *Arch Phys Med Rehabil*. (1973) 54:129–35.
41. Araneda R, Ebner-Karestinos D, Paradis J, Saussez G, Friel KM, Gordon AM, et al. Reliability and responsiveness of the Jebsen-Taylor Test of Hand Function and the Box and Block Test for children with cerebral palsy. *Dev Med Child Neurol*. (2019) 61:1182–8. doi: 10.1111/dmcn.14184
42. Mathiowetz V, Federman S, Wiemer D. Box and block test of manual dexterity: norms for 6-19 year olds. *Can J Occup Ther*. (1985) 52:241–5. doi: 10.1177/000841748505200505
43. Law M, Baptiste S, McColl M, Opzoomer A, Polatajko H, Pollock N. The Canadian occupational performance measure: an outcome measure for occupational therapy. *Can J Occup Ther Revue Canadienne d'ergotherapie*. (1990) 57:82–7. doi: 10.1177/000841749005700207
44. Verkerk GJ, Wolf MJ, Louwers AM, Meester-Delver A, Nollet F. The reproducibility and validity of the Canadian occupational performance measure in parents of children with disabilities. *Clin Rehabil*. (2006) 20:980–8. doi: 10.1177/0269215506070703
45. Arnould C, Penta M, Renders A, Thonnard JL. ABILHAND-Kids: a measure of manual ability in children with cerebral palsy. *Neurology*. (2004) 63:1045–52. doi: 10.1212/01.WNL.0000138423.77640.37
46. Bleyenheuft Y, Gordon AM, Rameckers E, Thonnard JL, Arnould C. Measuring changes of manual ability with ABILHAND-Kids following intensive training for children with unilateral cerebral palsy. *Dev Med Child Neurol*. (2017) 59:505–11. doi: 10.1111/dmcn.13338
47. Feldman AB, Haley SM, Coryell J. Concurrent and construct validity of the pediatric evaluation of disability inventory. *Phys Ther*. (1990) 70:602–10. doi: 10.1093/ptj/70.10.602
48. Haley SM, New England Medical Center H, PEDI Research Group. *Pediatric Evaluation of Disability Inventory (PEDI)*. Boston, MA: PEDI Research Group (1992).
49. Kuo HC, Ferre CL, Carmel JB, Gowatsky JL, Stanford AD, Rowny SB, et al. Using diffusion tensor imaging to identify corticospinal tract projection patterns in children with unilateral spastic cerebral palsy. *Dev Med Child Neurol*. (2017) 59:65–71. doi: 10.1111/dmcn.13192
50. Rothwell JC, Hallett M, Berardelli A, Eisen A, Rossini P, Paulus W. Magnetic stimulation: motor evoked potentials. The international federation of clinical neurophysiology. *Electroencephalogr Clin Neurophysiol Suppl*. (1999) 52:97–103.
51. Paixão S, Balijepalli A, Serradj N, Niu J, Luo W, Martin JH, et al. EphrinB3/EphA4-mediated guidance of ascending and descending spinal tracts. *Neuron*. (2013) 80:1407–20. doi: 10.1016/j.neuron.2013.10.006
52. Serradj N, Paixão S, Sobocki T, Feinberg M, Klein R, Kullander K, et al. EphA4-mediated ipsilateral corticospinal tract misprojections are necessary for bilateral voluntary movements but not bilateral stereotypic locomotion. *J Neurosci*. (2014) 34:5211–21. doi: 10.1523/JNEUROSCI.4848-13.2014
53. Simon-Martinez C, Mailleux L, Hoskens J, Ortibus E, Jaspers E, Wenderoth N, et al. Randomized controlled trial combining constraint-induced movement therapy and action-observation training in unilateral cerebral palsy: clinical effects and influencing factors of treatment response. *Ther Adv Neurol Disord*. (2020) 13:1756286419898065. doi: 10.1177/1756286419898065
54. Jackman M, Lannin N, Galea C, Sakzewski L, Miller L, Novak I. What is the threshold dose of upper limb training for children with cerebral palsy to improve function? A systematic review. *Aust Occup Ther J*. (2020) 67:269–80. doi: 10.1111/1440-1630.12666
55. Sakzewski L, Provan K, Ziviani J, Boyd RN. Comparison of dosage of intensive upper limb therapy for children with unilateral cerebral palsy: how big should the therapy pill be? *Res Dev Disabil*. (2015) 37:9–16. doi: 10.1016/j.ridd.2014.10.050
56. Kleim JA, Barbay S, Cooper NR, Hogg TM, Reidel CN, Remple MS, et al. Motor learning-dependent synaptogenesis is localized to functionally reorganized motor cortex. *Neurobiol Learn Mem*. (2002) 77:63–77. doi: 10.1006/nlme.2000.4004
57. Friel K, Chakrabarty S, Kuo H-C, Martin J. Using motor behavior during an early critical period to restore skilled limb movement after damage to the corticospinal system during development. *J Neurosci*. (2012) 32:9265–76. doi: 10.1523/JNEUROSCI.1198-12.2012
58. Schertz M, Shiran SI, Myers V, Weinstein M, Fattal-Valevski A, Artzi M, et al. Imaging predictors of improvement from a motor learning-based intervention for children with unilateral cerebral palsy. *Neurorehabil Neural Repair*. (2015) 30:647–60. doi: 10.1177/1545968315613446
59. Simon-Martinez C, Jaspers E, Alaerts K, Ortibus E, Balsters J, Mailleux L, et al. Influence of the corticospinal tract wiring pattern on sensorimotor functional connectivity and clinical correlates of upper limb function in unilateral cerebral palsy. *Sci Rep*. (2019) 9:8230. doi: 10.1038/s41598-019-44728-9
60. Brown JK, van Rensburg F, Walsh G, Lakie M, Wright GW. A neurological study of hand function of hemiplegic children. *Dev Med Child Neurol*. (1987) 29:287–304. doi: 10.1111/j.1469-8749.1987.tb02482.x
61. Gordon AM, Duff SV. Fingertip forces during object manipulation in children with hemiplegic cerebral palsy. I: anticipatory scaling. *Dev Med Child Neurol*. (1999) 41:166–75. doi: 10.1017/S0012162299000353
62. Arnfield E, Guzzetta A, Boyd R. Relationship between brain structure on magnetic resonance imaging and motor outcomes in children with cerebral palsy: a systematic review. *Res Dev Disabil*. (2013) 34:2234–50. doi: 10.1016/j.ridd.2013.03.031
63. Gupta D, Barachant A, Gordon AM, Ferre C, Kuo HC, Carmel JB, et al. Effect of sensory and motor connectivity on hand function in pediatric hemiplegia. *Ann Neurol*. (2017) 82:766–80. doi: 10.1002/ana.25080
64. Staudt M. Reorganization of the developing human brain after early lesions. *Dev Med Child Neurol*. (2007) 49:564. doi: 10.1111/j.1469-8749.2007.00564.x
65. Ferre CL, Carmel JB, Flamand VH, Gordon AM, Friel KM. Anatomical and functional characterization in children with unilateral cerebral palsy: an atlas-based analysis. *Neurorehabil Neural Repair*. (2020) 34:148–58. doi: 10.1177/1545968319899916
66. Weinstein M, Green D, Geva R, Schertz M, Fattal-Valevski A, Artzi M, et al. Interhemispheric and intrahemispheric connectivity and manual skills in children with unilateral cerebral palsy. *Brain Struct Func*. (2014) 219:1025–40. doi: 10.1007/s00429-013-0551-5
67. Ferre C, Brandao M, Chin K, Flamand V, Bonouvrie-Smorenburg A, Campos T, et al. Improvements in hand function after unimanual or bimanual training are independent of corticospinal tract laterality. *Dev Med Child Neurol*. (2020) 62:36.

Conflict of Interest: The authors declare that the research was conducted in the absence of any commercial or financial relationships that could be construed as a potential conflict of interest.

Copyright © 2021 Friel, Ferre, Brandao, Kuo, Chin, Hung, Robert, Flamand, Smorenburg, Bleyenheuft, Carmel, Campos and Gordon. This is an open-access article distributed under the terms of the Creative Commons Attribution License (CC BY). The use, distribution or reproduction in other forums is permitted, provided the original author(s) and the copyright owner(s) are credited and that the original publication in this journal is cited, in accordance with accepted academic practice. No use, distribution or reproduction is permitted which does not comply with these terms.

frontiers in Neurology

CASE REPORT
published: 14 May 2021
doi: 10.3389/fneur.2021.662910

Deep Brain Stimulation in KMT2B-Related Dystonia: Case Report and Review of the Literature With Special Emphasis on Dysarthria and Speech

*Maria Abel[1], Robert Pfister[1], Iman Hussein[2], Fahd Alsalloum[2], Christina Onyinzo[1], Simon Kappl[2], Michael Zech[3,4], Walter Demmel[1], Martin Staudt[2], Manfred Kudernatsch[1,5] and Steffen Berweck[2,6]**

[1] Department of Neurosurgery and Epilepsy Surgery, Spine- and Scoliosis Surgery, Schön Klinik Vogtareuth, Vogtareuth, Germany, [2] Departmemt of Pediatric Neurology, Neuro-Rehabilitation and Epileptology, Schön Klinik Vogtareuth, Vogtareuth, Germany, [3] Helmholtz Centre Munich, Institute of Neurogenomics, Neuherberg, Germany, [4] Institute of Human Genetics, Technical University of Munich, Munich, Germany, [5] Research Institute Rehabilitation, Transition, Palliation, Paracelsus Medical University, Salzburg, Austria, [6] Dr. Von Hauner Children's Hospital, Ludwig-Maximilians- University Munich, Munich, Germany

Objective: KMT2B-related dystonia is a progressive childhood-onset movement disorder, evolving from lower-limb focal dystonia into generalized dystonia. With increasing age, children frequently show prominent laryngeal or facial dystonia manifesting in dysarthria. Bilateral deep brain stimulation of the globus pallidus internus (GPi-DBS) is reported to be an efficient therapeutic option. Especially improvement of dystonia and regaining of independent mobility is commonly described, but detailed information about the impact of GPi-DBS on dysarthria and speech is scarce.

Methods: We report the 16-months outcome after bilateral GPi-DBS in an 8-year-old child with KMT2B-related dystonia caused by a *de-novo* c.3043C>T (p.Arg1015*) non-sense variant with special emphasis on dysarthria and speech. We compare the outcome of our patient with 59 patients identified through a PubMed literature search.

Results: A remarkable improvement of voice, articulation, respiration and prosodic characteristics was seen 16 months after GPi-DBS. The patients' speech intelligibility improved. His speech became much more comprehensible not only for his parents, but also for others. Furthermore, his vocabulary and the possibility to express his feelings and wants expanded considerably.

Conclusion: A positive outcome of GPi-DBS on speech and dysarthria is rarely described in the literature. This might be due to disease progression, non-effectiveness of DBS or due to inadvertent spreading of the electrical current to the corticobulbar

OPEN ACCESS

Edited by:
Volker Mall, Technical University of Munich, Germany

Reviewed by:
Leonardo Almeida, University of Florida, United States
Laura Cif, Université de Montpellier, France
Takashi Tsuboi, Nagoya University, Japan

***Correspondence:**
Steffen Berweck
SBerweck@schoen-klinik.de

Specialty section:
This article was submitted to Pediatric Neurology, a section of the journal Frontiers in Neurology

Received: *01 February 2021*
Accepted: *12 April 2021*
Published: *14 May 2021*

Citation:
Abel M, Pfister R, Hussein I, Alsalloum F, Onyinzo C, Kappl S, Zech M, Demmel W, Staudt M, Kudernatsch M and Berweck S (2021) Deep Brain Stimulation in KMT2B-Related Dystonia: Case Report and Review of the Literature With Special Emphasis on Dysarthria and Speech. Front. Neurol. 12:662910. doi: 10.3389/fneur.2021.662910

tract causing stimulation induced dysarthria. This highlights the importance of optimal lead placement, the possibility of horizontal steering of the electrical field by applying directional stimulation with segmented leads as well as the use of the lowest possible effective stimulation intensity.

Keywords: KMT2B-related dystonia, globus pallidus internus, internal capsule, dysarthria, case report, deep brain stimulation

INTRODUCTION

Dystonia is a movement disorder characterized by abnormal and uncontrolled hyperkinetic movements as a result of sustained or intermittent muscle contractions (1). Dystonic symptoms can affect only one or several sites of the body, resulting in twisting and repetitive postures and movements (2). The etiology of dystonias is quite heterogeneous (3). With the advancement of next-generation sequencing techniques, several genetic causes of isolated and combined dystonia have been identified (4). Since 2016, several mutations in the *KMT2B* gene have been identified as a new etiology of early-onset dystonia (5–9). *KMT2B*-related dystonia is a progressive childhood-onset disorder, commonly evolving from a focal, mainly lower-limb dystonia into generalized dystonia with cranio-cervical involvement. Further clinical characteristics such as intellectual disability, psychiatric comorbidities and dysmorphic features have been reported in several patients with *KMT2B*-related dystonia (7). Bilateral deep brain stimulation of the globus pallidus internus (GPi-DBS) has been reported as an efficient therapeutic option. Especially improvement of the movement disorder and regaining of independent mobility is commonly described (8). Dysarthria is one of the most commonly described stimulation-induced side effects when GPi-DBS is used in dystonia (10). Nevertheless, detailed information about the impact of GPi-DBS on speech in *KMT2B*-related dystonia is scarce. Here, we report the 16-months outcome after bilateral GPi-DBS in an 8-year-old child with *KMT2B*-related dystonia with special emphasis on dysarthria and speech. We compare the outcome of our patient with 59 patients identified through a PubMed literature search.

CASE REPORT

A 6-year-old Arabic boy with generalized dystonia affecting the limbs, trunk, cervical muscles and facial muscles, resulting in severe disability in gait, speech and daily life activities was admitted to our inpatient department.

Pregnancy, perinatal, birth and early infantile history were unremarkable. Gross motor development was normal until the age of 3 years, when the child started limping. Few months later, he lost the ability to walk and reverted to crawling. After several years, dystonia also involved the cervical, oromandibular and laryngeal muscles, as well as both upper limbs. The patients' speech and language development were delayed: At the age of 18 months, the child could pronounce "dad" and "mum." At the age of 2 years, the patient could speak two-word sentences in Arabic and English. Swallowing and chewing have not been affected by dystonia. The development of social and cognitive skills has also been delayed. Psychiatric comorbidities have not been reported.

On admission, the patient presented with already generalized dystonia and severe dysarthria. The child was wheelchair bound and sat unsteadily. Dystonia symptoms worsened at night, resulting in frequent nocturnal restlessness. Physical examination revealed intermittent myoclonus in both legs but no spasticity or other neurological symptoms. The patient showed developmental delay, a short stature (percentile: $<$ 3) and low body weight (percentile: $<$ 3). His face showed no dysmorphic features. The family history was negative for neurologic conditions. The Burke-Fahn-Marsden Dystonia Rating Scale (BFMDRS) score was 59 of 120 on the dystonia movement scale and 22 of 30 on the disability scale. Magnetic Resonance Imaging (MRI) of the brain and spine revealed no abnormalities. Also in retrospect, no symmetrical hypointensities of the globus pallidi commonly described in *KMT2B* mutations were present. Lumbar puncture to analyze neurotransmitters was denied.

Trio whole-exome sequencing, performed in a diagnostic laboratory had shown that the patient carried a heterozygous *de-novo* non-sense variant, c.3043C>T (p.Arg1015*), in *KMT2B* (11). According to American College of Medical Genetics & Genomics (ACMG) criteria, the variant was classified as "pathogenic."

The patient was treated with retarded Carbidopa 25 mg / Levodopa 100 mg and Gabapentin 300 mg. The dystonic movement disorder did not improve significantly. The dystonia was generalized, and therefore injections of botulinum toxin were not performed.

After intensive rehabilitation including orthotic management and supplying the patient with a posterior walker, the child could walk a few steps (see Video 2 in the **Supplementary Material**). For longer distances a wheelchair was necessary.

After an extensive interdisciplinary discussion, GPi-DBS was performed at the age of eight years under general anesthesia. Stereotactic planning was done with the Brainlab Elements software, using MRI T1- and T2- sequences (T1 1 mm isotropic 3D with Gadolinium and T2 space 0.65 mm isotropic). The GPi could be visualized on the T2- images, as shown in **Figure 1**. Stereotactical electrode placement was done with a Leksell Multipurpose Arc G-Frame. Directional leads (Model Vercise TM Cartesia directional Lead, Boston Scientific), targeting the caudal part of the GPi were implanted successfully and a rechargeable as well as MRI-compatible impulse generator (Model Gevia Boston Scientific) was placed subcutaneously in the right infraclavicular region. Correct position of the leads was confirmed by postoperative computed tomography (CT) and

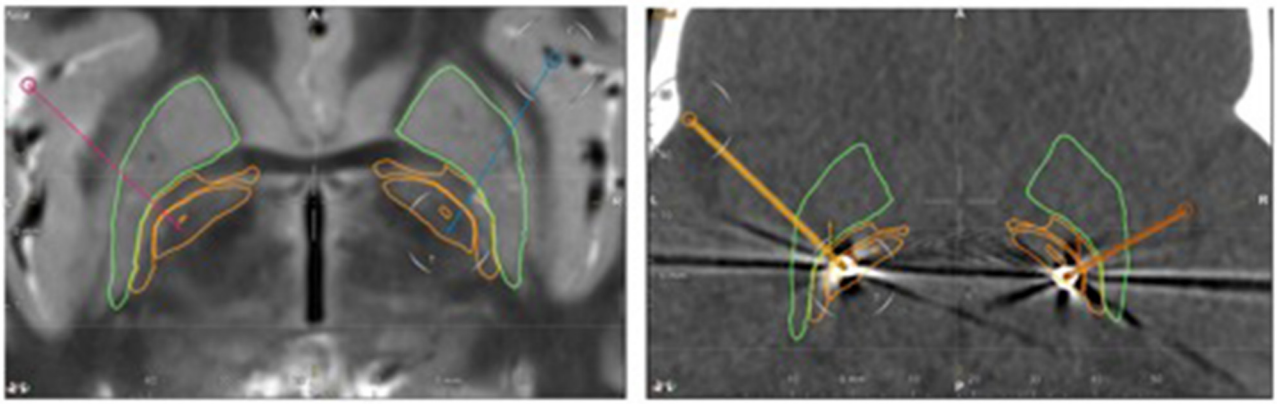

FIGURE 1 | Left: Pre-operative axial T2-weighted MRI. Stereotactic planning performed with the Brainlab Elements software shows the planned trajectories (red and blue line). Right: postoperative axial CT. The pre-calculated electrode position is projected to the CT artifacts of the real electrode (yellow on the right side, orange on the left side). The leads are located within the caudal part of the GPi. Green outline: putamen, outer orange outline: globus pallidus externus, inner orange outline: globus pallidus internus.

image fusion to the planning scans in Brainlab Elements (see **Figure 1**).

Initially the amplitude was set to 2 mA on both sides with a pulse width of 80 μs and a frequency of 130 Hz. Due to the short attention span, a structured test by monopolar review at each contact was not possible. Therefore, we decided to start a non-segmental stimulation at contact 2–4 on the left and 10–12 on the right side. During the following weeks, we tested different amplitudes of 2–4 mA and pulse widths between 80 and 100 μs. A clinical improvement was already observed after several days, especially for motor symptoms of the arms and legs but speech did not improve at the same pace. During subsequent visits, we changed the programming at the right lead to a segmental stimulation with a current flow steering to a lateral direction (contact 10:25, 11:0, 12:75%). Parallel to this change the parents noticed a reduced stiffness in the left arm during active movements and a significant, but still variable improvement of speech fluency in addition to the already achieved amelioration of symptoms.

Six and sixteen months after surgery, the boy underwent a follow-up investigation and neurological rehabilitation. Six months after surgery, his father reported impressive improvement of dystonia. The child had already achieved independent walking. Nocturnal restlessness and involuntary motor movements had disappeared. On admission, the patient appeared more settled, confident and focused. His concentration, and consequently, his performance in activities of daily living had significantly improved. The BFMDRS score 6 months after GPi-DBS was considerably reduced, counting 28 of 120 (reduction of eight points in the categories "mouth/speech/swallowing" and 23 points in the categories "trunk/extremities") on the dystonia movement scale and 11 of 30 on the disability scale.

An amelioration in speech and dysarthria after GPi-DBS was noticed. The modified Bogenhausen Dysarthria Scales as a clinical assessment with a defined scoring system (0 = most severe disorder; 1 = severe disorder; 2 = moderate disorder; 3 = mild disorder; 4 = no disorder) were applied before GPi-DBS as well as 6 and 16 months after surgery, by an Arabic speaking doctor and an Arabic speaking speech therapist. A moderate improvement from scale 1 to scale 2 was seen in articulation, voice quality, speech fluency and prosodic characteristics 6 months after surgery. A remarkable improvement from scale 1 to scale 3 was seen in articulation, voice quality, speech fluency and prosodic characteristics 16 months after surgery. The patients' speech intelligibility improved as well. His speech became much more comprehensible not only for his parents, but also for others. Furthermore, his vocabulary and the possibility to express his feelings and wants expanded considerably (Video 1 in the **Supplementary Material** shows the child counting in Arabic before and 16 months after GPi-DBS).

LITERATURE REVIEW

We did not follow the methodology of a systematic review. We analyzed the cohort studies performed by Cif et al. (7) and Zech et al. (8) as these studies are the largest KMT2B-DBS cohorts reported to date. Further, we have performed a PubMed Search using the terms "*KMT2B*" and "*dystonia*" and Deep Brain stimulation.

We identified 15 studies including a total of 59 patients with *KMT2B*-related dystonia who underwent DBS between 2016 and 2020 (see Table 1 in the **Supplementary Material**).

In 56 cases, the GPi was targeted for lead implantation. In one case, the leads were implanted within the subthalamic nucleus. In two cases, lead placement was not described.

In 3/59 patients, improvement of speech ("articulation"/"dysphonia"/"orolingual dystonia") was described (12–14). Amelioration of jaw opening dystonia was reported in 2/59 cases (5, 15). Persisting dysarthria/dysphonia after performance of DBS was described in 4/59 patients (6, 8, 13, 16). In 50/59 patients, the outcome of dysarthria and speech after DBS has not been specifically described.

Cif et al. reported a total of 18 patients with *KMT2B*-related dystonia who underwent GPi-DBS. In this study cohort, only 3.4 % of all patients showed benefit on speech at the last assessment (7). Carecchio et al. (9) reported eight patients with *KMT2B*-related dystonia, who underwent GPi-DBS. They observed laryngeal dystonia in some patients only after DBS was performed (9).

DISCUSSION

We report the 16-months GPi-DBS outcome of an 8-year-old child with *KMT2B*-related generalized dystonia.

Since 2016, mutations in the *KMT2B* gene have been identified in patients with early-onset dystonia (5–9). *KMT2B* encodes a lysine-specific histone methyltransferase, which is involved in an important methylation process for epigenetic modification linked to active gene transcription (17). Dysfunction or haploinsufficiency of *KMT2B* is assumed to affect the downstream expression of key genes that regulate neurodevelopment and motor control (7). *KMT2B*-related dystonia typically presents in childhood, commonly evolving from a lower-limb dystonia into generalized dystonia with cranio-cervical involvement (5–7). In our case, dystonia also started in the lower limbs, involving the cervical, oromandibular, and laryngeal muscles as well as the trunk and upper limbs a few years later. The median onset of age of *KMT2B*-related dystonia is reported to be 6 years, varying according to the subtype of *KMT2B* variants (17). In our patient, dystonia symptoms started at the age of 3 years. Facial dysmorphic features, developmental delay and intellectual disability are frequently observed in *KMT2B*-related dystonia patients as non-dystonic abnormalities (8, 17). Our patient showed development delay including short stature, low body weight and microcephaly as well as poor development of speech and language. There were no facial dysmorphic features.

Bilateral GPi-DBS is reported to be an overall efficient therapeutic option. Especially improvements of the movement disorder and regaining of independent mobility are commonly described (8). Oromandibular involvement of dystonia frequently results in disorders in speech and articulation in *KMT2B*-related dystonia (7–9). Furthermore, dysarthria additionally can occur as stimulation-induced side effect of GPi-DBS. A differentiation between dysarthria as a symptom of dystonia, regarding orofacial and buccolingual dystonia, that may or may not be responsive to GPi-DBS and dysarthria as a result of stimulation-induced side effect is necessary. In primary dystonia, the most common stimulation-induced side effect of GPi-DBS is reported to be dysarthria with a prevalence of up to 12 %. Dystonic patients who underwent DBS described a slowing of speech as well as requiring more effort for speech production even without clinically evident dysarthria (10). In terms of the established literature, studies with detailed information about the impact of GPi-DBS on dysarthria and speech in *KMT2B*-related dystonia are scarce. Speech disturbances can, however, severely impair the patients' quality of life. In only 3/59 patients in the literature, improvement of speech has been described (12–14). Nevertheless, persisting dysarthria / dysphonia after performance of DBS has been reported in 4/59 patients (6, 8, 13, 16). In addition, Carecchio et al. observed no improvement or even newly developing laryngeal dystonia in some *KMT2B* patients only after DBS was performed (9). The underlying cause is not described, but probably related to laryngeal dystonia associated with the progression of disease.

In this case report, the patient presented with orofacial dystonia, which was responsive to GPi-DBS. Further, a stimulation-induced side effect resulting in dysarthria did not occur. Dysarthria as well as delayed speech and language development were identified and assessed before performance of GPi-DBS in our case. According to the modified Bogenhausen Dysarthria Scales, a remarkable improvement of voice, articulation, respiration and prosodic characteristics were found 16 months after GPi-DBS. Furthermore, the patient's vocabulary and the possibility to express his feelings and wants expanded considerably after surgery.

Up to now, little is known about possible mechanisms of stimulation-induced changes in speech associated with GPi-DBS. A possible neuroanatomical mechanism is described as an inadvertent spreading of the electrical current to the corticobulbar tract in the adjacent internal capsule that represents the face region somatotopically (18). Therefore, higher stimulation intensities as well as more posterior location of active lead contacts could result in stimulation-induced dysarthria associated with undesirable spreading of the stimulation to the corticobulbar tract in the adjacent internal capsule (10).

Stimulation settings, as well as specific positioning of the leads into the GPi, have not been described in the cases with improvement of speech after GPi-DBS identified in our literature review. We assume that the positive effects on dysarthria and speech in our case are achieved by low stimulation intensity, avoiding stimulation of the corticobulbar tract by lead positioning within the caudal part of the GPi, and horizontal steering of the electrical field, using the features of the directional DBS-leads. A standardized protocol to test directional vs. non-directional stimulation would be useful for every patient, but in the majority of our pediatric patients and in the patient reported in this case report, the compliance does not allow this lengthy procedure.

Moreover, our patient seemed to have a huge potential for speech development, which he could not take advantage of because of the severity of the dystonia. Therefore, minimizing dystonia-related disorders regarding speech as well as movement disturbances led to impressive amelioration in speech after GPi-DBS implantation.

One important limitation of our case report is the short follow-up after GPi-DBS. We take into consideration that our patient was very young at time of surgery. Performing GPi-DBS surgery is a symptomatic treatment. The course of disease cannot be influenced. Therefore, the disease can progress despite ongoing efficient DBS therapy. As *KMT2B*-related dystonia is a progressive disease, a long-term follow-up is necessary. A

decrease and even loss of stimulation effect as well as disease progression in our patient could occur in the future.

CONCLUSION

Our case report demonstrates an improvement of dysarthria and speech after GPi-DBS in an 8-year old boy with *KMT2B*-related generalized dystonia.

A positive outcome of GPi-DBS on speech and dysarthria is rarely described in the literature. This might be due to disease progression, non-effectiveness of DBS or due to inadvertent spreading of the electrical current to the corticobulbar tract causing stimulation induced dysarthria. This highlights the importance of optimal lead placement, the possibility of horizontal steering of the electrical field by applying directional stimulation with segmented leads as well as the use of the lowest possible effective stimulation intensity. Future studies should implicate specific speech and articulation outcome assessments before and after performance of GPi-DBS associated with *KMT2B*-related dystonia as well as long-term outcomes after GPi-DBS.

DATA AVAILABILITY STATEMENT

The original contributions presented in the study are included in the article/**Supplementary Materials**, further inquiries can be directed to the corresponding author/s.

ETHICS STATEMENT

Ethical review and approval was not required for the study on human participants in accordance with the local legislation and institutional requirements. Written informed consent to participate in this study was provided by the participants' legal guardian/next of kin. Written informed consent was obtained from the minor(s)' legal guardian/next of kin for the publication of any potentially identifiable images or data included in this article.

AUTHOR CONTRIBUTIONS

MA and SB planned the article concept and design. RP and WD performed the surgery planning. WD and RP performed the surgery. IH and FA conducted the modified Bogenhausen Dysarthria Scales. MA performed the literature review. MA wrote the manuscript with support from RP, MZ, MS, and SB. All authors discussed the results and contributed to the final manuscript.

SUPPLEMENTARY MATERIAL

The Supplementary Material for this article can be found online at: https://www.frontiersin.org/articles/10.3389/fneur.2021.662910/full#supplementary-material

REFERENCES

1. Albanese A, Bhatia K, Bressman SB, Delong MR, Fahn S, Fung VS, et al. Phenomenology and classification of dystonia: a consensus update. *Mov Disord.* (2013) 28:863–73. doi: 10.1002/mds.25475
2. Charlesworth G, Bhatia KP. Primary and secondary dystonic syndromes: an update. *Curr Opin Neurol.* (2013) 26:406–12. doi: 10.1097/WCO.0b013e3283633696
3. Jinnah HA, Alterman R, Klein C, Krauss JK, Moro E, Vidailhet M, et al. Deep brain stimulation for dystonia: a novel perspective on the value of genetic testing. *J Neural Transm.* (2017) 124:417–30. doi: 10.1007/s00702-016-1656-9
4. Lohmann K, Klein C. Update on the genetics of dystonia. *Curr Neurol Neurosci Rep.* (2017) 17:26. doi: 10.1007/s11910-017-0735-0
5. Meyer E, Carss KJ, Rankin J, Nichols JM, Grozeva D, Joseph AP, et al. Mutations in the histone methyltransferase gene KMT2B cause complex early-onset dystonia. *Nat Genet.* (2017) 49:223–37. doi: 10.1038/ng.3740
6. Zech M, Boesch S, Maier EM, Borggraefe I, Vill K, Laccone F, et al. Haploinsufficiency of KMT2B, encoding the lysine-specific histone methyltransferase 2b, results in early-onset generalized dystonia. *Am J Hum Genet.* (2016) 99:1377–87. doi: 10.1016/j.ajhg.2016.10.010
7. Cif L, Demailly D, Lin JP, Barwick KE, Sa M, Abela L, et al. KMT2B-related disorders: expansion of the phenotypic spectrum and long-term efficacy of deep brain stimulation. *Brain.* (2020) 143:3242–61. doi: 10.1093/brain/awaa304
8. Zech M, Lam DD, Winkelmann J. Update on KMT2B-Related dystonia. *Curr Neurol Neurosci Rep.* (2019) 19:92. doi: 10.1007/s11910-019-1007-y
9. Carecchio M, Invernizzi F, Gonzàlez-Latapi P, Panteghini C, Zorzi G, Romito L, et al. Frequency and phenotypic spectrum of KMT2B dystonia in childhood: a single-center cohort study. *Mov Disord.* (2019) 34:1516–27. doi: 10.1002/mds.27771
10. Pauls KAM, Bröckelmann PJ, Hammesfahr S, Becker J, Hellerbach A, Visser-Vandewalle V, et al. Dysarthria in pallidal deep brain stimulation in dystonia depends on the posterior location of active electrode contacts: a pilot study. *Parkinsonism Relat Disord.* (2018) 47:71–5. doi: 10.1016/j.parkreldis.2017.11.002
11. Mahfouz NA, Kizhakkedath P, Ibrahim A, El Naofal M, Ramaswamy S, Harilal D, et al. Utility of clinical exome sequencing in a complex emirati pediatric cohort. *Comput Struct Biotechnol J.* (2020) 18:1020–7. doi: 10.1016/j.csbj.2020.04.013
12. Li XY, Dai LF, Wan XH, Guo Y, Dai Y, Li SL, et al. Clinical phenotypes, genotypes and treatment in Chinese dystonia patients with KMT2B variants. *Parkinsonism Relat Disord.* (2020) 77:76–82. doi: 10.1016/j.parkreldis.2020.06.002
13. Kawarai T, Miyamoto R, Nakagawa E, Koichihara R, Sakamoto T, Mure H, et al. Phenotype variability and allelic heterogeneity in KMT2B-Associated disease. *Parkinsonism Relat Disord.* (2018) 52:55–61. doi: 10.1016/j.parkreldis.2018.03.022
14. Cao Z, Yao H, Bao X, Wen Y, Liu B, Wang S, et al. DYT28 responsive to pallidal deep brain stimulation. *Mov Disord Clin Pract.* (2020) 7:97–9. doi: 10.1002/mdc3.12862

15. Kumar KR, Davis RL, Tchan MC, Wali GM, Mahant N, Ng K, et al. Whole genome sequencing for the genetic diagnosis of heterogenous dystonia phenotypes. *Parkinsonism Relat Disord.* (2019) 69:111–8. doi: 10.1016/j.parkreldis.2019.11.004
16. Garrido C, Simonet C, Marti MJ, Perez-Duenas B, Valldeoriola. Good response to bilateral GPI-DBS after 2 years in generalized dystonia due to a mutation in the KMT2B gene (DYT28). Mov. Disorder. (2018) 33 (Suppl. 2).
17. Mun JK, Kim AR, Ahn JH, Kim M, Cho JW, Lee JI, et al. Successful pallidal stimulation in a patient with KMT2B-related dystonia. *J Mov Disord.* (2020) 13:154–8. doi: 10.14802/jmd.19087
18. Risch V, Staiger A, Ziegler W, Ott K, Schölderle T, Pelykh O, et al. How does GPi-DBS affect speech in primary dystonia? *Brain Stimul.* (2015) 8:875–80. doi: 10.1016/j.brs.2015.04.009

Conflict of Interest: WD serves as a teacher of implantation techniques to Boston Scientific, Inc. and receives compensation for these services.

The remaining authors declare that the research was conducted in the absence of any commercial or financial relationships that could be construed as a potential conflict of interest.

The handling Editor declared a shared affiliation, though no other collaboration, with one of the authors MZ.

Copyright © 2021 Abel, Pfister, Hussein, Alsalloum, Onyinzo, Kappl, Zech, Demmel, Staudt, Kudernatsch and Berweck. This is an open-access article distributed under the terms of the Creative Commons Attribution License (CC BY). The use, distribution or reproduction in other forums is permitted, provided the original author(s) and the copyright owner(s) are credited and that the original publication in this journal is cited, in accordance with accepted academic practice. No use, distribution or reproduction is permitted which does not comply with these terms.

frontiers in Pediatrics

BRIEF RESEARCH REPORT
published: 31 May 2021
doi: 10.3389/fped.2021.660096

Non-verbal Intelligence in Unilateral Perinatal Stroke Patients With and Without Epilepsies

Alisa Gschaidmeier[1,2], Magdalena Heimgärtner[1], Lukas Schnaufer[1,3], Pablo Hernáiz Driever[4], Marko Wilke[1,3], Karen Lidzba[1,5] and Martin Staudt[1,2]*

[1] Department of Pediatric Neurology and Developmental Medicine, University Children's Hospital, Tübingen, Germany, [2] Center for Pediatric Neurology, Neurorehabilitation and Epileptology, Schön Klinik Vogtareuth, Vogtareuth, Germany, [3] Experimental Pediatric Neuroimaging, Children's Hospital and Department of Neuroradiology, University Hospital, Tübingen, Germany, [4] Department of Pediatric Oncology and Hematology, Berlin Institute of Health, Charité-Universitätsmedizin Berlin, Freie Universität Berlin, Humboldt-Universität zu Berlin, Berlin, Germany, [5] Division of Neuropediatrics, Development, and Rehabilitation, University Children's Hospital Inselspital, Bern University Hospital, University of Bern, Bern, Switzerland

OPEN ACCESS

Edited by:
Volker Mall, Technical University of Munich, Germany

Reviewed by:
Patricia Rzezak, University of São Paulo, Brazil
Lino Nobili, University of Genoa, Italy
Chao-Ying Chen, Hong Kong Polytechnic University, China

***Correspondence:**
Alisa Gschaidmeier
agschaidmeier@schoen-klinik.de

Specialty section:
This article was submitted to Pediatric Neurology, a section of the journal Frontiers in Pediatrics

Received: *28 January 2021*
Accepted: *06 May 2021*
Published: *31 May 2021*

Citation:
Gschaidmeier A, Heimgärtner M, Schnaufer L, Hernáiz Driever P, Wilke M, Lidzba K and Staudt M (2021) Non-verbal Intelligence in Unilateral Perinatal Stroke Patients With and Without Epilepsies. Front. Pediatr. 9:660096. doi: 10.3389/fped.2021.660096

Background: The risk factors for impaired cognitive development after unilateral perinatal stroke are poorly understood. Non-verbal intelligence seems to be at particular risk, since language can shift to the right hemisphere and may thereby reduce the capacity of the right hemisphere for its originary functions. Pharmaco-refractory epilepsies, a frequent complication of perinatal strokes, often lead to impaired intelligence. Yet, the role of well-controlled epilepsies is less well-understood. Here, we investigated whether well-controlled epilepsies, motor impairment, lesion size, lesion side, and lateralization of language functions influence non-verbal functions.

Methods: We recruited 8 patients with well-controlled epilepsies (9–26 years), 15 patients without epilepsies (8–23 years), and 23 healthy controls (8–27 years). All underwent the Test of Non-verbal Intelligence, a motor-independent test, which excludes biased results due to motor impairment. Language lateralization was determined with functional MRI, lesion size with MRI-based volumetry, and hand motor impairment with the Jebson-Taylor Hand Function-Test.

Results: Patients with epilepsies showed significantly impaired non-verbal intelligence [Md = 89.5, interquartile range (IQR) = 13.5] compared with controls (Md = 103, IQR = 17). In contrast, patients without epilepsies (Md = 97, IQR = 15.0) performed within the range of typically developing children. A multiple regression analysis revealed only epilepsy as a significant risk factor for impaired non-verbal functions.

Conclusion: In patients with unilateral perinatal strokes without epilepsies, the neuroplastic potential of one healthy hemisphere is able to support the development of normal non-verbal cognitive abilities, regardless of lesion size, lesion side, or language lateralization. In contrast, epilepsy substantially reduces this neuroplastic potential; even seizure-free patients exhibit below-average non-verbal cognitive functions.

Keywords: early brain lesion, functional magnet resonance imaging, lesion size, motor impairment, cognitive function

INTRODUCTION

Perinatal stroke has an estimated birth-prevalence of 37–64/100,000 (1, 2). It affects mostly term-born newborns, and presents with diverse signs and symptoms (2). Outcome is quite variable, with many children achieving normal levels of function (3, 4), while others experience difficulties, such as impairment in different domains of cognitive functions (5–7) as well as in motor skills (8–10). Potentially modifying factors explaining the variability in cognitive outcome are lesion size, the severity of hand motor impairment (6), and the side of the lesion (11–13).

In addition, for non-verbal functions in patients with left-sided lesions, language reorganization has been proposed as a modifying factor (6, 7, 14). This has been explained in the context of the "crowding hypothesis" (15–17), suggesting that cognitive processes originally located in the right hemisphere such as non-verbal intelligence show deficits when language functions shift to the right hemisphere. Following this hypothesis, non-verbal functions seem to be at a particular risk for lower performance; hence, in this study, we chose to focus on the development of non-verbal functions after perinatal stroke.

The threat most feared by families of children with perinatal stroke, however, is the development of epilepsy. Indeed, patients with perinatal stroke have a significant risk to develop epilepsy, which was estimated between 15% (18) and 54% (19). Not surprisingly, the type of the lesion also plays an important role, since children with cortico-subcortical lesions (commonly due to arterial ischemic strokes, AIS), are much more prone to develop epilepsies than children with white matter lesions (usually due to periventricular venous infarctions, PVI) (7, 20). In addition to the burden of seizures and side effects of anti-epileptic medication, epilepsy may also hamper cognitive development. For children with pharmaco-refractory epilepsies due to perinatal strokes, it is well-known that cognitive development can be severely compromised (3, 4, 21, 22). Much less is known, whether less severe, well-controlled epilepsies also play a role in this regard.

A frequent methodological problem in almost all previous studies on non-verbal cognitive abilities after perinatal stroke was the application of tests requiring bimanual activities, like the Wechsler Intelligence Scales (3, 4, 23–25), the Kaufman Assessment Battery for Children (7), or the Beery Developmental Test of Visual-Motor Integration (4). Administering such tests in hemiparetic patients—a frequent consequence of perinatal stroke (9, 10)—can lead to artificially lower scores for non-verbal functions [see (26) for review]. To overcome this problem, some authors [e.g., (6)] simply excluded patients with substantial motor impairments that prevented valid administration of the measures. As this potentially biases the outcomes, we here opted to use a different approach: the assessment of non-verbal cognitive abilities with completely motor-free tests. In a previous study (14), we had used the Block Tapping test and the Tube Figures Test; in the current study, we used the Test Of Non-verbal Intelligence (TONI-4) which measures the ability for abstract reasoning and the problem-solving capability—without involving any motor component (27, 28).

Motor impairment may therefore influence the result of cognitive tests by different mechanism. First, as described above, motor impairment can artificially influence the test procedure itself. Second, impaired motor abilities might limit a child's abilities to explore its environment, and thereby impair also the development of cognitive functions (29).

The aim of our study therefore was to assess the influence of well-controlled epilepsy (which we arbitrarily defined as seizure-freedom for at least 6 months) on non-verbal cognitive development of children with perinatal strokes, as assessed using appropriate test procedures. Furthermore, we wanted to clarify the influence of lesion size, hand motor impairment, side of the lesion, and language lateralization on non-verbal cognitive performances.

METHOD

Subjects

Participants were recruited in the University Children's Hospital Tübingen and in the Center for Pediatric Neurology, Neurorehabilitation and Epileptology, Schön Klinik Vogtareuth.

In Tübingen, participants were recruited by searching the clinical database for relevant diagnoses in electronic patient charts and by personal contacts to patients who had participated in previous studies. Healthy controls were recruited *via* advertisements in the local press and in the clinic internal information system. Patients in Vogtareuth were recruited *via* personal invitations after searching the clinical database and during hospitalization for a motor skills rehabilitation training. These differences in recruitment strategies may explain why the two cohorts of patients differed in terms of age (median age Tübingen = 18.13 years, median age Vogtareuth = 10.15 years). Inclusion criteria, however, were the same, and all participants were included following telephone interviews with identical questionnaires.

We included 23 patients (11 females; age range 8–26 years; median age 12.56 years) with a diagnosis of a pre-, peri-, or neonatally acquired unilateral arterial ischemic stroke (AIS) or unilateral periventricular hemorrhagic infarction (PVI). In order to be able to participate in all tests, patients had to be native German-speaking and aged 8 years or older. Patients with a previous diagnosis of intellectual disability (defined as IQ below 70) were excluded. Controls were screened using a questionnaire asking for any neurological or psychiatric diagnosis and for problems in cognitive or language development. We did not, however, use any formal assessment confirming normal development.

Additionally, patients with seizures during the last 6 months were excluded. Hemiparesis was present in 21/23 patients (no hemiparesis in #V13, #T12).

Patients were diagnosed with epilepsy ($n = 8$; age range, 9–26 years; median age, 16.40; 2 females) when at least two afebrile, unprovoked seizures had occurred in the post-neonatal period [definition as suggested in (19, 30)]. All but one of these patients (#T28) were on anti-convulsive medication at the time of the study. Of the patients without epilepsies ($n = 15$; age range, 8–23 years; median age, 11.80; 9 females), one patient (#V03) had suffered one single seizure, but was never treated with anti-convulsive medication. The other 14 patients never

had experienced epileptic seizures. Twenty-three age-matched healthy volunteers (age range 8–27 years; median age, 12.42 years; 8 females) served as controls. For every single patient, we age-matched a person from our cohort of 38 controls—irrespective of epilepsy.

The study was approved by the local ethics committee (Nr. 693/2014B01). All adult participants and the parents of underage participants gave their written, informed consent, and all underage participants gave verbal assent. The study was in accordance with the Code of Ethics of the World Medical Association (Declaration of Helsinki, 1964 in its latest version).

Neuropsychological Assessment

All participants completed the Test of Non-verbal Intelligence, Fourth Edition (TONI-4), which measures the ability for abstract reasoning and the problem-solving capability (28). It contains of 60 graphical items, arranged in order from easy to difficult. The participants analyze similarities and differences between the items, which are defined by the characteristics shape, position, direction, rotation, contiguity, shading, size and movement. The age-adjusted test results are not confounded by motor deficits and are therefore suitable for patients with motor impairments such as hemiparesis (27).

Structural and Functional Magnetic Resonance Imaging

Subjects were either scanned on a Siemens 1.5 T Avanto (Tübingen) or Symphony (Vogtareuth) MRI scanner (Siemens Medizintechnik, Erlangen, Germany), using the same sequences and a standard quadrature head coil. An echo-planar imaging (EPI) sequence was used to acquire functional series (repetition time = 3,000 ms, echo time = 40 ms, 40 axial slices, in plane matrix = 64 × 64, covering the whole brain with a voxel size = 3 × 3 × 3 mm^3). Anatomical images were acquired as T1-weighted 3D-datasets (repetition time = 1,300 ms, echo time = 2.92 ms, 167 contiguous sagittal slices, in plane matrix 265 × 265, resulting in a voxel size of 1 × 1 × 1 mm^3).

Functional and anatomical images were pre-processed and analyzed using SPM12 (Statistical Parametric Mapping; Wellcome Department of Imaging Neurosciences, UCL, UK), the Computational Anatomy Toolbox extension to SPM12 (CAT12, by Christian Gaser and Robert Dahnke, Departments of Psychiatry and Neurology, Jena University Hospital), as well as custom scripts and functions running within Matlab (Mathworks, Natrick MA, USA).

For the determination of lesion size, individual lesion masks were manually drawn in native space on the anatomical T1-weighted image using MRIcron (31). To compensate for asymmetric ventricular enlargement, the mirrored ventricles of the contra-lesional hemisphere were excluded from the lesion masks for all subjects. Lesion volumes were calculated from the lesion masks using a custom script.

For the determination of language lateralization, all patients with left-sided lesions underwent fMRI and performed the *Vowel Identification Task* (32) as a word generation task. Methodological details have been described elsewhere (32–34). In brief, pictures of everyday objects were presented visually to the participants, who were asked to decide if the name of the object contained the phoneme <i> by silently generating the name of the object. In the control condition, participants were presented an abstract puzzle and were asked to decide if a small piece fitted into a larger one. Laterality of language activation was calculated as described in Lidzba et al. (35). Based on the resulting laterality index (LI), patients were classified as "left-dominant" ($LI > +0.2$), as "right-dominant" ($LI < -0.2$) or as "bilateral" ($-0.2 \leq LI \leq +0.2$).

Motor Assessment

Hand motor function was assessed with the Jebson Taylor Hand function test (JTHFT). The test provides quantitative measurements of standardized unimanual hand function tasks that are frequently used in everyday activities (36). We calculated the median of six subtests (card turning, picking up small objects, stacking checkers, simulated feeding, lifting light objects and lifting heavy objects) (37). As suggested previously, we did not perform the subtest "writing" due to possible distortion by the different ages and performance levels of the participants (38–40). The test was initially developed for adults, but recently showed a good test-retest reliability in children aged 6–10 years (41). For our analysis, we calculated the ratio of the medians "non-dominant"/"dominant" hand motor function to control for inter-individual differences not related to the hemiparesis.

Statistics

The statistical analyzes were performed using SPSS 25. For correlation analyses, we used Spearman rank correlations; for correlations including dichotomous variables, we used the point-biserial correlations. Significance was assumed at $p \leq 0.05$, For group comparisons between the three groups, we used the non-parametric Kruskal-Wallis-test, corrected for multiple comparisons where appropriate by Bonferroni correction. A Chi-Square-test was used for a distribution measurement of the control group. Multiple regression analyses were used for the assessment of several predictor variables for the outcome variable non-verbal intelligence.

RESULTS

Table 1 summarizes demographic and clinical data of all 23 patients. Lesion size could be calculated in 21/23 patients, ranging from 1.16 to 220.71 cm^3. In the other two, dental braces (#V04) or an implanted shunt system (#T28) prevented the reliable determination of lesion size (**Table 1**). The presence of epilepsy correlated significantly with lesion size (point-biserial correlation, $r = -0.47$, $p < 0.01$) and with the type of the lesion (AIS vs. PVI, Phi $p < 0.05$).

The Kruskal Wallis-test for the three groups—patients with epilepsy, patients without epilepsy, and controls—yielded a significant main effect for non-verbal intelligence [$H(2) = 9.06$, $n = 46$, $p < 0.05$]. Pairwise comparisons with Bonferroni-adjusted p-values demonstrated that patients with epilepsy scored significantly lower than controls ($p = 0.010$), while no significant differences were observed between patients without epilepsy and

TABLE 1 | Patient characteristics.

ID	Age at study (years)	Sex	Lesion type	TONI	Epilepsy	Lesion size (ml)	JTHFT (ratio)	Lesion side	LI	Age of onset (years)	Time since seizure-freedom (years)	History of status epilepticus	History of AEDs	Time between first and last seizure (years)
T14	16	M	AIS	77	Yes	133.93	1.37	Left	−0.5	11	1.25	No	LEV BRIV, OXC	4
T39	26	M	AIS	87	Yes	167.79	25.34	Left	−0.87	11.5	8	No	STM	1.5
T44	16	M	AIS	87	Yes	84.97	9.48	Right		N/A	N/A	N/A	OXC	
T41	22	M	PVI	89	Yes	200.57	6.49	Right		15.5	6	No	OXC	1
V11	10	M	PVI	90	No	50.29	4.69	Left	+0.63					
T28	16	M	Not classified*	90	Yes	N/A	1.52	Left	+0.69	4	1	Yes	STM, LEV, CLB, PHT	12
V04	15	F	PVI	91	No	N/A	5.75	Right						
T21	23	F	PVI	92	No	29.57	6.64	Left	−0.25					
V14	10	M	PVI	93	No	79.38	18.65	Right						
V06	8	M	PVI	93	No	28.83	2.40	Left	+0.78					
T57	19	F	PVI	93	No	1.16	1.97	Left	+0.64					
T33	23	M	PVI	97	No	161.77	4.08	Left	−0.66					
V03	11	F	PVI	97	No	55.82	2.94	Left	+0.67					
T19	23	F	PVI	99	No	36.05	2.42	Left	−0.83					
T13	9	M	PVI	99	Yes	22.82	1.58	Left	+0.85	0.25	0.5	Yes	LEV, ACTH, PB, STM, CLB, Steroids, ESM	8
V01	8	M	PVI	100	No	24.80	15.25	Left	+0.61					
V12	10	F	PVI	101	Yes	220.71	5.05	Right		1	3	No	OXC, TPM, LEV	6
V13	10	F	PVI	102	No	85.36	0.95	Left	−0.31					
V02	8	F	PVI	104	Yes	45.11	2.04	Right		4.5	3	No	LEV	1.5
V09	10	F	PVI	108	No	1.24	2.17	Left	N/A					
T12	12	F	PVI	109	No	97.30	1.12	Left	−0.32					
T56	12	M	PVI	109	No	9.08	2.39	Right						
V08	11	F	AIS	121	No	41.65	3.85	Left	−0.53					

Patients are sorted by TONI. Hand motor function is calculated by the ratio (non-dominant/dominant) hand function of the median scores of JTHFT.

AIS, arterial ischemic stroke; LI, laterality index (positive: left; negative: right); N/A, no data available due to incompliance or technical failure; PVI, periventricular venous infarction; JTHFT, Jebson Taylor Hand function test; TONI, Test of non-verbal intelligence. LEV, Levetiracetam; BRV, Brivaracetam; OXC, Oxcarbazepine; STM, Sulthiame; CLB, Clobazam; PHT, Phenytoin; PB, Phenobarbital; ESM, Ethosuximide; TPM, Topiramate.

**The lesion in T28 could not unequivocally be classified as AIS or PVI because only MRI after implantation of a ventriculoperitoneal shunt were available.*

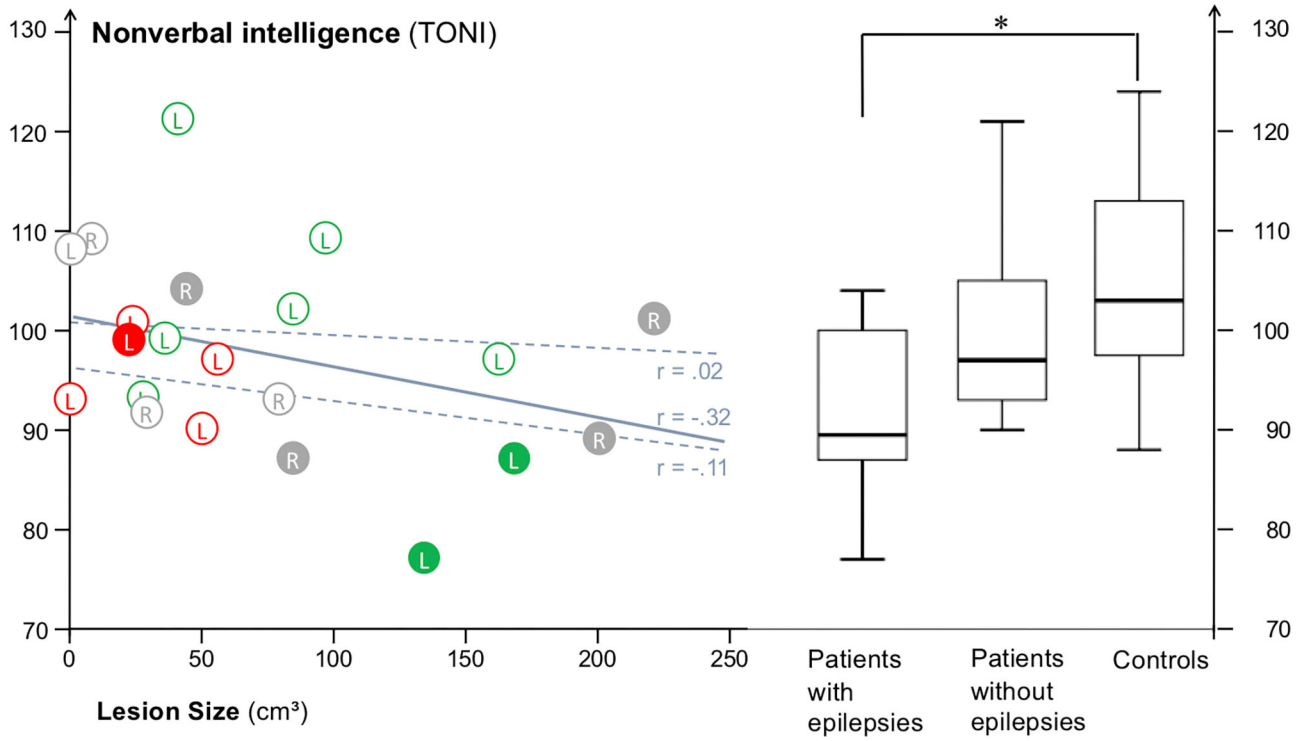

FIGURE 1 | Scatterplot of all 21 patients with lesion size data available, marked with solid circles (with epilepsy) or open circles (without epilepsy). Capital letters mark the side of the lesion (L, R), colors mark the lateralization of language (red = left-dominant; green = right-dominant; gray = no information). The solid line indicates the correlation between lesion size and TONI for all patients, the dashed lines the correlations for the subgroups of patients with epilepsies (lower line) and without epilepsies (upper line). The median TONI scores were about 7.5 points lower for patients with epilepsies (Md = 89.5, SD = 9.0) vs. those without epilepsies (Md = 97, SD = 8.8), and almost one standard deviation lower for patients with epilepsy vs. typically developing controls (Md = 103, SD = 10.0). Patients with epilepsy differed significantly (Kruskal-Wallis-test) from controls (marked with *), while patients with and without epilepsy and patients without epilepsy and controls did not differ.

TABLE 2 | Correlation coefficients.

	Epilepsy	JTHFT (ratio)	Lesion size	Lesion side	LI (left-sided lesions only)
TONI-4	**−0.405***	**−0.359***	−0.324	−0.042	−0.075

Correlation coefficients between non-verbal intelligence (TONI), hand motor impairment (JTHFT-ratio), lesion size, lesion side, and language lateralization (Spearman rank, one-tailed; for lesion side as a dichotomous variable: point-biserial correlation, one-tailed). Note that lesion size was available for only 21/23 patients, and only 15/16 patients with left-sided lesions contributed data for language lateralization.
*The bold values with *indicate a statistically significant correlation.*

controls ($p = 0.364$) and between patients with and without epilepsy ($p = 0.341$; **Figure 1**).

Results of the assessment of potential modifiers of non-verbal intelligence are displayed in **Table 2**. TONI scores were negatively correlated with the presence of epilepsy (point-biserial correlation, $r = -0.41$, $p < 0.05$) and with motor impairment of the paretic hand (Spearman Rank, $r = -0.36$, $p < 0.05$). Lesion size showed a trend ($r = -0.32$; $p = 0.078$) toward inferior non-verbal intelligence scores in patients with larger lesions. No significant correlations were observed for lesion side ($r = 0.04$; $p = 0.42$) nor, in patients with left-sided lesions, for language lateralization ($r = 0.08$; $p = 0.40$).

To investigate the differential effects of the potential modifiers epilepsy, hand motor impairment, lesion size, and lesion type, we conducted a stepwise linear multiple regression analysis in the order of the strength of the correlation coefficients. Only the factor epilepsy ($R^2 = 0.17$, beta $= -0.410$, $t = -2.0$, $p < 0.05$, one-tailed) was retained in the model as a statistically significant predictor, with epilepsy explaining 17 % of the variance in non-verbal intelligence. Neither hand motor impairment ($p = -0.13$, one-tailed) nor lesion size ($p = 0.34$, one-tailed) provided additional information.

Non-verbal intelligence did not correlate with epilepsy onset ($r = -0.61$, $p = 0.15$), time since seizure freedom ($r = 0.20$, $p = 0.67$), number of different antiepileptic drugs ever used ($r = 0.19$; $p = 0.65$), time between first and last seizure ($r = 0.20$, $p = 0.67$) or history of status epilepticus ($r = -0.10$, $p = 0.85$).

Seven patients had right-sided lesions, 16 patients had left-sided lesions (**Figure 2**). In the 16 patients with left-sided lesions, functional MRI revealed left-lateralized language in 7/16 patients and right-lateralized language in 8/16 patients. Patient V09 could not be classified due to technical failure, and no patient showed bilateral language. Language lateralization indices ranged from +0.85 to −0.87 and correlated significantly with lesion size ($r = -0.67$, $p < 0.05$; Spearman rank): the larger the left-sided lesion, the stronger the right-sided language dominance.

In our healthy control group, the median in non-verbal intelligence (IQ = 103) was slightly above the population-based average (IQ = 100), but they did not differ from the population-based estimated distribution (Chi Square = 5.590; $p = 0.232$). Overperformance of our healthy peer group can therefore be ruled out as the decisive factor.

DISCUSSION

The major finding of our study was that epilepsy is a key risk factor for impaired non-verbal cognitive abilities in children with perinatal stroke. This has already been known for severe pharmaco-refractory epilepsies (3, 4, 21, 22); in the current study, we could demonstrate that negative effects can also be seen even in patients with well-controlled epilepsies, i.e., with seizure-freedom for at least 6 months. Despite our comprehensive assessment, none of the other potentially modifying factors lesion size, lesion side, language lateralization, or hand motor impairment played any role beyond the deleterious effects of epilepsy.

According to our analyses, **patients without epilepsies** after perinatal stroke can be expected to develop normal non-verbal cognitive functions. This is in line with other studies (3, 4) reporting non-verbal cognitive performances in the range of typically developing children for non-epileptic patients after perinatal stroke. Furthermore, we found no correlation between TONI scores and lesion size in this group ($r = 0.02$). This confirms the report by Lõo et al., demonstrating that, in non-epileptic children with PVI, lesion size did not correlate with cognitive abilities (7). These patients provide impressive examples of the neuroplastic potential of the developing human brain: Even patients with very large lesions (e.g., patient T33) have the potential to develop non-verbal intelligence in the normal range (TONI = 97). This neuroplastic potential basically of one hemisphere seems sufficient even in patients who shift language to the right hemisphere as a consequence of large left-sided lesions—thus apparently contradicting the "crowding hypothesis" (see below).

In contrast, **in patients with epilepsies**, we observed a significant impairment of non-verbal cognitive abilities, with scores ranging between 77 and 104, hence from "poor" to "average" cognitive ability according to the TONI-4-manual (28).

This is all the more striking as we had already excluded patients with pharmaco-refractory epilepsies (i.e., with ongoing seizures) and patients with a previous diagnosis of intellectual disability. Apparently, in the presence of epilepsy, the neuroplastic potential of the contra-lesional hemisphere is not sufficient to allow for an undisturbed cognitive development. Network formation must be expected to be an important step in establishing the neural substrates for higher cognitive functions. Several mechanism have been discussed how perinatal lesions lead to epileptogenesis later in life; it seems likely that epilepsy impairs neuroplasticity by interfering with network formation (42).

In order to exclude that our results are mostly driven by the one patient with seizure-freedom for <1 year (T13), we conducted all analyses again without this patient T13. We found that neither the results in the correlation analysis, nor the group comparisons changed after the exclusion of this patient; patients with epilepsy still scored significantly lower than controls ($p = 0.007$).

The same holds true for the multiple regression analysis; only the factor epilepsy ($R^2 = 0.20$, beta = −0.444, $t = -2.1$, $p < 0.05$, one-tailed) was retained in the model as a statistically significant predictor, with epilepsy explaining 20 % of the variance in non-verbal intelligence.

In our cohort, none of the parameters characterizing epilepsy (i.e., epilepsy onset, time since last seizure, number of different antiepileptic drugs ever used, time between first and last seizure, or history of status epilepticus) correlated with non-verbal intelligence. This negative result must be interpreted, however, in the context of our small number of only eight patients with epilepsy and the limited dataset we obtained. We would expect that a more detailed analysis of a larger cohort of patients with stroke-induced epilepsy reveals such correlations.

Supporting our findings, impaired development of cognitive abilities in patients with epilepsies after perinatal stroke was also reported in previous studies (3, 4, 7). Two of these studies (3, 4) added a longitudinal aspect to this negative influence of epilepsy, describing a decline of cognitive functions over time associated with post-neonatal epilepsy in cohorts of children with perinatal AIS. Since our study was cross-sectional in nature, we are unable to provide such insights into the time-course of the development of cognitive impairment in our patients. Furthermore, these studies (3, 4, 7), reported on cohorts of patients with various seizure severities, ranging from seizure-free patients on anti-convulsive medication (as in most of our patients) to patients with drug-resistant epilepsies with ongoing seizures. The new aspect of our study in this respect, with seizure-freedom for at least 6 months as an inclusion criterion, was that the presence of even well-controlled epilepsy can significantly impair the development of non-verbal cognitive functions.

Nevertheless, children with **larger lesions** seem to be at higher risk to show impaired non-verbal cognitive abilities, since lesion size tended to correlate with non-verbal intelligence ($r = -0.32$). Our multiple regression analysis, however, demonstrated that this correlation is not an effect of lesion size *per se*, but arises as a consequence of the higher likelihood of larger lesions to result in epilepsies ($r = 0.55$). Hence, the effect of lesion size is biased by the higher likelihood of epilepsy in these patients.

In addition to the fact that motor impairment can artificially influence the test procedure itself, impaired motor abilities might limit a child's abilities to explore its environment, and thereby impair also the development of cognitive functions

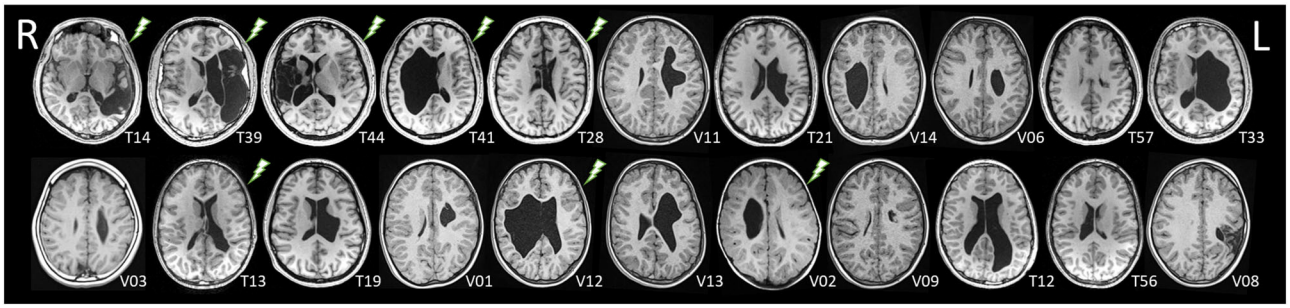

FIGURE 2 | Axial slices of the T1-weighted datasets of the 22 patients with MRI data available, sorted by TONI scores (as in **Table 1**). No MRI was available in patient V04 due to dental braces. A "lightning" symbol marks patients with epilepsies. Radiological orientation, R, right; L, left.

(29). Therefore, motor function is also an influencing factor when investigating cognitive outcome in children with unilateral perinatal stroke.

Similar to the lesion size analysis, children with hand motor impairment tend to show more severely impaired non-verbal cognitive abilities ($r = -0.36$). After inclusion of epilepsy as the first regressor, however, motor impairment ended up showing no additional significant effect in the regression model. This might indicate that epilepsy and motor impairment are epiphenomena of the same underlying feature of the lesion.

An interesting discrepancy arose when comparing our findings with previous data from our own group (14) regarding **the crowding hypothesis**. In this previous study (14), the degree of right-hemispheric language involvement did correlate with non-verbal cognitive parameters in a similar group of patients with unilateral PVI without epilepsies. Such a correlation was not only observed for the (potentially motor-contaminated) performance IQ scores of the Wechsler Intelligence Scales, but also for motor-free tests of visuospatial memory (Block-Tapping Test) and spatial ability (Tube Figures Test). To ensure that the presence of epilepsy in the current study did not wash out the influence of language lateralization or lesion size on the cognitive performances, we conducted the same analysis confined to patients without epilepsies—and again found no significant correlation between non-verbal intelligence and language lateralization ($n = 12$, $r = -0.54$, $p = 0.09$) or lesion size ($n = 14$, $r = 0.02$, $p = 0.96$).

This discrepancy may indicate that not all non-verbal cognitive functions are compromised to the same extent: In the current study, we found no evidence for non-verbal reasoning (as measured with the TONI) to be impaired by a right-shift of language. This is compatible with previous suggestions of spatial ability and reasoning tests being separable dimensions (43). Therefore, these two studies from our group seem to indicate that language shift to the right hemisphere may compromise some originary right hemispheric functions [such as visuospatial memory and spatial ability (14)] more than others (non-verbal reasoning—the current study).

Interestingly, the factor "**lesion side**" was irrelevant, which is compatible with recent studies that also failed to find such a difference using subtests of the Wechsler Intelligence Tests to assess non-verbal cognitive abilities (3, 4). This corroborates the hypothesis that cross-hemispheric reorganization may be an important mechanism underlying the neuroplastic potential of the developing human brain (44). In contrast, two studies reported lesion side-specific problems in cognition after perinatal strokes: In the first study (12), patients with perinatally acquired right-sided lesions were impaired in configural processing and made more global errors in reproducing memorized objects in drawing tasks, whereas patients with left-sided lesions were impaired in featural progressing and made more local errors. A possible explanation for this discrepancy is, again, that side-specific problems may exist for visuospatial memory functions, but that this side-specificity can not necessarily be transferred to the context of non-verbal reasoning as measured with the TONI in the current study. Second, in an earlier study from the same group (13), right-sided lesions lead to impaired visuospatial functions in pre-school children with perinatally acquired lesions. This specific impairment (which was revealed in drawing tasks) improved until school age, most likely by developing compensatory strategies. Therefore, the discrepancy to our data may not only be explained by the different cognitive functions tested, but also by the fact that we included only patients aged 8 years or older.

Limitations of our study include the following: First, we did not include patients with IQ < 70. Therefore, we have certainly underestimated the impairment of cognitive functions caused by epilepsies. Second, we have not collected data on learning disabilities. Hence, we cannot exclude that despite average score in non-verbal cognitive abilities, our patients show deficits in these aspects of cognition. Third, we did not analyze EEG data of our patients. Therefore, we could not assess the potential influence of interictal epileptic activity on non-verbal cognitive development.

Fourth, our patients showed a wide age range. We controlled for this issue by using age-adjusted norms and controls, but the inhomogeneity of the group might still be a confounding factor. Fifth, our sample size is relatively small. Given the

stringent inclusion criteria and the rarity of the underlying medical conditions, however, we attained an exceptional group size and used appropriate statistical approaches. We therefore interpret our results as valid. Sixth, our manual approach to determine lesion size is precise, but not at all topographically specific. We therefore cannot exclude that certain lesion topographies exert a more prominent effect on non-verbal cognitive abilities than what we report here. To this effect, lesion-symptom mapping approaches would have been necessary.

Seventh, AIS and PVI are two different pathological entities with different etiologies and different outcomes. Due to the small number of only 4 patients with AIS in our sample, we were unable to search for potential effects of lesion type.

Eighth, we did not control for the educational level of the parents—a factor which might also play a role in cognitive outcomes.

Ninth, with only two patients without CP in our cohort, we were unable to analyze the effect of presence vs. absence of CP on brain organization. Future studies could address this point by specifically recruiting patients without any motor impairment.

Our study has important **implications for patient counseling**: Patients with perinatal strokes without epilepsy can be expected to develop non-verbal intelligence within the range of typically developing children. If not hampered by epilepsy, the neuroplastic potential of one healthy hemisphere is able to support the development of normal non-verbal cognitive abilities, regardless of lesion size, lesion side, or language lateralization. Epilepsy, even when well-controlled, seems to substantially reduce this neuroplastic potential, resulting in impaired non-verbal abilities.

DATA AVAILABILITY STATEMENT

The original contributions presented in the study are included in the article/supplementary material, further inquiries can be directed to the corresponding author.

ETHICS STATEMENT

The studies involving human participants were reviewed and approved by Ethik-Kommission an der Medizinischen Fakultät der Eberhard Karls Universität und am Universitätsklinikum Tübingen (Nr. 693/2014B01). Written informed consent to participate in this study was provided by the participants' legal guardian/next of kin.

AUTHOR CONTRIBUTIONS

KL and MS conceptualized and initiated the study. AG, MH, LS, and MS collected the data. PH, MW, LS, AG, and MS conceptualized and interpreted the (f)MRI and lesion size data. AG and MS analyzed and interpreted the data and prepared the manuscript. KL, MH, LS, MW, and PH reviewed the manuscript. All authors approved the final manuscript as submitted.

FUNDING

This research study was supported by the German Research Foundation (DFG LI1925/4-1).

ACKNOWLEDGMENTS

PH was supported through a BIH Clinical Fellowship by Stiftung Charité.

REFERENCES

1. Laugesaar R, Kolk A, Tomberg T, Metsvaht T, Lintrop M, Varendi H, et al. Acutely and retrospectively diagnosed perinatal stroke: a population-based study. *Stroke*. (2007) 38:2234–40. doi: 10.1161/STROKEAHA.107.483743
2. Fluss J, Dinomais M, Chabrier S. Perinatal stroke syndromes: similarities and diversities in aetiology, outcome and management. *Eur J Paediatr Neurol*. (2019) 23:368–83. doi: 10.1016/j.ejpn.2019.02.013
3. Ballantyne AO, Spilkin AM, Hesselink J, Trauner DA. Plasticity in the developing brain: intellectual, language and academic functions in children with ischaemic perinatal stroke. *Brain*. (2008) 131:2975–85. doi: 10.1093/brain/awn176
4. van Buuren LM, van der Aa NE, Dekker HC, Vermeulen RJ, van Nieuwenhuizen O, van Schooneveld MM, et al. Cognitive outcome in childhood after unilateral perinatal brain injury. *Dev Med Child Neurol*. (2013) 55:934–40. doi: 10.1111/dmcn.12187
5. Greenham M, Anderson V, Mackay MT. Improving cognitive outcomes for pediatric stroke. *Curr Opin Neurol*. (2017) 30:127–32. doi: 10.1097/WCO.0000000000000422
6. Hajek CA, Yeates KO, Anderson V, Mackay M, Greenham M, Gomes A, et al. Cognitive outcomes following arterial ischemic stroke in infants and children. *J Child Neurol*. (2013) 29:887–94. doi: 10.1177/0883073813491828
7. Lõo S, Ilves P, Männamaa M, Laugesaar R, Loorits D, Tomberg T, et al. Long-term neurodevelopmental outcome after perinatal arterial ischemic stroke and periventricular venous infarction. *Eur J Paediatr Neurol*. (2018) 22:1006–15. doi: 10.1016/j.ejpn.2018.07.005
8. Nelson KB, Lynch JK. Stroke in newborn infants. *Lancet Neurol*. (2004) 3:150–8. doi: 10.1016/S1474-4422(04)00679-9
9. Dunbar M, Kirton A. Perinatal Stroke. *Semin Pediatr Neurol*. (2019) 32:100767. doi: 10.1016/j.spen.2019.08.003
10. Lehman LL, Rivkin MJ. Perinatal arterial ischemic stroke: presentation, risk factors, evaluation, and outcome. *Pediatr Neurol*. (2014) 51:760–8. doi: 10.1016/j.pediatrneurol.2014.07.031
11. Akshoomoff NA, Feroleto CC, Doyle RE, Stiles J. The impact of early unilateral brain injury on perceptual organization and visual memory. *Neuropsychologia*. (2002) 40:539–61. doi: 10.1016/S0028-3932(01)00129-4
12. Stiles J, Stern C, Appelbaum M, Nass R, Trauner D, Hesselink J. Effects of early focal brain injury on memory for visuospatial patterns: selective deficits of global-local processing. *Neuropsychology*. (2008) 22:61–73. doi: 10.1037/0894-4105.22.1.61
13. Stiles J, Trauner D, Engel M, Nass R. The development of drawing in children with congenital focal brain injury: evidence for limited functional recovery. *Neuropsychologia*. (1997) 35:299–312. doi: 10.1016/S0028-3932(96)00088-7
14. Lidzba K, Staudt M, Wilke M, Krägeloh-Mann I. Visuospatial deficits in patients with early left-hemispheric lesions and functional reorganization of language: consequence of lesion or reorganization? *Neuropsychologia*. (2006) 44:1088–94. doi: 10.1016/j.neuropsychologia.2005.10.022

15. Rasmussen T, Milner B. The role of early left-brain injury in determining lateralization of cerebral speech functions. *Ann N Y Acad Sci*. (1977) 299:355–69. doi: 10.1111/j.1749-6632.1977.tb41921.x
16. Strauss E, Satz P, Wada J. An examination of the crowding hypothesis in epileptic patients who have undergone the carotid amytal test. *Neuropsychologia*. (1990) 28:1221–7. doi: 10.1016/0028-3932(90)90057-U
17. Teuber H. Why two brains? In: Schmitt FO, Worden FG, editors. *Neurosciences: Third Study Program*. Boston, MA: MIT Press (1974). p. 71–4.
18. Chabrier S, Peyric E, Drutel L, Deron J, Kossorotoff M, Dinomais M, et al. Multimodal outcome at 7 years of age after neonatal arterial ischemic stroke. *J Pediatr*. (2016) 172:156–61.e3. doi: 10.1016/j.jpeds.2016.01.069
19. Wanigasinghe J, Reid SM, Mackay MT, Reddihough DS, Harvey AS, Freeman JL. Epilepsy in hemiplegic cerebral palsy due to perinatal arterial ischaemic stroke. *Dev Med Child Neurol*. (2010) 52:1021–7. doi: 10.1111/j.1469-8749.2010.03699.x
20. Laugesaar R, Vaher U, Lõo S, Kolk A, Männamaa M, Talvik I, et al. Epilepsy after perinatal stroke with different vascular subtypes. *Epilepsia Open*. (2018) 3:193–202. doi: 10.1002/epi4.12104
21. Wagenaar N, Martinez-Biarge M, van der Aa NE, van Haastert IC, Groenendaal F, Benders M, et al. Neurodevelopment after perinatal arterial ischemic stroke. *Pediatrics*. (2018) 142:e20174164. doi: 10.1542/peds.2017-4164
22. Bajer C, Hofer W, Pieper T, Kudernatsch M, Holthausen H, Staudt M. Correlates of intellectual development before and after hemispherotomy: an analysis of 75 children and adolescents. *Epileptic Disord*. (2020) 22:571–81. doi: 10.1684/epd.2020.1193
23. Levine SC, Kraus R, Alexander E, Suriyakham LW, Huttenlocher PR. IQ decline following early unilateral brain injury: a longitudinal study. *Brain Cognit*. (2005) 59:114–23. doi: 10.1016/j.bandc.2005.05.008
24. Ricci D, Mercuri E, Barnett A, Rathbone R, Cota F, Haataja L, et al. Cognitive outcome at early school age in term-born children with perinatally acquired middle cerebral artery territory infarction. *Stroke*. (2008) 39:403–10. doi: 10.1161/STROKEAHA.107.489831
25. Westmacott R, McDonald KP, Roberts SD, deVeber G, MacGregor D, Moharir M, et al. Predictors of cognitive and academic outcome following childhood subcortical stroke. *Dev Neuropsychol*. (2018) 43:708–28. doi: 10.1080/87565641.2018.1522538
26. Foo RY, Guppy M, Johnston LM. Intelligence assessments for children with cerebral palsy: a systematic review. *Dev Med Child Neurol*. (2013) 55:911–8. doi: 10.1111/dmcn.12157
27. Ritter N, Kilinc E, Navruz B, Bae Y. Test review. *J Psychoeduc Assess*. (2011) 29:484–8. doi: 10.1177/0734282911400400
28. Brown L, Sherbenou RJ, Johnsen SK. *Test of Nonverbal Intelligence: TONI-4*. Austin, TX: Pro-ed (2010).
29. Pavlova MA, Krägeloh-Mann I. Limitations on the developing preterm brain: impact of periventricular white matter lesions on brain connectivity and cognition. *Brain*. (2013) 136:998–1011. doi: 10.1093/brain/aws334
30. Raju TN, Nelson KB, Ferriero D, Lynch JK. Ischemic perinatal stroke: summary of a workshop sponsored by the National Institute of Child Health and Human Development and the National Institute of Neurological Disorders and Stroke. *Pediatrics*. (2007) 120:609–16. doi: 10.1542/peds.2007-0336
31. Rorden C, Karnath HO, Bonilha L. Improving lesion-symptom mapping. *J Cogn Neurosci*. (2007) 19:1081–8. doi: 10.1162/jocn.2007.19.7.1081
32. Wilke M, Lidzba K, Staudt M, Buchenau K, Grodd W, Krägeloh-Mann I. An fMRI task battery for assessing hemispheric language dominance in children. *NeuroImage*. (2006) 32:400–10. doi: 10.1016/j.neuroimage.2006.03.012
33. Meinhold T, Hofer W, Pieper T, Kudernatsch M, Staudt M. Presurgical language fMRI in children, adolescents and young adults. *Clin Neuroradiol*. (2020) 30:691–704. doi: 10.1007/s00062-019-00852-7
34. Máté A, Lidzba K, Hauser TK, Staudt M, Wilke M. A "one size fits all" approach to language fMRI: increasing specificity and applicability by adding a self-paced component. *Exp Brain Res*. (2016) 234:673–84. doi: 10.1007/s00221-015-4473-8
35. Lidzba K, de Haan B, Wilke M, Krägeloh-Mann I, Staudt M. Lesion characteristics driving right-hemispheric language reorganization in congenital left-hemispheric brain damage. *Brain Lang*. (2017) 173:1–9. doi: 10.1016/j.bandl.2017.04.006
36. Jebsen RH, Taylor N, Trieschmann RB, Trotter MJ, Howard LA. An objective and standardized test of hand function. *Arch Phys Med Rehabil*. (1969) 50:311–9.
37. Tipton-Burton M. Jebsen-Taylor hand function test. In: Kreutzer JS, DeLuca J, Caplan B, editors. *Encyclopedia of Clinical Neuropsychology*. New York, NY: Springer New York (2011). p. 1365.
38. Adler C, Berweck S, Lidzba K, Becher T, Staudt M. Mirror movements in unilateral spastic cerebral palsy: specific negative impact on bimanual activities of daily living. *Eur J Paediatr Neurol*. (2015) 19:504–9. doi: 10.1016/j.ejpn.2015.03.007
39. Islam M, Nordstrand L, Holmström L, Kits A, Forssberg H, Eliasson AC. Is outcome of constraint-induced movement therapy in unilateral cerebral palsy dependent on corticomotor projection pattern and brain lesion characteristics? *Dev Med Child Neurol*. (2014) 56:252–8. doi: 10.1111/dmcn.12353
40. Sakzewski L, Ziviani J, Boyd R. The relationship between unimanual capacity and bimanual performance in children with congenital hemiplegia. *Dev Med Child Neurol*. (2010) 52:811–6. doi: 10.1111/j.1469-8749.2009.03588.x
41. Reedman SE, Beagley S, Sakzewski L, Boyd RN. The Jebsen Taylor test of hand function: a Pilot test-retest reliability study in typically developing children. *Phys Occup Ther Pediatr*. (2016) 36:292–304. doi: 10.3109/01942638.2015.1040576
42. Becker AJ. Review: animal models of acquired epilepsy: insights into mechanisms of human epileptogenesis. *Neuropathol Appl Neurobiol*. (2018) 44:112–29. doi: 10.1111/nan.12451
43. Gittler G. Sind Raumvorstellung und Reasoning separierbare Fähigkeitsdimensionen? Dimensionalitätsanalysen zweier Rasch-skalierter Tests: 3 DW und WMT. *Diagnostica*. (1999) 45:69–81. doi: 10.1026//0012-1924.45.2.69
44. Krägeloh-Mann I, Lidzba K, Pavlova MA, Wilke M, Staudt M. Plasticity during early brain development is determined by ontogenetic potential. *Neuropediatrics*. (2017) 48:66–71. doi: 10.1055/s-0037-1599234

Conflict of Interest: The authors declare that the research was conducted in the absence of any commercial or financial relationships that could be construed as a potential conflict of interest.

Copyright © 2021 Gschaidmeier, Heimgärtner, Schnaufer, Hernáiz Driever, Wilke, Lidzba and Staudt. This is an open-access article distributed under the terms of the Creative Commons Attribution License (CC BY). The use, distribution or reproduction in other forums is permitted, provided the original author(s) and the copyright owner(s) are credited and that the original publication in this journal is cited, in accordance with accepted academic practice. No use, distribution or reproduction is permitted which does not comply with these terms.

frontiers in Neurology

ORIGINAL RESEARCH
published: 28 June 2021
doi: 10.3389/fneur.2021.673560

Double-Sine-Wave Quadri-Pulse Theta Burst Stimulation of Precentral Motor Hand Representation Induces Bidirectional Changes in Corticomotor Excitability

Nikolai H. Jung[1], Bernhard Gleich[2], Norbert Gattinger[2], Anke Kalb[1], Julia Fritsch[1], Elisabeth Asenbauer[1], Hartwig R. Siebner[3,4,5†] and Volker Mall[1†]*

[1] School of Medicine, Social Pediatrics, Technical University of Munich, Munich, Germany, [2] Munich School of Bioengineering (MSB), Technical University of Munich, Garching, Germany, [3] Danish Research Center for Magnetic Resonance, Centre for Functional and Diagnostic Imaging and Research, Copenhagen University Hospital, Amager and Hvidovre, Copenhagen, Denmark, [4] Institute for Clinical Medicine, Faculty of Medical and Health Sciences, University of Copenhagen, Copenhagen, Denmark, [5] Department of Neurology, Copenhagen University Hospital Bispebjerg and Frederiksberg, Copenhagen, Denmark

OPEN ACCESS

Edited by:
Kette D. Valente,
Universidade de São Paulo, Brazil

Reviewed by:
Igor Delvendahl,
University of Zurich, Switzerland
George M. Opie,
University of Adelaide, Australia

***Correspondence:**
Nikolai H. Jung
nikolai.jung@tum.de

† These authors share senior authorship

Specialty section:
This article was submitted to Pediatric Neurology, a section of the journal Frontiers in Neurology

Received: *27 February 2021*
Accepted: *24 May 2021*
Published: *28 June 2021*

Citation:
Jung NH, Gleich B, Gattinger N, Kalb A, Fritsch J, Asenbauer E, Siebner HR and Mall V (2021) Double-Sine-Wave Quadri-Pulse Theta Burst Stimulation of Precentral Motor Hand Representation Induces Bidirectional Changes in Corticomotor Excitability. Front. Neurol. 12:673560. doi: 10.3389/fneur.2021.673560

Neuronal plasticity is considered to be the neurophysiological correlate of learning and memory and changes in corticospinal excitability play a key role in the normal development of the central nervous system as well as in developmental disorders. In a previous study, it was shown that quadri-pulse theta burst stimulation (qTBS) can induce bidirectional changes in corticospinal excitability (1). There, a quadruple burst consisted of four single-sine-wave (SSW) pulses with a duration of 160 μs and inter-pulse intervals of 1.5 ms to match I-wave periodicity (666 Hz). In the present study, the pulse shape was modified applying double-sine-waves (DSW) rather than SSW pulses, while keeping the pulse duration at 160 μs. In two separate sessions, we reversed the current direction of the DSW pulse, so that its second component elicited either a mainly posterior-to-anterior (DSW PA-qTBS) or anterior-to-posterior (DSW AP-qTBS) directed current in the precentral gyrus. The after-effects of DSW qTBS on corticospinal excitability were examined in healthy individuals ($n = 10$) with single SSW TMS pulses. For single-pulse SSW TMS, the second component produced the same preferential current direction as DSW qTBS but had a suprathreshold intensity, thus eliciting motor evoked potentials (PA-MEP or AP-MEP). Single-pulse SSW TMS revealed bidirectional changes in corticospinal excitability after DSW qTBS, which depended on the preferentially induced current direction. DSW PA-qTBS at 666 Hz caused a stable increase in PA-MEP, whereas AP-qTBS at 666 Hz induced a transient decrease in AP-MEP. The sign of excitability following DSW qTBS at I-wave periodicity was opposite to the bidirectional changes after SSW qTBS. The results show that the pulse configuration and induced current direction determine the plasticity-effects of ultra-high frequency SSW and DSW qTBS at I-wave periodicity. These findings may offer new opportunities for short non-invasive

brain stimulation protocols that are especially suited for stimulation in children and patients with neurological or neurodevelopmental disorders.

Keywords: transcranial magnetic stimulation, double-sine pulses, non-invasive brain stimulation, neuronal plasticity, corticospinal excitability, human primary motor cortex, long-term potentiation, long-term depression

INTRODUCTION

Synaptic plasticity is considered to be the neurophysiological correlate of learning and memory and changes in corticospinal excitability play a key role in the normal development of the central nervous system as well as in developmental disorders (2, 3). Regular or patterned repetitive transcranial magnetic stimulation (rTMS) of the precentral motor representations can induce lasting bidirectional changes in corticomotor excitability revealed by a lasting change in the mean amplitude of the motor evoked potential (MEP). This change in corticomotor excitability is attributed to changes in synaptic efficacy in the stimulated corticospinal system and therefore referred to as long-term potentiation (LTP)-like or long-term depression (LTD)-like plasticity (4). LTP and LTD are supposed to be the neurophysiological correlate of learning and memory (5, 6).

Extending the classic rTMS protocols, we recently introduced a novel quadri-pulse theta-burst stimulation (qTBS) protocol (1). The burst protocol consisted of four single-sine-wave (SSW) pulses which were given at an ultra-high pulse repetition rate of 666 Hz and a burst repetition rate of 5 Hz. We chose a within-burst repetition rate of 666 Hz to mimic the periodicity of descending I-waves that are generated by TMS (7). Depending on the preferential current direction, our novel SSW qTBS protocol consistently induced lasting bidirectional changes in corticospinal excitability in the human precentral motor hand representation (1).

The SSW qTBS protocol recombined two established patterned rTMS protocols, namely theta-burst stimulation (TBS) and quadri-pulse stimulation (QPS) that were previously demonstrated to effectively induce changes in corticospinal excitability by primarily targeting two different mechanisms (8, 9). While TBS is Ca^{2+}-dependent with a frequency leading to an optimal post-synaptic Ca^{2+} influx that is required for LTP- and LTD–like plasticity (10, 11), QPS effectively induces synaptic plasticity at interstimulus intervals, mimicking the rhythmic pattern of multiple descending volleys (so-called I-wave rhythmicity) that can be recorded in the corticospinal tract (7, 9, 12). These descending volleys are composed of multiple excitatory and inhibitory (GABAergic) neurons and axons of different sizes, location, orientation, and function and activate presynaptic neural elements to the corticospinal cell (7, 13).

In the present study, we modified our novel qTBS with ultra-high within-burst frequency bursts. We altered the pulse configuration using double-sine-wave (DSW) pulses rather than single-sine-wave (SSW) while keeping the pulse duration constant. DSW pulses were generated by a new stimulation device designed and built by B.G. and N.G., Munich School of Bioengineering, Technical University of Munich, Garching, Germany, which enabled us to apply DSW pulses at ultra-high pulse repetition rates that mimic I-wave periodicity (i.e., 666 Hz). We hypothesized that DSW pulses would be more effective in inducing changes in corticomotor excitability. The use of DSW pulses was motivated by our own findings that concatenated full-sine cycles decrease the threshold of local excitability with a maximum at two sine (14). We assumed that these polyphasic TMS pulses at a sequence within the medium frequency band of 1–300 kHz may improve the effectiveness of high frequency patterned rTMS protocols such as qTBS by summation of subthreshold excitations within one pulse cycle, which is analogous to the so-called "Gildemeister effect" at peripheral nerves (15). This effect describes that highfrequency pulse cycles do not necessarily generate action potentials themselves, but subthreshold excitations of subsequent pulse phases may be integrated (15, 16). This has been shown in animal studies where electrical peripheral nerve stimulation of reversed DSW pulses resulted in a summation of the excitatory effect (16). Moreover, the stimulation effect of reverse DSW pulses depended on the sequence of polarity and the value of the membrane potential. At hyperpolarization of the membrane, the initial negative DSW pulse was more effective, whereas at depolarization of the membrane, the initial positive DSW was more effective (16). The coupling of full-sine pulses resulted in changes in the threshold voltage for nerve excitation (16).

In the present study, we aimed to investigate how DSW qTBS generating ultra-high frequency bursts at I-wave periodicity (666 Hz) shapes corticomotor excitability. For DSW pulses, we selected an initial current direction of the DSW to ensure that the second component of the DSW would elicit either a preferentially posterior-to-anterior (DSW PA-qTBS) or anterior-to-posterior (DSW AP-qTBS) directed current in the precentral gyrus. The aftereffects of DSW qTBS on corticomotor excitability were examined using single SSW TMS pulses as in our previous study in order to facilitate comparability of results (1). Single-pulse SSW TMS produced the same preferential current direction in the precentral gyrus as DSW qTBS but had a suprathreshold intensity, thus eliciting motor evoked potentials (PA-MEP or AP-MEP). We hypothesized that DSW pulses of the same total pulse length of 160 μs as used for SSW qTBS may introduce stronger plasticity-inducing effects.

MATERIALS AND METHODS

Participants

In DSW qTBS experiments, ten healthy volunteers (5 women, 5 men) aged 20–37 years (median age 22.5 years; SD 4.85) participated in the study after giving written informed consent. In SSW qTBS experiments, twelve healthy volunteers (7 women, 5 men) aged 18–36 years (median age 23.5 years; SD 4.45)

participated. Seven volunteers (4 women, 3 men, aged 20–37 years; median age 22 years; SD 5.55) took part in SSW qTBS and DSW qTBS experiments. The study was approved by the local Ethics Committee of the Technical University of Munich, Faculty of Medicine (vote 5423/12) and carried out according to the Code of Ethics of the World Medical Association (Declaration of Helsinki). Eight participants were right-handed and two were left-handed according to the Edinburgh Handedness Inventory (17). A structured interview according to existing guidelines revealed none of the participants as having either a history of neurological or psychiatric illnesses, nor meeting any exclusion criteria concerning the safety of TMS (18, 19). When comparing single-sine and double-sine data, we analyzed the same participants that took part in our previously published study (1).

Experimental Procedures

The experimental procedures closely resembled the procedures we had used previously for SSW qTBS (1). To investigate the direction dependency, the experiments were performed in PA (Experiment 1) and AP (Experiment 2) direction. A schematic drawing of the qTBS paradigm and a detailed timeline of Experiments 1 and 2 are depicted in **Figures 1A,B**. For DSW qTBS, the ISI of each pulse was set to 1.5 ms (666 Hz) to match I-wave periodicity (1, 12). Each DSW qTBS pulse consisted of two full-sine cycles with 80 μs duration, respectively, resulting in a total stimulus duration of 160 μs with a sine-frequency of 12.5 kHz (**Figure 2A**). We defined the direction of a DSW pulse according to which current direction is produced by its second component in the precentral gyrus. A DSW pulse has a PA direction if the second component of the pulse produces a posterior-to-anterior current in the precentral gyrus. Conversely, a DSW pulse has an AP direction, if its second phase produces an anterior-to-posterior current in the precentral gyrus (**Figure 2A**). The same nomenclature was used for SSW qTBS (**Figure 2B**) (1). To avoid carry-over effects, we randomized and counterbalanced the order of sessions between subjects and the minimum period between sessions was 1 week. Participants were not aware of the detailed experimental condition. As it has been introduced in our previous study using SSW qTBS (1), MEP and resting motor threshold (rMT) were recorded with single SSW TMS pulses before (pre-interventional at baseline) as well as at four time points after the end of qTBS (post-qTBS) in PA and AP directions (post 1: 0 min; post 2: 15 min; post 3: 30 min; post 4: 60 min) (**Figure 1**). Single-pulse SSW TMS produced the same preferential current direction in the precentral gyrus as DSW qTBS (**Figures 1**, **2A,B**). Therefore, the induced current direction in the brain (i.e., AP and PA, respectively) was always the same for evaluation (single-pulse SSW TMS) and intervention (DSW qTBS).

In addition, we compared the reported effects of SSW qTBS and DSW qTBS in the PA and AP directions (supporting information) using a between-subject design (1).

Electromyographic Recording

The methodological details of electromyographic recording match those reported in our previous study (1). In short, participants were seated comfortably in a chair resting both hands comfortably on a cushion or in their lap to ensure complete relaxation. MEPs were recorded by surface electromyography (EMG) from the non-dominant abductor pollicis brevis (APB) muscle using silver/silver chloride surface electrodes (surface area 263 mm^2; AMBU, Ballerup, Denmark) mounted according to the bipolar belly-tendon technique. Participants were asked to relax the target muscle throughout the measurement. MEP size was determined by measuring the two highest peaks of opposite polarity and then averaged over 20 trials (20). Trials that differed by more than three times the standard deviation (SD) from the mean were considered outliers and were excluded from the analysis as described previously, which was the case for only one trial (21). The data was bandpass filtered (20–2,000 Hz) and amplified by an Ekida DC universal amplifier (Ekida, Helmstadt, Germany) connected to a Micro 1401 *mk*II data acquisition unit (Cambridge Electronic Design, Cambridge, UK) with a sampling rate of 5 kHz and stored on a personal computer for online visual display and later offline analysis using Signal software version 5 (Cambridge Electronic Design).

Transcranial Magnetic Stimulation

Procedures of TMS were similar to those introduced previously (1). In detail, the intersection of an eight-shaped stimulation coil (diameter: 100 mm) was centered over the precentral motor hand representation of the non-dominant hand (M1-HAND). The handle pointed in a posterior direction and was lateralized at an angle of ∼45° away from the midline.

For single-pulse SSW TMS, the coil was connected to a custom-made magnetic stimulation device (QuattroMag, Munich School of Bioengineering (MSB), Technical University Munich, Munich, Germany) with a biphasic SSW of 160 μs pulse duration (**Figure 2B**), as reported previously (1, 22). For single-pulse DSW and DSW qTBS, another custom-made magnetic stimulation device (QuattroBurst, MSB, Technical University of Munich, Munich, Germany) with a DSW of the same total pulse duration of 160 μs was used resulting in two concatenated full-sine cycles of 80 μs, respectively (**Figure 2A**). The reverse of the current direction from PA to AP was performed using a cable that was connected to the coil changing the polarity of each pulse (AP-PA-switch) (1). For single-pulse SSW TMS and SSW qTBS, we refer to PA stimulation when the induced current in the precentral gyrus had a posterior-to-anterior direction, and AP stimulation refers to stimulation producing a preferentially anterior-to-posterior current flow (**Figure 2B**) (1).

Before each experiment, the optimal site for stimulation ('hotspot') was determined using single pulse SSW TMS of slightly suprathreshold intensities. The position of the coil was marked with a felt-tip pen. The procedure was repeated prior to DSW qTBS using single pulse DSW TMS to ensure the location of the hotspot for DSW qTBS and to determine the active motor threshold (AMT) for DSW qTBS intensity. Single-pulse SSW TMS used to identify the hotspot and motor thresholds was administered at a frequency of 0.25 Hz. Single-pulse SSW TMS to measure MEP was applied at a pulse repetition rate of 0.1 Hz with a jitter of 15%. Both, rMT and AMT, were determined by a maximum-likelihood threshold-hunting procedure (23) using

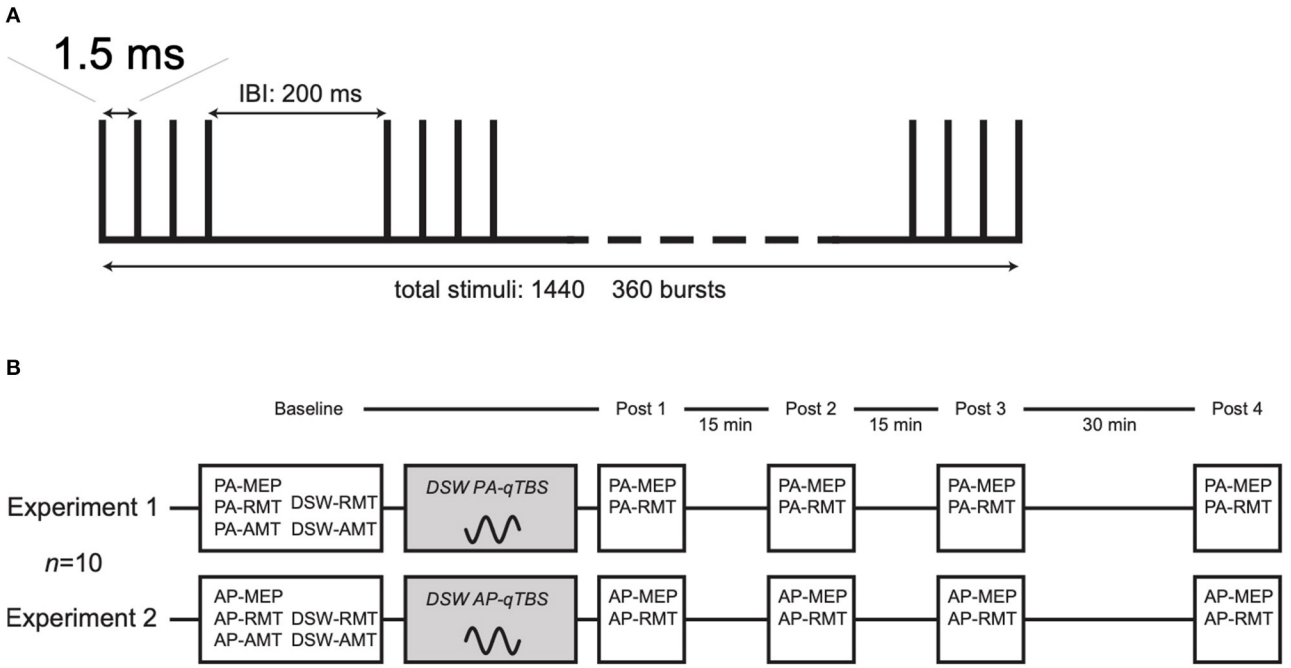

FIGURE 1 | Schematic drawing of DSW and SSW qTBS pulse sequence and experimental procedures **(A)** qTBS consists of 360 trains of DSW or SSW TMS pulses. Each train consists of magnetic pulses delivered at interstimulus intervals of 1.5 ms resulting in a total of 1,440 stimuli. Trains were repeated every 200 ms. **(B)** Experimental procedures, a timeline of experiments and number of participants for DSW Experiments 1 and 2. Experimental procedures and timelines resembled those introduced in our previous study for SSW qTBS (1). In Experiment 1, the interstimulus interval (ISI) of each double-sine-wave (DSW) qTBS pulse was set to 1.5 ms (666 Hz) to test the potential I-wave frequency-dependent patterns of DSW qTBS with an effective induced current in the precentral gyrus flowing from posterior to anterior (PA). In Experiment 2, the direction of the induced current was changed to an anterior-posterior direction (AP). For single-sine-wave (SSW) pulse TMS, cycles of corresponding current direction were applied. Details of waveforms and preferentially induced current directions are presented in **Figure 2**. The prefix PA and AP indicates the respective current direction in the precentral gyrus. MEP, motor evoked potential; RMT, resting motor threshold; AMT, active motor threshold; qTBS, quadri-pulse theta burst stimulation; DSW-RMT, resting motor threshold with double-sine-wave pulses; DSW-AMT, active motor threshold with double-sine-wave pulses; PA, posterior-anterior; AP, anterior-posterior.

the TMS Motor Threshold Assessment Tool, version 2 (http://www.clinicalresearcher.org/software.htm). A MEP was defined as a potential larger than 50 μV in peak-to-peak amplitude.

AMT was defined as the lowest intensity that evoked a small response (>100 μV) while participants maintained a slight contraction of the APB of 5–10% of the maximum voluntary contraction, as previously described for quadri-pulse stimulation (1, 9). Voluntary contraction of adequate force was controlled by a manometer. After determination of the motor threshold, we adjusted the stimulator output to elicit mean MEP amplitudes of 800–1,200 μV peak-to-peak (SI1mV) with single pulse SSW TMS for evaluation.

Double-Sine-Wave (DSW) Quadri-Pulse TBS (qTBS)

DSW qTBS was applied with a double-sine waveform over the precentral motor hand representation of the non-dominant hemisphere, as described previously for SSW qTBS (1). DSW qTBS consisted of bursts with four pulses of the same intensity in intervals of 1.5 ms (∼666 Hz). Each burst was separated by 200 ms (5 Hz). A total of 1,440 pulses was delivered in each session with 360 bursts. The stimulus intensity of each pulse was set to 90% DSW AMT (1). Mean stimulation intensity for DSW AP-qTBS at 1.5 ms ISI was 48.00%MSO ± 5.79 and 42.90%MSO ± 6.10 for DSW PA-qTBS at 1.5 ms ISI.

For comparison with SSW qTBS, we evaluated the same participants with the same dataset as reported in our previous study (1).

Analyses and Statistics

The analyses and statistics of DSW PA-qTBS and DSW AP-qTBS match those reported in our previous manuscript (1). We ensured a sufficient relaxation of the APB by monitoring the electromyographic activity online and by inspecting each MEP sweep again offline. The pre-stimulus time window for determining if MEPs were contaminated by muscle activity was 120 ms. If the electromyographic activity exceeded 0.05 mV, the trial was excluded from further analyses.

All statistical analyses were computed using IBM SPSS Statistics software, version 20.0 (IBM SPSS Statistics Inc., Chicago, IL, USA). Statistical evaluation of DSW qTBS data was performed using repeated-measure analysis of variance (ANOVA) with the inner-subject factors TIME (5 levels: PRE, POST 1, POST 2, POST 3, POST 4) and DIRECTION (2 levels:

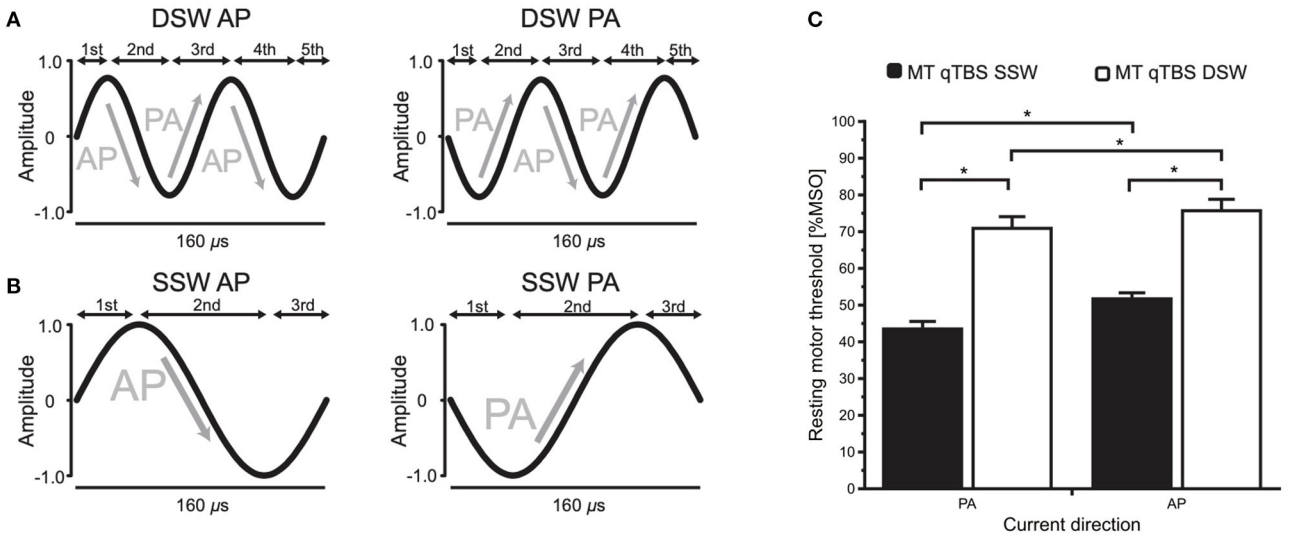

FIGURE 2 | qTBS pulse sequence and current waveforms for double-sine-wave (DSW) and single-sine-wave (SSW) stimuli. **(A)** DSW pulses in PA and AP directions had a biphasic current waveform with 5 components with 160 μs total pulse duration. Current directions always refer to the electrical current produced by the second component of the DSW or SSW pulse in M1-HAND. **(B)** SSW pulses in PA and AP directions with 3 components and 160 μs total pulse duration were used for assessing corticomotor excitability. **(C)** Comparison of rMT data revealed by single pulse TMS using SSW and DSW pulses. RMT was significantly higher with DSW as compared to SSW pulses in PA- and AP-current directions (*post hoc t*-test: $p = 0.02$). Asterisks (*) indicate significant differences between measurements ($p < 0.05$). Error bars display the standard error of the mean (S.E.M.). qTBS, quadri-pulse theta burst stimulation; SSW, single-sine-wave; DSW, double-sine-wave; ISI, interstimulus interval; MEP, motor evoked potential; MSO, maximum stimulator output; IBI, interburst interval; AP, anterior-posterior; PA, posterior-anterior.

PA and AP) after the Kolmogorov-Smirnov test revealed no violations of the assumption of normality.

DSW qTBS and SSW qTBS were compared using a rmANOVA with the inner-subject factors TIME (5 levels: PRE, POST 1, POST 2, POST 3, POST 4) and between-subject factor PULSE SHAPE (2 levels: SSW and DSW). No transformations were required.

All statistics were performed using the mean single pulse SSW MEP amplitude of each case computed of 20 MEP trials averaged to a mean, or rMT value (%MSO). Accordingly, the figures display the mean SSW TMS MEP amplitude, or rMT, of all cases. If necessary, we used the Greenhouse-Geisser correction to adjust for violations of sphericity, resulting in adjusted *p*-values based on adjusted degrees of freedom. In the case of significant main effects or interactions, we conducted *post-hoc* two-tailed paired *t*-tests for PRE-POST investigations and for inter-group comparisons, if the same participants took part in the experiment. For inter-group comparisons between DSW qTBS and SSW qTBS data, we computed *post-hoc* two-tailed unpaired *t*-tests. Data was corrected using the Bonferroni correction for multiple comparisons by multiplication of the *p*-values by the number of tests, in this case four. This method was used for MEP and resting motor threshold data. The significance level was set at $\alpha = 0.05$ for all statistical analyses. All values given are mean group values ± SD, if not indicated otherwise.

RESULTS

None of the participants reported any adverse events during or after the experiments. Detailed MEP values, standard deviations, and mean TMS intensities (%MSO) in the AP and PA directions, respectively, for each condition at SI1mV are depicted below. We observed no changes in hotspots between single pulse SSW TMS and single pulse DSW TMS which was administered prior to the DSW qTBS in AP and PA directed currents in the precentral motor hand representation.

Comparison of rMT between SSW TMS and DSW TMS recorded prior to DSW qTBS revealed significantly higher threshold values ($p < 0.01$) for DSW TMS in AP and PA directed currents, respectively (**Figure 2C**).

Double-Sine Wave (DSW) qTBS at I-Wave Periodicity

Ten volunteers participated in Experiment 1 (DSW PA-qTBS) and Experiment 2 (DSW AP-qTBS), assessing the effect of DSW qTBS at I-wave periodicity with ISI of 1.5 ms. Mean intensity of SSW TMS to target SI1mV was 60.80%MSO ± 14.44 for PA-MEP amplitudes (Experiment 1) and 70.20%MSO ± 11.04 for AP-MEP amplitudes (Experiment 2). rmANOVA of MEP showed a significant main effect of DIRECTION [$F_{(1;9)} = 18.246$, $p = 0.002$] and TIME x DIRECTION interaction [$F_{(4;36)} = 5.466$, $p = 0.002$], but no effect of TIME [$F_{(4;36)} = 1.738$, $p = 0.163$].

PA-MEP amplitudes significantly increased on all time points (*post hoc t*-tests: POST 1: $p = 0.036$; POST 2: $p = 0.00014$; POST 3: $p = 0.012$; POST 4: $p = 0.004$) (**Figure 3A**).

In the AP direction, mean AP-MEP amplitudes significantly decreased on time point POST 1 (*post hoc t*-test: $p = 0.004$) (**Figure 3A**).

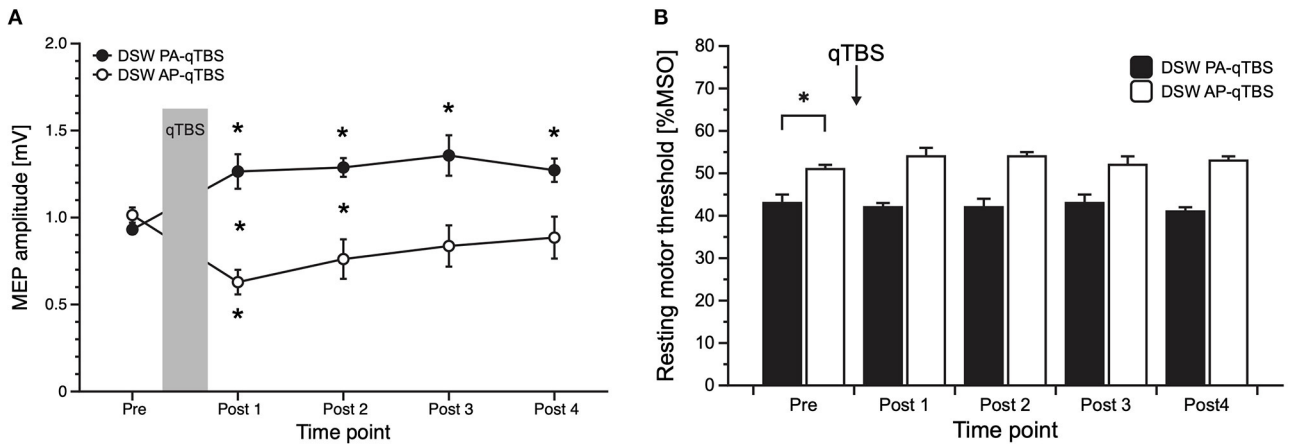

FIGURE 3 | Results of MEP data with corresponding current direction after double-sine-wave (DSW) qTBS in AP and PA directions at ISI of 1.5 ms **(A)** and resting motor threshold following DSW qTBS in AP and PA directions at ISI of 1.5 ms **(B)**. For evaluation, we always used single-sine-wave TMS (SSW TMS) pulses with corresponding current direction as used for qTBS. **(A)** Changing the current flow in M1-HAND from AP to PA led to bidirectional changes in corticospinal excitability with a significant increase of PA-MEP and a significant decrease of AP-MEP, opposite to the bi-directionality observed after SSW qTBS. **(B)** Resting motor threshold of SSW TMS following DSW qTBS in AP and PA directions at ISI of 1.5 ms did not demonstrate significant changes. As observed previously (1), RMT in AP and PA directions significantly differed at pre measurements. Pre: before qTBS, POST1: immediately after qTBS, POST2: 15 min, POST3: 30 min, POST4: 60 min after qTBS. Asterisks indicate significant differences between pre and post measurements ($p < 0.05$). Error bars indicate the standard error of the mean (S.E.M.). qTBS, quadri-pulse theta burst stimulation; PA, posterior-anterior; AP, anterior-posterior; ISI, interstimulus interval; MEP, motor evoked potential; MSO, maximum stimulator output.

Between group comparisons revealed significant differences at time points POST 1 ($p = 0.004$) and POST 2 ($p = 0.008$) (**Figure 3A**).

rmANOVA on rMT data revealed a significant main effect of DIRECTION [$F_{(1;9)} = 42.178$, $p = 0.000112$] but no effect of TIME [$F_{(4;36)} = 0.809$, $p = 0.528$] or TIME x DIRECTION interaction [$F_{(4;36)} = 2.523$, $p = 0.058$]. As expected, and previously observed in the study using SSW qTBS (1), baseline data of SSW TMS rMT prior to DSW qTBS differed significantly (*post hoc t*-test: $p = 0.000464$), with higher thresholds in the AP direction (**Figure 3B**). Mean SSW TMS AP- and PA-rMT data are presented in **Table 1**.

Single-Sine Wave (SSW) qTBS and Double-Sine Wave (DSW) qTBS in PA-Directed Currents

We compared the effect of single-sine wave (SSW) qTBS and double-sine waves (DSW) qTBS, and analyzed for SSW AP- and PA-qTBS the same dataset as previously published (1). Of these participants ($n = 12$), seven took also part in DSW AP- and PA-qTBS experiments. rmANOVA of raw MEP in PA- and AP-directed currents in the brain were computed.

For the PA direction, rmANOVA showed a significant main effect of PULSE SHAPE [$F_{(1;20)} = 14.308$, $p = 0.001$] and TIME x PULSE SHAPE interaction [$F_{(1;20)} = 10.590$, $p = 0.004$] with no significant main effects of TIME [$F_{(4;80)} = 0.561$, $p = 0.692$]. Mean single-sine wave MEP amplitudes significantly increased after double-sine wave (DSW) PA-qTBS at all time points, as demonstrated above. Conversely, mean single-sine wave (SSW) MEP amplitude after SSW PA-qTBS significantly decreased at time points POST 1 and POST 3 (*post hoc t*-test: $p = 0.008$, $p = 0.037$, respectively; (**Figure 4B**). *Post hoc* unpaired *t*-tests revealed a significant difference in SSW MEP amplitudes after SSW and DSW PA-qTBS at all time points (POST 1: $p = 0.004$; POST 2: $p = 0.012$; POST 3: $p = 0.004$; POST 4: $p = 0.048$) (**Figure 4B**).

After SSW and DSW PA-qTBS, significant main effects on rMT data were observed for PULSE SHAPE [$F_{(1;20)} = 6.872$, $p = 0.016$] but not for TIME [$F_{(4;80)} = 0.642$, $p = 0.634$] or TIME x PULSE SHAPE interaction [$F_{(4;80)} = 2.469$, $p = 0.051$]. *Post hoc* analyses (unpaired *t*-test) revealed no significant differences of baseline data of rMT prior to single- and double-sine PA-qTBS ($p = 0.058$), but between all time points after stimulation (post 1: $p = 0.013$; post 2: $p = 0.025$; post 3: $p = 0.036$; post 4: $p = 0.006$) (**Table 1**).

SSW qTBS and DSW qTBS in AP Directed Currents

Comparing AP directed SSW and DSW qTBS effects, rmANOVA revealed a significant TIME x PULSE SHAPE interaction [$F_{(4;80)} = 3.929$, $p = 0.006$] with significant main effects for PULSE SHAPE [$F_{(1;20)} = 11.070$, $p = 0.003$] but not for TIME [$F_{(4;80)} = 1.839$, $p = 0.129$] (**Figure 4A**). Mean SSW MEP amplitudes after DSW AP-qTBS significantly decreased at time point POST 1 ($p = 0.004$). Mean SSW MEP amplitudes increased after SSW AP-qTBS at time point POST 4 (*post hoc t*-test: $p = 0.014$). Comparing SSW and DSW AP-qTBS, SSW MEP amplitudes were significantly different (*post-hoc* unpaired *t*-test) at time points POST 1 ($p = 0.008$) and POST 4 ($p = 0.044$) (**Figure 4A**). Detailed MEP values are provided in **Table 1**.

TABLE 1 | Raw data of motor evoked potential (MEP) in millivolts (mV) and resting motor threshold (rMT) in percent of maximum stimulator output (%MSO) in the respective effective current direction in the brain anterior-posterior (AP) and posterior-anterior (PA) before and after double-sine wave (DSW) qTBS and single-sine wave (SSW) qTBS.

			Timepoint				
		Current direction	**Pre**	**POST 1**	**POST 2**	**POST 3**	**POST 4**
DSW qTBS	MEP ± SD (mV)	PA	0.93 ± 0.08	1.26 ± 0.31	1.29 ± 0.17	1.36 ± 0.37	1.27 ± 0.24
		AP	1.01 ± 0.14	0.63 ± 0.22	0.76 ± 0.36	0.83 ± 0.38	0.88 ± 0.38
	RMT ± SD (%MSO)	PA	43.50 ± 6.52	42.70 ± 5.60	42.80 ± 6.73	43.30 ± 7.59	41.10 ± 6.10
		AP	51.70 ± 5.23	54.20 ± 8.27	54.80 ± 4.92	52.90 ± 7.26	53.40 ± 5.99
SSW qTBS	MEP ± SD (mV)	PA	0.99 ± 0.14	0.77 ± 0.32	0.81 ± 0.42	0.73 ± 0.42	0.81 ± 0.49
		AP	0.98 ± 0.10	1.20 ± 0.47	1.25 ± 0.48	1.19 ± 0.42	1.41 ± 0.49
	RMT ± SD (%MSO)	PA	50.25 ± 2.53	52.17± 2.78	50.17 ± 2.12	51.83 ± 2.81	52.42 ± 2.93
		AP	59.33 ± 8.40	61.00 ± 11.98	60.58 ± 12.19	61.33 ± 9.74	59.00 ± 10.04

Analyses of rMT data (rmANOVA) measured with SSW pulses of the same direction revealed no significant main effect of PULSE SHAPE [$F_{(1;20)} = 3.648$, $p = 0.071$], TIME [$F_{(4;80)} = 1.543$, $p = 0.198$] or TIME x PULSE SHAPE [$F_{(4;80)} = 0.635$, $p = 0.639$] after SSW and DSW AP-qTBS.

Comparing the changes in corticospinal excitability between DSW and SSW qTBS of opposite current directions but with the same sign of plasticity (1), we observed a tendency toward a more stable increase in corticospinal excitability after DSW qTBS and a decrease in corticospinal excitability after SSW qTBS (**Table 1**).

DISCUSSION

This study extends the findings of previous research on the ability of TBS to alter corticomotor excitability. Using pulses with a double-sine-wave configuration, the present study is the first investigating the after-effects of DSW qTBS and the impact of induced current direction on corticospinal excitability. DSW pulses were applied as quadruple bursts at I-wave periodicity (666 Hz) to preferentially interact with the intracortical circuits in the precentral cortex that project onto the fast-conducting corticospinal neurons. After effects of DSW qTBS on corticospinal excitability were examined using single SSW TMS pulses that produced the same preferential current direction as DSW pulses during qTBS. We found that DSW qTBS at 666 Hz produced lasting changes in corticomotor excitability. The temporal order of phase-related reversals and the resulting order of current reversals in the precentral gyrus determined whether DSW qTBS at I-wave periodicity produced an increase or decrease in corticospinal excitability. If the second component of DSW induced an anterior-to-posterior current in the cortex, DSW AP-qTBS transiently decreased AP-MEP amplitudes. Conversely, DSW PA-qTBS increased PA-MEP amplitudes, if the second component of DSW induced a posterior-to-anterior current in the cortex.

Double-Sine Wave (DSW) qTBS in PA and AP direction

Biphasic SSW pulses with cycle durations >160 μs are commonly used for TBS. But so far, there is no research on the plasticity inducing effects of TMS pulses that consist of two concatenated full-sine cycles. In this study, we matched the total duration (160 μs) of the DSW pulse to the duration of an SSW pulse (**Figures 2A,B**). Hence, a single DSW pulse produced five reversals of the induced current direction in the stimulated motor cortex within the 160 μs (**Figures 2A,B**). Inducing very fast oscillating tissue currents, DSW PA-qTBS at 666 Hz (i.e., at I-wave periodicity) caused a stable increase in PA-MEP amplitudes, whereas DSW AP-qTBS at 666 Hz induced a transient decrease in AP-MEP amplitudes.

These after effects are novel and interesting, but a neurobiological interpretation is challenging and remains in many aspects speculative. Previous electrophysiological TBS studies are of little help as they used biphasic SSW pulses with longer single-cycle duration. Given the short cycle length of our DSW pulse, polarity reversals occurred at a faster rate and thus, the rise times of the electrical field during a single pulse component were steeper, but shorter. Therefore, the biophysical effects of a given AP or PA component of the DSW pulse can be expected to differ substantially from the effects evoked by the AP or PA component of a standard SSW pulse. Due to the shorter duration, the depolarizing and hyperpolarizing effects of the DSW components on the axonal membrane may interact. The earlier components of the DSW pulse may enhance or attenuate the likelihood of the later components of the DSW pulse to alter the membrane state and to evoke changes in corticomotor excitability by eliciting action potentials in the targeted cortex region with DSW qTBS.

Computational models and experimental observations suggest that the effect of electrical stimulation with reversed double pulses on the probability to elicit an action potential depends on the sequence of polarity within a pulse and on the value of the membrane potential at the time of stimulation (16). In a hyperpolarized membrane state, an initial negative double-sine shaped pulse is more effective in generating action potentials in animal models, while in a depolarized membrane, an initially positive pulse is more effective (16). It has been argued, using biphasic pulses, that the initially negative short falling component of the pulse leads to a hyperpolarization of the nerve membrane and removes a small degree of the

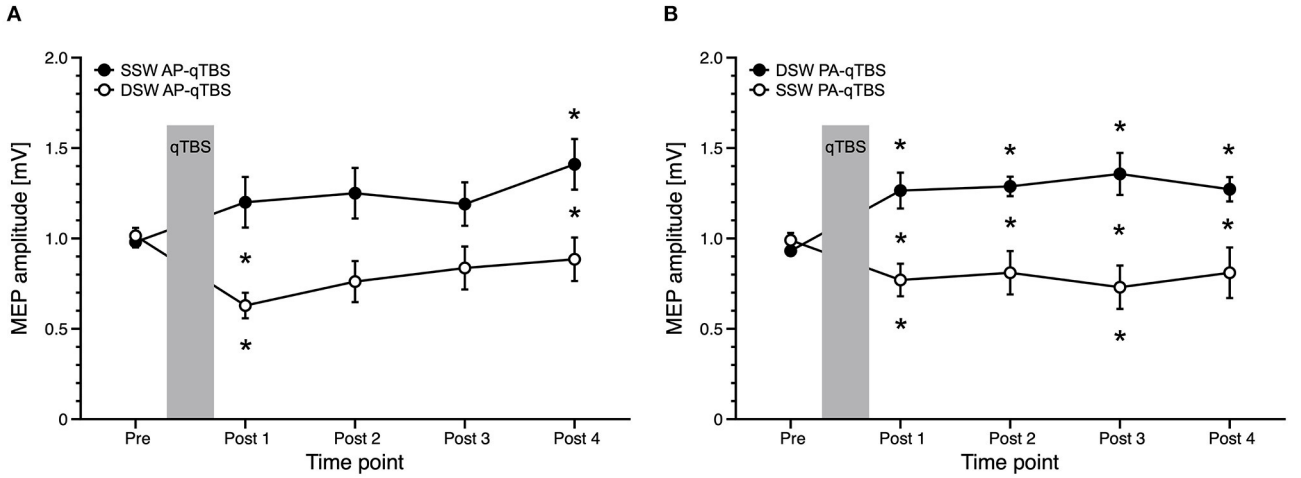

FIGURE 4 | Comparison of MEP data with corresponding current direction after single-sine wave (SSW) and double-sine wave (DSW) qTBS in AP and PA directions, respectively, at ISI of 1.5 ms **(A,B)**. Data are replotted from **Figure 3A** and from the previous manuscript (1). For evaluation, we always used single-sine wave (SSW) TMS pulses of corresponding current direction. **(A)** Differences of MEP course after SSW AP-qTBS and DSW AP-qTBS demonstrate bidirectional changes in corticomotor excitability in the precentral motor hand representation with a significant increase of AP-MEP after DSW AP-qTBS and a significant decrease of AP-MEP after SSW AP-qTBS. **(B)** Conversely, PA-MEP amplitudes as a sign of changes in corticomotor excitability significantly increased after SSW PA-qTBS and transiently decreased following DSW PA-qTBS. SSW TMS results shown here are the same as previously published (1). Pre: before qTBS, POST1: immediately after qTBS, POST2: 15 min, POST3: 30 min, POST4: 60 min after qTBS. Asterisks indicate significant differences between pre and post measurements or between SSW and DSW measurements within one time point ($p < 0.05$, unpaired *t*-test). Error bars indicate the standard error of the mean (S.E.M.). qTBS, quadri-pulse theta burst stimulation; PA, posterior-anterior; AP, anterior-posterior; ISI, interstimulus interval; MEP, motor evoked potential.

resting level of sodium channel inactivation (24). This, in turn, renders the following long rising component more effective in depolarizing the nerve membrane and eliciting action potentials (24). The long rising or falling second component in biphasic pulses dominates the depolarizing or hyperpolarizing effect which is primed by the initial current of the short component (24). In this context, a hyperpolarization of the nerve has been shown to increase the availability of sodium channels during the subsequent depolarizing component of the pulse and triggers action potentials elicited by the pulse (24). However, the situation may be much more complex using DSW pulses due to the many reversals of the current. In this case, we may only speculate about the mechanisms and further investigations of the detailed neurophysiological mechanisms are needed, as these hypotheses of different membrane states are not directly supported by our experiments.

The preceding components of DSW used in the present study may have influenced the responsiveness of the cortical target structures (axons) to the depolarizing or hyperpolarizing effects of the tissue current induced by later phases of a DSW pulse, while the priming effect of a preceding hyperpolarization may explain the sign of the aftereffects induced by DSW qTBS. We speculate that this leads to an increase in corticomotor excitability after DSW PA-qTBS, which is explained by a higher efficacy of this double-sine shaped pulse to elicit action potentials.

In contrast, the transient decrease in corticomotor excitability after DSW AP-qTBS may be due to the hyperpolarization of predominantly AP directed currents. Thus, DSW AP-qTBS may generate action potentials in fewer neurons (16, 24–26). However, we remain very speculative as the detailed cellular mechanisms have not been directly investigated (e.g., on single neurons).

Another explanation of the effects may be that each DSW pulse of the respective current direction results in a greater net activation of AP- and PA-directed currents (here, DSW AP-qTBS and DSW PA-qTBS), respectively. Comparing the results of SSW qTBS and DSW qTBS of the same preferential current direction in the brain, we demonstrated an opposite sign of plasticity (**Figures 4A,B**). The idea of the same effective current direction in the brain (i.e., AP and PA) is supported by the directional dependency of rMT values, which is in agreement with our hypothesis, that DSW AP-qTBS mainly induces an AP-directed current in the brain while DSW PA-qTBS mainly induces a PA-directed current flow in the brain (**Figure 2C**). Hence, we assume further mechanisms of DSW pulses to be responsible for the bidirectional effects of DSW qTBS on corticospinal excitability.

The interpretation of our findings is further complicated by the assumption that AP and PA currents in the precentral gyrus may produce preferential excitation of different sets of cortical neurons (27). Implementing realistic models of cortical neurons, a recent modeling study of TMS-induced electrical fields in the precentral gyrus identified intracortical axonal terminations in the superficial crown and lip regions as primary stimulation target sites (28). Relevant to our study, varying the induced current direction (AP vs. PA) caused an anterior-posterior shift in precentral activation for both monophasic and biphasic pulse (SSW) configurations (28). This leads to a preferential excitation

of differently oriented axon terminals in the anterior (AP current) or posterior (PA current) lip regions of the precentral gyrus. Since cortical neurons in the precentral crown display marked regional differences in their sensitivity to fire in response to the rapidly changing AP or PA-directed currents, we argue that DSW PA-qTBS and AP-qTBS targeted spatially distinct sets of cortical neurons in the precentral cortex. This may be an important additional cause for why DSW PA-qTBS induced opposite effects on corticomotor excitability compared to AP-qTBS.

Double-Sine-Wave (DSW) qTBS and Single-Sine-Wave (SSW) qTBS

The direction of plasticity produced by DSW qTBS at I-wave periodicity was opposite in sign compared to the bidirectional excitability changes that we had previously observed after SSW qTBS at I-wave periodicity. This was the case when we compared the SSW qTBS conditions (applied in our previous study) and the DSW qTBS conditions (applied in this study) of the same preferential current direction in the precentral motor hand representation. We found an increase in corticomotor excitability after DSW PA-qTBS and a decrease after SSW PA-qTBS, while DSW AP-qTBS led to a decrease and SSW AP-qTBS to an increase (**Figure 4**). Comparing the changes in corticospinal excitability between DSW and SSW qTBS of opposite current direction but with same sign of plasticity (1), the increase in corticospinal excitability was slightly more evident after DSW PA-qTBS than SSW AP-qTBS indicating DSW qTBS is more effective.

The burst frequency (666 Hz) for both, DSW qTBS and SSW qTBS, was chosen to interact with I-wave periodicity, for instance by modifying the fidelity of spike timing mechanisms for single-sine qTBS (1, 29). We consider a differential effect of DSW and SSW pulses on the high-fidelity spike-timing mechanisms at I-wave periodicity to be unlikely, given the very high frequency of the alternating tissue current in the kHz range. Rather, we propose that the aforementioned mechanisms of change in membrane states and action potential generation account for the differences in current-orientation specific effects. However, we may not exclude a rather simple explanation that DSW PA-qTBS has an AP-like stimulation effect and, consequently, DSW AP-qTBS has a PA-like stimulation effect. Although this seems to be unlikely since an evaluation in the opposite current direction of SSW TMS to DSW qTBS demonstrated no changes in corticospinal excitability (**Supplementary Material**). Moreover, I-wave excitability appears to play a central role in modulating corticospinal excitability (30). Regardless of what the underlying mechanisms may be, the results of our qTBS work highlights the pulse configuration as an important variable of TMS interventions. Our observation motivates future research examining, in detail, how the number of cycles and cycle length of SSW, DSW, and poly-sine wave pulses influence the efficacy of inducing action potentials in axonal structures in the targeted cortex. Such research may inform future attempts to optimize the pulse configurations used for interventional rTMS in a therapeutic setting.

Differences to Previous Findings and Safety Issues

In a therapeutic setting, the motivation for applying rTMS is to induce stable changes in cortical excitability and function (31). Here, we introduce a modified version of the existing qTBS protocol using a novel pulse configuration which may draw on mechanisms of neuronal excitation that could not be investigated previously with conventional either monophasic or biphasic single-sine-wave pulse configurations. Comparing our findings to other TMS studies that investigated corticospinal plasticity in humans, the increase or decrease in corticomotor excitability resembles previously reported LTP- and LTD-like plasticity (8). Yet, the mechanisms that determine the induction of action potentials with DSW pulses remain to be explored. Further investigations using DSW to better understand the mechanisms of the new stimulation protocol are needed.

Our previous findings demonstrated that using pulses that consisted of multiple sine cycles is more effective in exciting corticospinal output neurons in the precentral motor hand representation than single-sine cycles (14). Here, we observed a slightly higher threshold for DSW pulses of app. 10 %MSO as compared to our previous findings (14). Since we did not use the same stimulation device, this difference may be attributed to the technical pattern because of different capacitors and repetition of the pulses or neurophysiological differences in chronaxie and rheobase. Additional experiments comparing SSW pulses of 80 μs and DSW pulses of 160 μs may provide additional insights.

Furthermore, it is worth mentioning that the directional dependency of rMT values is in line with our hypothesis, that the preferential currents in the brain induced by DSW stimulation cause higher rMT values for AP-directed currents than for PA-directed currents. This may support the idea of predominantly PA- and AP-directed tissue currents and activation as illustrated in **Figure 2C**.

As a limitation, we evaluated changes in corticospinal excitability only by SSW single-pulse TMS. As we used amplitudes with an intensity to target 1 mV (SI1mV) and rMT of DSW TMS was high (**Figure 2C**) we were unable to target SI1mV by DSW single-pulse TMS. Moreover, we limited the stimuli count before experiments to avoid occlusion of possible plasticity effects in human primary motor cortex (21). The study is further limited by a rather small numbers of participants. However, we tried to minimize any confounding factors by choosing an intra-subject design for DSW qTBS (and for SSW qTBS). Even then, DSW qTBS has demonstrated clear (bidirectional) effects on corticospinal plasticity.

In this study, DSW pulses were used for the first time for ultra-high-frequent qTBS. This raises the question whether the novel protocol is equally as safe as previously introduced rTMS protocols. We performed the intervention with stimulation intensities below active motor thresholds according to existing safety guidelines (18). The protocol was well-tolerated by all participants with no adverse effects or spread of excitation to neighboring muscles during stimulation. However, further studies are needed to confirm the safety and clinical use of patterned rTMS protocols using DSW pulses.

CONCLUSIONS

We demonstrated bi-directional changes in corticospinal excitability after ultra-high frequency DSW qTBS over human precentral motor hand representation. The induced current direction in the brain determined the sign of plasticity of DSW qTBS at ISI that target I-wave periodicity (i.e., 666 Hz). Bi-directional effects were opposite to those observed after SSW qTBS in the respective current direction. The results may be explained by the effects of alternating medium frequency current at axonal membranes. Our findings may be of relevance when designing new and effective non-invasive TMS protocols for research and therapeutic purposes and may provide new insights into mechanisms of corticospinal excitability in the human precentral gyrus. The results of this study may offer new opportunities for short non-invasive brain stimulation protocols that are especially suited for transcranial magnetic stimulation in children and patients with neurological or neurodevelopmental disorders.

DATA AVAILABILITY STATEMENT

The original contributions presented in the study are included in the article/**Supplementary Material**, further inquiries can be directed to the corresponding authors.

ETHICS STATEMENT

The studies involving human participants were reviewed and approved by Ethics Committee of the Technical University of Munich, Faculty of Medicine. The patients/participants provided their written informed consent to participate in this study.

AUTHOR CONTRIBUTIONS

NJ, BG, HS, and VM conceptualized and designed the study and supervised the work. NJ, BG, NG, AK, EA, and JF were involved in data acquisition, including patient recruitment, and data analysis. NJ, BG, NG, AK, and JF were involved in the analysis and interpretation of the data. NJ wrote the first draft of the manuscript. All authors approved the final manuscript.

FUNDING

HS received financial support from the Novo Nordisk Foundation Interdisciplinary Synergy Program 2014 [Biophysically adjusted state-informed cortex stimulation (BASICS); Grant No. NNF14OC0011413].

ACKNOWLEDGMENTS

We would like to thank Julia Knürr, M.Sc. (Munich School of BioEngineering, Technical University Munich), and Ing. John LaMaster (Department of Bioengineering, Faculty of Computer Science, Technical University Munich) for proofreading and critically revising the language of the manuscript. The authors would also like to thank all volunteers for participating in the present study. HS holds a 5-year professorship in precision medicine at the Faculty of Health Sciences and Medicine at the University of Copenhagen which is sponsored by the Lundbeck Foundation (Grant No. R186-2015-2138).

SUPPLEMENTARY MATERIAL

The Supplementary Material for this article can be found online at: https://www.frontiersin.org/articles/10.3389/fneur.2021.673560/full#supplementary-material

REFERENCES

1. Jung NH, Gleich B, Gattinger N, Hoess C, Haug C, Siebner HR, et al. Quadri-pulse theta burst stimulation using ultra-high frequency bursts - a new protocol to induce changes in cortico-spinal excitability in human motor cortex. *PLoS ONE*. (2016) 11:e0168410. doi: 10.1371/journal.pone.0168410
2. Bliss TV, Lomo T. Long-lasting potentiation of synaptic transmission in the dentate area of the anaesthetized rabbit following stimulation of the perforant path. *J Physiol*. (1973) 232:331–56. doi: 10.1113/jphysiol.1973.sp010273
3. Ismail FY, Fatemi A, Johnston MV. Cerebral plasticity: windows of opportunity in the developing brain. *Eur J Paediatr Neurol*. (2017) 21:23–48. doi: 10.1016/j.ejpn.2016.07.007
4. Ziemann U, Paulus W, Nitsche MA, Pascual-Leone A, Byblow WD, Berardelli A, et al. Consensus: motor cortex plasticity protocols. *Brain Stimul*. (2008) 1:164–82. doi: 10.1016/j.brs.2008.06.006
5. Bliss TV, Collingridge GL. A synaptic model of memory: long-term potentiation in the hippocampus. *Nature*. (1993) 361:31–9. doi: 10.1038/361031a0
6. Feldman DE. Synaptic mechanisms for plasticity in neocortex. *Annu Rev Neurosci*. (2009) 32:33–55. doi: 10.1146/annurev.neuro.051508.135516
7. Di Lazzaro V, Profice P, Ranieri F, Capone F, Dileone M, Oliviero A, et al. I-wave origin and modulation. *Brain Stimul*. (2012) 5:512–25. doi: 10.1016/j.brs.2011.07.008
8. Huang YZ, Edwards MJ, Rounis E, Bhatia KP, Rothwell JC. Theta burst stimulation of the human motor cortex. *Neuron*. (2005) 45:201–6. doi: 10.1016/j.neuron.2004.12.033
9. Hamada M, Terao Y, Hanajima R, Shirota Y, Nakatani-Enomoto S, Furubayashi T, et al. Bidirectional long-term motor cortical plasticity and metaplasticity induced by quadripulse transcranial magnetic stimulation. *J Physiol*. (2008) 586:3927–47. doi: 10.1113/jphysiol.2008.152793
10. Huang YZ, Rothwell JC, Chen RS, Lu CS, Chuang WL. The theoretical model of theta burst form of repetitive transcranial magnetic stimulation. *Clin Neurophysiol*. (2011) 122:1011–8. doi: 10.1016/j.clinph.2010.08.016
11. Weise D, Mann J, Rumpf JJ, Hallermann S, Classen J. Differential regulation of human paired associative stimulation-induced and theta-burst stimulation-induced plasticity by L-type and T-type Ca2+ channels. *Cereb Cortex*. (2017) 27:4010–21. doi: 10.1093/cercor/bhw212
12. Di Lazzaro V, Oliviero A, Profice P, Meglio M, Cioni B, Tonali P, et al. Descending spinal cord volleys evoked by transcranial magnetic and electrical stimulation of the motor cortex leg area in conscious humans. *J Physiol*. (2001) 537(Pt 3):1047–58. doi: 10.1111/j.1469-7793.2001.01047.x
13. Ziemann U. I-waves in motor cortex revisited. *Exp Brain Res*. (2020) 238:1601–10. doi: 10.1007/s00221-020-05764-4
14. Pechmann A, Delvendahl I, Bergmann TO, Ritter C, Hartwigsen G, Gleich B, et al. The number of full-sine cycles per pulse influences the efficacy of multicycle transcranial magnetic stimulation. *Brain Stimul*. (2012) 5:148–54. doi: 10.1016/j.brs.2011.02.006

15. Gildemeister M. Untersuchungen über die Wirkung der Mittelfrequenzströme auf den Menschen. *Pflüger's Archiv für die gesamte Physiologie des Menschen und der Tiere*. (1944) 247:366–404. doi: 10.1007/BF01759722
16. Bromm B, Girndt E. [Demonstration, extinction and summation of subliminal stimuli in the isolated node of Ranvier by stimulation with short reverse double pulse]. *Pflugers Arch Gesamte Physiol Menschen Tiere*. (1967) 296:1–13. doi: 10.1007/BF00363475
17. Oldfield RC. The assessment and analysis of handedness: the Edinburgh inventory. *Neuropsychologia*. (1971) 9:97–113. doi: 10.1016/0028-3932(71)90067-4
18. Rossi S, Hallett M, Rossini PM, Pascual-Leone A, Safety of TMSCG. Safety, ethical considerations, and application guidelines for the use of transcranial magnetic stimulation in clinical practice and research. *Clin Neurophysiol*. (2009) 120:2008–39. doi: 10.1016/j.clinph.2009.08.016
19. Rossi S, Hallett M, Rossini PM, Pascual-Leone A. Screening questionnaire before TMS: an update. *Clin Neurophysiol*. (2011) 122:1686. doi: 10.1016/j.clinph.2010.12.037
20. Ziemann U, Muellbacher W, Hallett M, Cohen LG. Modulation of practice-dependent plasticity in human motor cortex. *Brain*. (2001) 124(Pt 6):1171–81. doi: 10.1093/brain/124.6.1171
21. Delvendahl I, Jung NH, Mainberger F, Kuhnke NG, Cronjaeger M, Mall V. Occlusion of bidirectional plasticity by preceding low-frequency stimulation in the human motor cortex. *Clin Neurophysiol*. (2010) 121:594–602. doi: 10.1016/j.clinph.2009.09.034
22. Gattinger N, Jung NH, Mall V, Gleich B. Transcranial magnetic stimulation devices for biphasic and polyphasic ultra-high frequency protocols. *Biol Eng Med*. (2018) 3:8–8. doi: 10.15761/BEM.1000136
23. Awiszus F. TMS and threshold hunting. *Suppl Clin Neurophysiol*. (2003) 56:13–23. doi: 10.1016/S1567-424X(09)70205-3
24. Clay JR, Forger DB, Paydarfar D. Ionic mechanism underlying optimal stimuli for neuronal excitation: role of Na+ channel inactivation. *PLoS ONE*. (2012) 7:e45983. doi: 10.1371/journal.pone.0045983
25. Maccabee PJ, Nagarajan SS, Amassian VE, Durand DM, Szabo AZ, Ahad AB, et al. Influence of pulse sequence, polarity and amplitude on magnetic stimulation of human and porcine peripheral nerve. *J Physiol*. (1998) 513 (Pt 2):571–85. doi: 10.1111/j.1469-7793.1998.571bb.x
26. Sommer M, Rummel M, Norden C, Rothkegel H, Lang N, Paulus W. Mechanisms of human motor cortex facilitation induced by subthreshold 5-Hz repetitive transcranial magnetic stimulation. *J Neurophysiol*. (2013) 109:3060–6. doi: 10.1152/jn.01089.2012
27. Hamada M, Galea JM, Di Lazzaro V, Mazzone P, Ziemann U, Rothwell JC. Two distinct interneuron circuits in human motor cortex are linked to different subsets of physiological and behavioral plasticity. *J Neurosci*. (2014) 34:12837–49. doi: 10.1523/JNEUROSCI.1960-14.2014
28. Aberra AS, Wang B, Grill WM, Peterchev AV. Simulation of transcranial magnetic stimulation in head model with morphologically-realistic cortical neurons. *Brain Stimul*. (2020) 13:175–89. doi: 10.1016/j.brs.2019.10.002
29. Cash RF, Mastaglia FL, Thickbroom GW. Evidence for high-fidelity timing-dependent synaptic plasticity of human motor cortex. *J Neurophysiol*. (2013) 109:106–12. doi: 10.1152/jn.00584.2011
30. Volz L, Hamada M, Michely J, Pool EM, Nettekoven C, Rothwell JC, et al. Modulation of I-wave generating pathways by TBS: a model of plasticity induction. *J Physiol*. (2019) 597:5963–71. doi: 10.1113/JP278636
31. Rossini PM, Burke D, Chen R, Cohen LG, Daskalakis Z, Di Iorio R, et al. Non-invasive electrical and magnetic stimulation of the brain, spinal cord, roots and peripheral nerves: Basic principles and procedures for routine clinical and research application. An updated report from an IFCN Committee. *Clin Neurophysiol*. (2015) 126:1071–107. doi: 10.1016/j.clinph.2015.02.001

Conflict of Interest: HS has received honoraria as speaker from Sanofi Genzyme, Denmark and Novartis, Denmark, as a consultant from Sanofi Genzyme, Denmark and as editor-in-chief (NeuroImage Clinical) and senior editor (NeuroImage) from Elsevier Publishers, Amsterdam, Netherlands. He has received royalties as book editor from Springer Publishers, Stuttgart, Germany and Gyldendal Publishers, Copenhagen, Denmark.

The remaining authors declare that the research was conducted in the absence of any commercial or financial relationships that could be construed as a potential conflict of interest.

Copyright © 2021 Jung, Gleich, Gattinger, Kalb, Fritsch, Asenbauer, Siebner and Mall. This is an open-access article distributed under the terms of the Creative Commons Attribution License (CC BY). The use, distribution or reproduction in other forums is permitted, provided the original author(s) and the copyright owner(s) are credited and that the original publication in this journal is cited, in accordance with accepted academic practice. No use, distribution or reproduction is permitted which does not comply with these terms.

frontiers in Neurology

REVIEW
published: 23 July 2021
doi: 10.3389/fneur.2021.668081

Sensorimotor Integration in Childhood Dystonia and Dystonic Cerebral Palsy—A Developmental Perspective

Verity M. McClelland[1,2]* *and Jean-Pierre Lin*[2]

[1] Department of Basic and Clinical Neuroscience, Institute of Psychiatry, Psychology and Neuroscience, King's College London, London, United Kingdom, [2] Children's Neurosciences Department, Evelina London Children's Hospital, Guy's and St Thomas' NHS Foundation Trust, London, United Kingdom

Dystonia is a disorder of sensorimotor integration, involving dysfunction within the basal ganglia, cortex, cerebellum, or their inter-connections as part of the sensorimotor network. Some forms of dystonia are also characterized by maladaptive or exaggerated plasticity. Development of the neuronal processes underlying sensorimotor integration is incompletely understood but involves activity-dependent modeling and refining of sensorimotor circuits through processes that are already taking place *in utero* and which continue through infancy, childhood, and into adolescence. Several genetic dystonias have clinical onset in early childhood, but there is evidence that sensorimotor circuit development may already be disrupted prenatally in these conditions. Dystonic cerebral palsy (DCP) is a form of acquired dystonia with perinatal onset during a period of rapid neurodevelopment and activity-dependent refinement of sensorimotor networks. However, physiological studies of children with dystonia are sparse. This discussion paper addresses the role of neuroplasticity in the development of sensorimotor integration with particular focus on the relevance of these mechanisms for understanding childhood dystonia, DCP, and implications for therapy selection, including neuromodulation and timing of intervention.

Keywords: dystonia, children, dystonic cerebral palsy, sensorimotor integration, plasticity, critical windows, neurodevelopment, neuromodulation

OPEN ACCESS

Edited by:
Volker Mall, Technical University of Munich, Germany

Reviewed by:
Fumiaki Yokoi, University of Florida, United States
Bhooma Aravamuthan, Washington University School of Medicine in St. Louis, United States

***Correspondence:**
Verity M. McClelland
verity.McClelland@kcl.ac.uk

Specialty section:
This article was submitted to Pediatric Neurology, a section of the journal Frontiers in Neurology

Received: *15 February 2021*
Accepted: *07 June 2021*
Published: *23 July 2021*

Citation:
McClelland VM and Lin J-P (2021) Sensorimotor Integration in Childhood Dystonia and Dystonic Cerebral Palsy—A Developmental Perspective. Front. Neurol. 12:668081. doi: 10.3389/fneur.2021.668081

INTRODUCTION

Dystonia is a neurological syndrome characterized by involuntary, sustained, or intermittent, muscle contractions causing abnormal, often repetitive, movements, postures, or both. Dystonic movements are typically patterned, twisting, and associated with overflow muscle activation (1). Healthy babies and infants also express involuntary, sustained, patterned, and repetitive contraction of non-synergistic muscles, causing twisting movements or postures (**Figure 1**) which are replaced through development by skilled, purposeful, and economic movements (2). Although the underlying pathophysiological mechanisms of dystonia are still not fully understood, several common themes have emerged from physiological studies, including reduced inhibition within the CNS (4), exaggerated plasticity (5, 6), abnormal patterns of basal ganglia neuronal firing (7–10), and enhanced low-frequency oscillatory activity in the basal ganglia (11, 12), and an abnormal

excessive low frequency drive to muscles (13–16). Another striking feature is aberrant sensorimotor processing, with the implication that distorted perception of incoming afferent information and its abnormal integration with motor commands leads to excessive and undesired dystonic movements (16–20). Abnormal sensorimotor processing, particularly measures of spatial or temporal tactile sensory discrimination, appears to be an "endophenotype" in certain genetic dystonias, being observed also in non-manifesting DYT1 carriers (21) or asymptomatic first degree relatives of patients with adult-onset primary torsion dystonia (22).

Unfortunately, despite the onset of many genetic dystonias in mid-childhood (e.g., DYT1 and DYT6), neurophysiological studies in children with dystonia are sparse (23). This leaves a significant gap in our knowledge of the impact of these genetic abnormalities on the sensorimotor system as it develops and matures through infancy, childhood, and adolescence, and during critical windows of neurodevelopment (23, 24) when neuroplasticity is naturally heightened compared with adults, facilitating development, learning, and adaptation in typically developing children (24). As will be seen below, these mutations may have an impact on sensorimotor development even *in utero*. Moreover, many acquired dystonias arise from brain injury in the perinatal period [i.e., dystonic cerebral palsy (DCP)], when the presence of transient neuronal structures or critical periods of synaptic plasticity and activity-dependent refinement of neuronal circuits gives rise to specific periods of vulnerability to insult (2, 24–26). To gain a thorough understanding of these processes, and the options for therapeutic intervention, it is important to study neurophysiological mechanisms of disease in infants and children rather than extrapolate from adult studies (23).

This article brings together literature on the neurophysiology of normal development of the sensorimotor system in the pre-natal and perinatal periods, childhood and adolescence, to consider the role of plasticity mechanisms during these times, and then to consider how these processes are relevant to dystonia, with an emphasis on both isolated genetic dystonias with onset in childhood and DCP.

NEUROPLASTICITY AND ITS MECHANISMS

Neuroplasticity refers to the dynamic biological capacity of the central nervous system to undergo structural and functional change in response to experience, and to adapt following injury (24). These experience-driven changes are mediated by a variety of mechanisms, including neurogenesis, apoptosis, synaptogenesis, and synaptic pruning, as reviewed in detail elsewhere (24, 27). Two main forms of plasticity are described–Hebbian and homeostatic–and both play a critical role in nervous system maturation.

Hebbian Plasticity

Hebbian mechanisms include changes in synaptic strength mediated via long-term potentiation (LTP) or long-term depression (LTD) following high frequency or prolonged, patterned pre-synaptic stimulation, respectively (28). See also **Figure 1**. LTP or LTD can also be induced by repeated pairing of single presynaptic stimuli with post-synaptic depolarisation, with the relative timing of the pre- and post-synaptic action potentials determining the direction of synaptic change (28). If Hebbian forms of plasticity are unregulated, there is the potential for neural circuit activity to become unstable and to "runaway" toward hyperactivity or quiescence (29). Homeostatic plasticity mechanisms are therefore required to guard against this possibility and stabilize the system.

Homeostatic Plasticity

Homeostatic mechanisms regulate both synaptic numbers and synaptic strength (30) and act to adjust neuronal firing in response to changes in post-synaptic activity. Thus, when cortical networks are deprived of activity, network properties are altered to promote excitability, for example by an increase in strength of excitatory synapses onto excitatory neurons (29). In contrast, an elevation in network activity leads to a reduction in the strength of excitatory synapses. Homeostatic mechanisms thus restore activity to a "set-point" following perturbations (30) and act throughout the nervous system, both centrally and at the neuromuscular junction (29), thus tuning the central and peripheral mechanisms for action.

These homeostatic changes in synaptic strength occur relatively slowly over several hours and are mediated in various ways, such as proportional scaling of synaptic currents (i.e., each synapse is strengthened or weakened in proportion to its initial strength, allowing the relative differences between synapses to be preserved), changes in the clustering of postsynaptic receptors (i.e., prolonged synaptic inactivity leads to an increase in the insertion of post-synaptic receptors), presynaptic transmitter release or reuptake and changes to the number of functional synapses (29). Combinations of these mechanisms can also allow "sliding plasticity thresholds," which adjust the ease with which LTP and LTD can be induced in an activity—dependent manner (29).

NEUROPLASTICITY AND DYSTONIA

Neurophysiological Tools Used to Assess Plasticity

The paired associative stimulation (PAS) protocol involves coupling of low frequency electrical peripheral nerve stimulation with transcranial magnetic stimulation (TMS) over primary motor cortex. This leads to an increase or decrease in the amplitude of the motor evoked potential (MEP), depending on the inter-stimulus interval between the peripheral and TMS stimuli, reflecting an increase or decrease in excitability of the corticospinal neurons (31). These effects are both enduring and show topographical specificity, and are therefore considered to represent LTP-like and LTD-like neuroplasticity within the sensorimotor system (31). Paired associative stimulation has been demonstrated in adults (31, 32) and in children from age seven upwards (33). The theta burst stimulation (TBS) paradigm applies bursts of high frequency TMS pulses to the motor cortex, each burst comprising three pulses at 50 Hz,

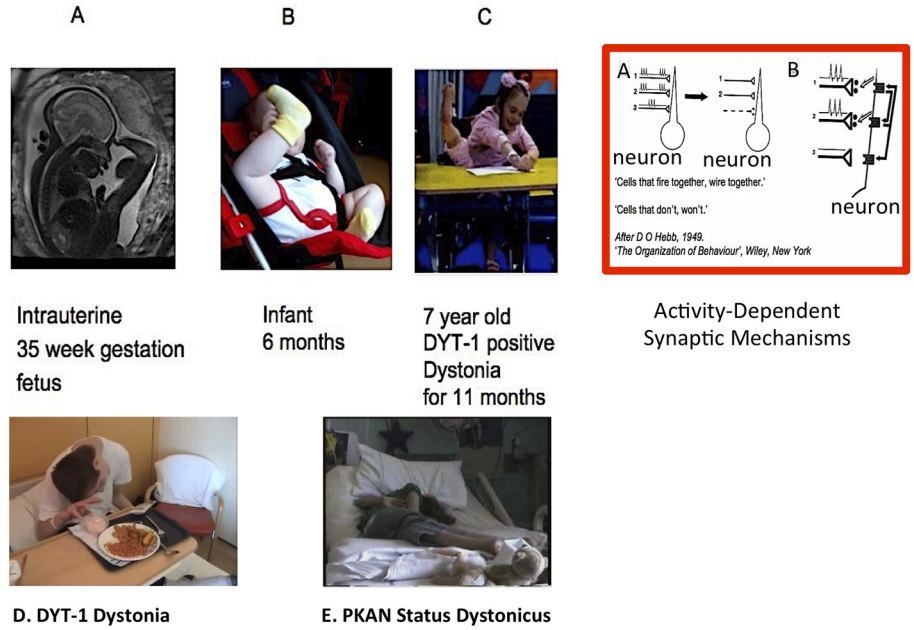

FIGURE 1 | Normal development, dystonia, and role for activity-dependent plasticity. [**Top** (L-R)]: Thirty-five week gestation fetus; typically developing 6 month old infant; 7 year old girl with DYT-1 dystonia (2); Red Rectangle: **(A)** Example of activity-dependent synaptic plasticity. The two synchronously firing neurons (1 and 2) are retained by a "retrograde messenger" from the post-synaptic receptors shown in **(B)** while the asynchronously firing neuronal connection (3) is lost. From Penn and Shatz (3) annotated from *DO Hebb 1949: "The Organisation of Behaviour"*. [**Lower** (L-R)]: Adolescent with generalized DYT-1 Dystonia attempting to eat; Adolescent in status dystonicus due to Pantothenate Kinase associate Neurodegeneration (PKAN); *Clinical cases courtesy J-P Lin*.

FIGURE 2 | DYT-1 dystonia and intrusive "ballerina postures" and improvements with Deep Brain Stimulation (DBS). Video frames over time before and after DBS. Onset age 6.0 years with rapid progression to wheel-chair mobility by age 6.5 years. **(Top)** "Ballerina posturing" of the right leg interferes with lying and sitting (see also **Figure 1C**). [**Lower** (left-right)]: unable to stand or walk; head and chest X-ray post ACTIVA RC rechargeable DBS implant, age 7 years; standing unsupported within days of DBS; walking unsupported 3 months post DBS with a left circumducting gait; fully recovered at 3 years post-DBS. *Courtesy J-P Lin*.

with the bursts repeated at 5 Hz intervals. Intermittent TBS (comprising runs of 2 s on and 8 s off, repeated 20 times) gives rise to MEP facilitation (an LTP-like response), whereas continuous TBS for 40 s gives rise to an LTD-like response with suppression of MEP amplitude (34). The TBS paradigm therefore assesses plasticity in the motor cortex. Plasticity in the sensory cortex can be induced using high frequency repetitive somatosensory stimulation (HF-RSS), a protocol which applies patterned cutaneous electrical stimulation, and which can improve both two-point spatial discrimination and temporal discrimination in the stimulated area in healthy adults (35).

Abnormalities of Hebbian and Homeostatic Plasticity in Adults With Genetic or Idiopathic Dystonias

Adults with focal hand dystonia show abnormal LTP-like plasticity, as measured with PAS, with a larger and less focal increase in corticospinal excitability compared with controls (5, 36) which could represent an over-recruitment and "blurring" of the distinct functions and characteristics between primary (SI) and secondary (SII) somatosensory cortices and primary and supplementary motor (MI and MII, respectively) cortices. This in turn can be related to dystonic symptoms, in which there is a loss of specificity in muscle activation, with overflow to other muscles, including antagonists. Additionally, excessive LTP-like plasticity may strengthen inappropriate sensory-motor associations, particularly with excessive practice or training, as is seen in musician's dystonias or writer's cramp (5). Abnormal plasticity is also present in adults with idiopathic dystonia or isolated DYT1 genetic dystonia, as demonstrated by enhanced long-lasting effects of TBS (37), while homeostatic plasticity, assessed with combined repetitive TMS and transcranial direct current stimulation, is abnormal in patients with focal hand dystonia (38). Furthermore, cerebellar modulation of motor cortex plasticity is impaired in patients with writer's cramp (39) and sensory cortex plasticity is abnormal in patients with cervical dystonia, in whom a paradoxical response to HF-RSS was seen, with a deterioration in somatosensory temporal discrimination (40).

Quartarone et al. postulated that abnormal or excessive cortical plasticity may lead to the consolidation of incorrect motor programmes (or "engrams") containing redundant muscular activation, which in turn are manifest as overt dystonic movements (5). Examples are shown in **Figure 2**. Interestingly, restoration of plasticity levels (measured with PAS) toward those seen in controls is observed in patients who have responded clinically to pallidal Deep Brain Stimulation (DBS) (41, 42). The observation that improvement in dystonia occurs in proportion to the reduction in cortical plasticity implies that this effect on plasticity makes an important contribution toward the mechanisms of GPi DBS in dystonia (43), in turn suggesting an important pathophysiological role of the exaggerated plasticity response.

Assessment of Plasticity in Acquired Dystonia

In contrast to idiopathic or genetic dystonias, patients with acquired hemidystonia have shown normal responses to both PAS (44) and HF-RSS (45), suggesting that abnormal plasticity, at least in the form measured with these particular protocols, may not be essential for the development of dystonia (45). On the other hand, in patients with acquired dystonia secondary to basal ganglia lesions, there is usually a delay between the time of injury and the onset of dystonic symptoms (46), which would be consistent with a maladaptive plasticity response.

How do we explain this conundrum? Examining the developmental origins of these disorders and how each may impact on sensorimotor circuit development may help to reconcile these findings. In this context it is also important to appreciate that, as well as plasticity generally being greater in early life, the site and extent to which various homeostatic plasticity mechanisms are active alters during different stages of neurodevelopment (30). For example, genetic dystonias, although often not manifesting until mid-childhood or later, are likely to influence development even during embryogenesis, when circuits are initially forming. In contrast, many acquired dystonias arise from injury in the perinatal period (DCP) when prior embryonic development of sensorimotor circuits has been normal, but is then impaired abruptly at a critical time when activity-dependent refinement of sensorimotor circuits would normally be heightened. Understanding the role of neuroplasticity mechanisms in the developing sensorimotor system may therefore provide critical insights in this regard.

PRENATAL AND PERINATAL PERIODS ARE CRITICAL FOR ESTABLISHMENT AND EXPERIENCE-DRIVEN REFINEMENT OF SENSORIMOTOR CIRCUITS

During embryonic and fetal development, thalamocortical neurones destined for sensory cortex pass via the transient structure of the sub-plate, and subsequently to the cortical plate, reaching the cortex around 24 weeks gestational age (25). Whilst the sub-plate is considered fundamental in establishing thalamo-cortical connections, more detailed connectivity depends on neuronal activity, including endogenous neural activity generated by the nervous system itself before sensory input is available (3).

Evidence for the Role of Neuronal Activity in Sensorimotor Circuit Development

In humans, endogenously generated bursts of neuronal activity are seen in preterm infants from 26 weeks gestational age. From 28 weeks, "delta brushes" are seen, comprising slow delta waves (0.3–2 Hz) with superimposed fast (8–25 Hz) activity (47, 48), initially over central regions, but with the topography and predominant frequencies changing with gestational age (49). Delta brushes occur spontaneously, but can also be triggered by contralateral limb movements or somatosensory stimulation with a somatotopic distribution (47).

Animal models, particularly rodents in which early postnatal stages are comparable to late fetal stages of human development (50), support the concept that neuronal oscillatory activity in the developing somatosensory cortex plays a role in establishing early networks (51–54). Newborn rats demonstrate several patterns of spontaneous and sensory stimulus-induced oscillatory neuronal activity in somatosensory cortex, including 1–2 s runs of alpha frequency (8–12 Hz) activity, termed "spindle bursts" due to their typical appearance (52). *In vitro* and *in vivo* studies suggest that sub-plate neurones are involved in the generation or amplification of spindle bursts, which are considered to be the correlate of human delta brushes (25, 50). As with delta brushes, spindle bursts in newborn rat primary somatosensory (S1) cortex are triggered by muscle twitches with a somatotopic distribution. Inactivation of peripheral input using lidocaine leads to a significant reduction in the occurrence of spindle bursts in contralateral barrel cortex of newborn rats (54), indicating that a substantial proportion of spontaneous spindle burst activity in developing sensory neocortex is triggered by events in the sensory periphery (50, 54).

Recent fMRI studies show a somatotopic organization of sensorimotor cortex even in preterm human infants (55), suggesting early intrinsic determination of a broad somatotopic map. This is supported by the topography of sensory evoked responses to tactile stimulation of the upper and lower limbs in preterms (56). However, the fine-tuning of somatotopic organization within sensory and motor cortices requires experience-dependent synaptic plasticity. For example, in the rat, neonatal asphyxia and hind limb immobilization leads to disorganization of primary somatosensory (S1) cortex with abnormally large and overlapping hind limb receptive fields (57) indicative of a lack of activity-dependent synaptic pruning. Taken together the above observations suggest that early oscillatory neuronal activity, both spontaneous and sensory-evoked, plays an important role in the development and refinement of sensorimotor networks.

Evidence of Activity-Dependent Refinement of Efferent Projections

During this same time period (24–34 weeks GA), efferent projection tracts are also developing, connecting the cortex with sub-cortical nuclei, cerebellum, and spinal cord (58). The corticospinal projections are initially bilateral but, during typical development, the ipsilateral projection is gradually withdrawn though a neuroplastic process of activity-dependent competition, particularly during the first 15–18 months after birth (59). The "rewiring" of descending motor pathways in individuals with hemiplegic CP provides another example of how activity, or lack of activity, during critical developmental windows shapes the development of structural and functional sensorimotor connections. Unilateral brain lesions disrupt the usual process of activity-dependent competition between ipsilateral and contralateral corticospinal projections, such that uncrossed ipsilateral projections from the non-lesioned hemisphere survive and are strengthened due to lack of competition from contralateral corticospinal fibers arising from the lesioned hemisphere, which end up being withdrawn (59, 60). The pattern of re-organization and relative strength of descending ipsilateral and contralateral projections varies depending on the timing and extent of the lesion (61, 62) and have been reviewed in detail elsewhere (58). However, the ascending somatosensory pathway retains its projection to the contralateral sensory cortex (63) and may even take a longer route to bypass a periventricular lesion and reach its intended destination in the postcentral gyrus (64).

It is clear that the prenatal and perinatal periods are critical for both the establishment and the experience-driven refinement of sensorimotor circuits. A pathological process that disrupts the normal pattern of events during these periods will therefore have a profound effect on sensorimotor development, whether it be via genetically determined abnormalities of synaptogenesis and synaptic plasticity, or due to a lack of the normal activity responsible for experience-dependent synaptic modification and the consequential effect on homeostatic plasticity set-points.

HOW ARE SYNAPTIC PLASTICITY AND EXPERIENCE-DRIVEN REFINEMENT OF SENSORIMOTOR CIRCUITS IN THE PRENATAL AND PERINATAL PERIODS RELEVANT TO GENETIC DYSTONIA?

There is growing evidence that several genetic dystonias are associated with abnormal synaptogenesis and synaptic plasticity.

DYT1 Dystonia

One well-studied example from the myriad of genetic dystonias is DYT1, a severe generalized dystonia with typical onset in mid-childhood (**Figures 1C,D**, **2**), resulting from a mutation in *TOR1A*, (typically a three base pair deletion leading to loss of a glutamic acid residue at the carboxyl-terminal region). This mutation leads to impaired function of the protein TorsinA which is thought to pay a role in the function of the endoplasmic reticulum and nuclear envelope as well as in interactions between the cytoskeleton and nuclear membrane and regulation of cellular lipid metabolism (65). These are all key processes in synaptogenesis and synaptic plasticity, since changes in the numbers of post-synaptic receptors involves changes in the turnover and synaptic localization of many post-synaptic scaffolding proteins (29). Mouse models of TorsinA hypofunction display altered protein homeostasis and abnormal synaptic transmission and plasticity (66, 67). One model has shown subtle neurodegeneration in several regions of the sensorimotor network, including sensorimotor cortex, thalamus, globus pallidus, and deep cerebellar nuclei (67). It is noted that the double knock-out model used in the Liang study is genetically quite different from DYT1 patients, who usually have a single heterozygous mutation, and that other studies using *Dyt1* heterozygous knock-out mice have not demonstrated neurodegeneration (66). However, evidence from several animal model studies indicates that TorsinA hypofunction affects multiple regions of the sensorimotor network and that there are early critical windows in which sensorimotor circuit

development may be vulnerable to TorsinA hypofunction, particularly during periods of intense synaptogenesis (67–70).

DYT6 Dystonia

Mutations in *THAP1*, a zinc-finger transcription factor, which lead to DYT6 dystonia, have also been associated with dysfunction of molecular pathways leading to defective neuritogenesis, with implications for axonal guidance, and defects in synaptic plasticity (71). Although these deficits were observed in early development of the mutant mouse, Zakirova et al. raise the interesting suggestion that any effects on neuritogenesis that persist into adulthood might be offset by the synaptic changes (71). Interestingly these abnormalities show convergence with those disrupted in DYT1 dystonia i.e., in both DTY1 and DYT6 there is a defect of neuritogenesis and synaptic plasticity (71). In human functional imaging studies, both DYT1 and DYT6 are associated with abnormal connectivity in cerebello-thalamo-cortical pathways (72). Importantly, these findings emphasize that the disrupted plasticity and activity in the sensorimotor network caused by *TOR1A* or *THAP1* dysfunction are not just manifest at the time of clinical onset (usually mid-childhood) but are likely to impact on the early development of sensorimotor circuits and also on their function, perhaps shifting the balance between excitation and inhibition.

Relevance of Abnormal Synaptic Plasticity in Genetic Dystonias to Sensorimotor Network Development

Neuroplasticity is generally enhanced during development compared with adulthood (24). In addition, the extent to which various plasticity mechanisms are operative fluctuates during development and across different parts of the brain (30). In humans, synaptogenesis starts around 27 weeks gestational age and intensifies during the first 2 years of life, with maturation patterns varying across different cortical regions (24). Abnormal synaptic plasticity within the sensorimotor network due to *TOR1A* hypofunction is therefore likely to have a significant impact during early sensorimotor development, including prenatally. Synaptic pruning also peaks at different times for different brain regions, earlier in auditory than in pre-frontal cortex, the latter continuing into adolescence (24). Furthermore, the pattern of expression of CNS receptors changes with a sequential (but partly overlapping) expression of GABA-A, then NMDA and then AMPA receptors, supporting the development of LTP and LTD and a transition from neonatal to adult forms of plasticity (73–75).

Although originally identified in DYT1 dystonia, there is now evidence of an association between variant mutations within the *TOR1A* gene and focal dystonia and writer's cramp (65), disorders which tend to occur with overuse, and to present in adulthood. Further studies will be required to delineate the possible effect of these particular mutations on sensorimotor circuits during development (including prenatally) and the intriguing possibility of preventing manifestation of the disorder by modulating neuroplasticity in early life.

HOW ARE SYNAPTIC PLASTICITY AND EXPERIENCE-DRIVEN REFINEMENT OF SENSORIMOTOR CIRCUITS IN THE PRENATAL AND PERINATAL PERIODS RELEVANT TO DYSTONIC CEREBRAL PALSY?

Dystonic cerebral palsy (DCP) refers to dystonia that arises from a brain insult in the perinatal period. This encompasses individuals with acquired dystonia due to hypoxic ischaemic-encephalopathy (HIE) at term (i.e., birth asphyxia), extreme prematurity, or unconjugated hyperbilirubinaemia-induced kernicterus, or indeed a combination of these.

Patterns of Brain Injury in DCP

The patterns of brain lesions seen on MRI in DCP differ with timing of injury: typical MRI findings in HIE due to acute severe asphyxia reflect those areas of high metabolic rate at the time of injury, with classical involvement of the thalamus, basal ganglia (especially posterior putamen), peri-rolandic (sensorimotor) cortex, and sometimes also the cerebellum (76–79). The overlap between these areas and those implicated in the functional neuroanatomy of dystonia is striking (80–82). In extreme prematurity one is more likely to observe periventricular leukomalacia or the sequelae of intraventricular hemorrhage, but a normal structural MRI is reported in up to 50% of prematurely born children with DCP (83). In kernicterus, the injury on MRI is localized to the globus pallidus internus and subthalamic nuclei but is notoriously transient in many cases. Although imaging cohorts find "normal" structural MRI scan reports in 17–20% of children with CP (76–78), it is important to remember that changes to the *development and function* of sensorimotor networks are still likely to be present.

Impact of Brain Injury on Sensorimotor Circuit Development in DCP

Although a broad somatotopic map is usually present in sensory cortex by term (or before), its further development is refined by experience-dependent connectivity changes.

Neonatal Asphyxia

For those with HIE, the development of sensorimotor circuits will have proceeded normally up until the time of injury, but then the injury to the thalamus, a crucial relay in the passage of sensory information to the cortex, and the subsequent disruption of thalamocortical pathway activity, will disrupt the on-going refinement of sensorimotor circuitry that usually occurs in the post-natal period. There is also injury to the sensorimotor cortex itself (peri-rolandic cortex) and to the basal ganglia and cerebellum, all important sub-cortical structures in the sensorimotor network. Thus, several nodes of the network may be disrupted.

As noted above, rat models demonstrate that neonatal asphyxia with hind limb immobilization leads to impaired somatotopic organization of primary sensory cortex with abnormally large and overlapping hind limb receptive fields

(57) suggesting a lack of activity-dependent synaptic pruning. It is notable that in adults with focal or generalized dystonias, widened and overlapping sensory receptive fields have also been demonstrated, both in the cortex [e.g., (84) and in the globus pallidus (7)]. Even in the absence of asphyxia, early restriction of sensorimotor activity in newborn rats gave rise to maladaptive plasticity in the SM cortex (85, 86) with degradation- "blurring"- of the somatotopic organization of somatosensory cortex. Importantly, neuronal responses in sensorimotor cortex remained abnormal even after sensorimotor activity was no longer restricted (86), emphasizing the long-lasting impact of an insult within this critical window. Whilst equivalent experimental paradigms are not feasible in human infants, there is clear evidence from clinical studies that abnormal sensory evoked potentials (SEPs) have high predictive value for neurological sequelae in post-asphyxiated neonates (25).

Extreme Prematurity

In individuals with cerebral palsy born pre-term with periventricular white matter injury on MRI, diffusion tensor imaging studies show injury to the posterior thalamic radiation, indicating disruption of thalamocortical connections (87, 88). Moreover, the injury in the posterior thalamic radiation pathways is more severe than that in the descending corticospinal tracts and correlates with clinical measures of severity (88). These seminal findings emphasized the importance of disruption to sensory and not just motor pathways in cerebral palsy due to prematurity. As indicated by the animal studies outlined above, reduction or loss of peripheral input leads to reduced oscillatory activity in the developing sensorimotor cortex (52, 54). It can be envisaged that injury or dysfunction of the ascending sensory tracts of the posterior thalamic radiation will disrupt the passage of sensory information to the sensory cortex, and that the subsequent disruption of sensorimotor cortex neuronal oscillatory activity will in turn affect the development of sensorimotor circuits, even if the dysfunction of ascending pathways is only transient. Indeed, in preterm infants with structural brain lesions (bilateral intraventricular hemorrhage) somatosensory evoked responses to tactile stimuli are abnormal (56). Interestingly, the responses only became abnormal after a delay of several weeks (56), suggesting that the abnormality may reflect a neuroplastic response with re-organization of the relevant neuronal networks.

Role of Somatosensory Evoked Potentials

Importantly, abnormal somatosensory evoked potentials have a high predictive value for adverse neurodevelopmental outcome in both preterm infants and term infants with HIE (25, 89–92), with SEPs evoked from posterior tibial nerve stimulation having particular sensitivity for predicting development of CP in preterms (90, 91). In addition to the clear clinical application of these studies, the findings are also concordant with the notion that sensory pathway dysfunction has a negative impact on the normal activity-dependent development of sensorimotor networks.

In a study of upper and lower limb SEPs in young people with dystonia, 47% of patients showed an abnormality in at least one of their SEP responses (93). A similar proportion of 40% was confirmed in a larger cohort (94). The abnormalities were seen predominantly in the acquired dystonia group, of which the majority had dystonic-dyskinetic CP (93, 94). Although this was not a longitudinal study, it is likely that these abnormalities were long-standing and therefore that sensory pathway dysfunction had been present since the perinatal period in these individuals, with a consequent adverse impact on the activity-dependent refinement of sensorimotor circuits in the early post-natal period, and an enduring effect on their function (86).

SENSORIMOTOR DEVELOPMENT IN CHILDHOOD AND ADOLESCENCE

Neuronal sensorimotor development continues throughout childhood and into adolescence and is associated with age-related improvements in sensorimotor skills, leading to a reduction in associated postures and unwanted overflow (95–98). The neurophysiological mechanisms of motor performance enhancement and refinement also reflect activity-dependent plasticity.

Postnatal Cortical Oscillatory Activities and Reactivity

In humans, the post-natal development of cortical oscillatory activities and their reactivity to sensory stimulation is well-documented (99). A 6 Hz rhythm is seen over central regions from as early as 5–6 months (99). The peak frequency of this central rhythm increases with age, especially in the first year of life (99–101) when motor skills are developing rapidly. By the end of the first year of life, a 6–9 Hz rhythm is present over sensorimotor cortex which displays the typical characteristics of the adult mu rhythm (adult mu having a frequency of 8–12 Hz and a distinctive arciform morphology), showing suppression in response to movement and/or somatosensory stimulation (101, 102). Thus, mu event-related desynchronisation (ERD), which is considered to reflect sensorimotor processing (103–105), is present in infancy, at a time of rapid sensorimotor development. Stroganova et al. (100) observed that the peak frequency of mu rhythm in the second half-year of life, depended on the duration of intra- and extra-uterine development, whereas the frequency of the occipital alpha rhythm depended only on extra-uterine development i.e., the presence of visual input, suggesting that the development of the sensorimotor mu rhythm itself is influenced by somatosensory stimulation, which is present even in the uterus (100).

Mu Rhythm Modulation

The mu rhythm and its modulation continues to develop throughout childhood, with the mu/alpha ERD being followed by a mu/alpha *event related synchronization* (ERS) (20) and the emergence of a beta range (14–30 Hz) ERD and ERS also in response to movement (20, 102, 106, 107). Whilst ERD is considered to reflect activation of sensorimotor networks, ERS is considered to reflect active inhibition or "resetting" within the sensorimotor cortex (103–105). Evidence from adult studies

suggests that post-movement beta ERS may relate to erasing working memory information after task completion, or an integration between feedback and reward (108). Development proceeds further during adolescence before reaching an adult pattern (109). For example, recent observations suggest a relative "overshoot" in the mu/alpha ERS response in 10–14 year olds, which becomes more refined in 15–21 year olds (20). Similarly, in a recent MEG study of alpha-beta cortical oscillations in response to lower limb somatosensory stimulation applied during isometric force production, adolescents showed a more enhanced modulation compared with adults (109). Thus, the balance between excitation and inhibition may still be maturing at this stage.

Patterns of Neuronal Oscillatory Activities in Dystonia

Dystonia is associated with enhanced low frequency (4–12 Hz) neuronal oscillatory activity in the basal ganglia (11, 12, 110) and also in the motor cortex (111). The exaggerated low frequency basal ganglia oscillations are coherent with activity in other parts of the sensorimotor network, including the cerebellum (12), correlate with symptom severity (112), and are coherent with dystonic EMG (14). An abnormal excessive low frequency drive to muscles has been shown in several forms of dystonia (13–16). The enhanced low frequency oscillations in the basal ganglia and motor cortex are suppressed by DBS (11, 111), as is the exaggerated low frequency muscular drive (15). Interestingly the performance of an effective sensory trick in two patients with cervical dystonia has been associated with a bilateral desynchronisation in the 6–8 Hz and beta band in both the globus pallidus and sensorimotor cortices (113), while a similar maneuver in two patients wtihout an effective sensory trick induced a worsening of dystonia and an increase in 6–8 Hz oscillations. These observations support the notion that exaggerated low frequency oscillations play an important role in the pathophysiology of dystonia.

Much of this work involves invasive recordings and has therefore focused on adults with dystonia. The development of cortical and basal ganglia oscillatory activity in young patients with dystonia remains largely unexplored. Normal patterns of development of cortical oscillatory activities are well-documented, as noted above, with the proportion of low frequencies [delta (1–3 Hz) and theta (3–7 Hz)] generally decreasing with age, and the proportion of higher frequencies [alpha (8–12 Hz) and beta (14–30 Hz) ranges] generally increasing with age. A recent study found that the spectral content of scalp EEG over sensorimotor cortex in children with dystonia follows a similar general pattern with age, but that power in the theta range is relatively higher than in typically developing children (20). This study found that children with either isolated genetic dystonia or with DCP show impaired mu modulation in response to a proprioceptive stimulus, indicating an abnormality in sensorimotor processing which is common across different dystonia etiologies (20)—**Figure 3**. Importantly, this abnormality was present even in the youngest age-group tested (5–9 years). It is possible that this form of sensorimotor processing does not develop adequately in dystonia, either due to genetic abnormalities of synaptogenesis and synaptic plasticity (for example as in DYT1 or DYT6 dystonia) or due to lack of sensory input during a critical window of sensorimotor circuit development (e.g., in DCP). However, it is also possible that the observations reflect a secondary plastic change in the sensorimotor cortex due to abnormal feedback from dystonic muscle activity. This remains to be tested.

Neurophysiological Phenomena Show Different Maturational Profiles

Different neurophysiological phenomena relevant to sensorimotor function show different maturational profiles. For example, TMS studies have shown that short-latency intracortical inhibition is present but at significantly lower levels in children under the age of 10 compared with adults (114). Intercortical inhibition, as measured by the ipsilateral silent period, is absent in pre-school children: it can be seen by age 6–7 years, but with a delayed latency and short duration compared with the adult ipsilateral silent period, and tends to mature by early adolescence (115, 116). Somatosensory gating, investigated using a paired-pulse electrical stimulus paradigm in children aged 10–18 years, appears to show a fully mature pattern by age 10 years (117). Interestingly it has been suggested that alpha/mu ERD may in part reflect somatosensory gating (118). The earlier development of mu ERD compared with mu or beta ERS (20) in this context is thus concordant with the suggestion that somatosensory gating mechanisms develop earlier than the (motor cortical) inhibitory mechanisms measured with TMS, or those reflected by movement related beta and gamma oscillations, which continue to develop during childhood and adolescence and into young adulthood (119). The lower levels of intracortical inhibition in children have been suggested to facilitate greater plasticity and motor learning during normal development (114, 120). In dystonia/DCP, these lower levels of inhibition may contribute toward a destabilization of pathologically enhanced plasticity at a critical stage in mid-childhood, but could also provide a window of opportunity for intervention.

RELEVANCE OF NEUROPLASTICITY AND SENSORIMOTOR DEVELOPMENT FOR TIMING OF NEUROMODULATION THERAPIES

Overall, these different developmental disorders, all with the clinical manifestation of dystonia, are each characterized by disruption to the early development of sensorimotor networks, although at different stages and with different impacts on and responses from neuroplastic mechanisms.

Timing of Injury and Disruption to Sensorimotor Development

Individuals with dystonic CP due to prematurity may experience a disruption of thalamocortical pathway activity, through damage to posterior thalamic radiation fibers, at a developmental stage

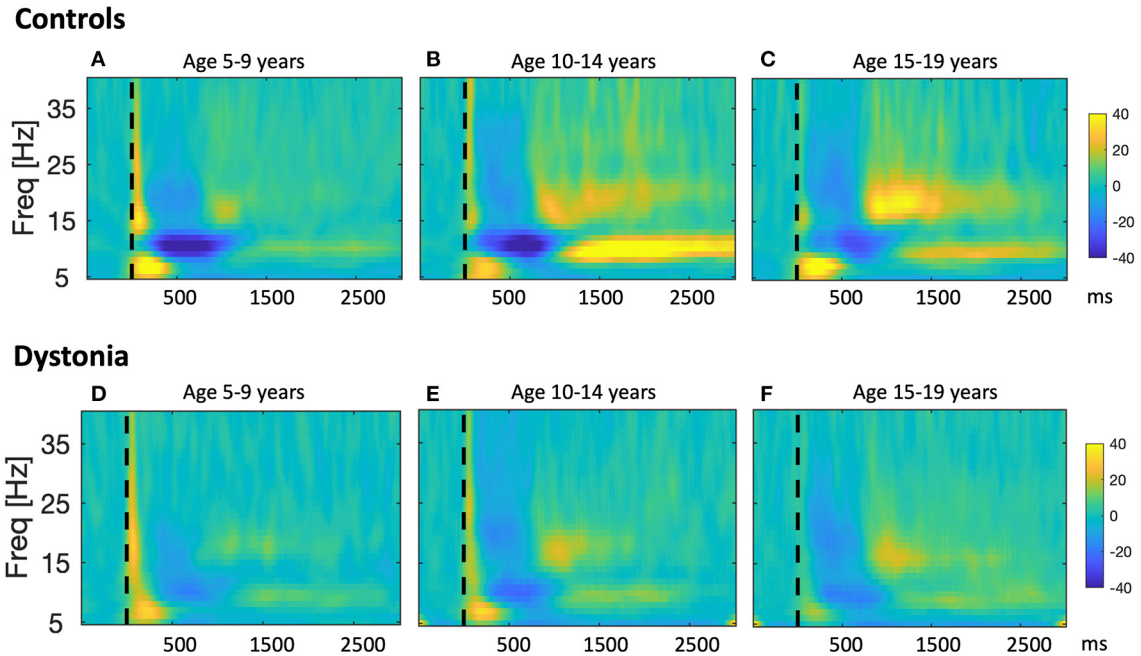

FIGURE 3 | Developmental sequence of event-related changes in EEG power in relation to a proprioceptive stimulus in typically developing children and children with dystonia. Results from a study in which changes in sensorimotor cortex EEG were recorded in response to proprioceptive stimuli in 30 young people with dystonia and 22 controls (20). Participants sat at a table with their arm positioned in the arm-rest of a robotic wrist interface which delivered controlled passive wrist extension movements, resulting in brief stretches of the wrist flexors, with rise-time of 240 ms, and a target of 12° from the neutral position. Up to 160 wrist extension movements were recorded for each hand. Scalp EEG was recorded using a BrainVision system (BrainAmp MR Plus) and stimulus timing was synchronized with the EEG recordings via an electrical marker designating the movement onset. Offline, data were segmented into epochs comprising 1 s pre-stimulus and 3.5 s post-stimulus. After artifact rejection, remaining epochs were averaged to produce a stretch evoked potential for each hand in each subject. EEG power was calculated in 1 Hz bins from 5 to 40 Hz using the continuous Morlet wavelet transform with eight wavelet cycles. Relative changes in post-stimulus EEG power with respect to the pre-stimulus period were calculated. The figure shows pooled time-frequency plots across subjects showing the response over the contralateral hemisphere to stretch of the dominant hand wrist flexors i.e., right sensorimotor cortex for left hand movement, left sensorimotor cortex for right hand movement for controls **(A–C),** and individuals with dystonia **(D–F),** grouped by age. Left column: Young age group (5–9 years, $n = 10$), middle column: Intermediate age group (10–14 years, $n = 6$), right column: Older age group (15–19 years, $n = 6$). x-axis shows time in ms after the stimulus (dashed vertical line), y-axis shows frequency, color scale shows relative power at each frequency with respect to the pre-stimulus period, such that dark blue indicates event-related desynchronisation (ERD) and yellow-orange indicates event-related synchronization (ERS). The sharp increase in power with respect to baseline at time zero, extending up to 40 Hz, and the brief, early increase in theta range (4–7 Hz) power from 0 to 300 ms are likely to reflect movement artifact and a contribution from the stretch evoked potential, respectively. Figure adapted from McClelland et al. (20).

when the subplate is still guiding the development of sensory cortex and somatotopic maps are still being formed. Those with dystonic CP due to term HIE will have had normal prenatal development of sensorimotor circuits followed by sudden and profound disruption of thalamocortical pathway activity and thus of the neuronal activity which would normally determine the on-going refinement of sensorimotor circuitry that occurs in the post-natal period. In addition, other nodes of the sensorimotor network will have been damaged (basal ganglia, cerebellum, sensorimotor cortex itself). Individuals with genetic dystonias (including for example *TOR1A* or *THAP1* related dystonias), although not manifesting clinically until mid-childhood, may actually have had an even earlier prenatal onset of sensorimotor circuit dysfunction, perhaps so early that functional circuits could still develop through compensatory mechanisms, as alluded to by Zakirova et al., with defects in neuritogenesis being offset by synaptic changes (71). One could speculate that an abnormality of dendrite formation leads to reduced neural activity at a critical time-point in prenatal development, which in turn leads to a change in the plasticity threshold due to homeostatic mechanisms, or even in the *range* of the plasticity response, which enhances the effect of LTP-like mechanisms. Whilst this enhanced LTP-like plasticity may initially be an advantage, there may come a point in mid-childhood, when LTP is enhanced as part of normal maturation, where the system is tipped out of a functional range and into an unstable range causing hyper-excitability i.e., the destabilizing effect of Hebbian plasticity is unchecked and leads to a driving of synaptic strengths toward maximum values.

In contrast, in acquired dystonia due to perinatal brain injury, the "plasticity machinery" itself may be intact (44, 45), but the consequence of reduced and atypical patterns of afferent feedback in early life induces a different form of maladaptive neuroplasticity. The "set-point" around which these processes function may well have been affected by the relative deprivation of afferent input induced by the lesion (30), even if this was only temporary. This can be considered a type of reactive plasticity, following sensory deprivation or CNS insult (24). Interestingly, a

cTBS (continuous Theta Burst Stimulation) study demonstrated that adolescents who had been born pre-term showed a reduced LTD-like response to cTBS compared with adolescents born at term, suggesting that LTD-like neuroplasticity regulation is impaired in this group (121). These were not individuals with dystonia, but the study emphasizes that pre-term birth can have an impact on the function of plasticity mechanisms.

Thus, the ultimate effects of sensory deprivation on cortical circuitry are the result of a complex interplay between Hebbian and homeostatic forms of synaptic plasticity (29). These considerations could help to explain the conundrum presented earlier. For example, it is possible that patients with acquired dystonia may show normal PAS or HF-RSS responses, but that the set-point around which the underlying plasticity mechanisms are working has been changed due to the relative deprivation of sensory input resulting from the CNS insult.

Timing of Intervention

The observation that there is often a delay between the time of insult and the development of symptoms in acquired dystonia suggests a maladaptive plasticity response and raises the exciting possibility that intervention within this time could be beneficial in preventing the development of dystonia. Even after the onset of dystonia, timing of intervention is important. Early presentation of dystonia in childhood is often followed by gradual worsening without remission despite attempted pharmacological and physical support interventions (122). There is evidence from clinical studies that the duration of dystonic symptoms or the proportion of life lived with dystonia has an influence on DBS response: outcomes from DBS showed a negative correlation with dystonia duration, normalized for age at surgery (123) and this relationship was observed for both primary (isolated genetic or idiopathic) and acquired dystonia (123). Marks and colleagues emphasize that DYT1 dystonia progresses quite rapidly during its early course, and that the initial goal of DBS is to arrest or slow this deterioration before actual improvement can occur (124), another factor in favor of early intervention.

A meta-analysis of 321 patients (from 72 articles) confirms that shorter duration of life lived with dystonia (or older age at onset) is associated with better improvement scores, as measured with the Burke Fahn Marsden Dystonia Rating Scale (125).

The foregoing review of time-critical events in the developing brain is sharply illustrated by the success of cochlear implantation to augment hearing (a special sensory input) in late infancy and early childhood with a view to promote language recognition and speech production, which has a greater chance of success if cochlear neuromodulation is performed before the age of 5 years when auditory and language plasticity windows are open (126). Comparable studies of intervention in early life for children with acquired dystonia (in particular DCP) are not yet available, with most reported cases of DBS surgery taking place from 5 years of age onwards (127). However, the findings above, regarding the relationship between proportion of life lived with dystonia and DBS response, combined with the documented success of early cochlear implantation, indicate that neuromodulation for movement disorders in childhood constitutes a race against time before the dysfunctional movement patterns and sensory experiences are neuroanatomically and neurophysiologically set (126).

Abnormal neuronal activity during critical windows in the prenatal and perinatal periods clearly has enduring effects on neural circuit activity for later life. This is demonstrated by the studies in rats, discussed above (85, 86), and also by studies in drosophila, in which increased neuronal excitation during a critical embryonic period could permanently induce seizure behavior in post-embryonic stages (128). An opportunity for "rescue" might be possible, but only during these critical early time-periods (128). Interestingly, in a study of neuromotor outcome in very preterm infants, Pike and Marlow describe a phenomenon of "transient dystonia" (or dystonia of prematurity), in which infants showed abnormalities of tone and dynamic function over the first postnatal year, but were neurologically normal by the age of 2 years. The authors speculated that these infants had sustained a less severe brain injury, but the observations could also suggest that these early years represent a period in which "rescue" is still possible through early intervention.

Very early intervention with neuromodulation, including DBS, in younger children will require not only the further development of surgical methods and age-appropriate equipment, but also, and indeed more importantly, a greater in-depth understanding of the pathophysiology of sensorimotor circuit development in infants with, or at risk of developing, dystonia/dystonic CP. Herein, lies a huge and critical gap in scientific knowledge which needs urgently to be addressed. Technology is advancing rapidly, but without this fundamental scientific understanding, trials of DBS neuromodulation in very young children and infants will not be possible or ethically acceptable. Other potential considerations include the use of non-invasive neuromodulation techniques to harness neuroplasticity within critical windows for sensorimotor circuit development. This could include non-invasive neurostimulation methods such as TMS, or targeted occupational or physical therapy techniques aiming to modulate neural activity by enhancing sensorimotor afferent input in infants who would otherwise experience a restriction or deprivation or sensory stimulation following a CNS insult. Such approaches could be used independently or as an adjunct to DBS, or could help to achieve a situation where the child is more likely to respond to DBS at a later stage, when the risk/benefit ratio of neurosurgery may be more favorable. Again, these potential interventions need to be based upon a robust understanding of the fundamental mechanisms and the critical time windows for neuroplasticity in sensorimotor circuit development in human infants. These studies need to be performed in order to establish a strong evidence-base and to provide the confidence and impetus for clinical trials of such early interventions.

CONCLUSION

It is clear that critical windows exist, during which abnormal neural activity has enduring effects on future neuronal

function and also during which restoration of normal activity might prevent long-term, persistent disruptions of neuronal circuit function (128). This is highly relevant to our understanding of dystonic CP and genetic dystonias with onset in childhood, but also provides insights into the mechanisms underlying dystonias with onset in later life. We are currently missing out on opportunities to intervene early and improve neuromotor developmental outcomes due to critical gaps in scientific knowledge and a sparsity of research in pediatric dystonia/dystonic CP. Further study is urgently needed to understand in detail how neuroplasticity processes influence sensorimotor circuit development and function in dystonic CP and to define the potential time windows in which intervening to modulate neural activity may induce a more normal pattern of development, either through invasive or non-invasive methods of therapy, or their combination.

AUTHOR CONTRIBUTIONS

VM wrote the first draft of the manuscript. J-PL wrote sections of the manuscript. All authors provided material for figures and read and approved the final version.

FUNDING

VM is currently supported by the Medical Research Council (Post-doctoral Clinical Research Training Fellowship MR/P006868/1) and the Rosetrees Trust and has been supported previously by the National Institute for Health Research and the Academy of Medical Sciences, for research work in clinical neurophysiology and childhood dystonia. J-PL has received support from the Guy's and St Thomas Charity New Services and Innovation Grant G060708; the Dystonia Society UK Grants 01/2011 and 07/2013 and Action Medical Research GN2097 for work in childhood dystonia and deep brain stimulation neuromodulation.

ACKNOWLEDGMENTS

We would like to thank the children with dystonia, their families and referring clinical services without whose help our clinical studies and observations would not have been possible. Particular thanks to our neurosurgical colleagues at King's College Hospital, Richard Selway, Keyoumars Ashkan, and Harutomo Hasegawa and to the multidisciplinary team within the Complex Motor Disorders Service, Evelina London Children's Hospital.

REFERENCES

1. Albanese A, Bhatia K, Bressman SB, Delong MR, Fahn S, Fung VS, et al. Phenomenology and classification of dystonia: a consensus update. *Mov Disord.* (2013) 28:863–73. doi: 10.1002/mds.25475
2. Lin JP, Nardocci N. Recognizing the common origins of dystonia and the development of human movement: a manifesto of unmet needs in isolated childhood dystonias. *Front Neurol.* (2016) 7:226. doi: 10.3389/fneur.2016.00226
3. Penn AA, Shatz CJ. Brain waves and brain wiring: the role of endogenous and sensory-driven neural activity in development. *Pediatr Res.* (1999) 45:447–58. doi: 10.1203/00006450-199904010-00001
4. Hallett M. Neurophysiology of dystonia: the role of inhibition. *Neurobiol Dis.* (2011) 42:177–84. doi: 10.1016/j.nbd.2010.08.025
5. Quartarone A, Morgante F, Sant'angelo A, Rizzo V, Bagnato S, Terranova C, et al. Abnormal plasticity of sensorimotor circuits extends beyond the affected body part in focal dystonia. *J Neurol Neurosurg Psychiatry.* (2008) 79:985–90. doi: 10.1136/jnnp.2007.121632
6. Quartarone A, Pisani A. Abnormal plasticity in dystonia: disruption of synaptic homeostasis. *Neurobiol Dis.* (2011) 42:162–70. doi: 10.1016/j.nbd.2010.12.011
7. Vitek JL, Chockkan V, Zhang JY, Kaneoke Y, Evatt M, Delong MR, et al. Neuronal activity in the basal ganglia in patients with generalized dystonia and hemiballismus. *Ann Neurol.* (1999) 46:22–35. doi: 10.1002/1531-8249(199907)46:1andlt;22::AID-ANA6andgt;3.0.CO;2-Z
8. Starr PA, Rau GM, Davis V, Marks WJ Jr, Ostrem JL, Simmons D, et al. Spontaneous pallidal neuronal activity in human dystonia: comparison with Parkinson's disease and normal macaque. *J Neurophysiol.* (2005) 93:3165–76. doi: 10.1152/jn.00971.2004
9. Vitek JL, Delong MR, Starr PA, Hariz MI, Metman LV. Intraoperative neurophysiology in DBS for dystonia. *Mov Disord.* (2011) 26(Suppl 1):S31–6. doi: 10.1002/mds.23619
10. McClelland VM, Valentin A, Rey HG, Lumsden DE, Elze MC, Selway R, et al. Differences in globus pallidus neuronal firing rates and patterns relate to different disease biology in children with dystonia. *J Neurol Neurosurg Psychiatry.* (2016) 87:958–67. doi: 10.1136/jnnp-2015-311803
11. Barow E, Neumann WJ, Brucke C, Huebl J, Horn A, Brown P, et al. Deep brain stimulation suppresses pallidal low frequency activity in patients with phasic dystonic movements. *Brain.* (2014) 137:3012–24. doi: 10.1093/brain/awu258
12. Neumann WJ, Jha A, Bock A, Huebl J, Horn A, Schneider GH, et al. Cortico-pallidal oscillatory connectivity in patients with dystonia. *Brain.* (2015) 138:1894–906. doi: 10.1093/brain/awv109
13. Grosse P, Edwards M, Tijssen MA, Schrag A, Lees AJ, Bhatia KP, et al. Patterns of EMG-EMG coherence in limb dystonia. *Mov Disord.* (2004) 19:758–69. doi: 10.1002/mds.20075
14. Sharott A, Grosse P, Kuhn AA, Salih F, Engel AK, Kupsch A, et al. Is the synchronization between pallidal and muscle activity in primary dystonia due to peripheral afferance or a motor drive? *Brain.* (2008) 131:473–84. doi: 10.1093/brain/awm324
15. Doldersum E, Van Zijl JC, Beudel M, Eggink H, Brandsma R, Pina-Fuentes D, et al. Intermuscular coherence as biomarker for pallidal deep brain stimulation efficacy in dystonia. *Clin Neurophysiol.* (2019) 130:1351–7. doi: 10.1016/j.clinph.2019.04.717
16. McClelland VM, Cvetkovic Z, Lin JP, Mills KR, Brown P. Abnormal patterns of corticomuscular and intermuscular coherence in childhood dystonia. *Clin Neurophysiol.* (2020) 131:967–77. doi: 10.1016/j.clinph.2020.01.012
17. Tinazzi M, Priori A, Bertolasi L, Frasson E, Mauguiere F, Fiaschi A. Abnormal central integration of a dual somatosensory input in dystonia. Evidence for sensory overflow. *Brain.* (2000) 123(Pt 1):42–50. doi: 10.1093/brain/123.1.42
18. Avanzino L, Tinazzi M, Ionta S, Fiorio M. Sensory-motor integration in focal dystonia. *Neuropsychologia.* (2015) 79:288–300. doi: 10.1016/j.neuropsychologia.2015.07.008
19. Sakellariou, DF, Dall'orso S, Burdet E, Lin JP, Richardson MP, McClelland VM. Abnormal microscale neuronal connectivity triggered by a proprioceptive stimulus in dystonia. *Sci Rep.* (2020). 10:20758. doi: 10.1038/s41598-020-77533-w
20. McClelland VM, Fischer P, Foddai E, Dall'orso S, Burdet E, Brown P, et al. EEG measures of sensorimotor processing and their development are abnormal in children with isolated dystonia and dystonic cerebral palsy. *Neuroimage Clin.* (2021) 30:102569. doi: 10.1016/j.nicl.2021.102569

21. Fiorio M, Gambarin M, Valente EM, Liberini P, Loi M, Cossu G, et al. Defective temporal processing of sensory stimuli in DYT1 mutation carriers: a new endophenotype of dystonia? *Brain.* (2007) 130:134–42. doi: 10.1093/brain/awl283
22. Kimmich O, Bradley D, Whelan R, Mulrooney N, Reilly RB, Hutchinson S, et al. Sporadic adult onset primary torsion dystonia is a genetic disorder by the temporal discrimination test. *Brain.* (2011) 134:2656–63. doi: 10.1093/brain/awr194
23. McClelland VM. The neurophysiology of paediatric movement disorders. *Curr Opin Pediatr.* (2017) 29:683–90. doi: 10.1097/MOP.0000000000000547
24. Ismail FY, Fatemi A, Johnston MV. Cerebral plasticity: windows of opportunity in the developing brain. *Eur J Paediatr Neurol.* (2017) 21:23–48. doi: 10.1016/j.ejpn.2016.07.007
25. Vanhatalo S, Lauronen L. Neonatal SEP - back to bedside with basic science. *Semin Fetal Neonatal Med.* (2006) 11:464–70. doi: 10.1016/j.siny.2006.07.009
26. Millar LJ, Shi L, Hoerder-Suabedissen A, Molnar Z. Neonatal hypoxia ischaemia: mechanisms, models, and therapeutic challenges. *Front Cell Neurosci.* (2017) 11:78. doi: 10.3389/fncel.2017.00078
27. Johnston MV. Plasticity in the developing brain: implications for rehabilitation. *Dev Disabil Res Rev.* (2009) 15:94–101. doi: 10.1002/ddrr.64
28. Bliss TV, Cooke SF. Long-term potentiation and long-term depression: a clinical perspective. *Clinics (São Paulo).* (2011) 66(Suppl 1):3–17. doi: 10.1590/S1807-59322011001300002
29. Turrigiano GG, Nelson SB. Homeostatic plasticity in the developing nervous system. *Nat Rev Neurosci.* (2004) 5:97–107. doi: 10.1038/nrn1327
30. Tien NW, Kerschensteiner D. Homeostatic plasticity in neural development. *Neural Dev.* (2018) 13:9. doi: 10.1186/s13064-018-0105-x
31. Stefan K, Kunesch E, Cohen LG, Benecke R, Classen J. Induction of plasticity in the human motor cortex by paired associative stimulation. *Brain.* (2000) 123(Pt 3):572–84. doi: 10.1093/brain/123.3.572
32. Kujirai K, Kujirai T, Sinkjaer T, Rothwell JC. Associative plasticity in human motor cortex during voluntary muscle contraction. *J Neurophysiol.* (2006) 96:1337–46. doi: 10.1152/jn.01140.2005
33. Damji O, Keess J, Kirton A. Evaluating developmental motor plasticity with paired afferent stimulation. *Dev Med Child Neurol.* (2015) 57:548–55. doi: 10.1111/dmcn.12704
34. Huang YZ, Edwards MJ, Rounis E, Bhatia KP, Rothwell JC. Theta burst stimulation of the human motor cortex. *Neuron.* (2005) 45:201–6. doi: 10.1016/j.neuron.2004.12.033
35. Erro R, Rocchi L, Antelmi E, Palladino R, Tinazzi M, Rothwell J, et al. High frequency repetitive sensory stimulation improves temporal discrimination in healthy subjects. *Clin Neurophysiol.* (2016) 127:817–20. doi: 10.1016/j.clinph.2015.06.023
36. Quartarone A, Bagnato S, Rizzo V, Siebner HR, Dattola V, Scalfari A, et al. Abnormal associative plasticity of the human motor cortex in writer's cramp. *Brain.* (2003) 126:2586–96. doi: 10.1093/brain/awg273
37. Edwards MJ, Huang YZ, Mir P, Rothwell JC, Bhatia KP. Abnormalities in motor cortical plasticity differentiate manifesting and nonmanifesting DYT1 carriers. *Mov Disord.* (2006) 21:2181–6. doi: 10.1002/mds.21160
38. Quartarone A, Rizzo V, Bagnato S, Morgante F, Sant'angelo A, Romano M, et al. Homeostatic-like plasticity of the primary motor hand area is impaired in focal hand dystonia. *Brain.* (2005) 128:1943–50. doi: 10.1093/brain/awh527
39. Hubsch C, Roze E, Popa T, Russo M, Balachandran A, Pradeep S, et al. Defective cerebellar control of cortical plasticity in writer's cramp. *Brain.* (2013) 136:2050–62. doi: 10.1093/brain/awt147
40. Erro R, Rocchi L, Antelmi E, Liguori R, Tinazzi M, Berardelli A, et al. High frequency somatosensory stimulation in dystonia: Evidence fordefective inhibitory plasticity. *Mov Disord.* (2018) 33:1902–9. doi: 10.1002/mds.27470
41. Ruge D, Cif L, Limousin P, Gonzalez V, Vasques X, Hariz MI, et al. Shaping reversibility? Long-term deep brain stimulation in dystonia: the relationship between effects on electrophysiology and clinical symptoms. *Brain.* (2011) 134:2106–15. doi: 10.1093/brain/awr122
42. Ruge D, Tisch S, Hariz MI, Zrinzo L, Bhatia KP, Quinn NP, et al. Deep brain stimulation effects in dystonia: time course of electrophysiological changes in early treatment. *Mov Disord.* (2011) 26:1913–21. doi: 10.1002/mds.23731
43. Tisch S, Limousin P. Neurophysiological insights in dystonia and its response to deep brain stimulation treatment. *Exp Brain Res.* (2020) 238:1645–57. doi: 10.1007/s00221-020-05833-8
44. Kojovic M, Parees I, Kassavetis P, Palomar FJ, Mir P, Teo JT, et al. Secondary and primary dystonia: pathophysiological differences. *Brain.* (2013) 136:2038–49. doi: 10.1093/brain/awt150
45. Latorre A, Cocco A, Bhatia KP, Erro R, Antelmi E, Conte A, et al. Defective somatosensory inhibition and plasticity are not required to develop dystonia. *Mov Disord.* (2020) 36:1015–21. doi: 10.1002/mds.28427
46. Trompetto C, Avanzino L, Marinelli L, Mori L, Pelosin E, Roccatagliata L, et al. Corticospinal excitability in patients with secondary dystonia due to focal lesions of the basal ganglia and thalamus. *Clin Neurophysiol.* (2012) 123:808–14. doi: 10.1016/j.clinph.2011.06.033
47. Milh M, Kaminska A, Huon C, Lapillonne A, Ben-Ari Y, Khazipov R. Rapid cortical oscillations and early motor activity in premature human neonate. *Cereb Cortex.* (2007) 17:1582–94. doi: 10.1093/cercor/bhl069
48. Andre M, Lamblin MD, D'allest AM, Curzi-Dascalova L, Moussalli-Salefranque FT, SN.T., et al. Electroencephalography in premature and full-term infants. Developmental features and glossary. *Neurophysiol Clin.* (2010) 40:59–124. doi: 10.1016/j.neucli.2010.02.002
49. Whitehead K, Pressler R, Fabrizi L. Characteristics and clinical significance of delta brushes in the EEG of premature infants. *Clin Neurophysiol Pract.* (2017) 2:12–8. doi: 10.1016/j.cnp.2016.11.002
50. Kirischuk S, Sinning A, Blanquie O, Yang JW, Luhmann HJ, Kilb W. Modulation of neocortical development by early neuronal activity: physiology and pathophysiology. *Front Cell Neurosci.* (2017) 11:379. doi: 10.3389/fncel.2017.00379
51. Banerjee A, Ellender TJ. Oscillations in the developing cortex: a mechanism for establishing and synchronizing an early network? *J Neurosci.* (2009) 29:15029–30. doi: 10.1523/JNEUROSCI.4567-09.2009
52. Yang JW, Hanganu-Opatz IL, Sun JJ, Luhmann HJ. Three patterns of oscillatory activity differentially synchronize developing neocortical networks *in vivo*. *J Neurosci.* (2009) 29:9011–25. doi: 10.1523/JNEUROSCI.5646-08.2009
53. An S, Kilb W, Luhmann HJ. Sensory-evoked and spontaneous gamma and spindle bursts in neonatal rat motor cortex. *J Neurosci.* (2014) 34:10870–83. doi: 10.1523/JNEUROSCI.4539-13.2014
54. Yang JW, Reyes-Puerta V, Kilb W, Luhmann HJ. Spindle bursts in neonatal rat cerebral cortex. *Neural Plast.* (2016) 2016:3467832. doi: 10.1155/2016/3467832
55. Dall'orso S, Steinweg J, Allievi AG, Edwards AD, Burdet E, Arichi T. Somatotopic mapping of the developing sensorimotor cortex in the preterm human brain. *Cereb Cortex.* (2018). 28:2507–15. doi: 10.1093/cercor/bhy050
56. Leikos S, Tokariev A, Koolen N, Nevalainen P, Vanhatalo S. Cortical responses to tactile stimuli in preterm infants. *Eur J Neurosci.* (2020) 51:1059–73. doi: 10.1111/ejn.14613
57. Coq JO, Strata F, Russier M, Safadi FF, Merzenich MM, Byl NN, et al. Impact of neonatal asphyxia and hind limb immobilization on musculoskeletal tissues and S1 map organization: implications for cerebral palsy. *Exp Neurol.* (2008) 210:95–108. doi: 10.1016/j.expneurol.2007.10.006
58. Jaspers E, Byblow WD, Feys H, Wenderoth N. The corticospinal tract: a biomarker to categorize upper limb functional potential in unilateral cerebral palsy. *Front Pediatr.* (2015) 3:112. doi: 10.3389/fped.2015.00112
59. Eyre JA, Taylor JP, Villagra F, Smith M, Miller S. Evidence of activity-dependent withdrawal of corticospinal projections during human development. *Neurology.* (2001) 57:1543–54. doi: 10.1212/WNL.57.9.1543
60. Eyre JA, Smith M, Dabydeen L, Clowry GJ, Petacchi E, Battini R, et al. Is hemiplegic cerebral palsy equivalent to amblyopia of the corticospinal system? *Ann Neurol.* (2007) 62:493–503. doi: 10.1002/ana.21108
61. Staudt M, Grodd W, Gerloff C, Erb M, Stitz J, Krageloh-Mann I. Two types of ipsilateral reorganization in congenital hemiparesis: a TMS and fMRI study. *Brain.* (2002) 125:2222–37. doi: 10.1093/brain/awf227
62. Staudt M, Gerloff C, Grodd W, Holthausen H, Niemann G, Krageloh-Mann I. Reorganization in congenital hemiparesis acquired at different gestational ages. *Ann Neurol.* (2004) 56:854–63. doi: 10.1002/ana.20297
63. Thickbroom GW, Byrnes ML, Archer SA, Nagarajan L, Mastaglia FL. Differences in sensory and motor cortical organization following brain injury early in life. *Ann Neurol.* (2001) 49:320–7. doi: 10.1002/ana.68

64. Staudt M, Braun C, Gerloff C, Erb M, Grodd W, Krageloh-Mann I. Developing somatosensory projections bypass periventricular brain lesions. *Neurology.* (2006) 67:522–5. doi: 10.1212/01.wnl.0000227937.49151.fd
65. Siokas V, Dardiotis E, Tsironi EE, Tsivgoulis G, Rikos D, Sokratous M, et al. The role of TOR1A polymorphisms in dystonia: a systematic review and meta-analysis. *PLoS ONE.* (2017) 12:e0169934. doi: 10.1371/journal.pone.0169934
66. Yokoi F, Chen HX, Dang MT, Cheetham CC, Campbell SL, Roper SN, et al. Behavioral and electrophysiological characterization of Dyt1 heterozygous knockout mice. *PLoS ONE.* (2015) 10:e0120916. doi: 10.1371/journal.pone.0120916
67. Liang CC, Tanabe LM, Jou S, Chi F, Dauer WT. TorsinA hypofunction causes abnormal twisting movements and sensorimotor circuit neurodegeneration. *J Clin Invest.* (2014) 124:3080–92. doi: 10.1172/JCI72830
68. Vanni V, Puglisi F, Bonsi P, Ponterio G, Maltese M, Pisani A, et al. Cerebellar synaptogenesis is compromised in mouse models of DYT1 dystonia. *Exp Neurol.* (2015) 271:457–67. doi: 10.1016/j.expneurol.2015.07.005
69. Desimone JC, Febo M, Shukla P, Ofori E, Colon-Perez LM, Li Y, et al. In vivo imaging reveals impaired connectivity across cortical and subcortical networks in a mouse model of DYT1 dystonia. *Neurobiol Dis.* (2016) 95:35–45. doi: 10.1016/j.nbd.2016.07.005
70. Maltese M, Stanic J, Tassone A, Sciamanna G, Ponterio G, Vanni V, et al. Early structural and functional plasticity alterations in a susceptibility period of DYT1 dystonia mouse striatum. *Elife.* (2018) 7. doi: 10.7554/eLife.33331.019
71. Zakirova Z, Fanutza T, Bonet J, Readhead B, Zhang W, Yi Z, et al. Mutations in THAP1/DYT6 reveal that diverse dystonia genes disrupt similar neuronal pathways and functions. *PLoS Genet.* (2018) 14:e1007169. doi: 10.1371/journal.pgen.1007169
72. Niethammer M, Carbon M, Argyelan M, Eidelberg D. Hereditary dystonia as a neurodevelopmental circuit disorder: evidence from neuroimaging. *Neurobiol Dis.* (2011) 42:202–9. doi: 10.1016/j.nbd.2010.10.010
73. Crair MC, Malenka RC. A critical period for long-term potentiation at thalamocortical synapses. *Nature.* (1995) 375:325–8. doi: 10.1038/375325a0
74. Ben-Ari Y, Khazipov R, Leinekugel X, Caillard O, Gaiarsa JL. GABAA, NMDA and AMPA receptors: a developmentally regulated 'menage a trois'. *Trends Neurosci.* (1997) 20:523–9. doi: 10.1016/S0166-2236(97)01147-8
75. Citri A, Malenka RC. Synaptic plasticity: multiple forms, functions, and mechanisms. *Neuropsychopharmacology.* (2008) 33:18–41. doi: 10.1038/sj.npp.1301559
76. Bax M, Tydeman C, Flodmark O. Clinical and MRI correlates of cerebral palsy: the European Cerebral Palsy Study. *JAMA.* (2006) 296:1602–8. doi: 10.1001/jama.296.13.1602
77. Korzeniewski SJ, Birbeck G, Delano MC, Potchen MJ, Paneth N. A systematic review of neuroimaging for cerebral palsy. *J Child Neurol.* (2008) 23:216–27. doi: 10.1177/0883073807307983
78. Robinson MN, Peake LJ, Ditchfield MR, Reid SM, Lanigan A, Reddihough DS. Magnetic resonance imaging findings in a population-based cohort of children with cerebral palsy. *Dev Med Child Neurol.* (2009) 51:39–45. doi: 10.1111/j.1469-8749.2008.03127.x
79. De Vries LS, Groenendaal F. Patterns of neonatal hypoxic-ischaemic brain injury. *Neuroradiology.* (2010) 52:555–66. doi: 10.1007/s00234-010-0674-9
80. Neychev VK, Gross RE, Lehericy S, Hess EJ, Jinnah HA. The functional neuroanatomy of dystonia. *Neurobiol Dis.* (2011) 42:185–201. doi: 10.1016/j.nbd.2011.01.026
81. Corp DT, Joutsa J, Darby RR, Delnooz CCS, Van De Warrenburg BPC, Cooke D, et al. Network localization of cervical dystonia based on causal brain lesions. *Brain.* (2019) 142:1660–74. doi: 10.1093/brain/awz112
82. Latorre A, Rocchi L, Bhatia KP. Delineating the electrophysiological signature of dystonia. *Exp Brain Res.* (2020) 238:1685–92. doi: 10.1007/s00221-020-05863-2
83. Towsley K, Shevell MI, Dagenais L, Consortium R. Population-based study of neuroimaging findings in children with cerebral palsy. *Eur J Paediatr Neurol.* (2011) 15:29–35. doi: 10.1016/j.ejpn.2010.07.005
84. Nelson AJ, Blake DT, Chen R. Digit-specific aberrations in the primary somatosensory cortex in Writer's cramp. *Ann Neurol.* (2009) 66:146–54. doi: 10.1002/ana.21626
85. Delcour M, Massicotte VS, Russier M, Bras H, Peyronnet J, Canu MH, et al. Early movement restriction leads to enduring disorders in muscle and locomotion. *Brain Pathol.* (2018) 28:889–901. doi: 10.1111/bpa.12594
86. Delcour M, Russier M, Castets F, Turle-Lorenzo N, Canu MH, Cayetanot F, et al. Early movement restriction leads to maladaptive plasticity in the sensorimotor cortex and to movement disorders. *Sci Rep.* (2018) 8:16328. doi: 10.1038/s41598-018-34312-y
87. Hoon AH Jr, Lawrie WT Jr, Melhem ER, Reinhardt EM, Van Zijl PC, Solaiyappan M, et al. Diffusion tensor imaging of periventricular leukomalacia shows affected sensory cortex white matter pathways. *Neurology.* (2002) 59:752–6. doi: 10.1212/WNL.59.5.752
88. Hoon AH Jr, Stashinko EE, Nagae LM, Lin DD, Keller J, Bastian A, et al. Sensory and motor deficits in children with cerebral palsy born preterm correlate with diffusion tensor imaging abnormalities in thalamocortical pathways. *Dev Med Child Neurol.* (2009) 51:697–704. doi: 10.1111/j.1469-8749.2009.03306.x
89. De Vries LS, Eken P, Pierrat V, Daniels H, Casaer P. Prediction of neurodevelopmental outcome in the preterm infant: short latency cortical somatosensory evoked potentials compared with cranial ultrasound. *Arch Dis Child.* (1992) 67:1177–81. doi: 10.1136/adc.67.10_Spec_No.1177
90. Pierrat V, Eken P, De Vries LS. The predictive value of cranial ultrasound and of somatosensory evoked potentials after nerve stimulation for adverse neurological outcome in preterm infants. *Dev Med Child Neurol.* (1997) 39:398–403. doi: 10.1111/j.1469-8749.1997.tb07453.x
91. Pike AA, Marlow N. The role of cortical evoked responses in predicting neuromotor outcome in very preterm infants. *Early Hum Dev.* (2000) 57:123–35. doi: 10.1016/S0378-3782(99)00061-4
92. Suppiej A, Cappellari A, Franzoi M, Traverso A, Ermani M, Zanardo V. Bilateral loss of cortical somatosensory evoked potential at birth predicts cerebral palsy in term and near-term newborns. *Early Hum Dev.* (2010) 86:93–8. doi: 10.1016/j.earlhumdev.2010.01.024
93. McClelland VM, Fialho D, Flexney-Briscoe D, Holder GE, Elze MC, Gimeno H, et al. Somatosensory evoked potentials and central motor conduction times in children with dystonia and their correlation with outcomes from deep brain stimulation of the globus pallidus internus. *Clin Neurophysiol.* (2018) 129:473–86. doi: 10.1016/j.clinph.2017.11.017
94. Shah SA, Brown P, Gimeno H, Lin JP, McClelland VM. Application of machine learning using decision trees for prognosis of deep brain stimulation of globus pallidus internus for children with dystonia. *Front Neurol.* (2020) 11:825. doi: 10.3389/fneur.2020.00825
95. Fog E, Fog M. Cerebral inhibition examined by associated movements, minimal cerebral dysfunction. In: Bax M, Mac Keith R, editors. *Clinics in Developmental Medicine*, Vol. 10. London: Heinemann Medical (1963) p. 52–7.
96. Lin JP, Brown JK, Walsh EG. The maturation of motor dexterity: or why Johnny can't go any faster. *Dev Med Child Neurol.* (1996) 38:244–54. doi: 10.1111/j.1469-8749.1996.tb15086.x
97. Quatman-Yates CC, Quatman CE, Meszaros AJ, Paterno MV, Hewett TE. A systematic review of sensorimotor function during adolescence: a developmental stage of increased motor awkwardness? *Br J Sports Med.* (2012) 46:649–55. doi: 10.1136/bjsm.2010.079616
98. Holst-Wolf JM, Yeh IL, Konczak J. Development of proprioceptive acuity in typically developing children: normative data on forearm position sense. *Front Hum Neurosci.* (2016) 10:436. doi: 10.3389/fnhum.2016.00436
99. Marshall PJ, Bar-Haim Y, Fox NA. Development of the EEG from 5 months to 4 years of age. *Clin Neurophysiol.* (2002) 113:1199–208. doi: 10.1016/S1388-2457(02)00163-3
100. Stroganova TA, Orekhova EV, Posikera IN. EEG alpha rhythm in infants. *Clin Neurophysiol.* (1999) 110:997–1012. doi: 10.1016/S1388-2457(98)00009-1
101. Berchicci M, Zhang T, Romero L, Peters A, Annett R, Teuscher U, et al. Development of mu rhythm in infants and preschool children. *Dev Neurosci.* (2011) 33:130–43. doi: 10.1159/000329095
102. Thorpe SG, Cannon EN, Fox NA. Spectral and source structural development of mu and alpha rhythms from infancy through adulthood. *Clin Neurophysiol.* (2016) 127:254–69. doi: 10.1016/j.clinph.2015.03.004

103. Pfurtscheller G, Lopes Da Silva FH. Event-related EEG/MEG synchronization and desynchronization: basic principles. *Clin Neurophysiol.* (1999) 110:1842–57. doi: 10.1016/S1388-2457(99)00141-8
104. Pineda JA. The functional significance of mu rhythms: translating "seeing" and "hearing" into "doing". *Brain Res Brain Res Rev.* (2005) 50:57–68. doi: 10.1016/j.brainresrev.2005.04.005
105. Demas J, Bourguignon M, Perivier M, De Tiege X, Dinomais M, Van Bogaert P. Mu rhythm: state of the art with special focus on cerebral palsy. *Ann Phys Rehabil Med.* (2019) 63: 439–46. doi: 10.1016/j.rehab.2019.06.007
106. Cheyne D, Jobst C, Tesan G, Crain S, Johnson B. Movement-related neuromagnetic fields in preschool age children. *Hum Brain Mapp.* (2014) 35:4858–75. doi: 10.1002/hbm.22518
107. Johnson B, Jobst C, Al-Loos R, He W, Cheyne D. Individual differences in motor development during early childhood: an MEG study. *Dev Sci.* (2019) 23:e12935. doi: 10.1111/desc.12935
108. Schmidt R, Herrojo Ruiz M, Kilavik BE, Lundqvist M, Starr PA, Aron AR. Beta oscillations in working memory, executive control of movement and thought, and sensorimotor function. *J Neurosci.* (2019) 39:8231–8. doi: 10.1523/JNEUROSCI.1163-19.2019
109. Gehringer JE, Arpin DJ, Vermaas JR, Trevarrow MP, Wilson TW, Kurz MJ. the strength of the movement-related somatosensory cortical oscillations differ between adolescents and adults. *Sci Rep.* (2019) 9:18520. doi: 10.1038/s41598-019-55004-1
110. Silberstein P, Kuhn AA, Kupsch A, Trottenberg T, Krauss JK, Wohrle JC, et al. Patterning of globus pallidus local field potentials differs between Parkinson's disease and dystonia. *Brain.* (2003) 126:2597–608. doi: 10.1093/brain/awg267
111. Miocinovic S, Miller A, Swann NC, Ostrem JL, Starr PA. Chronic deep brain stimulation normalizes scalp EEG activity in isolated dystonia. *Clin Neurophysiol.* (2017) 129:368–76. doi: 10.1016/j.clinph.2017.11.011
112. Moll CK, Galindo-Leon E, Sharott A, Gulberti A, Buhmann C, Koeppen JA, et al. Asymmetric pallidal neuronal activity in patients with cervical dystonia. *Front Systems Neurosci.* (2014) 8:15. doi: 10.3389/fnsys.2014.00015
113. Tang JK, Mahant N, Cunic D, Chen R, Moro E, Lang AE, et al. Changes in cortical and pallidal oscillatory activity during the execution of a sensory trick in patients with cervical dystonia. *Exp Neurol.* (2007) 204:845–8. doi: 10.1016/j.expneurol.2007.01.010
114. Mall V, Berweck S, Fietzek UM, Glocker FX, Oberhuber U, Walther M, et al. Low level of intracortical inhibition in children shown by transcranial magnetic stimulation. *Neuropediatrics.* (2004) 35:120–5. doi: 10.1055/s-2004-815834
115. Heinen F, Glocker FX, Fietzek U, Meyer BU, Lucking CH, Korinthenberg R. Absence of transcallosal inhibition following focal magnetic stimulation in preschool children. *Ann Neurol.* (1998) 43:608–12. doi: 10.1002/ana.410430508
116. Garvey MA, Ziemann U, Bartko JJ, Denckla MB, Barker CA, Wassermann EM. Cortical correlates of neuromotor development in healthy children. *Clin Neurophysiol.* (2003) 114:1662–70. doi: 10.1016/S1388-2457(03)00130-5
117. Wiesman AI, Heinrichs-Graham E, Coolidge NM, Gehringer JE, Kurz MJ, Wilson TW. Oscillatory dynamics and functional connectivity during gating of primary somatosensory responses. *J Physiol.* (2017) 595:1365–75. doi: 10.1113/JP273192
118. Cheng CH, Chan PY, Baillet S, Lin YY. Age-related reduced somatosensory gating is associated with altered alpha frequency desynchronization. *Neural Plast.* (2015) 2015:302878. doi: 10.1155/2015/302878
119. Trevarrow MP, Kurz MJ, Mcdermott TJ, Wiesman AI, Mills MS, Wang YP, et al. The developmental trajectory of sensorimotor cortical oscillations. *Neuroimage.* (2019) 184:455–61. doi: 10.1016/j.neuroimage.2018.09.018
120. Walther M, Berweck S, Schessl J, Linder-Lucht M, Fietzek UM, Glocker FX, et al. Maturation of inhibitory and excitatory motor cortex pathways in children. *Brain Dev.* (2009) 31:562–7. doi: 10.1016/j.braindev.2009.02.007
121. Pitcher JB, Riley AM, Doeltgen SH, Kurylowicz L, Rothwell JC, Mcallister SM, et al. Physiological evidence consistent with reduced neuroplasticity in human adolescents born preterm. *J Neurosci.* (2012) 32:16410–6. doi: 10.1523/JNEUROSCI.3079-12.2012
122. Lin JP, Lumsden DE, Gimeno H, Kaminska M. The impact and prognosis for dystonia in childhood including dystonic cerebral palsy: a clinical and demographic tertiary cohort study. *J Neurol Neurosurg Psychiatry.* (2014) 85:1239–44. doi: 10.1136/jnnp-2013-307041
123. Lumsden DE, Kaminska M, Gimeno H, Tustin K, Baker L, Perides S, et al. Proportion of life lived with dystonia inversely correlates with response to pallidal deep brain stimulation in both primary and secondary childhood dystonia. *Dev Med Child Neurol.* (2013) 55:567–74. doi: 10.1111/dmcn.12117
124. Marks W, Bailey L, Reed M, Pomykal A, Mercer M, Macomber D, et al. Pallidal stimulation in children: comparison between cerebral palsy and DYT1 dystonia. *J Child Neurol.* (2013) 28:840–8. doi: 10.1177/0883073813488674
125. Elkaim LM, Alotaibi NM, Sigal A, Alotaibi HM, Lipsman N, Kalia SK, et al. Deep brain stimulation for pediatric dystonia: a meta-analysis with individual participant data. *Dev Med Child Neurol.* (2019) 61:49–56. doi: 10.1111/dmcn.14063
126. Hudson VE, Elniel A, Ughratdar I, Zebian B, Selway R, Lin JP. A comparative historical and demographic study of the neuromodulation management techniques of deep brain stimulation for dystonia and cochlear implantation for sensorineural deafness in children. *Eur J Paediatr Neurol.* (2017) 21:122–35. doi: 10.1016/j.ejpn.2016.07.018
127. Koy A, Hellmich M, Pauls KA, Marks W, Lin JP, Fricke O, et al. Effects of deep brain stimulation in dyskinetic cerebral palsy: a meta-analysis. *Mov Disord.* (2013) 28:647–54. doi: 10.1002/mds.25339
128. Giachello CN, Baines RA. Inappropriate neural activity during a sensitive period in embryogenesis results in persistent seizure-like behavior. *Curr Biol.* (2015) 25:2964–8. doi: 10.1016/j.cub.2015.09.040

Conflict of Interest: J-PL received unrestricted educational support for instructional courses and consultancy fees from Medtronic Ltd.

The remaining author declares that the research was conducted in the absence of any commercial or financial relationships that could be construed as a potential conflict of interest.

Publisher's Note: All claims expressed in this article are solely those of the authors and do not necessarily represent those of their affiliated organizations, or those of the publisher, the editors and the reviewers. Any product that may be evaluated in this article, or claim that may be made by its manufacturer, is not guaranteed or endorsed by the publisher.

Copyright © 2021 McClelland and Lin. This is an open-access article distributed under the terms of the Creative Commons Attribution License (CC BY). The use, distribution or reproduction in other forums is permitted, provided the original author(s) and the copyright owner(s) are credited and that the original publication in this journal is cited, in accordance with accepted academic practice. No use, distribution or reproduction is permitted which does not comply with these terms.

frontiers in Pediatrics

CASE REPORT
published: 22 October 2021
doi: 10.3389/fped.2021.732645

Case Report: Paternal Uniparental Isodisomy and Heterodisomy of Chromosome 16 With a Normal Phenotype

*Xu Zhang, Li Liu, Yang Liu and Xin Pan**

The Department of Obstetrics and Gynecology, The Second Affiliated Hospital of Chongqing Medical University, Chongqing, China

Uniparental disomy (UPD) is a specific type of chromosomal variant that has been detected in both prenatal diagnosis and neonates with advances in molecular genetic testing technologies [mainly chromosome microarray analysis (CMA) technologies containing single-nucleotide polymorphism (SNP) probes]. In this case, we performed non-invasive prenatal genetic testing (NIPT) to screen fetuses for aneuploidy and detected the presence of aneuploidy chimerism and UPD by CMA, including SNP analysis and whole-exome sequencing, to detect pathogenic variants within the genome. The NIPT results suggested an increased number of fetal chromosome 16, and the CMA results indicated that it was the first case of holistic paternal UPD16 with isodisomy combined with heterodisomy, although no abnormal phenotype was seen in the newborn at postnatal follow-up. The homozygous region of the isodimer combined with the heterodimer is smaller than that of the complete isodimer, and it is less prone to recessive genetic diseases. A retrospective analysis of this case of paternally derived UPD16 was used to explore the uniparental diploid origin of chromosome 16 and to provide some reference for genetic counseling and prenatal diagnosis.

Keywords: paternal uniparental disomy, UPD 16, SNP array, prenatal diagnosis, chromosomal variant

OPEN ACCESS

Edited by:
Volker Mall, Technical University of Munich, Germany

Reviewed by:
Aleksandra Jezela-Stanek, National Institute of Tuberculosis and Lung Diseases, Poland
Antonella Riva, University of Genoa, Italy

****Correspondence:***
Xin Pan
panxin@cqmu.edu.cn

Specialty section:
This article was submitted to Pediatric Neurology, a section of the journal Frontiers in Pediatrics

Received: *29 June 2021*
Accepted: *14 September 2021*
Published: *22 October 2021*

Citation:
Zhang X, Liu L, Liu Y and Pan X (2021) Case Report: Paternal Uniparental Isodisomy and Heterodisomy of Chromosome 16 With a Normal Phenotype. Front. Pediatr. 9:732645. doi: 10.3389/fped.2021.732645

INTRODUCTION

Eric Engel first proposed the concept of a single-parent diploid in 1980, which described the situation in which two homologous chromosomes are inherited from the same parent and have no genetic relationship with the other parent (1). The incidence of uniparental diploidy in newborns is ∼0.029%. As of 2010, statistics in the literature have reported ∼1,100 cases of whole uniparental disomy (UPD) and 120 cases of partial UPD (2). Recent data from more than 4 million subjects studied by the personal genetics companies 23 and Me and Biobankhave led to the estimation that all chromosomes (not only chromosomes with imprinted regions) have a UPD incidence of 1/2,000 (3). Chromosome 16 is one of the chromosomes that are prone to non-integration, which also causes a high incidence of chromosome 16 UPD, but most cases are maternal UPD. According to statistics from Kotzor and other scholars in 2005, there have been more than 50 cases of maternal chromosome 16 UPD reported in the literature, and their clinical phenotypes have varied, ranging from no abnormal clinical phenotypes to mental retardation, developmental delay, and structural abnormalities (4). However, only two cases of paternal UPD16 have been reported, and its clinical

manifestations range from no abnormal clinical manifestations to the onset of Mendelian genetic disease (5, 6).

UPD includes three subtypes: heterodisomy, isodisomy, and partial isodisomy. Heterodisomy is caused by non-segregation in stage I meiosis, and the affected individual inherits two homologous chromosomes from the same parent; isodisomy is caused by non-segregation in stage II meiosis, and the affected individual inherits two sister chromatids of one homologous chromosome from one parent. For the simple type of uniparental diploid (referring to the absence of combined trisomy or other abnormal mosaicism), its pathogenicity mainly lies in two aspects. One is caused by the influence of imprinted genes from this perspective. In other words, most chromosomal UPDs do not have clear and characteristic clinical symptoms. Currently, UPDs on chromosomes 6, 7, 11, 14, 15, and 20 can cause clinical symptoms. The second type is the onset of recessive genetic diseases on the chromosome where the UPD is located. For example, UPD on the X chromosome may cause the onset of X-linked recessive genetic diseases in female patients (7). As the known cases of UPD on chromosome 16 belong to the overall UPD involving the entire chromosome, the segments and genes that cause UPD on chromosome 16 cannot be located, and its pathogenic mechanism is also difficult to analyze. Although partial UPD16 cases involving only partial fragments of chromosome 16 can help researchers determine the chromosome segment that causes specific clinical symptoms, further determine the key genes that cause the disease, and clarify gene functions and pathogenic mechanisms, there is no literature support at present.

This study used single-nucleotide polymorphism (SNP) array technology to perform copy number analysis and SNP genome typing on a prenatal diagnosis sample with abnormal non-invasive prenatal genetic testing (NIPT) and found a case of paternal UPD16. The results of the whole-exome sequencing (WES) test showed no abnormalities, the neonatal follow-up after birth did not show abnormal phenotypes, and all developmental indicators were normal. Similar to the previous two reports on paternal upd16, no abnormal syndrome was found in the cases. The cases reported by Kohlhase et al. found bilateral calcaneal and mandibular arch hypoplasia. In the cases reported by Donova et al., Fanconi anemia was mainly caused by homozygous mutation of the *FANCA* gene (5, 6). No significant gene mutation on the chromosome of UPD was found in this case report; the two previous reports were isodimers, whereas this case report describes isodimers combined with heterodimers. Compared with a complete isodimer, the homozygous region is relatively small, and the risk of recessive diseases is lower. This study conducted a retrospective analysis of this case of UPD16 to explore the source and pathogenic mechanism of chromosome 16-UPD and its application value in clinical response and genetic counseling.

CLINICAL REPORT

We present a case of a 26-year-old pregnant woman, G2P0 (gravida 2, para 0), with both pregnancies from the same non-consanguineous male partner. The couple had normal physical conditions, normal mental development, and no adverse contact or exposure in the working environment. The first abortion of the pregnant woman was an induced abortion, and the aborted tissue was not examined for genetics. The present pregnancy was spontaneous. The results of NIPT at 13 weeks of gestation showed that the number of chromosomes at 16 was excessive. Chromosome microarray analysis (CMA) results after amniocentesis at 18 weeks showed that there were two regional homozygous fragments around the centromere of chromosome 16. CMA family analysis suggested that fetal chromosome 16 was an integral paternal UPD with isodisomy and heterodisomy. Consecutive systematic ultrasound examinations throughout pregnancy were as follows: ultrasonography at 12 weeks of gestation showed no significant abnormality (**Figures 1A,B**). On ultrasound performed at 25 weeks, abnormal echogenicity of the fetal left lower lung (possible isolated lung) and slight polyhydramnios were observed (**Figures 1C,D**). At 30 weeks of gestation, the ultrasound results were the same as before, but the amniotic fluid volume had returned to normal (**Figures 1E,F**). Ultrasonography at 34 and 37 weeks showed no significant abnormality (**Figures 1G,H**). There were no abnormalities in blood pressure, weight, uterine height, or abdominal circumference during pregnancy and no abnormalities in any fetal heart rate test. In the first trimester of pregnancy, she had been treated with infusion for cold and fever, but the specific medication was unknown. The pregnant woman delivered a boy by cesarean section at 38 weeks 3 days. A physical examination was performed after birth, and the weight of the newborn was 3.25 kg.

At 1 month and 5 days old, the baby's weight was 4.7 kg, his height was 52.0 cm, his head circumference was 39.0 cm, his facial features were normal, his mental development was within the normal range, his prehalogen was 2.0 × 2.0 cm, and his hearing oral, chest, abdominal, and umbilical examinations were unremarkable. At 4 months 18 days old, the baby's weight was 6.8 kg, his height was 59.0 cm, his head circumference was 43.5 cm, his facial features were normal, his mental condition was good, his front halogen was 1.0 × 1.0 cm, his physical examination is normal, and his movement and language development were normal. At 6 months old, the baby's weight was 7.2 kg, his height was 64.0 cm, his head circumference was 43.8 cm, his front halogen was 1.0 × 1.0 cm, his physical examination showed no abnormalities, and his hemoglobin value was 105 g/L. At 10 months 26 days old, the baby's weight was 8.9 kg, his height was 70.5 cm, and his head circumference was 48.9 cm. There were no abnormalities in facial features or in his gross motor, fine motor, or speech development. After birth, peripheral blood was retrieved for karyotyping and SNP array analysis, and the results were consistent with the prenatal results. A WES test was also performed and showed no abnormal results. Overall, to the date of this article, the clinical presentation of the newborn did not show any adverse conditions. All data were collected after obtaining informed consent from the patient.

MATERIALS AND METHODS

Non-invasive Prenatal Genetic Testing

Peripheral venous blood (5 mL) was collected from the pregnancy at 19 weeks of gestation, anticoagulated by

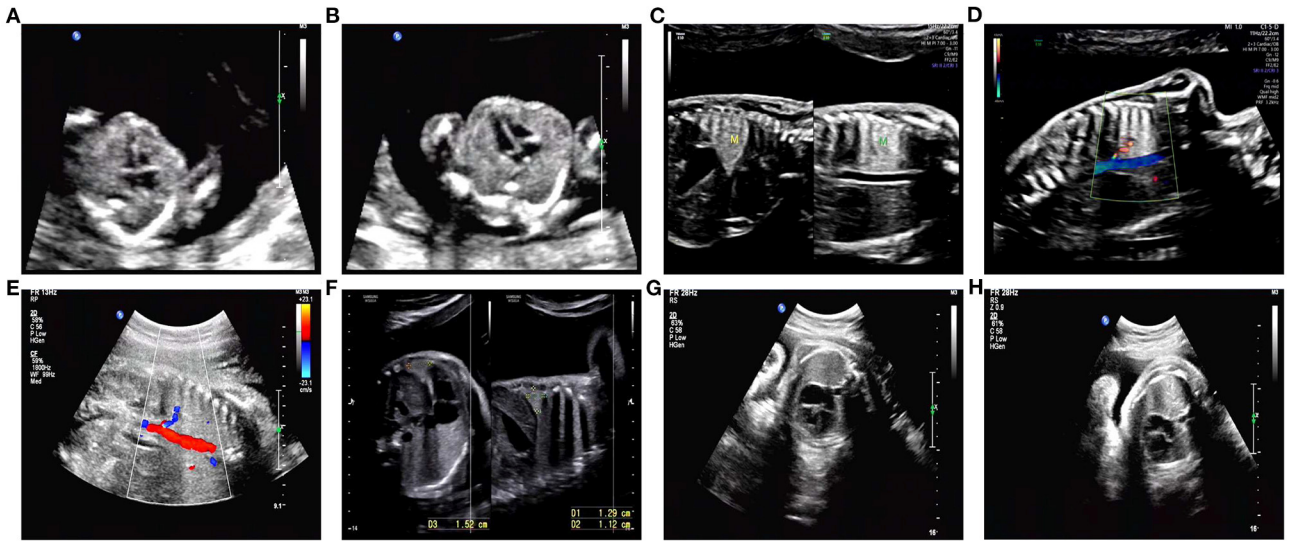

FIGURE 1 | Detailed ultrasound images. **(A,B)** No abnormalities were observed in this fetus at 12 weeks of gestation. **(C,D)** An ultrasound scan revealed abnormal echogenicity of the left lower lung (isolated lung possible) and hydramnion at 25 weeks of gestation. **(E,F)** Ultrasound image of abnormal echogenicity of the left lower lung (isolated lung possible) and normal amniotic fluid volume at 30 weeks of gestation. **(G,H)** At 34 and 37 weeks of gestation, no abnormalities were observed on ultrasound.

ethylenediaminetetraacetic acid, and then transferred into a sterile centrifuge tube for NIPT (The Beijing Genomics Institute). The procedure was performed as described in a previous study (8). Then, cell-free DNA from plasma was extracted and stored at −80°C. The kits were purchased from BGI Biotechnology Co., Ltd. (Wuhan, China). Cell-free DNA was sequenced using the MGISeq-2000 sequencing system (BGI, China) to obtain the exact DNA fragment distribution on each chromosome. The coverage depths (Cov-chrN) of the test and standard samples were calculated based on bioinformatics analysis and then converted into a specific risk index, which was eventually used to determine the sample risks of trisomy 21 (T21), trisomy 18 (T18), and trisomy 13 (T13).

Cytogenetic Analysis

Peripheral blood samples were collected from both parents. Chromosome analysis was performed according to the standard protocol using G-banding at a 450-band resolution. At least 25 metaphases were read for each sample.

Chromosome Microarray Analysis

In this study, an SNP array was used to confirm the existence of genomic variation that was detected by NIPT. Genomic DNA was extracted from peripheral blood or amniotic fluid cells from pregnant women using the QIAamp DNA Mini Kit (Qiagen, Hilden, Germany). The Infinium Global Screening Array (Illumina, San Diego, CA), consisting of ∼700,000 marker genome-wide tag SNPs and markers targeting all regions of known cytogenetic importance, was applied for the whole-genome scan. Molecular karyotype analysis was performed using GenomeStudio V2011.1 software (Illumina, San Diego, CA). Automated detection of copy number changes was carried out using the cnvPartition algorithm (versions 1.2.1–3.1.6) in GenomeStudio V2011.1 software. All identified abnormalities were further characterized by visual inspection of the Log R and BAF chromosomal plots (9).

WES Analysis

WES is a high-throughput sequencing analysis that captures and enriches DNA from all exome regions of the genome using exome sequence-specific capture technology. WES analysis was performed by BGI-Shenzhen Clinical Laboratory Centre. The exome describes the protein-coding regions of the human genome; most pathogenic gene mutations occur in exome regions. WES captures probes that cover only 1–1.5% of the human genome, allowing for the accurate detection of multiple exome disease-causing variants at once (10). Genomic DNA from the blood of the subject was used as the test material. The DNA was first sheared, and libraries were prepared. Then, the exons of the target gene and the DNA in the adjacent shear region were captured and enriched by the BGI V4 chip. Finally, the MGISEQ-2000 sequencing platform (Shenzhen, China) was used for variant detection. Sequencing data quality control indicators were as follows: the average sequencing depth of the target region was ≥180×, and the percentage of loci with average depth >20× in the target region was >95%.

Data Analysis

Sequenced fragments were aligned to the UCSC hg19 human reference genome by BWA to remove duplicates. GATK was used for base mass value correction and SNV, INDEL, and genotype detection. Exome depth was used for copy number variation detection at the exon level. The specific experimental procedure was performed according to the kit instructions (11–15).

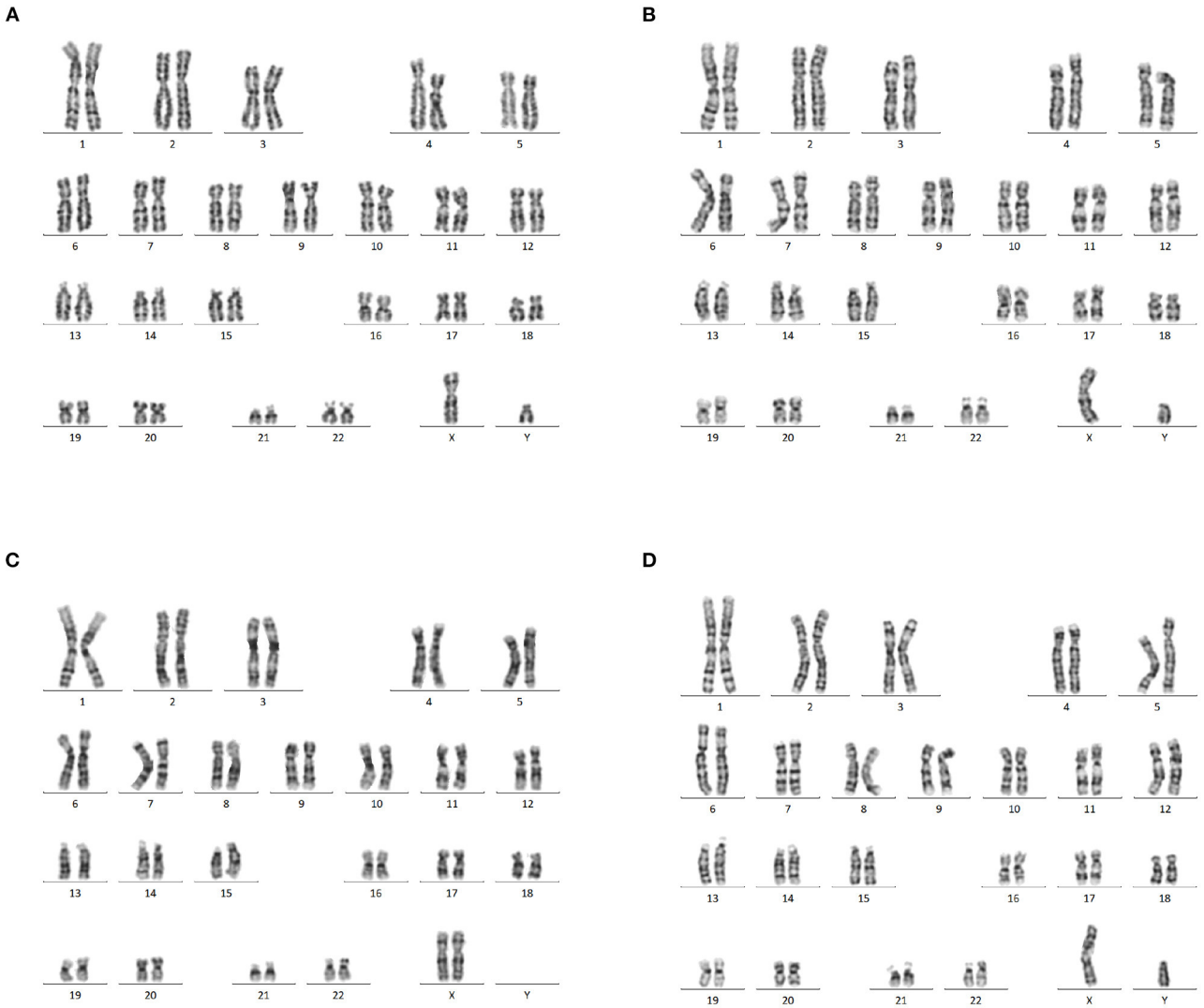

FIGURE 2 | Karyotype analysis. **(A)** Normal karyotype analysis of amniotic fluid cells (46,XY). **(B)** Karyotype analysis of newborn peripheral blood, showing a 46, XY karyotype as the fetal amniotic fluid sample. **(C,D)** The peripheral blood of the couple showed a normal 46, XX and 46, XY karyotype.

We evaluated the chromosome region with the information provided by the Online Mendelian Inheritance in Man database (OMIM, http://omim.org/), the DECIPHER Database (http://decipher.sanger.ac.uk), the UCSC database (http://genome.ucsc.edu), and the Geneimprint database (http://www.geneimprint.com/).

RESULTS

Results of NIPT

The NIPT of this case report indicated that the fetus had a high risk of an increased number of chromosome 16 and no other chromosomal abnormalities (data not shown). Further amniocentesis or cord blood aspiration for karyotyping and gene chip analysis was required to confirm the diagnosis.

Karyotype Results

Karyotyping of the fetus, consistent with his newborn's peripheral blood, revealed a normal karyotype (46, XY) (**Figures 2A,B**). The couple had normal karyotype results (46, XX and 46, XY) (**Figures 2C,D**).

CMA Detected UPD of Chromosome 16

The CMA results of the peripheral blood of the newborn after birth were consistent with the CMA results of the amniotic fluid (16). In this case, the log R ratio of chromosome 16 was consistent with a normal copy number; in addition, some genotypes present were homozygous (genotypes as AA or BB). There was partial isodisomy of chromosome 16 with loss of heterozygosity (genotypes as AB). This is consistent with the mechanism of trisomy/monosomy rescue. Whole-genome SNP array analysis can detect all chromosome

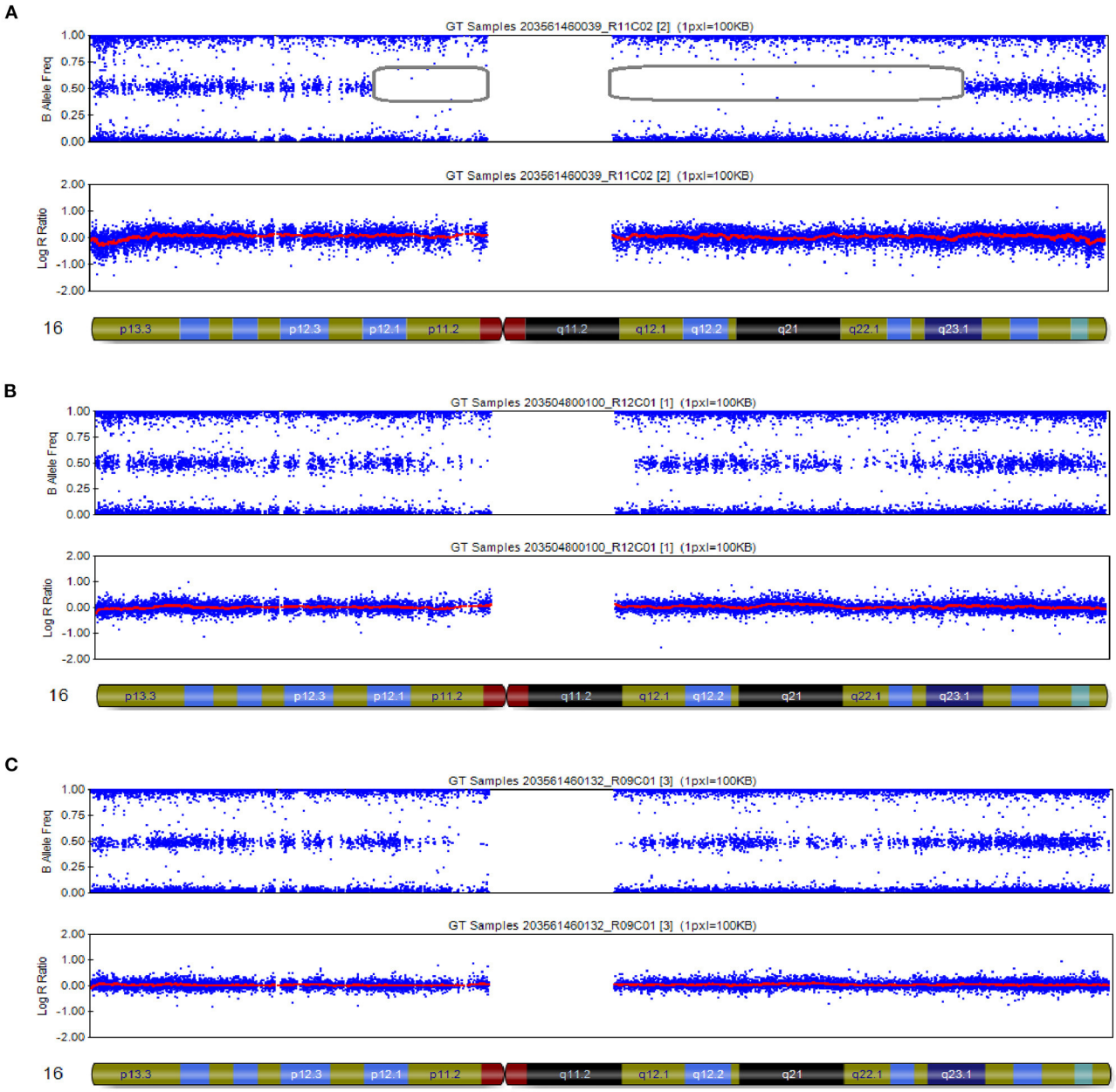

FIGURE 3 | SNP array results of these cases involved imprinted chromosome 16. **(A)** The fetus was chromosome 16 combined with UPD: 16p12.1p11.1 (25,079,459–35,257,261) × 2 hmz pat, 16q11.2q23.1 (46,394,361–77,737,858) × 2 hmz pat. **(B,C)** SNP arrays revealed no abnormalities at chromosome 16 in females and males.

number abnormalities; identify and detect chromosome rearrangements, including genomic sequence gains and losses; and are effective in detecting genomic imbalances. In this case, whole-genome SNP array analysis on uncultured amniocytes detected arr [hg19] 16p12.1p11.1 (25,079,459–35,257,261) × 2 hmz and 16q11.2q23.1 (46,394,361–77,737,858) × 2 hmz, which indicated a case of isodimeric merged heterodimeric holomeric paternal UPD (**Figure 3A**). The results of SNP typing for all chromosomes except chromosome 16 supported the parentage of the fetus to both spouses (**Figures 3B,C**). The comparative results of typing in neonates are shown in **Table 1**.

Analysis of Pathogenic Variants in the Genome

In this case, WES did not detect pathogenic/suspected pathogenic variants within the subject's genome.

TABLE 1 | Comparative results of SNP in neonates.

Chromosomal segment	Length (bp)	Total number of SNP probes	Number of SNP probe detections	SNP probe detection rate	Number of AB heterozygotes	AB heterozygous ratio	Fractal and paternal concordance rate	UPD type
16:88,366–25,068,754	24,980,388	7,419	6,843	92.24%	1,126	16.45%	100%	Heterodisomy
16:25,079,459–35,257,261	10,177,802	1,628	1,490	91.52%	0	0	100%	Isodisomy
16:46,394,361–77,737,858	31,343,497	7,354	6,866	93.36%	0	0	100%	Isodisomy
16:77,741,596–90,161,959	12,420,363	5,273	4,961	94.08%	912	18%	100%	Heterodisomy

TABLE 2 | Case review of the f parentage UPD16.

Date	Author	UPD detection method	Isodimer/heterodimer	Genetic mutation	Sex	Age	Phenotype
2000	Kohlhase et al. (5)	STR	Isodimers (technical limitation, cannot confirm the presence of heterodimeric regions)	Untested	Female	Prenatal—13 months	Normal phenotype and no syndromic picture with the exception of bilateral achilles and mandibular arch hypoplasia
2016	Donovan et al. (6)	STR, SNP array	Complete isomorphism	FANCA homozygous mutation (inherited from father)	Female	9 years old	No synthetic picture with the exception of Fanconi anemia that due to the homozygous state of FANCA gene.

DISCUSSION

This case of prenatal diagnosis was clinically specific, with limited testing and difficulty in obtaining comprehensive phenotypic information. The detection and diagnosis method of UPD is based on the relevant guidelines published by the American College of Medical Genetics and Genomics in 2020, which describes the adaptation of UPD detection in prenatal diagnosis. Based on the case we reported, the chromosomal abnormalities detected by NIPT during pregnancy may indicate the existence of UPD. When specific chromosomes are involved, such as chromosomes 6, 7, 11, 14, 15, and 20, we recommend the detection of UPD.

UPD can occur during meiosis of gametes or mitosis of oosperm and is most commonly seen in the q11.2-q13.1 imprinted region of chromosome 15, as in Prader Willi/Angelman. Most of the reported UPDs on chromosome 16 are of maternal origin; as of 2005, more than 50 cases of maternal UPD (16) have been reported, whereas only two cases of paternal UPD have been reported (**Table 2**).

Chromosome 16 in this case was identified as a chromosomal paternal UPD with an isodimeric merger of heterodimers based on SNP typing results. Thus, our report is the first confirmed case of a parental UPD (16) with both regional isodimers and regional heterodimers. This case is a newborn boy currently without any abnormal phenotype. The mechanisms of occurrence of complete and regional isodysomy are different. Chromosomal errors occur at different stages of cell division, and types of UPDs may not have the same effects on fetal development.

UPD is usually caused by two non-disjunction events, the first occurring during meiosis and the second during mitosis. Meiosis I non-disjunction is the failure of two homologous chromosomes to separate, resulting in an increased probability of two different homologous chromosomes or uniparental heterodimers from the same parent. After fertilization with a normal haploid gamete, the chromosomes affected in the zygote may be trisomic or monosomic. Mitotic non-disjunction after the formation of a zygote may then occur as a second event, with aneuploidy being rescued by the loss of a third chromosome (trisomic rescue) or the duplication of a monosomic chromosome (monosomic rescue) (7). Given that most non-disjunctions occur in maternal meiosis I, trisomies consisting of two different maternal chromosomes and one paternal chromosome are more common. Subsequent trisomic rescue is achieved by the loss of a paternal chromosome, which makes maternal heterodimers more common. Thus, as described in the background of this article, we found that most of the reports of UPD16 are maternal UPD16.

The specific mechanism of paternal UPD on chromosome 16 in this case is not clear. Based on the abovementioned mechanism of UPD formation, we suggest that it may be caused by an error in meiosis II during the formation of the father's sperm, resulting in the formation of sperm with two chromosomes 16 of paternal origin. As a result of meiotic recombination, the two chromosomes appear as alternate regions of heterozygotes

and homozygotes, but there are homozygous regions around the centromere, that is, regional isodisomes. This sperm–ovum union forms a zygote with two paternal chromosomes 16, after which the zygote undergoes trisomy rescue, loses one maternal chromosome 16, and finally develops into an embryo carrying a paternal UPD of chromosome 16.

Incomplete trisomic rescue or monosomic rescue can result in chimeric cell lines, some of which have residual chromosomal trisomies or monosomes, leading to pathogenicity. In this case, we ruled out trisomic or monosomic chimerism by two karyotypic analyses with prenatal amniocentesis and peripheral blood taken from the newborn. At present, only UPD on chromosomes 6, 7, 11, 14, 15, and 20 clearly causes clinical symptoms, and no clearly pathogenic imprinted genes have been identified on chromosome 16. Related cases have reported that chromosome 16 contains 2 clear maternally imprinted genes: *ZNF597* and *NAA60* (17, 18), and genes with possible imprinting effects include *SALL*, *C16orf57/USB1*, *ACD*, and *FOXF1*; therefore, paternally derived chromosome 16 uniparental diploidy may be pathogenic (19–22). None of the above six genes was found to be clearly related to the occurrence of diseases. This case also proves that there is no pathogenic maternally imprinted gene on chromosome 16, and WES analysis showed no meaningful gene mutations, which is consistent with the currently observed phenotype. Of course, this conclusion will need to be supported by additional clinical evidence.

Most cases of UPD (16) are of maternal origin, and the available reports of paternal UPD (16) are all complete isodimers. Our report suggests that regional isodimers merging with regional heterodimers can also exist. In the process of sperm formation, errors may also occur during the meiotic phase. The follow-up of this case, with a normal neonatal phenotype, demonstrates the absence of maternally imprinted pathogenic genes on chromosome 16, at least not maternally imprinted pathogenic genes that affect intrauterine fetal development or cause early infant morbidity. In addition, compared with complete isodysomy, homozygous regions of isodysomy combined with heterodysomy are relatively less likely to result in recessive genetic diseases. Clinically, in cases of prenatal diagnosis or postnatal detection of paternal UPD16, the pathogenicity of the UPD itself may not be prioritized, but the fetus/affected child should be recommended for WES analysis to look for genetic mutations. This case may provide some guidance for eugenics on the male side.

DATA AVAILABILITY STATEMENT

The raw data supporting the conclusions of this article will be made available by the authors, without undue reservation.

ETHICS STATEMENT

The studies involving human participants were approved by the Ethics Committee of the Second Affiliated Hospital of Chongqing Medical University (Approval number: 2021(651)-1.0). Written informed consent was obtained from the minor(s)' legal guardian/next of kin for the publication of any potentially identifiable images or data included in this article.

AUTHOR CONTRIBUTIONS

XP carried out study design. YL and LL performed the experiments. XZ wrote the paper. All authors read and approved the final manuscript.

ACKNOWLEDGMENTS

We are grateful for the participation of the family in this study.

REFERENCES

1. Engel E. [A new genetic concept: the uniparental disomy and its potential effect, the isodisomy (author's transl)]. *J De Genetique Humaine.* (1980) 28:11.
2. Liehr T. Cytogenetic contribution to uniparental disomy (UPD). *Mol Cytogenet.* (2010) 3:8. doi: 10.1186/1755-8166-3-8
3. Nakka P, Pattillo Smith S, O'Donnell-Luria AH, McManus KF. Characterization of prevalence and health consequences of uniparental disomy in four million individuals from the general population. *Am J Hum Genet.* (2019) 105:921–32. doi: 10.1101/540955
4. Kotzot D, Utermann G. Uniparental disomy (UPD) other than 15: phenotypes and bibliography updated. *Am J Med Genet A.* (2005) 136:287–305. doi: 10.1002/ajmg.a.30483
5. Kohlhase J, Janssen B, Weidenauer K, Harms K, Bartels I. First confirmed case with paternal uniparental disomy of chromosome 16. *Am J Med Genet.* (2000) 91:190–1. doi: 10.1002/(SICI)1096-8628(20000320)91:3<190::AIDAJMG6>3.0.CO;2-I
6. Donovan FX, Kimble DC, Kim Y, Lach FP, Harper U, Kamat A, et al. Paternal or maternal uniparental disomy of chromosome 16 resulting in homozygosity of a mutant allele causes fanconi anemia. *Hum Mutat.* (2016) 37:465–8. doi: 10.1002/humu.22962
7. Del Gaudio D, Shinawi M, Astbury C, Tayeh MK, Deak KL, Raca G, et al. Diagnostic testing for uniparental disomy: a points to consider statement from the American College of Medical Genetics and Genomics (ACMG). *Genet Med.* (2020) 22:1133–41. doi: 10.1038/s41436-020-0782-9
8. Lau TK, Cheung SW, Lo PS, Pursley AN, Chan MK, Jiang F, et al. Non-invasive prenatal testing for fetal chromosomal abnormalities by low-coverage whole-genome sequencing of maternal plasma DNA: review of 1982 consecutive cases in a single center. *Ultrasound Obstet Gynecol.* (2014) 43:254–64. doi: 10.1002/uog.13277
9. Usui H, Nakabayashi K, Kaku H, Maehara K, Hata K, Shozu M. Elucidation of the developmental mechanism of ovarian mature cystic teratomas using B allele-frequency plots of single nucleotide polymorphism array data. *Genes Chromosomes Cancer.* (2018) 57:409–19. doi: 10.1002/gcc.1
10. Pauta M, Grande M, Rodriguez-Revenga L, Kolomietz E, Borrell A. Added value of chromosomal microarray analysis over karyotyping in early pregnancy loss: systematic review and meta-analysis. *Ultrasound Obstet Gynecol.* (2018) 51:453–62. doi: 10.1002/uog.18929
11. Shen Q, Lee K, Han SK, Ahn HJ, Kim S, Lee JH. Variants at potential loci associated with Sjogren's syndrome in Koreans: a genetic association study. *Clin Immunol.* (2019) 207:79–86. doi: 10.1016/j.clim.2019.07.010
12. Wei X, Ju X, Yi X, Zhu Q, Qu N, Liu T, et al. Identification of sequence variants in genetic disease-causing genes using targeted next-generation sequencing. *PLoS ONE.* (2011) 6:e29500. doi: 10.1371/journal.pone.0029500
13. Li H, Durbin R. Fast and accurate short read alignment with Burrows-Wheeler transform. *Bioinformatics.* (2009) 25:1754–60. doi: 10.1093/bioinformatics/btp324

14. McKenna A, Hanna M, Banks E, Sivachenko A, Cibulskis K, Kernytsky A, et al. The Genome Analysis Toolkit: a MapReduce framework for analyzing next-generation DNA sequencing data. *Genome Res.* (2010) 20:1297–303. doi: 10.1101/gr.107524.110
15. San Lucas FA, Wang G, Scheet P, Peng B. Integrated annotation and analysis of genetic variants from next-generation sequencing studies with variant tools. *Bioinformatics.* (2012) 28:421–2. doi: 10.1093/bioinformatics/btr667
16. Richards S, Aziz N, Bale S, Bick D, Das S, Gastier-Foster J, et al. Standards and guidelines for the interpretation of sequence variants: a joint consensus recommendation of the American College of Medical Genetics and Genomics and the Association for Molecular Pathology. *Genet Med*. (2015) 17:405–24. doi: 10.1038/gim.2015.30
17. Yamazawa K, Inoue T, Sakemi Y, Nakashima T, Yamashita H, Khono K, et al. Loss of imprinting of the human-specific imprinted gene ZNF597 causes prenatal growth retardation and dysmorphic features: implications for phenotypic overlap with Silver-Russell syndrome. *J Med Genet.* (2021) 58:427–32. doi: 10.1136/jmedgenet-2020-107019
18. Van Damme P, Hole K, Pimenta-Marques A, Helsens K, Vandekerckhove J, Martinho RG, et al. NatF contributes to an evolutionary shift in protein N-terminal acetylation and is important for normal chromosome segregation. *PLoS Genet.* (2011) 7:e1002169. doi: 10.1371/journal.pgen.1002169
19. Webb BD, Metikala S, Wheeler PG, Sherpa MD, Houten SM, Horb ME, et al. Heterozygous pathogenic variant in DACT1 causes an autosomal-dominant syndrome with features overlapping townes-brocks syndrome. *Hum Mutat.* (2017) 38:373–377. doi: 10.1002/humu.23171
20. Wang LL, Gannavarapu A, Clericuzio CL, Erickson RP, Irvine AD, Plon SE. Absence of RECQL4 mutations in poikiloderma with neutropenia in Navajo and non-Navajo patients. *Am J Med Genet A*. (2003) 118A:299–301. doi: 10.1002/ajmg.a.10057
21. Kocak H, Ballew BJ, Bisht K, Eggebeen R, Hicks BD, Suman S, et al. Hoyeraal-Hreidarsson syndrome caused by a germline mutation in the TEL patch of the telomere protein TPP1. *Genes Dev*. (2014) 28:2090–102. doi: 10.1101/gad.248567.114
22. Boggs S, Harris MC, Hoffman DJ, Goel R, McDonald-McGinn D, Langston C, et al. Misalignment of pulmonary veins with alveolar capillary dysplasia: affected siblings and variable phenotypic expression. *J Pediatr.* (1994) 124:125–8. doi: 10.1016/S0022-3476(94)70267-5

Conflict of Interest: The authors declare that the research was conducted in the absence of any commercial or financial relationships that could be construed as a potential conflict of interest.

Publisher's Note: All claims expressed in this article are solely those of the authors and do not necessarily represent those of their affiliated organizations, or those of the publisher, the editors and the reviewers. Any product that may be evaluated in this article, or claim that may be made by its manufacturer, is not guaranteed or endorsed by the publisher.

Copyright © 2021 Zhang, Liu, Liu and Pan. This is an open-access article distributed under the terms of the Creative Commons Attribution License (CC BY). The use, distribution or reproduction in other forums is permitted, provided the original author(s) and the copyright owner(s) are credited and that the original publication in this journal is cited, in accordance with accepted academic practice. No use, distribution or reproduction is permitted which does not comply with these terms.

frontiers in Pediatrics

CASE REPORT
published: 27 October 2021
doi: 10.3389/fped.2021.725868

Case Report: The JAK-Inhibitor Ruxolitinib Use in Aicardi-Goutieres Syndrome Due to *ADAR1* Mutation

Marco Cattalini[1,2*†], *Jessica Galli*[2,3†], *Fiammetta Zunica*[2], *Rosalba Monica Ferraro*[4,5], *Marialuisa Carpanelli*[6], *Simona Orcesi*[7,8], *Giovanni Palumbo*[9,10], *Lorenzo Pinelli*[11], *Silvia Giliani*[4,5], *Elisa Fazzi*[2,3‡] *and Raffaele Badolato*[1,2‡]

[1] Pediatrics Clinic, Azienda Socio Sanitaria Territoriale Spedali Civili di Brescia, Brescia, Italy, [2] Department of Experimental and Clinical Sciences, University of Brescia, Brescia, Italy, [3] Child Neurology and Psychiatry Unit, Azienda Socio Sanitaria Territoriale Spedali Civili di Brescia, Brescia, Italy, [4] "Angelo Nocivelli" Institute for Molecular Medicine, Azienda Socio Sanitaria Territoriale Spedali Civili, Brescia, Italy, [5] Department of Molecular and Translational Medicine, University of Brescia, Brescia, Italy, [6] Child Neurology and Psichiatry Unit, Azienda Socio Sanitaria Territoriale Valtellina e Alto Lario, Sondrio, Italy, [7] Child Neurology and Psychiatry Unit, Istituto di Ricovero e Cura a Carattere Scientifico Mondino Foundation, Pavia, Italy, [8] Department of Brain and Behavioral Sciences, University of Pavia, Pavia, Italy, [9] Radiology Unit Department of Medical and Surgical Specialties, Radiological Sciences, and Public Health, University of Brescia, Brescia, Italy, [10] Radiology Unit, Azienda Socio Sanitaria Territoriale Spedali Civili di Brescia, Brescia, Italy, [11] Neuroradiology Unit, Azienda Socio Sanitaria Territoriale Spedali Civili di Brescia, Brescia, Italy

Type I Interferonopathies comprise inherited inflammatory diseases associated with perturbation of the type I IFN response. Use of *Janus* kinase (JAK) inhibitors has been recently reported as possible tools for treating some of those rare diseases. We describe herein the clinical picture and treatment response to the JAK-inhibitor ruxolitinib in a 5-year-old girl affected by Aicardi-Goutières Syndrome type 6 (AGS6) due to *ADAR1* mutation. The girl's interferon score (IS) was compared with that of her older brother, suffering from the same disorder, who was not treated. We observed a limited, but distinct neurological improvement (Gross Motor Function and Griffiths Mental Development Scales). Analysis of IS values of the two siblings during the treatment showed several changes, especially related to infections; the IS values of the child treated with ruxolitinib were consistently lower than those measured in her brother. Based on these observations we suggest that the use of ruxolitinib in children with the same condition might be effective in inhibiting type I interferon response and that starting this therapy at early age in children with AGS could mitigate the detrimental effects of type I interferon hyperproduction.

Keywords: interferonopathies, JAK-inhibitor, Aicardi-Goutières syndrome, ruxolitinib, type I interferon

OPEN ACCESS

Edited by:
Jean-Pierre Sao-Ming Lin, Guy's and St Thomas' NHS Foundation Trust, United Kingdom

Reviewed by:
Bruria Ben-Zeev, Sheba Medical Center, Israel
Giuseppe Battaglia, University of Palermo, Italy

***Correspondence:**
Marco Cattalini
marco.cattalini@unibs.it

†These authors have contributed equally to this work

‡These authors share senior authorship

Specialty section:
This article was submitted to Pediatric Neurology, a section of the journal Frontiers in Pediatrics

Received: *12 July 2021*
Accepted: *22 September 2021*
Published: *27 October 2021*

Citation:
Cattalini M, Galli J, Zunica F, Ferraro RM, Carpanelli M, Orcesi S, Palumbo G, Pinelli L, Giliani S, Fazzi E and Badolato R (2021) Case Report: The JAK-Inhibitor Ruxolitinib Use in Aicardi-Goutieres Syndrome Due to ADAR1 Mutation. Front. Pediatr. 9:725868. doi: 10.3389/fped.2021.725868

INTRODUCTION

Type I interferonopathies constitute a recently identified group of Mendelian autoinflammatory diseases characterized by an aberrant and uncontrolled activation of the IFN-alpha pathway leading to multisystemic involvement in the first years of life (1). In physiological conditions, the activation of type I IFN pathway is strictly dependent on interferon binding to IFNAR receptor, which is expressed on all the nucleated cells; this results in the activation of the membrane receptor-associated *Janus* kinases (JAKs) TYK2 and JAK1. Activated JAKs phosphorylate the signal transducer and activator of transcription (STAT) proteins which, in turn, induce transcription

of interferon stimulated genes (ISGs) (2, 3). The evaluation of interferon activity by quantitative analysis of ISGs transcription, through the so-called interferon signature, has recently been used in clinical practice and therapeutic trials in children with AGS and other interferonopathies, although its capacity to finely intercept disease activity has still to be clearly determined (4).

Aicardi-Goutières Syndrome (AGS) is a rare subacute monogenic encephalopathy which represents the prototype of type I interferonopathies (5). To date, mutations in 9 genes (TREX1, RNASEH2A, RNASEH2B, RNASEH2C, SAMHD1, ADAR, IFIH1, PNPT1, MDA5, LSM11, and RNU7-1) have been associated with the disease. Between them *ADAR*, which encodes for the RNA editing enzyme ADAR1, which destabilizes the double-stranded RNA by hydrolytic deamination of adenosine to inosine (6). Although AGS clinical picture is heterogeneous in terms of severity of the neurological involvement and for the extent of extra neurological manifestations, neuroimaging findings in subjects with AGS are typical and constitute a useful tool for the diagnostic work-up and follow-up monitoring (6–9). To date, no definite treatment is available to prevent progressive encephalopathy resulting in neurological damage. Therefore, the management of children with AGS can only be based on supportive measures for limiting late sequelae. Recent studies showed that the use of JAK-inhibitors could be effective for controlling the disease in children with AGS (10–14).

CASE PRESENTATION

We report the case of a 5-year-old girl born to unrelated parents who had been identified in the prenatal period as a carrier of compound heterozygous mutations in *ADAR1*: p.P193A (c.577C>G) and p.LYS359Argfs*S14 (c.1076_1080 del). The same genotype was originally observed in the older brother who was born 6 years before from an uneventful pregnancy and delivery (*see* **Figure 1A**). The boy was well-until 7 months of age when he started to suffer from irritability, dystonic movements, and progressive loss of psychomotor skills that lead to the final picture of spastic-dystonic tetraparesis within few months. Extensive workup showed basal ganglia calcifications on CT scan and brain MRI. Genetic analysis lead to the final diagnosis of AGS. The boy was regularly followed at our Units since then. At last evaluation before treatment with ruxolitinib was started in his sister, the boy was suffering from severe neurological involvement (spastic-dystonic tetraparesis, severe intellectual disability, enteral feeding) and his last available MRI confirmed the basal ganglia calcifications and showed cortical-subcortical atrophy and leukodystrophy. The girl had no symptoms of disease in the early years of life and showed adequate psychomotor development. Analysis of IFN signature, performed at birth, showed high values, which spontaneously returned to normal in the second year of life. Neuroimaging study of the child at that age by MRI was also normal (**Figure 1A**). When the girl reached 3 years of age, she presented with symptoms related to mild recurrent upper respiratory tract infections. Thereafter, her neurological conditions began to deteriorate with the appearance of asthenia, irritability, disturbed sleep-wake patterns, and signs of extrapyramidal involvement (see below for details). Brain MRI showed bilateral symmetrical signal abnormality of the striatum, with volume loss of both putamina (**Figure 1B**), suggesting bilateral striatal necrosis (BSN), a typical although not a pathognomonic finding of AGS6. Additionally, brain CT showed an isolated calcification in the left anterior periventricular white matter, and evaluation of IS was suggestive of increased type I activity (IS 2.88 with normal values 0–2.22). Because these features are usually observed when AGS subjects develop encephalopathy, we started infection prophylaxis with Immunoglobulins i.v. (1 g/kg/4 weeks) and corticosteroids (prednisone 2 mg/kg for a week followed by weaning over 1 month). Re-evaluation of the child at 40 months of age, failed to demonstrate clinical signs of improvement and on MRI there was a slight increase of the signal abnormality in both striatal nuclei (**Figure 1C**), which prompted us to taper prednisone and start treatment with a JAK-inhibitor, in an attempt to prevent disease progression.

Ruxolitinib was started at 2.5 mg twice daily; 10 weeks later the dose was increased to 5 mg BID. The child underwent a neurological examination before starting any treatment (at 37 and 38 months of age), 1 month after starting i.v. immunoglobulins (39 months) and after 1 (41 months), 2, 4, 6, 18, and 24 months from the start of ruxolitinib treatment. The motor function and the developmental profile were videotaped and assessed by a physician blinded to treatment, using the Gross Motor Function Measure (GMFM)-88 at the same timepoints and the Griffiths Mental Development Scales-Extended Revised (GMDS-ER) at baseline (38 months) and after 9 and 18 months from the beginning of ruxolitinib. Quantification of IS was also performed before and during treatment and compared with the IS values measured in her older brother on the same occasions.

The neurological examination of the girl before treatment showed signs of extrapyramidal involvement: "tonus changing" pattern, dystonic posturing of the left hand, and fingers associated with difficulties in manual ability, asymmetrically impaired gait characterized by excessive internal rotation of right side of the body, bradykinesia, difficulty maintaining balance, and increased gait velocity. Spontaneous speech was severely impaired, making verbal communication slower and less accurate, which was associated with a deficit of verbal fluency and naming. GMDS-ER and GMFM-88 scores are reported in **Tables 1**, **2**.

A mild but significant improvement of the neurological picture was evident, especially after 18 months of follow-up, with

Abbreviations: ADAR, adenosine deaminase acting on RNA; AGS, aicardi-goutières syndrome; BID, Twice a day; CNS, central nervous system; CT, computed tomography; GMDS-ER, griffiths mental development scales-extended revised; GMFM-88, gross motor function measure-88; HIB, hemophilus influenzae type B; HPIV-1, human parainfluenza virus-1; IFIH1, interferon induced with helicase C domain 1; IFN, interferon; IFNAR, Type 1 interferon receptor; IS, interferon score; ISGs, interferon stimulated genes; JAK, janus kinase; LSM11, LSM11, U7 small nuclear RNA associated; MRI, magnetic risonance imaging; MRSA, methicillin-resistant *Staphylococcus aureus*; RNASEH2 (A-B-C), ribonuclease H2 subunit A-B-C; RNU7-1, RNA, U7 Small Nuclear 1; SAMHD1, SAM And HD Domain Containing Triphosphate Triphosphohydrolase 1; STAT1, Signal Transducer And Activator of transcription 1; TREX1, three prime repair exonuclease 1; TYK2, tyrosine kinase 2.

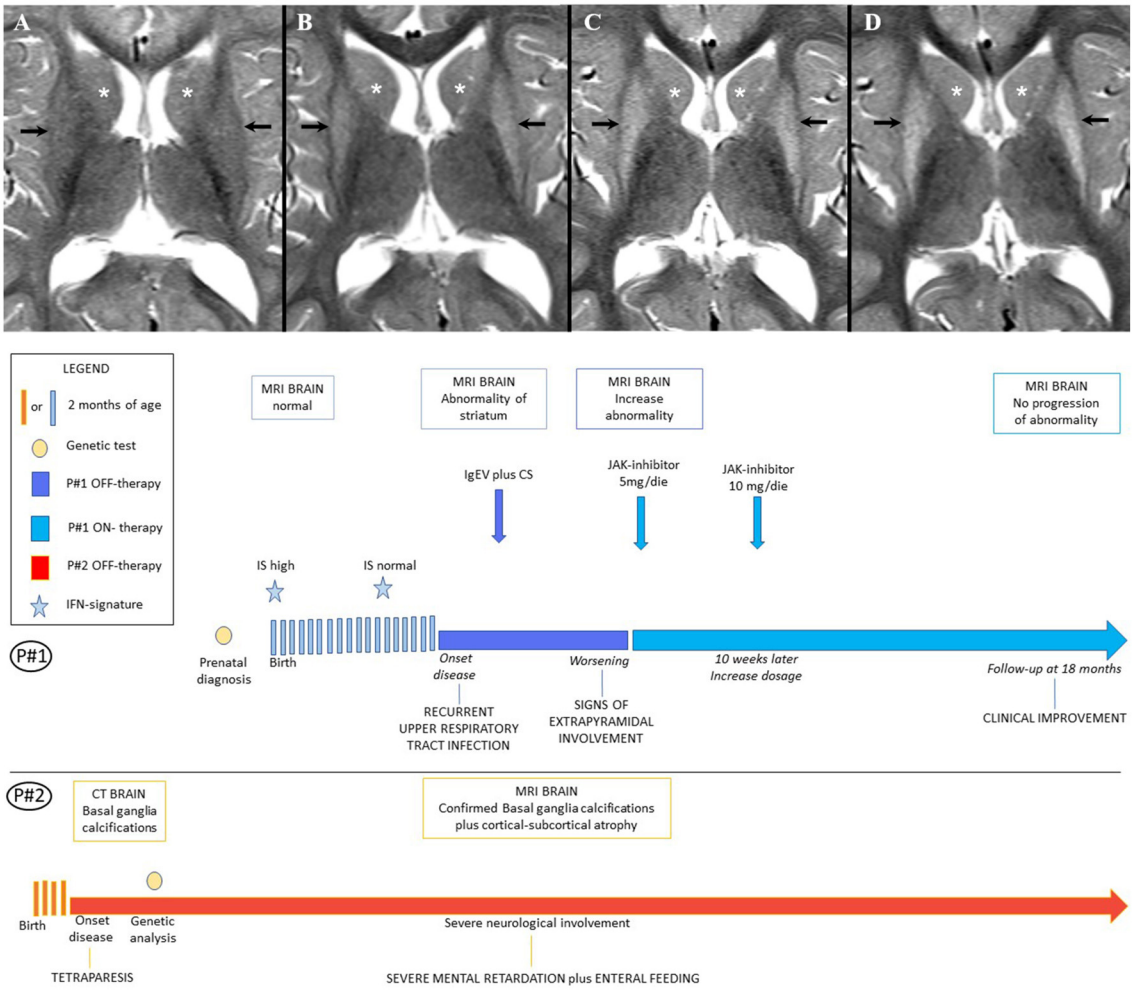

FIGURE 1 | (A) Patients' Timeline. **(B)** Brain MRI. Brain MRI, axial T2-weighted image at the age of 18 months **(A)**, 36 months **(B)**, 40 months **(C)**, 5 years **(D)**. Putamen (black arrow) and head of caudate nucleus (white asterisk), show normal signal at 18 months **(A)**; follow-up MRIs **(B,C)** show progressively increasing diffuse hyperintensity in both gray matter nuclei with volume loss of the putamina, consistent with bilateral striatal necrosis; after 18 months of therapy with Ruxolitinib the MRI **(D)** showed no progression of the basal ganglia abnormality.

a reduction of bradykinesia, better fine motor skills and balance competencies, and vocabulary expansion, even if the dystonic posturing, asymmetrical gait, and verbal fluency deficit persisted. The GMFM-88 evaluation showed a progressive increase in the global score (from 68 to 82%) and all the subscales at every timepoint, as summarized in **Table 1**. Moreover, GMDS-ER documented increased scores in language (from 34th to 43th percentile), performance (from 3rd to 41rd percentile), and practical reasoning (from 8th to 58th percentile) subscales at 18 months/follow-up.

The IS values were fluctuating between 36.24 and 69.30 (notably the IS was performed by a different lab than previously, with the normal cohort range between 0 and 4.67). At her last follow-up visit, evaluation of IS showed lower values when compared with measurements performed before starting ruxolitinib treatment (see **Figure 2**). In addition, when comparing the IS of the girl with her brother's IS we found that her values were consistently lower. In particular, the child treated with ruxolitinib presented a mild increase of IFN score during infections, while her brother (off-therapy) had significant increments of IS ranging from 53.02 up to 851.45. The peak values of IS in both subjects were observed during an episode of *Pseudomonas aeruginosa* infection, which occurred ∼9 months after starting treatment with ruxolitinib. During a pulmonary infectious episode by a Methicillin Resistant *Staphylococcus aureus* (MRSA) and *Haemophilus influenzae type B* which affected both patients, we observed that IS remained unchanged in the treated child, whereas the IS value increased in her brother. Moreover, when the two siblings were free of infections, we detected consistently lower levels of IS in the ruxolitinib-treated child than in her brother. Neuroimaging assessment after 18 months of ruxolitinib therapy by MRI showed no change of the signal intensity abnormality in the basal ganglia (**Figures 1A,D**).

TABLE 1 | Gross motor function measure-88 from the treated patient.

Chronological age (months)	37	38	39	41	42	44	47	58	64
GMFM-88 domain									
Lying & rolling (%)	84	92	94	94	94	94	96	96	96
Sitting (%)	92	87	88	93	96	97	97	97	97
Crawling & kneeling (%)	67	62	71	69	74	83	83	86	86
Standing (%)	74	56	72	72	72	64	69	72	72
Walking, running, & jumping (%)	40	43	49	49	49	48	50	53	57
Total score (%)	71	68	75	75	77	77	79	81	82

TABLE 2 | Griffiths mental development scales-extended revise from the treated patient.

Chronological age (months)	38	47	58
GMDS-Er subscale			
Locomotor (percentile)	<1/	<1	<1
Personal-Social (percentile)	42	9	30
Hearing and speech (percentile)	34	76	43
Eye and hand coordination (percentile)	5	10	2
Performance (percentile)	3	57	41
Practical reasoning (percentile)	8	40	58
Total score (percentile)	2	6	4

DISCUSSION

Aicardi-Goutières Syndrome is a disorder of the aberrant activation of the immune system, in particular of IFN-alpha pathway. Over the years, some features of the disease have been clarified: the disease is characterized by a first subacute phase, were children affected show the neurological deterioration, followed by a more chronic course. Although the majority of patients with AGS demonstrate the disease onset in the first months of life, there is extreme variability in age at onset and severity of the clinical picture. Also, a wide intrafamilial variability has been observed. These observations suggest that treatment in the early stages could result in the mitigation of inflammation associated with tissue damage and therefore mitigate the sequelae. Defining a standardized treatment is difficult, also for the small number of patients and the clinical heterogeneity. Empirical therapy with immunosuppressor drugs (corticosteroids, azathioprine, IVIG) has been attempted in the past, without clear evidence of benefits.

A better understanding of the pathogenesis of AGS, with the focus on type I interferon production, suggested new therapeutic strategies based on the use of JAK-inhibitors. Indeed, promising results came from the use of JAK-inhibitors in various interferonopathies. Beneficial effects are reported after JAK-inhibitor therapy in patients with other distinct interferonopathies such as SAVI, USP18, CANDLE (14–17). There is also mounting evidence on the possible beneficial effect of JAK-inhibitors in subjects with AGS, as reported in a large cohort published by Vanderver et al. which included 35 AGS subjects, −7 with AGS6–treated with baricitinib, analyzing the response to treatment with interferon signaling gene-expression score (18). Ruxolitinib has also been shown to be effective in the treatment of lesions in patients with FCL mutated in TREX1 and on systemic inflammation in patients with IFIH1 mutations (13). Also, two AGS2 patients with a severe developmental delay with unspecified age of onset, both treated with ruxolitinib 0.2 mg/kg/day, increased after 7 days−0.5 mg/kg/day starting from the age of 23 months, showed an improvement in psychomotor retardation with a reduction in dystonic movements and Interferon Score (19). In addition, a patient with AGS7 at 32 months of age, without response to therapy with IVIG and corticosteroids, started ruxolitinib 5 mg/2 vv/day with clinical improvement, recovery of neuromotor skills, increase in neuropsychiatric function scales and improvement of neuroradiological findings (12).

These positive effects are less striking compared to other type I interferonopathies, probably because the clinical picture is dominated by severe CNS damage, which is peculiar to AGS and is almost irreversible. Nonetheless, our patient showed mild signs of improvement of her neurological picture since the start of ruxolitinib. We acknowledge that firm conclusions could not be reached from a single case report, and that other factors may have contributed to the clinical improvement of our patient. AGS is a two-phase disease, with the first encephalitic phase where the neurological damage occurs and a second chronic phase. Disease severity is very variable, even in patients carrying the same mutations. It is possible, however unlikely, that our treated patient reached the "stable" phase of the disease just at the same time the treatment was started, with an overall better clinical picture than her brother. It is also important to underline that the motor skills improvement observed in the treated patient may be due to the time-lapse of observation, as it is expected that motor skills improve with age. Nonetheless, it is striking to note that all the data from the patient before treatment were consistent with active disease with worsening clinical picture, while treatment start was followed by mild improvement in the clinical picture, reduction in the IS, and stabilization of MRI findings.

As interferon signature reproducibility is sub-optimal and the test may be influenced by a concomitant infection, and given the unique family history of two AGS siblings who shared the same *ADAR* genotype and environmental milieau, we decided to compare IS values between the child receiving ruxolitinib and her brother, who had advanced AGS-associated encephalopathy and did not receive any specific treatment. IS levels were fluctuating during observations, the higher levels being during infections, but the girl's IS levels were always lower than those measured in her brother who had the same infections. This observation is consistent with the induction of type I interferon during infections and with the biologic activity of JAK inhibitors. Although the better clinical evolution of the treated patient, compared to her brother, may be due to many factors -as already discussed- we suggest that the use of JAK-inhibitors may influence the clinical evolution of AGS patients by downregulation of the type I interferon response and that our case report seems to confirm a possible efficacy of ruxolitinib in

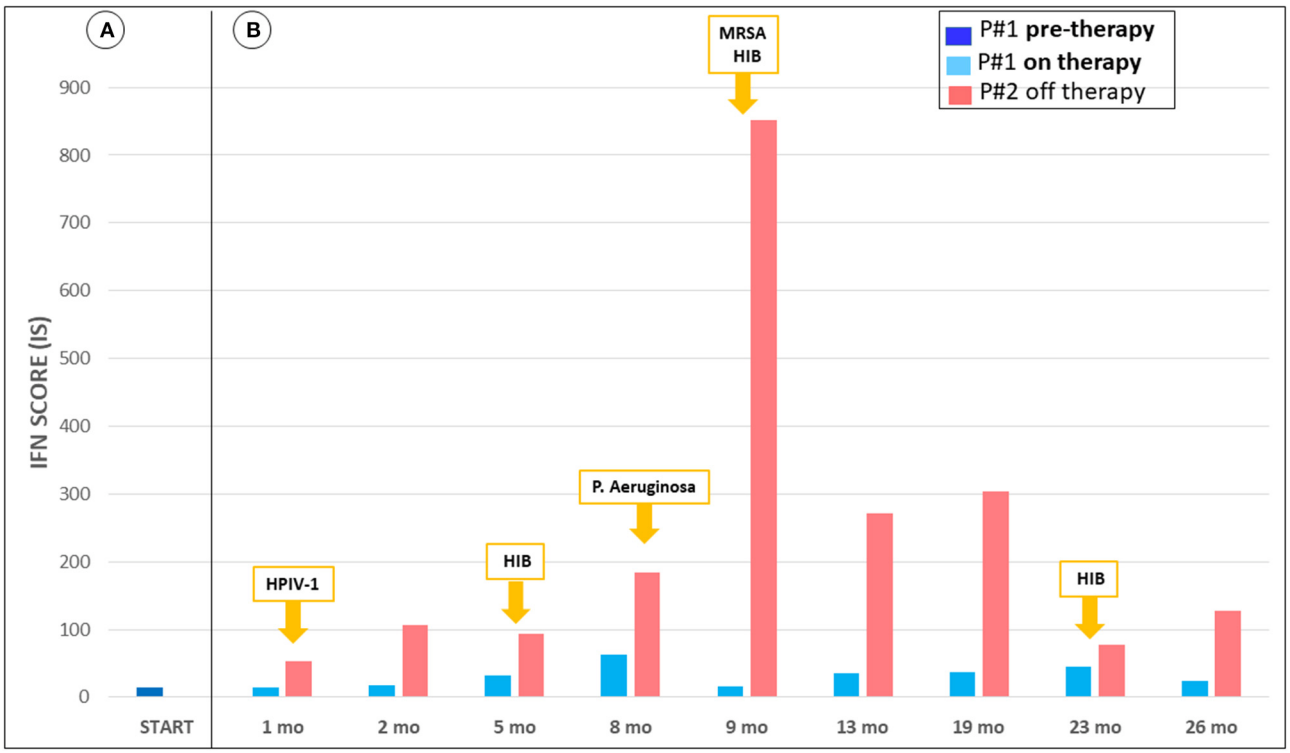

FIGURE 2 | Trend of interferon-signaling gene expression score from June 2018 to August 2020. **(A)** IFN score P#1 pre-therapy, not available measurement of P#2. **(B)** IFN score during treatment of P#1, in parallel with P#2, and report of simultaneous respiratory infections. P#1 shows mild increment of IFN score during infections, while P#2 presents significant increments. Also, during infection free periods, there is discrepancy of the values. The interferon score was calculated as the median fold changes of expression of a panel of interferon-stimulated genes (ISGs: IFI27, IFI44L, IFIT1, RSAD2, ISG15, and SIGLEC1). The gene expression was analyzed by quantitative reverse transcription polymerase chain reaction (qPCR) using 18s as gene housekeeping to normalize the results. Relative quantification (RQ) was calculated with the formula $2^{-\Delta\Delta Ct}$, using as calibrator a pool of 17 healthy controls. The mean interferon score of the healthy donors plus two standard deviations above the mean was calculated. Scores higher than this value (4.67) were designated as positive.

AGS6. The early use of these drugs, before neurological damage occurs, could also give insights for a better understanding of their possible efficacy on this severe disease.

DATA AVAILABILITY STATEMENT

The raw data supporting the conclusions of this article will be made available by the authors, without undue reservation.

ETHICS STATEMENT

The studies involving human participants were reviewed and approved by Ethics Committee of Brescia ASST Spedali Civili Brescia Piazzale Spedali Civili, 1 25123 Brescia (BS). Written informed consent to participate in this study was provided by the participants' legal guardian/next of kin. Written informed consent was obtained from the individual(s), and minor(s)' legal guardian/next of kin, for the publication of any potentially identifiable images or data included in this article.

AUTHOR CONTRIBUTIONS

All authors listed have made a substantial, direct and intellectual contribution to the work, and approved it for publication.

FUNDING

RB received partial funding from Italian Ministry of Health (Grant RF-2016-02362384). EF and SO received funding from the NIH Project Clinical Outcomes in Aicardi Goutières Syndrome (01NS106845-01A1).

ACKNOWLEDGMENTS

The Authors would like to thank Prof. Yanick Crow, University of Edinburgh for running the genetic analysis and the first interferon signatures on the patient and her brother and for many fruitful discussions on the patient picture. Many thanks also to Chiara Fumagalli, from Neuroradiology Unit, ASST Lecco, for providing the first MRI of the patient.

REFERENCES

1. Crow YJ, Manel N. Aicardi-Goutières syndrome and the type I interferonopathies. *Nat Rev Immunol.* (2015) 15:429–40. doi: 10.1038/nri3850
2. Crow YJ. Type I interferonopathies: a novel set of inborn errors of immunity. *Ann N Y Acad Sci.* (2011) 1238:91–8. doi: 10.1111/j.1749-6632.2011.06220.x
3. Rodero MP, Decalf J, Bondet V, Hunt D, Rice GI, Werneke S, et al. Detection of interferon alpha protein reveals differential levels and cellular sources in disease. *J Exp Med.* (2017) 214:1547–55. doi: 10.1084/jem.20161451
4. Rice GI, Forte GM, Szynkiewicz M, Chase DS, Aeby A, Abdel-Hamid MS, et al. Assessment of interferon-related biomarkers in Aicardi-Goutières syndrome associated with mutations in TREX1, RNASEH2A, RNASEH2B, RNASEH2C, SAMHD1, and ADAR: a case-control study. *Lancet Neurol.* (2013) 12:1159–69. doi: 10.1016/S1474-4422(13)70258-8
5. Harapas CR, Steiner A, Davidson S, Masters SL. An update on autoinflammatory diseases: inflammasomopathies. *Curr Rheumatol Rep.* (2018) 20:40. doi: 10.1007/s11926-018-0750-4
6. Uggenti C, Lepelley A, Depp M, Badrock AP, Rodero MP, El-Daher MT, et al. cGAS-mediated induction of type I interferon due to inborn errors of histone pre-mRNA processing. *Nat Genet.* (2020) 52:1364–72. doi: 10.1038/s41588-020-00737-3
7. Fazzi E, Cattalini M, Orcesi S, Tincani A, Andreoli L, Balottin U, et al. Aicardi-Goutieres syndrome, a rare neurological disease in children: a new autoimmune disorder? *Autoimmun Rev.* (2013) 12:506–9. doi: 10.1016/j.autrev.2012.08.012
8. Cattalini M, Galli J, Andreoli L, Olivieri I, Ariaudo G, Fredi M, et al. Exploring autoimmunity in a cohort of children with genetically confirmed aicardi-goutières syndrome. *J Clin Immunol.* (2016) 36:693–9. doi: 10.1007/s10875-016-0325-y
9. Crow YJ, Chase DS, Lowenstein Schmidt J, Szynkiewicz M, Forte GM, Gornall HL, et al. Characterization of human disease phenotypes associated with mutations in TREX1, RNASEH2A, RNASEH2B, RNASEH2C, SAMHD1, ADAR, and IFIH1. *Am J Med Genet A.* (2015) 167A:296–312. doi: 10.1055/s-0036-1592307
10. Sanchez GAM, Reinhardt A, Ramsey S, Wittkowski H, Hashkes P, Berkun J, et al. JAK1/2 inhibition with baricitinib in the treatment of autoinflammatory interferonopathies. *J Clin Invest.* (2018) 128:3041–52. doi: 10.1172/JCI98814
11. Tonduti D, Fazzi E, Badolato R, Orcesi S. Novel and emerging treatments for Aicardi-Goutières syndrome. *Expert Rev Clin Immunol.* (2020) 16:189–98. doi: 10.1080/1744666X.2019.1707663
12. Kothur K, Bandodkar S, Chu S, Wienholt L, Johnson A, Barclay P, et al. An open-label trial of JAK 1/2 blockade in progressive IFIH1-associated neuroinflammation. *Neurology.* (2018) 90:289–91. doi: 10.1212/WNL.0000000000004921
13. Briand C, Frémond ML, Bessis D, Carbasse A, Rice GI, Bondet V, et al. Efficacy of JAK1/2 inhibition in the treatment of chilblain lupus due to TREX1 deficiency. *Ann Rheum Dis.* (2019) 78:431–3. doi: 10.1136/annrheumdis-2018-214037
14. Alsohime F, Martin-Fernandez M, Temsah MH, Alabdulhafid M, Le Voyer T, Alghamdi M, et al. JAK inhibitor therapy in a child with inherited USP18 Deficiency. *N Engl J Med.* (2020) 382:256–65. doi: 10.1056/NEJMoa1905633
15. Neven B, Al Adba B, Hully M, Desguerre I, Pressiat C, Boddaert N, et al. JAK inhibition in the Aicardi-Goutières Syndrome. *N Engl J Med.* (2020) 383:2190–1. doi: 10.1056/NEJMc2031081
16. Kerrigan SA, McInnes IB. JAK inhibitors in rheumatology: implications for paediatric syndromes? *Curr Rheumatol Rep.* (2018) 20:83. doi: 10.1007/s11926-018-0792-7
17. Fragoulis GE, McInnes IB, Siebert S. JAK-inhibitors. New players in the field of immune-mediated diseases, beyond rheumatoid arthritis. *Rheumatology.* (2019) 58:i43–54. doi: 10.1093/rheumatology/key276
18. Vanderver A, Adang L, Gavazzi F, McDonald K, Helman G, Frank DB, et al. Janus kinase inhibition in the aicardi-goutières syndrome. *N Engl J Med.* (2020) 383:986–9. doi: 10.1056/NEJMc2001362
19. Tüngler V, König N, Günther C, Engel K, Fiehn C, Smitka M, et al. Response to: "JAK inhibition in STING-associated interferonopathy" by Crow et al. *Ann Rheumat Dis.* (2016) 75:e76. doi: 10.1136/annrheumdis-2016-210565

Conflict of Interest: The authors declare that the research was conducted in the absence of any commercial or financial relationships that could be construed as a potential conflict of interest.

Publisher's Note: All claims expressed in this article are solely those of the authors and do not necessarily represent those of their affiliated organizations, or those of the publisher, the editors and the reviewers. Any product that may be evaluated in this article, or claim that may be made by its manufacturer, is not guaranteed or endorsed by the publisher.

Copyright © 2021 Cattalini, Galli, Zunica, Ferraro, Carpanelli, Orcesi, Palumbo, Pinelli, Giliani, Fazzi and Badolato. This is an open-access article distributed under the terms of the Creative Commons Attribution License (CC BY). The use, distribution or reproduction in other forums is permitted, provided the original author(s) and the copyright owner(s) are credited and that the original publication in this journal is cited, in accordance with accepted academic practice. No use, distribution or reproduction is permitted which does not comply with these terms.

frontiers in Neurology

ORIGINAL RESEARCH
published: 30 November 2021
doi: 10.3389/fneur.2021.754701

Electrophysiological Signature and the Prediction of Deep Brain Stimulation Withdrawal and Insertion Effects

Carlos Trenado[1], *Laura Cif*[2], *Nicole Pedroarena-Leal*[1] *and Diane Ruge*[1]*

[1] *Laboratoire de Recherche en Neurosciences Cliniques, LRENC, Montpellier, France,* [2] *Département de Neurochirurgie, Centre Hospitalier Universitaire de Montpellier, Montpellier, France*

Deep brain stimulation (DBS) serves as a treatment for neurological and psychiatric disorders, such as Parkinson's disease (PD), essential tremor, dystonia, Tourette Syndrome (GTS), Huntington's disease, and obsessive-compulsive disorder (OCD). There is broad experience with the short-term effects of DBS in individual diseases and their signs/symptoms. However, even in acute treatment and for the same disorder or a given disorder, a prediction of effect is not perfect. Even further, the factors that influence the long-term effect of DBS and its withdrawal are hardly characterized. In this work, we aim to shed light on an important topic, the question of "DBS dependency." To address this, we make use of the Kuramoto model of phase synchronization (oscillation feature) endowed with neuroplasticity to study the effects of DBS under successive withdrawals and renewals of neuromodulation as well as influence of treatment duration in *de novo* DBS "patients." The results of our simulation show that the characteristics of neuroplasticity have a profound effect on the stability and mutability of oscillation synchronization patterns across successive withdrawal and renewal of DBS in chronic "patients" and also in *de novo* DBS "patients" with varying duration of treatment (here referred to as the "number of iterations"). Importantly, the results demonstrate the strong effect of the individual neuroplasticity makeup on the behavior of synchrony of oscillatory activity that promotes certain disorder/disease states or symptoms. The effect of DBS-mediated neuromodulation and withdrawal is highly dependent on the makeup of the neuroplastic signature of a disorder or an individual.

Keywords: electrophysiological signature, deep brain stimulation, dependency, neuropsychiatric disease, neuromodulation

OPEN ACCESS

Edited by:
Jean-Pierre Sao-Ming Lin, Guy's and St Thomas' NHS Foundation Trust, United Kingdom

Reviewed by:
Angelo Lavano, University of Magna Graecia, Italy
Alice Bonuccelli, Pisana University Hospital, Italy

***Correspondence:**
Diane Ruge
diane.ruge@gmail.com

Specialty section:
This article was submitted to Pediatric Neurology, a section of the journal Frontiers in Neurology

Received: *06 August 2021*
Accepted: *18 October 2021*
Published: *30 November 2021*

Citation:
Trenado C, Cif L, Pedroarena-Leal N and Ruge D (2021) Electrophysiological Signature and the Prediction of Deep Brain Stimulation Withdrawal and Insertion Effects. Front. Neurol. 12:754701. doi: 10.3389/fneur.2021.754701

INTRODUCTION

Deep brain stimulation (DBS) is a neuromodulation technique that is effective as a treatment for severe neurological and psychiatric disorders (1–4). It has been suggested that it modulates cortico-striatal brain circuitry with an indirect effect on cognitive and behavioral abilities (5, 6). The overall efficacy of DBS for different pathologies, such as Parkinson's disease (PD) and dystonia, has been well-established for months and a number of years. The long-term effects remain overall effective on motor symptoms and mood (7, 8); they have, however, to be characterized further

in terms of variability in efficacy and clinical adverse features, such as stimulation-related side effects or stimulation-independent effects. To further the demographic and history of disease-related predictors, understanding of relevant prediction factors for short- and long-term effects of DBS is required. Long-term neuromodulation with deep brain stimulation reorganizes the brain, changes the inherent patterns of cortical excitability typical of a particular disorder or symptom, and causes different individual clinical responses of a patient upon withdrawal of the stimulation input. One meaningful marker for the clinical withdrawal effect seems to be neuroplasticity which is quantifiable with electrophysiological recordings (9–12). Importantly, in patients *in vivo* it would be impossible to characterize the complex multifactorial patterns of neuroplasticity in a specific state (e.g., "ON DBS," "OFF DBS," and "symptom status") the patient is in. The reasons for this are technical in nature. This explains the high value of a computational simulation as used here. It allows consideration of an input as a function of complex patterns, supposedly reflecting an electrophysiological signature of a patient.

A mechanism by which complex systems reach a specific state is synchronization of the lower-level elements that are organized into a functional unit (13). Synchronization has been referred to as the property of a non-linear system in which the dynamics of individual elements are correlated in time (14). Computational models have shown that synchronized spiking within small neural populations in cortical and hippocampal areas may be enhanced through Hebbian learning, which is characterized by long-term potentiation (LTP) if a presynaptic spike precedes a postsynaptic spike within a brief time window or by long-term depression (LTD) if the temporal order of spikes is reversed, a relationship described as *neurons that fire together wire together* (15–18). The invasive and non-invasive brain stimulation approaches allow a quantification of synaptic strength in the human nervous system, and manipulation of it has implications for the treatment of neurological and psychiatric disorders (19, 20). Exaggerated oscillatory neuronal synchronization relates to the cardinal symptoms of bradykinesia, rigidity, dystonia, and levodopa-induced dyskinesias. Excessive theta synchronization is a finding in dystonia, sensorimotor integration, and motor learning (21–25). Excessive beta oscillations have often been linked to specific Parkinson symptoms. It has been hypothesized that DBS is able to interrupt pathological synchronization (26).

At large-scale levels, for instance by considering electroencephalography (EEG) and magnetoencephalography (MEG) data, a valid index of synchronization is in-phase activation of neural elements in relation to cognition and pathology. In particular, alpha-beta phase synchronization has been reported to mediate the recruitment of visuospatial attention (27), while the role of selective attention in controlling phase oscillatory neural activity to efficiently process relevant information at pre-stimulus stages has been emphasized (28). In addition, frontotemporal theta phase-synchronization has been shown to underlie music-evoked pleasantness (29), while inter-brain phase synchronization has been proposed to be a marker of human social interaction (30). With regards to pathology, previous studies reported that deficits in EEG phase synchrony may underlie cognitive disturbances in schizophrenia (31) and that aberrant multi-frequency MEG phase temporal synchronization may be useful to predict conversion from mild cognitive impairment to Alzheimer's disease (AD) (32). Likewise, EEG phase synchrony has been helpful to prognosticate the outcomes in pediatric coma (33). Mean phase coupling of the motor brain regions has been shown to be abnormally enhanced in patients with PD and isolated dystonia (34, 35). In contrast, pianists with musician's dystonia exhibited deficient phase coupling between the neuronal assemblies required to inhibit motor memory traces (36). Increased EEG phase synchronization in all bands has been shown to be present in patients with Huntington's disease and to correlate with cognitive decline (37). The enhanced coupling or synchronization seems to be a feature of pathology, e.g., rigidity in PD or dystonic symptoms in dystonia. The desynchronization (or decoupling) on the other hand rather reflects "leaving of (also pathological) state," in line with Pfurtscheller's work (38), while synchronization in the oscillations has a physiological healthy function (e.g., idling states) and the lack of mutability (change between states) bears pathology. For clinicians who use DBS as a treatment, pressing questions are: "What happens with the patient when I start DBS, when I switch off DBS after a short treatment duration, after a long treatment duration, when it accidentally stops working"? And moreover, "Is the patient dependent on the DBS or is there a window in time where I can ultimately stop DBS and the patient reaches independence?"

In the present study, we made use of computational modeling using an established network's model of synchronization, Kuramoto's model, endowed with plasticity (39). First, we targeted the effect of consecutive withdrawals and renewals of DBS by considering the different neuroplasticity conditions defined by the levels of (long term) potentiation and depotentiation. Second, we examined the effect of stimulation duration (by varying the number of iterations in the model) in *de novo* DBS "patients," again under different neuroplasticity conditions. The results of our computer simulation mirror relevant clinical observations and also broaden our understanding of the long-term effect of DBS under the considered conditions.

MATERIALS AND METHODS

Kuramoto's Model With Endowed Plasticity

As emphasized by previous DBS studies, the state of a neuron can be described by a set of variables that for certain parameters display a regular behavior. Therefore, such a state is susceptible to be described by the parameters that reflect changes in regularity as in the case of the phase (40). The same notion naturally applies to the ensembles of neurons whose regular behavior gives place to the patterns of regularity that have been linked to high cognitive functions and behavioral features as described earlier. On the basis of such an observation, we adopt Kuramoto's model of network synchronization to address the long-term effects of DBS.

In accordance with Kuramoto's model, the phase evolution equation for a network of coupled oscillators is given by:

$$\frac{\partial}{\partial t}\varphi_i = \omega_i + \frac{K_{ij}}{N}\sum_{i=1}^{N}\sin(\varphi_i - \varphi_j) + I_i,$$

where φ_i and ω_i represent the phase and natural frequency of oscillator i, K_{ij} refers to the coupling between the oscillators i and j, N represents the number of oscillators ($N = 100$), and I_i denotes the DBS input received by the oscillator i. The values for ω_i were uniformly distributed random numbers in the interval (0,1). The DBS input adopted was a stereotypical train of rectangular pulses with a 130 Hz frequency and a 3.0 amplitude. Note that a modified version of this model has been previously used to evaluate the efficacy of new therapeutic DBS protocols (40). As in previous studies (39), we assume a direct effect of plasticity on the coupling between the oscillators as defined by:

$$K_{ij} = a_p \star exp(\frac{r_1}{\tau_p}) - \alpha_d\, exp(\frac{r_2}{\tau_d}),$$

where α_p and α_d refer to the potentiation and depotentiation rates, τ_p and τ_d denote the damping parameters (set-up as 0.5), and r_1 and r_2 ($r_1 \neq r_2$) denote constant parameters that were selected from the uniformly distributed random values in the interval (0,1) for each pair of oscillators i, j.

Synchronization Quantification

To quantify global synchronization for the considered network of coupled oscillators, we make use of the phase locking value (PLV) (41), which provides a normalized synchronization index [ranging from 0 (no synchronization) to 1 (full synchronization)] between a pair of oscillators $i, j = 1.0.100$ as defined by:

$$PLV_{ij} = \frac{1}{N}\left|\sum_{i=1}^{N} e^{-i(\varphi_i - \varphi_j)}\right|,$$

where φ_i and φ_j denote the phase of oscillators i and j. The grand average of PLV_{ij} across all possible combinations of pairs of oscillators ($i \neq j$ and without repetition) represents a global index of network synchronization for a given plasticity and DBS condition.

Plasticity Conditions

In the present study, we considered different plasticity conditions on the basis of previous studies addressing the assessment of neuroplasticity in the case of patients suffering from neurodegenerative and psychiatric disorders as well as healthy subjects. For instance, a reduction of neuroplasticity as reflected in decreased LTP and LTD has been suggested in subjects with depression by transcranial magnetic stimulation (TMS) studies utilizing paired associative stimulation (PAS) (42). A deficient plasticity that is reflected in strong asymmetry of LTP and LTD has been suggested in patients suffering from bipolar disorder by studies targeting the effect of lithium on human plasticity (43). With regards to PD, lack of LTP in the primary motor cortex has been stressed by TMS studies utilizing intermittent theta burst stimulation (iTBS) (44). An excess of LTP has been suggested in the case of patients with dystonia (45).

Note that the plasticity conditions in the adopted synchronization model are defined by setting up the specific values for the potentiation and depotentiation rate parameters; specifically the following plasticity conditions were considered:

(1) high level of potentiation ($\alpha_p = 8.0$) and low level of depotentiation ($\alpha_d = 0.001$); (2) low level of potentiation ($\alpha_p = 0.001$) and high level of depotentiation ($\alpha_d = 8.0$); (3) equally high level of potentiation ($\alpha_p = 8.0$) and depotentiation ($\alpha_d = 8.0$); (4) equally medium level of potentiation ($\alpha_p = 4.0$) and depotentiation ($\alpha_d = 4.0$); equally low level of potentiation and depotentiation: (5) ($\alpha_p = 0.7$) and ($\alpha_d = 0.7$); (6) ($\alpha_p = 0.1$) and ($\alpha_d = 0.1$); and (7) ($\alpha_p = 0.001$) and ($\alpha_d = 0.001$).

DBS Conditions

Focusing on the effect of consecutive withdrawal and renewal of DBS, the conditions DBS ON, DBS OFF, DBS ON2, DBS OFF2, and DBS ON3 were considered. For these conditions, duration and absence of DBS were set up to 2,000 iterations.

In the case of *de novo* DBS "patients," the conditions DBS OFF and DBS ON were considered. For these conditions, duration, and absence of DBS stimulation were set up to 500, 1,000, and 2,000 iterations.

Synchronization Percentage Change

For the long-term scenario of consecutive withdrawal and renewal of DBS, the condition DBS ON was defined as the baseline level (100%) so that percentage change in synchronization for the subsequent DBS conditions (DBS OFF, DBS ON2, DBS OFF2, and DBS ON3) was calculated in relation to DBS ON. Analogously, the initial condition DBS OFF was adopted as the baseline level (100%) in the case of *de novo* DBS "patients."

RESULTS

With a focus on the long-term effect of DBS under successive withdrawal and renewal of stimulation, we varied the level and balance of potentiation and depotentiation as depicted in **Figures 1A,B**, **2A,B**. Strikingly, a stable high phase locking value was noticeable in the case of high potentiation and low depotentiation (**Figures 1A**, **2A**), whereas PLV fluctuated between increased and decreased very low values. There is a stable increase of PLV during the successive DBS OFF states in the opposite constellation of potentiation and depotentiation (**Figures 1B**, **2B**). The case of symmetry (i.e., equally high, medium, or low) in the level of potentiation and depotentiation is depicted by **Figures 1C–G**, **2C–G**. It is noticeable that for the high levels of potentiation and depotentiation (8.0 and 8.0), PLV tended to decrease under successive DBS withdrawal and renewals (**Figures 1C**, **2C**); in the case of middle levels of potentiation and depotentiation (4.0 and 4.0), PLV showed a stable trend without fluctuations (**Figures 1D**, **2D**); in the case of low values of potentiation and depotentiation (0.7 and 0.7), PLV fluctuated between increased and decreased low values with a consistent increase during the successive DBS OFF states (**Figures 1E**, **2E**). In the case of very low levels of potentiation

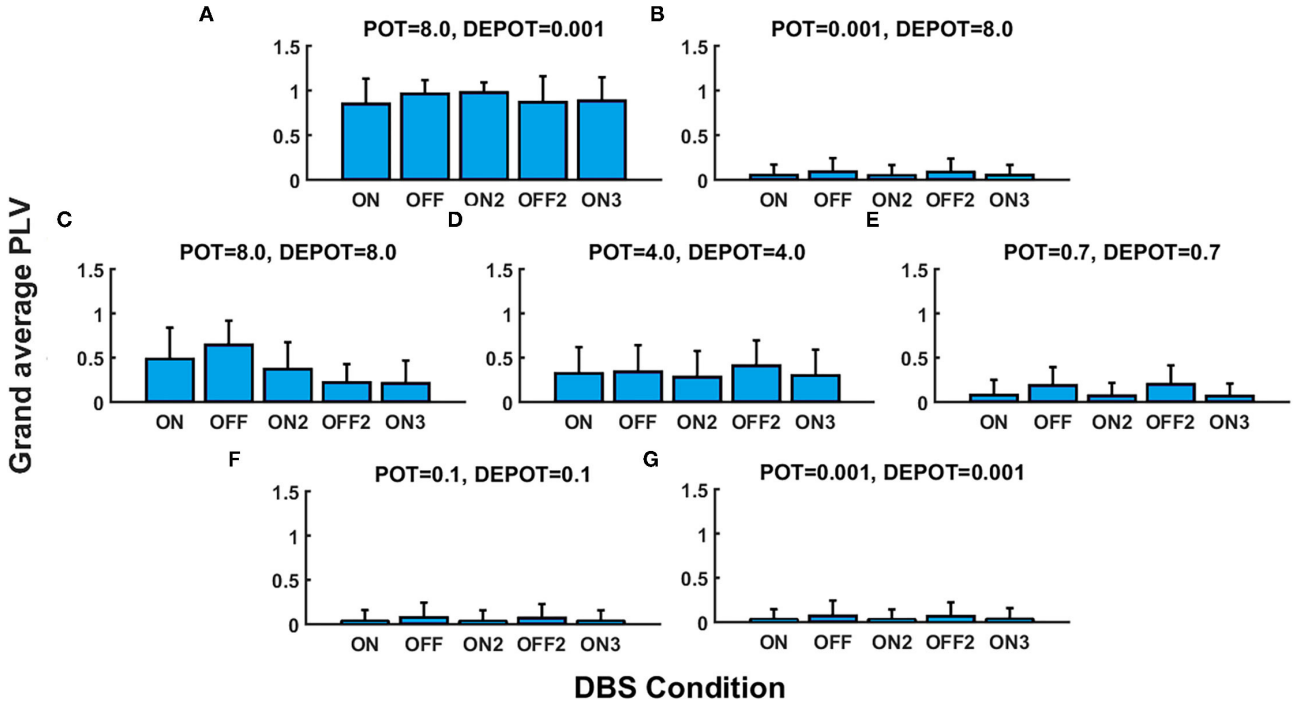

FIGURE 1 | The simulation results (mean and SD of the grand average phase locking value [PLV]) corresponding to the long-term effect of deep brain stimulation (DBS) under successive withdrawal and renewal of stimulation: unbalanced potentiation and depotentiation (high and low level) **(A,B)**; balance potentiation and depotentiation, i.e., equally high levels, **(C)**; equally medium levels **(D)**; equally low levels **(E–G)**.

and depotentiation (0.1 as well as 0.001), PLV fluctuated between increased and decreased very low values with a stable increase during the successive DBS OFF states (**Figures 1F,G**, **2F,G**).

With a focus on longitudinal development under DBS input in *de novo* DBS "patients," we again altered the level and balance of potentiation and depotentiation as depicted by **Figures 3A,B**, **4A,B**. Strikingly, a stable high level of PLV was noticeable across a number of iterations (500, 1,000, and 2,000) (**Figure 3A**) and thus reflected the duration of DBS input, with a slight increase during DBS ON (**Figure 4A**) in the case of high potentiation and low depotentiation. A stable low level of PLV was noticeable across a number of iterations (500, 1,000, and 2,000) (**Figure 3B**) with a tendency to decrease during DBS OFF and DBS ON (**Figure 4B**) in the case of low potentiation and high depotentiation. The case of symmetry in the level of potentiation and depotentiation is depicted in **Figures 3C–E**, **4C–E**. It is noticeable that for high levels of potentiation and depotentiation (8.0 and 8.0), PLV first increased and then showed a tendency to decrease in the transition from DBS OFF to DBS ON across a number of iterations (**Figures 3C**, **4C**); in the case of middle values of potentiation and depotentiation (4.0 and 4.0), PLV first increased and then showed a tendency to decrease during DBS OFF while a tendency to decrease was observed during DBS ON across a number of iterations (**Figures 3D**, **4D**); in the case of very low levels of potentiation and depotentiation (0.001 and 0.001), PLV showed low values with a tendency to decrease during DBS OFF and DBS ON across a number of iterations (**Figures 3E**, **4E**).

DISCUSSION

This paper summarizes a computational modeling study in scenarios with different neuroplasticity distributions, reflecting virtual "patients" with different neurophysiological signatures. When a powerful treatment, such as deep brain stimulation gets introduced in a new patient, questions arise as to "Why there is no effect? Will there be an effect when I stimulate for a longer time? What happens when the DBS machinery fails or a planned interruption of the stimulation occurs?" In long-term patients on this neuromodulation treatment, the question comes up whether a break or time off the intervention could be planned, or whether a life-long dependence on this input is likely.

In line with existing neurobiological models and neurophysiological findings in various DBS-treated conditions, our study looks at synchronization (coupling) of oscillatory activity, assuming that too much synchronization in certain frequency bands (beta in PD, theta in dystonia, etc.) maintains the pathological state (rigidity, dystonic symptoms, obsessive compulsive behavior, etc.), whereas a reduction in synchronization reflects the leaving of the symptom-stabilizing state. The *in vivo* situation of a biological system of course is complex and the exact mechanism of action leading to symptom improvement initiated by disruption of the synchronization patterns through DBS remains unclear (46).

The adopted computational simulation approach is particularly advantageous with regards to avoiding the risks

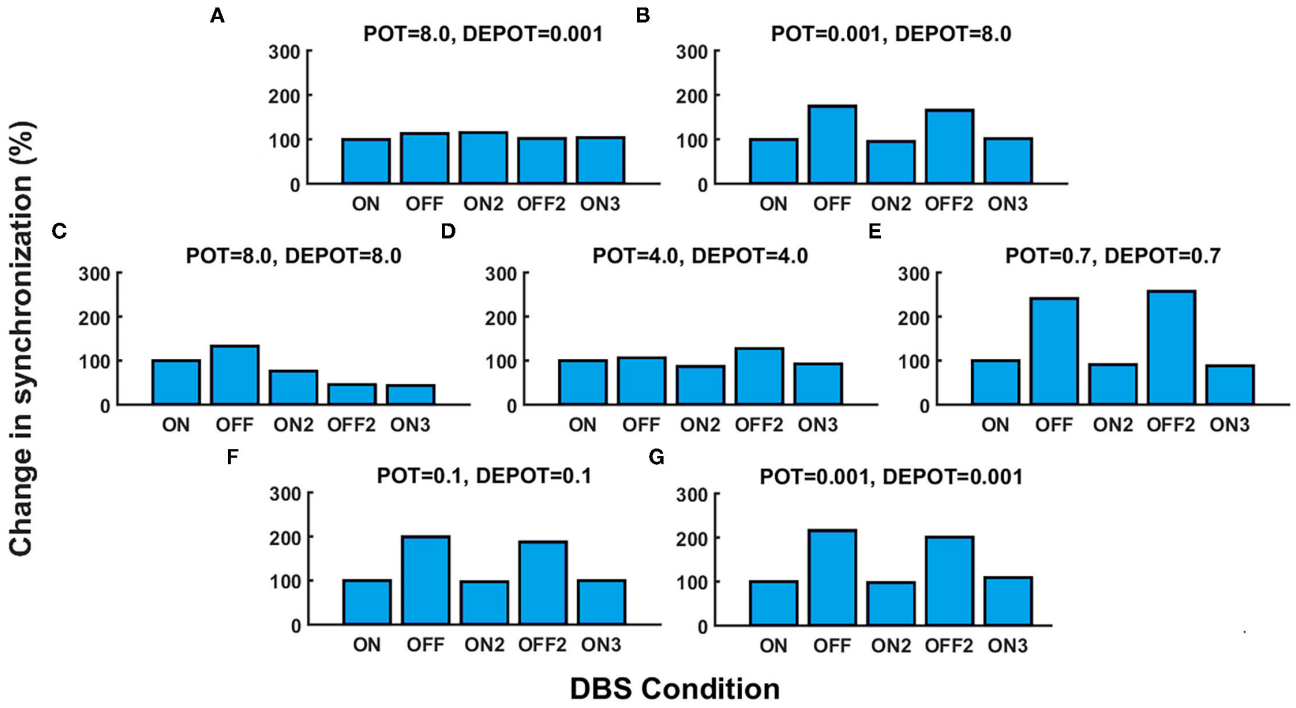

FIGURE 2 | The simulation results [percentage change of the grand average PLV, DBS ON represents the baseline level (100%)] corresponding to the long-term effect of DBS under successive withdrawal and renewal of stimulation: unbalanced potentiation and depotentiation (high and low level) **(A,B)**; balance potentiation and depotentiation, i.e., equally high levels, **(C)**; equally medium levels **(D)**; equally low levels **(E–G)**.

associated with turning on and off an implanted DBS device in patients suffering from neurological or psychiatric pathology and allowing flexibility in setting up the different plasticity scenarios that would not be accessible simultaneously under real (*in vivo*) patient conditions.

In the first part of our study, we simulated patients with DBS switched on long-term, and observed the effect of consecutive withdrawals and renewals of DBS. In the second part of the study, *de novo* "patients" (with no previous DBS treatment) received long-term DBS of various durations. On DBS treatment, the literature shows that certain symptoms seem to respond very quickly (tremor in PD) whereas others need longer, yet variable, time to allow the DBS effects on symptom alleviation to occur (dystonia) (9, 47). Particular patient profiles, that is, individual differences in baseline potentiation or depotentiation changes due to symptoms, have never been profiled and could provide information as to the potential response patients have to neuromodulation settings and treatment duration.

Our study introduces different neuroplasticity makeups, i.e., different levels and balances of potentiation and depotentiation. It assumes that this mirrors some real patient electrophysiological signatures. It is well-established that dystonia tends to show too much neuroplasticity, whereas it tends to be at normal levels in obsessive-compulsive disorders (OCD), and there is a lack of it in PD, Tourette Syndrome, bipolar disorder, and schizophrenia, as examples for abnormalities (48–50). These citations all represent group level studies, however, individual neuroplasticity levels are relevant for the personal effect of withdrawal or insertion of therapeutic input.

For the first part of the study, the simulations revealed that symmetry and asymmetry in the potentiation and depotentiation levels have a strong effect on the stability and level of synchronization patterns across the successive withdrawals and renewals of DBS input to the system. Our results reveal that, interestingly, a high level of potentiation in combination with a low level of depotentiation ensures the system is "stuck" in its current state (low mutability). Whether DBS is switched on or off does not affect the oscillatory state of the system. It remains stabilized at its observable high level of synchronization. On the contrary, when potentiation is low, independent of whether this is in combination with high or low depotentiation values, the oscillatory state of the system is highly mutable with a striking effect of switching DBS on or off. However, the effects of switching DBS on or off seem highly predictable. Intriguingly, when potentiation and depotentiation are balanced, both high or medium, the response to repeated insertions and withdrawals of DBS becomes less predictable and might suggest that they both counteract each other in line with a homeostatic regulation of the system, where a drive in one direction is counteracted *via* the other mechanism and driven into the opposite direction, with the goal of keeping the system in healthy boundaries. We conclude that the reaction of the oscillatory system highly depends on

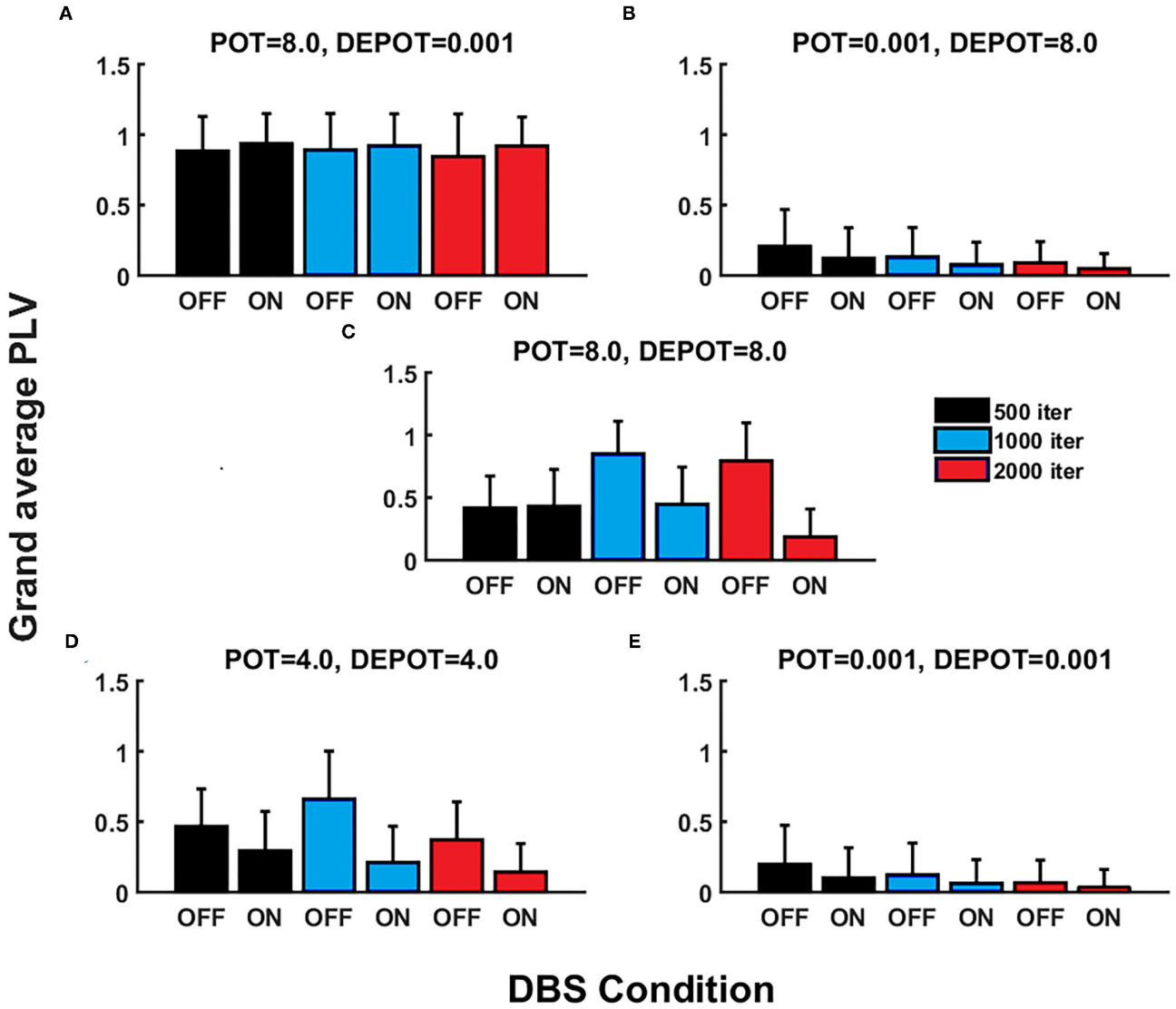

FIGURE 3 | The simulation results (mean and SD of the grand average PLV) corresponding to the influence of stimulation duration (500, 1,000, and 2,000 iterations) in *de novo* DBS "patients": unbalanced potentiation and depotentiation (high and low level) **(A,B)**; balance potentiation and depotentiation, i.e., equally high levels, **(C)**; equally medium levels **(D)**; and equally low levels **(E)**.

the neuroplasticity makeup of the "individual." Let us assume that there are disorders with too much plasticity, i.e., too much potentiation: In this case, the reaction of the system to DBS withdrawal or reinsertion is almost ineffective. The system is stabilized in its current status. This situation resembles that of many DBS naïve dystonia patients, for example. The long time to respond to initial treatment in dystonia or the strong resistance to neuromodulation and to occupational training might be due to such a neurophysiological signature. In the low potentiation constellation, the oscillatory system instantly responds to being switched on or off. The system is highly mutable, a response well-known for major symptoms of PD and long-term DBS-treated dystonia patients who have low potentiation as a cardinal neurophysiological feature (9, 47). The change of the oscillatory system directly matches the ON/OFF state and is highly predictable. The most complicated constellation arises with balanced high or medium levels of potentiation and depotentiation. Unlike what happens in the high unbalanced potentiation situation, in this case, the system responds to insertion and withdrawal of DBS. However, the contradictory forces of neuroplasticity seem to intermingle and one might speculate that the homeostatic mechanisms come into play to keep the system within healthy boundaries. Here, the outcome of DBS OFF and ON scenarios becomes unpredictable. However, change happens, and this stands in contrast to the unbalanced high potentiation-low depotentiation scenario where the oscillatory system remains immutable and "stuck" in its current state.

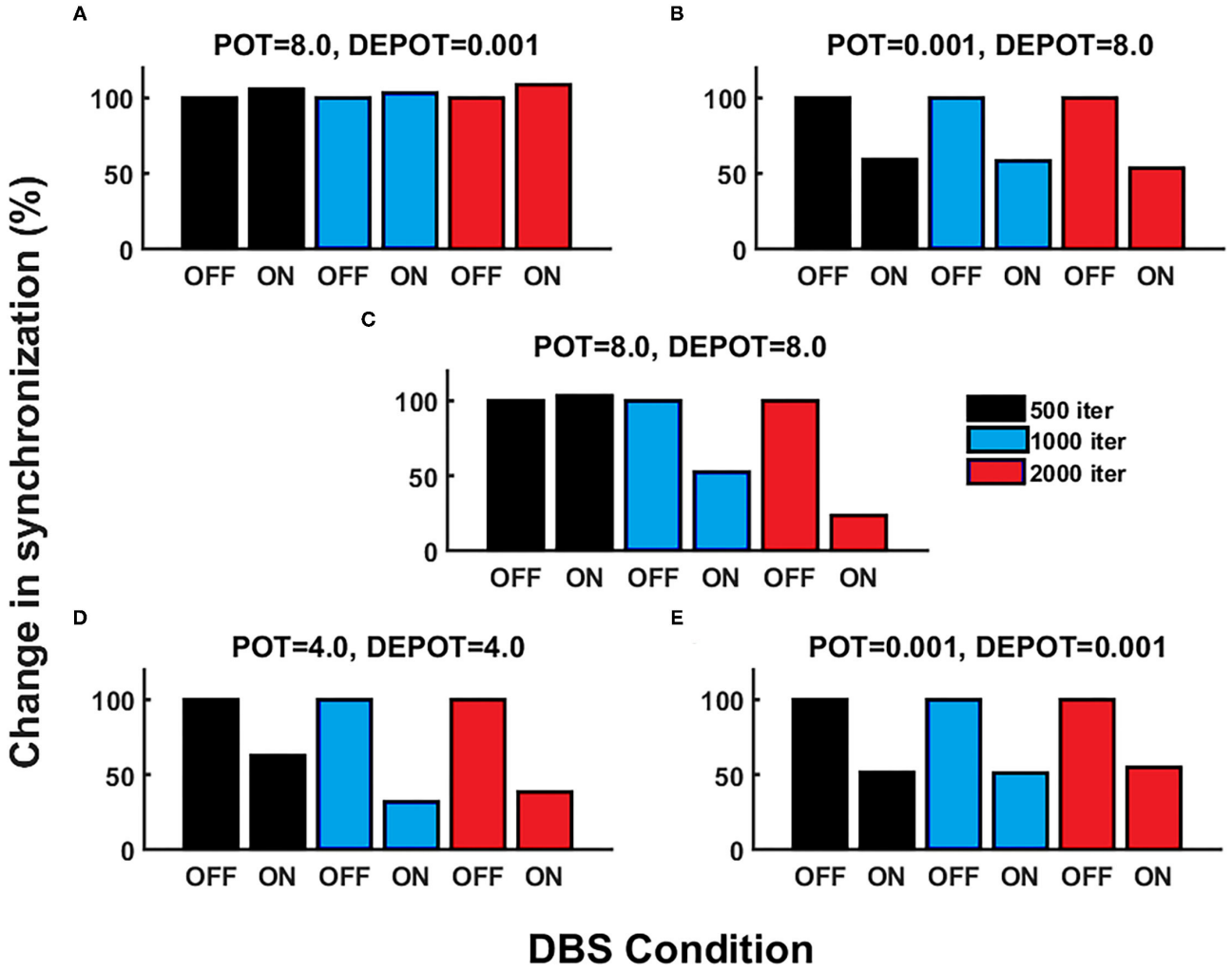

FIGURE 4 | The simulation results [percentage change of the grand average PLV, the initial DBS OFF represents the baseline level (100%)] corresponding to the influence of stimulation duration (500, 1,000, and 2,000 iterations) in *de novo* DBS "patients": unbalanced potentiation and depotentiation (high and low level) **(A,B)**; balance potentiation and depotentiation, i.e., equally high levels, **(C)**; equally medium levels **(D)**; and equally low levels **(E)**.

In the second part of our study, the computational simulation mimicked a *de novo* "patient" who then received DBS for various durations (iterations), and consecutively withdrawal of DBS was simulated at different time points along this time axis. Again, as in the first part of the study, the outcome was highly dependent on the synaptic plasticity signature. In the unbalanced high potentiation-low depotentiation situation, the system over time remains immutable and "stuck" in its oscillatory state. DBS insertion is not able to produce change in the system, resembling the situation of therapy-resistant patients. As an example, naïve patients with dystonia are known for their high potentiation. The removal of high potentiation, allowing the system to become mutable, might drive the change toward the beneficial effects of DBS as suggested before (9). In the balanced high and medium potentiation-depotentiation scenario, we observe effects in a monophasic positive direction after insertion of DBS with a gradual decrease in coupling in the oscillatory system. Interestingly, however, upon withdrawal of DBS, a rebound occurs that exceeds the level of the initial coupling by far. This might resemble a situation of dramatic, sometimes life threatening worsening of symptoms in dystonia patients with accidental or planned DBS switch OFF (51). In a scenario where there is an unbalanced or balanced low potentiation, the response to DBS is present and in a positive direction, it appears that the system is mutable. Intriguingly, the oscillatory system reverts back to the DBS naïve state upon DBS withdrawal, but not to the 100% baseline level of the naïve system, in other words some of the DBS-induced effect seems to be stabilized despite a relative lack of potentiation. However, this is only a mild deviation from the naïve 100% value in the OFF state (before treatment or DBS input was initiated).

The computational simulation study shows the strong effect of the individual neuroplasticity makeup on the insertion and

withdrawal of DBS as a therapeutic tool on the oscillatory system and thereby supposedly on disorder symptoms manifesting in brain coupling. How mutable a system is and thereby how effectively it responds to the treatment input might be linked to such individual signatures. Even in healthy people, neuroplasticity levels are variable and individual (52, 53). The meaning of such a marker setup or signature for personalized therapy and management of patients becomes clear by the usage of such computational approaches.

Limitations of the study or points to consider: This is a computational modeling and simulation approach and not *in vivo* data. However, in this limitation lies strength, because it is impossible, due to technical limitations, to obtain such data during acquisition of this type of neurophysiological recordings in real patients. Besides technical impossibility, the potential harm of switch OFF situations needs to be carefully considered by experienced clinicians who know the patients well. The second point to consider is that this modeling does not currently include the fact that the neuroplasticity itself is dependent on the oscillatory system and therefore will be dynamic over time. In other words, the results of the current study reflect the neuroplasticity conditions that once set up remain the same across iterations. As shown previously, the neuroplasticity is variable over time and also influences the switch OFF clinical outcome based on its potentiation as one form of neuroplasticity at that particular time point (9, 11, 12, 54). To explore the dynamics of the system would be a meaningful next study.

In conclusion, the electrophysiological signature has a profound impact on the effects of an intervention, such as DBS on the system, and can be used in future to narrow down potential outcomes in specific scenarios.

DATA AVAILABILITY STATEMENT

The raw data supporting the conclusions of this article will be made available by the authors, without undue reservation.

AUTHOR CONTRIBUTIONS

All authors listed have made a substantial, direct, and intellectual contribution to the work and approved it for publication.

ACKNOWLEDGMENTS

We acknowledge the Dorothy Feiss Scientific Research Grant.

REFERENCES

1. Vijverman AC, Fox SH. New treatments for the motor symptoms of Parkinson's disease. *Expert Rev Clin Pharmacol.* (2014) 7:761–77. doi: 10.1586/17512433.2014.966812
2. Groiss SJ, Wojtecki L, Südmeyer M, Schnitzler A. Deep brain stimulation in Parkinson's disease. *Ther Adv Neurol Disord.* (2009) 2:20–8. doi: 10.1177/1756285609339382
3. Lee DJ, Lozano CS, Dallapiazza RF, Lozano AM. Current and future directions of deep brain stimulation for neurological and psychiatric disorders. *J Neurosurg.* (2019) 131:333–42. doi: 10.3171/2019.4.JNS181761
4. Harmsen IE, Elias GJB, Beyn ME, Boutet A, Pancholi A, Germann J, et al. Clinical trials for deep brain stimulation: current state of affairs. *Brain Stimul.* (2020) 13:378–85. doi: 10.1016/j.brs.2019.11.008
5. Calabresi P, Ghiglieri V, Mazzocchetti P, Corbelli I, Picconi B. Levodopa-induced plasticity: a double-edged sword in Parkinson's disease? *Philos Trans R Soc Lond B Biol Sci.* (2015) 370:20140184. doi: 10.1098/rstb.2014.0184
6. Da Cunha C, Boschen SL, Gómez,-A. A., Ross EK, Gibson WSJ, Min HK, et al. Toward sophisticated basal ganglia neuromodulation: review on basal ganglia deep brain stimulation. *Neurosci Biobehav Rev.* (2015) 58:186–10. doi: 10.1016/j.neubiorev.2015.02.003
7. Cif L, Demailly D, Lin JP, Barwick KE, Sa M, Abela L, et al. KMT2B-related disorders: expansion of the phenotypic spectrum and long-term efficacy of deep brain stimulation. *Brain.* (2020) 143:3242–61. doi: 10.1093/brain/awaa304
8. Krause P, Völzmann S, Ewert S, Kupsch A, Schneider GH, Kühn AA. Long-term effects of bilateral pallidal deep brain stimulation in dystonia: a follow-up between 8 and 16 years. *J Neurol.* (2020) 267:1622–31. doi: 10.1007/s00415-020-09745-z
9. Ruge D, Tisch S, Hariz MI, Zrinzo L, Bhatia KP, Quinn NP, et al. Deep brain stimulation effects in dystonia: time course of electrophysiological changes in early treatment. *Mov Disord.* (2011) 26:1913–21. doi: 10.1002/mds.23731
10. Ruge D, Cif L, Limousin P, Gonzalez V, Vasques X, Hariz MI, et al. Shaping reversibility? Long-term deep brain stimulation in dystonia: the relationship between effects on electrophysiology and clinical symptoms. *Brain.* (2011) 134:2106–15. doi: 10.1093/brain/awr122
11. Ruge D, Cif L, Limousin P, Gonzalez V, Vasques X, Coubes P, et al. Longterm deep brain stimulation withdrawal: clinical stability despite electrophysiological instability. *J Neurol Sci.* (2014) 342:197–9. doi: 10.1016/j.jns.2014.05.011
12. Cif L, Ruge D, Gonzalez V, Limousin P, Vasques X, Hariz MI, et al. The influence of deep brain stimulation intensity and duration on symptoms evolution in an OFF stimulation dystonia study. *Brain Stimul.* (2013) 6:500–5. doi: 10.1016/j.brs.2012.09.005
13. Nowak A, Vallacher RR, Zochowski M, Rychwalska A. Functional synchronization: the emergence of coordinated activity in human systems. *Front Psychol.* (2017) 8:945. doi: 10.3389/fpsyg.2017.00945
14. Pikovsky A, Rosenblum MG, Kurths J. Synchronization: a universal concept in nonlinear sciences. *Am J Phys.* (2002) 70:655. doi: 10.1119/1.1475332
15. Suri RE, Sejnowski TJ. Spike propagation synchronized by temporally asymmetric Hebbian learning. *Biol Cybern.* (2002) 87:440–5. doi: 10.1007/s00422-002-0355-9
16. Debanne D, Gahwiler BH, Thompson SM. Long-term synaptic plasticity between pairs of individual CA3 pyramidal cells in rat hippocampal slice cultures. *J Physiol.* (1998) 507:237–47. doi: 10.1111/j.1469-7793.1998.237bu.x
17. Feldman DE. Timing-based LTP and LTD at vertical inputs to layer II/III pyramidal cells in rat barrel cortex. *Neuron.* (2000) 27:45–56. doi: 10.1016/S0896-6273(00)00008-8
18. Hebb DO. *The Organization of Behaviour. A Neuropsychological Theory.* John Wiley and Sons (1949).
19. Herrington TM, Cheng JJ, Eskandar EN. Mechanisms of deep brain stimulation. *J Neurophysiol.* (2016) 115:19–38. doi: 10.1152/jn.00281.2015
20. Terranova C, Rizzo V, Cacciola A, Chillemi G, Calamuneri A, Milardi D, et al. Is there a future for non-invasive brain stimulation as a therapeutic tool? *Front Neurol.* (2019) 24:1146. doi: 10.3389/fneur.2018.01146
21. Chen CC, Kuhn AA, Trottenberg T, Kupsch A, Schneider GH, Brown P. Neuronal activity in globus pallidus interna can be synchronized to local field potential activity over 3–12 Hz in patients with dystonia. *Exp Neurol.* (2006) 202:480–6. doi: 10.1016/j.expneurol.2006.07.011
22. Bland BH, Oddie SD. Theta band oscillation and synchrony in the hippocampal formation and associated structures: the case for its role in sensorimotor integration. *Behav Brain Res.* (2001) 127:119–36. doi: 10.1016/S0166-4328(01)00358-8

23. DeCoteau WE, Thorn C, Gibson DJ, Courtemanche R, Mitra P, Kubota Y, et al. Learning-related coordination of striatal and hippocampal theta rhythms during acquisition of a procedural maze task. *Proc Natl Acad Sci USA*. (2007) 104:5644–9. doi: 10.1073/pnas.0700818104
24. Gengler S, Mallot HA, Holscher C. Inactivation of the rat dorsal striatum impairs performance in spatial tasks and alters hippocampal theta in the freely moving rat. *Behav Brain Res*. (2005) 164:73–82. doi: 10.1016/j.bbr.2005.06.009
25. Trenado C, Hartmann CJ, Elben S, Pauls KAM, Friggemann L, Groiss SJ, et al. Local field potential oscillations of the globus pallidus in cervical and tardive dystonia. *J Neurol Sci*. (2016) 366:68–73. doi: 10.1016/j.jns.2016.04.033
26. Brown P. Abnormal oscillatory synchronisation in the motor system leads to impaired movement. *Curr Opin Neurobiol*. (2007) 17:656–64. doi: 10.1016/j.conb.2007.12.001
27. D'Andrea A, Chella F, Marshall TR, Pizzella V, Romani GL, Jensen O, et al. Alpha and alpha-beta phase synchronization mediate the recruitment of the visuospatial attention network through the Superior Longitudinal Fasciculus. *NeuroImage*. (2019) 188:722–32. doi: 10.1016/j.neuroimage.2018.12.056
28. Zareian B, Maboudi K, Daliri MR, Abrishami Moghaddam H, Treue S, Esghaei M. et al. Attention strengthens across-trial pre-stimulus phase coherence in visual cortex, enhancing stimulus processing. *Sci Rep*. (2020) 10:4837. doi: 10.1038/s41598-020-61359-7
29. Ara A, Marco-Pallarés J. Fronto-temporal theta phase-synchronization underlies music-evoked pleasantness. *Neuroimage*. (2020) 212:116665. doi: 10.1016/j.neuroimage.2020.116665
30. Ahn S, Cho H, Kwon M, Kim K, Kwon H, Kim BS, et al. Interbrain phase synchronization during turn-taking verbal interaction—a hyperscanning study using simultaneous EEG/MEG. *Hum Brain Mapp*. (2018) 39:171–88. doi: 10.1002/hbm.23834
31. Bob P, Palus M, Susta M, Glaslova K. EEG phase synchronization in patients with paranoid schizophrenia. *Neurosci Lett*. (2008) 447:73–7. doi: 10.1016/j.neulet.2008.09.055
32. Pusil S, Dimitriadis SI, López ME, Pereda E, Maestú F. Aberrant MEG multi-frequency phase temporal synchronization predicts conversion from mild cognitive impairment-to-Alzheimer's disease. *NeuroImage*. (2019) 24:101972. doi: 10.1016/j.nicl.2019.101972
33. Nenadovic V, Perez Velazquez JL, Hutchison JS. Phase synchronization in electroencephalographic recordings prognosticates outcome in paediatric coma. *PLoS ONE*. (2014) 9:e94942. doi: 10.1371/journal.pone.0094942
34. Miocinovic S, de Hemptinne C, Qasim S, Ostrem JL, Starr PA. Patterns of cortical synchronization in isolated dystonia compared with Parkinson disease. *JAMA Neurol*. (2015) 72:1244–51. doi: 10.1001/jamaneurol.2015.2561
35. Lee S, Liu A, Wang ZJ, McKeown MJ. Abnormal phase coupling in Parkinson's disease and normalization effects of subthreshold vestibular stimulation. *Front Hum Neurosc*. (2019) 13:118. doi: 10.3389/fnhum.2019.00118
36. Ruiz MH, Senghaas P, Grossbach M, Jabusch HC, Bangert M, Hummel F, et al. Defective inhibition and inter-regional phase synchronization in pianists with musician's dystonia: an EEG study. *Hum Brain Mapp*. (2009) 30:2689–700. doi: 10.1002/hbm.20700
37. Delussi M, Nazzaro V, Ricci K, de Tommaso M. EEG functional connectivity and cognitive variables in premanifest and manifest Huntington's disease: EEG Low-Resolution Brain Electromagnetic Tomography (LORETA) Study. *Front Physiol*. (2020) 11:612325. doi: 10.3389/fphys.2020.612325
38. Pfurtscheller G, Lopes da Silva FH. Event-related EEG/MEG synchronization and desynchronization: basic principles. *Clin Neurophysiol*. (1999) 110:1842–57. doi: 10.1016/S1388-2457(99)00141-8
39. Beuter A, Modolo J. Delayed and lasting effects of deep brain stimulation on locomotion in Parkinson's disease. *Chaos*. (2009) 19:026114. doi: 10.1063/1.3127585
40. Weerasinghe G, Duchet B, Cagnan H, Brown P, Bick C, Bogacz R. Predicting the effects of deep brain stimulation using a reduced coupled oscillator model. *PLoS Comput Biol*. (2019) 15:e1006575. doi: 10.1371/journal.pcbi.1006575
41. Lachaux JP, Rodriguez E, Martinerie J, Varela FJ. Measuring phase synchrony in brain signals. *Hum Brain Mapp*. (1999) 8:194–208. doi: 10.1002/(SICI)1097-0193(1999)8:4<194::AID-HBM4>3.0.CO;2-C
42. Noda Y, Zomorrodi R, Vila-Rodriguez F, Downar J, Farzan F, Cash RFH, et al. Impaired neuroplasticity in the prefrontal cortex in depression indexed through paired associative stimulation. *Depress Anxiety*. (2018) 35:448–56. doi: 10.1002/da.22738
43. Voytovych H, Kriváneková L, Ziemann U. Lithium: a switch from LTD- to LTP-like plasticity in human cortex. *Neuropharmacology*. (2012) 63:274–9. doi: 10.1016/j.neuropharm.2012.03.023
44. Suppa A, Marsili L, Belvisi D, Conte A, Iezzi E, Modugno N, et al. Lack of LTP-like plasticity in primary motor cortex in Parkinson's disease. *Exp Neurol*. (2011) 227:296–301. doi: 10.1016/j.expneurol.2010.11.020
45. Tisch S, Limousin P. Neurophysiological insights in dystonia and its response to deep brain stimulation treatment. *Exp Brain Res*. (2020) 238:1645–57. doi: 10.1007/s00221-020-05833-8
46. Brown P, Eusebio A. Paradoxes of functional neurosurgery: clues from basal ganglia recordings. *Mov Disord*. (2008) 23:12–20. doi: 10.1002/mds.21796
47. Krack P, Batir A, Van Blercom N, Chabardes S, Fraix V, Ardouin C, et al. Five year follow-up of bilateral stimulation of the subthalamic nucleus in advanced Parkinson's disease. *N Engl J Med*. (2003) 349:1925–34. doi: 10.1056/NEJMoa035275
48. Udupa K, Chen R. Motor cortical plasticity in Parkinson's disease. *Front Neurol*. (2013) 4:128. doi: 10.3389/fneur.2013.00128
49. Quartarone A, Ruge D. How many types of dystonia? pathophysiological considerations. *Front Neurol*. (2018) 9:12. doi: 10.3389/fneur.2018.00012
50. Suppa A, Marsili L, Di Stasio F, Berardelli I, Roselli V, Pasquini M, et al. Cortical and brainstem plasticity in Tourette syndrome and obsessive-compulsive disorder. *Mov Disord*. (2014) 29:1523–31. doi: 10.1002/mds.25960
51. Nerrant E, Gonzalez V, Milesi C, Vasques X, Ruge D, Roujeau T, et al. Deep brain stimulation treated dystonia-trajectory via status dystonicus. *Mov Disord*. (2018) 33:1168–73. doi: 10.1002/mds.27357
52. Wiethoff S, Hamada M, Rothwell JC. Variability in response to transcranial direct current stimulation of the motor cortex. *Brain Stimul*. (2014) 7:468–75. doi: 10.1016/j.brs.2014.02.003
53. Pedroarena-Leal N, Heidemeyer L, Trenado C, Ruge D. Human depotentiation following induction of spike timing dependent plasticity. *Biomedicines*. (2018) 6:71. doi: 10.3390/biomedicines6020071
54. Honkanen EA, Korpela J, Pekkonen E, Kaasinen V, Reich MM, Joutsa J. Reappearance of symptoms after GPi-DBS discontinuation in cervical dystonia. *Mov Disord*. (2021) 8:406–11. doi: 10.1002/mdc3.13162

Conflict of Interest: The authors declare that the research was conducted in the absence of any commercial or financial relationships that could be construed as a potential conflict of interest.

Publisher's Note: All claims expressed in this article are solely those of the authors and do not necessarily represent those of their affiliated organizations, or those of the publisher, the editors and the reviewers. Any product that may be evaluated in this article, or claim that may be made by its manufacturer, is not guaranteed or endorsed by the publisher.

Copyright © 2021 Trenado, Cif, Pedroarena-Leal and Ruge. This is an open-access article distributed under the terms of the Creative Commons Attribution License (CC BY). The use, distribution or reproduction in other forums is permitted, provided the original author(s) and the copyright owner(s) are credited and that the original publication in this journal is cited, in accordance with accepted academic practice. No use, distribution or reproduction is permitted which does not comply with these terms.

frontiers in Pediatrics

ORIGINAL RESEARCH
published: 01 March 2022
doi: 10.3389/fped.2022.763642

Epilepsy Combined With Multiple Gene Heterozygous Mutation

He Qiuju[1,2,3†], *Zhuang Jianlong*[4†], *Wen Qi*[1,2,3], *Li Zhifa*[5], *Wang Ding*[1,2], *Sun Xiaofang*[1,2*] and *Xie Yingjun*[1,2*]

[1] Department of Obstetrics and Gynaecology, Key Laboratory for Major Obstetric Diseases of Guangdong Province, The Third Affiliated Hospital of Guangzhou Medical University, Guangzhou, China, [2] Key Laboratory of Reproduction and Genetics of Guangdong Higher Education Institutes, The Third Affiliated Hospital of Guangzhou Medical University, Guangzhou, China, [3] Department of Clinical Medicine, The Third Clinical School of Guangzhou Medical University, Guangzhou, China, [4] Prenatal Diagnosis Center, Quanzhou Women's and Children's Hospital, Quanzhou, China, [5] Gastrointestinal Surgery, The Third Affiliated Hospital of Guangzhou Medical University, Guangzhou, China

The fast pace of gene discovery has resulted in groundbreaking advances in the field of epilepsy genetics. Clinical testing using comprehensive gene panels, exomes, or genomes is now increasingly available and has significantly increased the diagnostic yield for early-onset epilepsies and enabled precision medicine approaches. In this paper, we report a case of epilepsy in a pedigree. The proband had heterozygous mutations in *KCNC1* (NM_001112741.1:c.959G>A, p. Arg320His), *CAPN3* (NM_000070.2:c.526G>A, p. Val176Met), and *NEFH* (NM_021076.3:c. 2595 delC, p. Lys866Argfs*51). Sanger sequencing verification was consistent with the results of whole-exome sequencing. The *KCNC1* mutation was a *de novo* mutation, and the *CAPN3* and *NEFH* mutations were inherited from their father and mother, respectively. Based on the American College of Medical Genetics and Genomics (ACMG) guidelines, a heterozygous mutation was found for *APOB* (NM_000384.2: c.10579C > T, p. Arg3527Trp). The heterozygous mutation at this site was inherent in the pedigree. Coexpression analysis indicated that heterozygous mutations of *KCNC1, CAPN3, NEFH,* and *APOB* were closely related to the clinical phenotypes of the patient, and the clinical phenotypic heterogeneity of the disease may be the result of the interaction of multiple genes.

Keywords: whole exome sequencing, Sanger sequencing, epilepsy, coexpression analysis, heterozygous mutations

OPEN ACCESS

Edited by:
Piero Pavone,
University of Catania, Italy

Reviewed by:
Ruzica Kravljanac,
The Institute for Health Protection of Mother and Child Serbia, Serbia
Lorenzo Pavone,
University of Catania, Italy

***Correspondence:**
Sun Xiaofang
xiaofangsun@gzhmu.edu.cn
Xie Yingjun
xieyjun@mail2.sysu.edu.cn

[†] These authors have contributed equally to this work and share first authorship

Specialty section:
This article was submitted to Pediatric Neurology, a section of the journal Frontiers in Pediatrics

Received: *24 August 2021*
Accepted: *26 January 2022*
Published: *01 March 2022*

Citation:
Qiuju H, Jianlong Z, Qi W, Zhifa L, Ding W, Xiaofang S and Yingjun X (2022) Epilepsy Combined With Multiple Gene Heterozygous Mutation. Front. Pediatr. 10:763642. doi: 10.3389/fped.2022.763642

INTRODUCTION

Epilepsy is a disorder of the central nervous system caused by abnormal discharge of neurons that affects consciousness, sensation, temperament, and movement. The classification levels of epilepsy diagnosis are based on seizure type, epilepsy type (focal, generalized, combined generalized and focal, and unknown) and epilepsy syndrome, and 40% of epilepsy is related to genetic factors (1–4). More than half of active epilepsy cases are 12 years old. The clinical features of epilepsy are complex and diverse and can manifest as paroxysmal movement, abnormal autonomic nerve function, transient sensory disorders, limb convulsions, loss of consciousness, and mental disorders. The etiology of epilepsy is heterogeneous and includes genetic factors, brain diseases, and systemic diseases. An imbalance between excitation and inhibition of the central nervous system leads to epileptic attack, and ion-channel

abnormalities are closely related to the occurrence of disease. Mutations in coding genes can participate in the development of the disease by affecting the functioning of ion channels, including those for potassium, calcium, and sodium ions. Approximately 25% of hereditary epilepsy cases are caused by variations in ion channel-related genes (5). In addition, epilepsy is related to changes in neurotransmitters and glial cells (6). Epilepsy can be controlled in most patients through regular medication, but some patients develop refractory epilepsy. Long-term repeated seizures can lead to cognitive impairment, which places a heavy economic and psychological burden on patients and families. Defining the pathogenesis of epilepsy has practical significance for classification, prenatal diagnosis, genetic screening, and subsequent treatment. With the rapid development of high-throughput sequencing technology, whole-exome sequencing technology is playing an important role in the genetic diagnosis of hereditary diseases. Mutations in genetic diseases are mostly located in coding regions, which account for 1% of the whole genome. The whole-exome sequencing technique has the advantages of low cost and strong pertinence. This technique covers most variations associated with gene function (7), enabling screening for pathogenic genes for a variety of diseases (8–11). In the present report, we elucidate the causative role of the interaction of multiple heterozygous mutation genes in the pathogenesis of a severe form of epilepsy.

MATERIALS AND METHODS

Case Presentation

A 26-year-old man came to the hospital because of his recurrent limb convulsions, unstable gait, and ease of falling accompanied by loss of consciousness for more than 5 years. The first seizure occurred at the age of 6 years, and he manifested generalized convulsions, foaming at the mouth, a blue complexion, and non-responsivity. The seizure lasted approximately 2 min. Then, he exhibited no abnormality upon waking, later developed clonic attacks, unintentional movements, and hand and foot paralysis, and received Depakine treatment in the same year (sodium valproate syrup). The next year, the patient experienced large twitching of the legs for 2 min. When the patient discontinued the drug for 2 months, the symptoms were aggravated, characterized by handshaking and eyelid movements, followed by weakness of the legs, trembling of the limbs, and convulsions of the whole body when he was frightened or stressed.

The patient was a first full-term baby and was delivered *via* Cesarean section due to a misplaced position and a large head. The proband was in good condition after birth. Compared with children of the same age, the patient has poor balance function and poor coordination. The patient's parents denied a family history of epilepsy. At the age of 6, the proband underwent a computerized tomography (CT) examination of the brain, and no obvious abnormalities were found. Further electroencephalogram (EEG) and CT examinations were performed, and no obvious abnormalities were found. At the age of 8, the patient had a second seizure, and EEG examination showed inhibition of the α wave. Further 24-h dynamic EEG examination showed abnormal EEG (evident in the right frontotemporal central region, epileptiform discharge) and inhibition of α waves. Based on magnetic resonance imaging (MRI) results, sclerosis of the right hippocampus was suspected. At the age of 9, the proband underwent brain positron emission computed tomography (PET CT), which showed no significant abnormalities in interictal pet metabolic brain imaging and a single spike in the right frontal region during light sleep. At the age of 26, an MRI of the brain showed no significant abnormalities. Multiple external hospital examinations were performed, and no obvious abnormalities in the EEG, MRI, or CT results were found. The muscles were tested more than 10 years ago and have not since. No muscular problems were found by electromyography (EMG) and nerve conduction velocity (NCV). Recent clinical follow-up shows that a major seizure (violent convulsions) occurred once, in the last 2 years, and myoclonus often occurred.

Karyotyping Analysis

Peripheral blood was collected intravenously from the proband and his parents, and the peripheral blood lymphocytes were cultured and harvested. A karyotyping analysis was performed according to the conventional G-banding technique (550-band resolution) (12).

Chromosomal Microarray Analysis

The CytoScan HD chip has a 2 M-probe count and is a high-density chip for detecting copy number variations and single nucleotide polymorphisms. Blood samples of the proband and his parents were collected, and the Affymetrix cyto HD Array was performed in strict accordance with the chip operation manual using CytoScan chip technology provided by Affymetrix.

Library Preparation and Whole-Exome Sequencing

Venous blood was withdrawn from the proband and his parents, and genomic DNA was extracted according to the manufacturer's standard procedure for the MagPure Buffy Coat DNA Midi KF Kit (Magen, Guangzhou, China). Then, the genomic DNA was fragmented by Segmentase (BGI, China) to generate small DNA fragments (100–500 bp) that were further screened using magnetic beads to enrich the fragments with sizes ranging from 280 to 320 bp. After the ends were filled, an "A" base was added to the 3' end to enable ligation of the DNA fragment to an adapter with a "T" base at the 3' end. The DNA fragments were amplified by a ligation-mediated polymerase chain reaction and purified to form a library. The library was enriched by array hybridization following a protocol (Roche NimbleGen, Madison, USA), followed by elution and postcapture amplification. The magnitude of the enrichment of the products was measured using an Agilent 2100 Bioanalyzer. All the amplified libraries were subsequently sent to BGI for circularization and sequencing on the MGIseq-2000 platform with a paired-end 100 sequencing strategy. The sequenced data were automatically demultiplexed by index.

Bioinformatics Analysis

We used published filtering criteria to generate "clean reads" for further analysis (13). The "clean reads" were aligned to the human genome reference (hg19) using Burrows Wheeler Aligner (BWA) software (14). The output files were used to perform sequencing coverage and depth analysis of the target region and single-nucleotide variant (SNV), as well as insertion and deletion (indel) calling. We used GATK to detect SNVs and indels. All SNVs and indels were filtered and estimated *via* multiple databases, including dbSNP, HapMap, 1000 human genome datasets and databases of 100 healthy Chinese adults. We used the scale-invariant feature transform (SIFT) and Polyphen2 to predict the effect of variants. Pathogenic variants were assessed under the protocol issued by the American College of Medical Genetics (ACMG) (15). The Human Gene Mutation Database (HGMD) was used to screen for mutations reported in published studies.

Sanger Sequencing

Mutations in the targeted genes for the proband and his parents were validated using conventional Sanger sequencing methods. Segregation analysis was performed if DNA from family members was available.

Protein–Protein Interaction Analysis

The protein–protein interactions of targeted genes with the heterozygous mutations confirmed by Sanger sequencing were analyzed with STRING version 10.0 (16) (https://stringdb.org/cgi/input.pl?sessionId=GQHzYg5cCT15&input_page_show_search=on).

RESULTS

Karyotyping Analysis and Chromosomal Microarray Analysis

The results of a karyotyping analysis indicated that the karyotypes of the three blood samples were normal. Chromosomal microarray analysis did not identify obvious copy number variations, ruling out the contribution of chromosomal abnormalities and copy number variations to the disease in the family (data not shown).

Whole-Exome Sequencing Analysis

Whole-exome sequencing identified a new heterozygous mutation c.959G>A (p. Arg320His) in the *KCNC1* gene. *KCNC1* encodes a voltage-gated potassium channel expressed in inhibitory neurons, and mutations in the gene cause progressive myoclonus epilepsy and ataxia. A suspected pathogenic variation consistent with the phenotype of the subject was detected in the *CAPN3* gene associated with limb-band muscular dystrophy type 2A/limb-girdle muscular dystrophy II. Due to the absence of relevance to the pathogenicity of this variant, the mutation was considered a causative mutation according to the ACMG guidelines (15, 17–19). Whole-exome sequencing also detected a suspected pathogenic mutation in the axonal *NEFH* genes related to Charcot-Marie-Tooth disease type 2. There are no reports on the pathogenicity of this mutation (NEFH c.2595delC, p. Lys866Argfs∗51). According to the ACMG guidelines, this variation was considered a likely pathogenic variation. In addition, the WES test results indicated a heterozygous mutation (APOB, c.10579C>T, p. Arg3527Trp), and pathogenicity of this variant has been reported (20). According to the ACMG guidelines, the patient had no relevant clinical manifestations, and the mutation was suspected to be a disease-causing variant (**Table 1**).

Sanger Sequencing

Sanger sequencing confirmed that the c.959G>A mutation in the KCNC1 gene was a *de novo* mutation. The heterozygous mutation *CAPN3* c.526G > A (p. Val176Met) was detected in the proband and his father. The heterozygous variants c.2595delC (p. Lys866Argfs∗51) and c.10579C > T (p. Arg3527Trp) detected in the *NEFH* and *APOB* genes of the patient were inherited from his mother. The patient's parents did not report any history of seizures, myasthenia, or myoclonus problems (**Figure 1**).

Protein–Protein Interaction Analysis

A protein–protein interaction analysis was performed on the following targeted genes and their interacting genes: *KCNC1, CAPN3, NEFH* (interacting genes: *PKN1, CDK5*), and *APOB* (interacting genes: *SYNCRIP, A1CF, APOBR, APOBEC1, APOBEC2, SCARB1, AMFR, HNRNPAB, OSBPL10, APOA5*); the results indicated that the proteins were highly interacting (**Figures 2**, **3**), suggesting that the combination of heterozygous mutations in multiple genes led to a severe phenotype.

DISCUSSION

Significant advances in the understanding of the neurobiology of seizures and epileptic diseases have resulted in multiple etiologic categories for epilepsy classification. An initial investigation often involves neuroimaging, ideally MRI, where available. The clinician can thus determine whether there is a structural etiology for the patient's epilepsy. The five etiologic groups are genetic, infectious, metabolic, immune, and unknown (2). Therefore, elucidation of the etiology and pathogenesis of seizures is very important for genetic counseling, diagnosis, and effective treatment of seizures. Recent studies on the etiology of epilepsy have shown that genetic factors play an important role in the pathogenesis of epilepsy (21, 22). The whole-exome sequencing technique uses a specific probe to enrich the DNA of the protein-coding regions and detects gene mutations through high-throughput sequencing, which provides good support for the diagnosis of hereditary diseases. Whole-exome sequencing of 10 families of seizures has indicated mutations associated with severe epilepsy and several new disease-causing genes (23). Whole-exome sequencing technology provides new guidance on diseases that are difficult to diagnose only through clinical characterization and laboratory tests, as well as facilitating the diagnosis of diseases and an analysis of etiology and pathogenesis (24). In this study, we found that the presence of *KCNC1, CAPN3,* and *NEFH* mutations in probands was closely related to clinical manifestations such as seizures and muscle weakness. Among

TABLE 1 | Results of gene mutation in patients with whole exome sequencing.

Gene	Site	Coding DNA change	Protein change	Disease associated with the gene
KCNC1	Chr11: 17793600	NM_001112741.1:c.959G>A	p. Arg320His	Progressive myoclonic epilepsy type 7
CAPN3	Chr15: 42679978	NM_000070.2: c.526G>A	p. Val176Met	Limb band muscular dystrophy type 2A/limb girdle muscular dystrophy 11
NEFH	Chr22: 29886222	NM_021076.3: c.2595delC	p. Lys866Arg fs*51	Charcot-Marie-Tooth disease type 2 hypercholesterol
APOB	Chr2: 21229161	NM_000384.2: c.10579C>T	p. Arg3527Trp	Type 1/autosomal dominant hypercholesterolemia type B

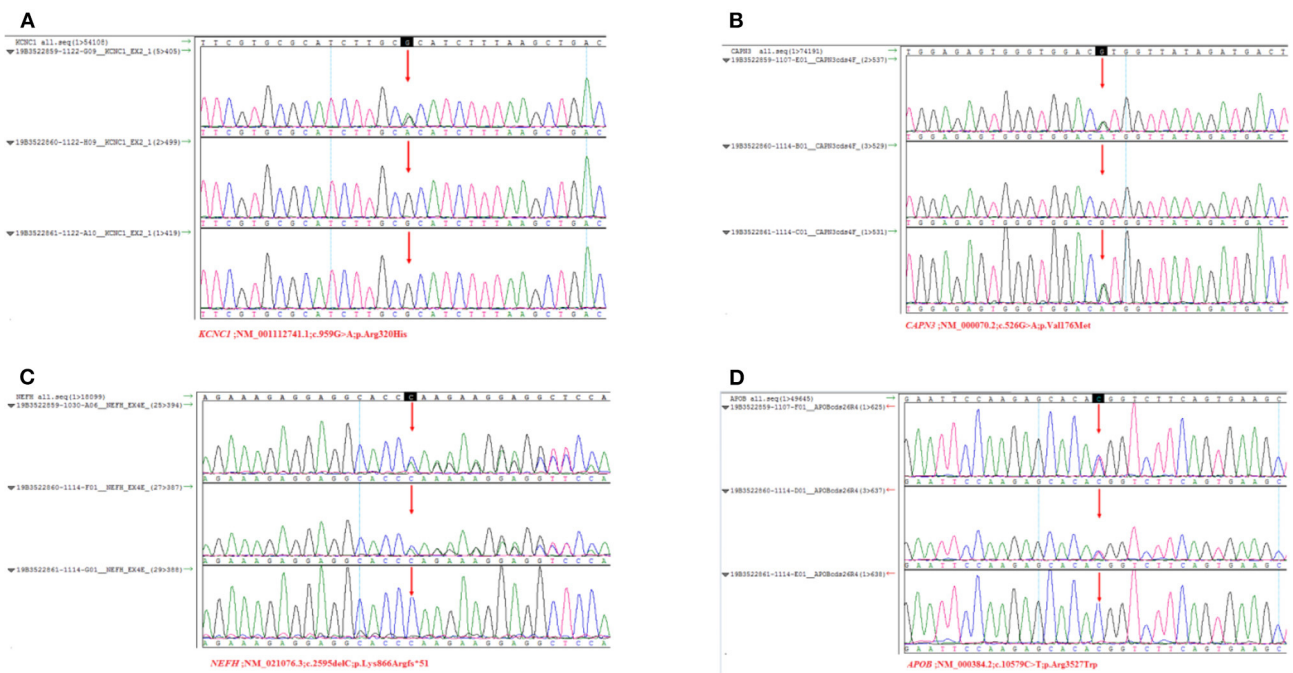

FIGURE 1 | Sanger sequencing results of the *KCNC1, CANP3, NEFH, APOB.* Arrows indicate the verification site of mutation. **(A)** The three results were sequencing results of proband, father and mother. KCNC1 was a new mutation (c. 959G > A, p. Arg320His). There was no heterozygous mutation of variant. **(B)** CAPN3 (c.526G > A, p. Val176Met) at this site, which was inherited from the father. **(C)** NEFH is a heterozygous mutation (c.259 5delC, p. Lys866Arg fs*51) inherited from the mother. **(D)** APOB belongs to heterozygous mutation (c.10579C > T, p. Arg3527Trp), inherited from its mother.

these mutations, *KCNC1* was a *de novo* mutation, and the latter two mutations were inherited from the proband's father and mother.

KCNC1 belongs to the gene family related to potassium-ion channels that are widely distributed in the central nervous system. This gene plays an important role in regulating a series of physiological activities, such as action potential formation, membrane repolarization, and creating tension in muscle cells. Voltage-gated potassium channels are critically important for the rapid repolarization of fast-discharging brain neurons, where Kv3 is a voltage-gated potassium channel consisting of six transmembrane segments (25). The Kv3 subfamily consists of four genes, Kv3.1, Kv3.2, Kv3.3, and Kv3.4. *KCNC1* encodes Kv3.1 and can activate the high-frequency discharge of cells, which is the main determinant of the discharge of high-frequency neurons and facilitates regulation of the excitability of cells (26). *KCNC1* is a highly conserved potassium channel subunit of the voltage-gated tetrameric potassium channel Kv3 subfamily. The Kv3 subfamily is closely associated with neurological disorders, such as *KCNC 3* (Kv3.3) missense mutations found in spinocerebellar ataxia (27) and the absence of KCNC2 chromosomes in patients with neurodevelopmental retardation and ataxia (28). Knocking out *KCNC1* in *KCNC1*-mutant mice has been reported to lead to myopathy and ataxia (29–31). Recently, a new mutation c.959G>A (p. (Arg320His) in *KCNC 1* was identified as a major cause of progressive myoclonic epilepsy (32, 33). Since 2015, exome sequencing has led to the identification of more than 24 *KCNC1* c.959G>A mutation cases in unrelated families (**Tables 2**, **3**). **Table 1** shows a list of variants, including those found in our patient and all cases reported thus far, as well as the major clinical symptoms observed in patients with this *KCNC1* c.959G>A mutation. A similar clinical phenotype and findings were obtained for our patients as for most reported patients reported thus far, and 10 patients manifested trembling (**Table 3**). Being positively charged, the arginine residue contributes to the gated charge (37, 38). This

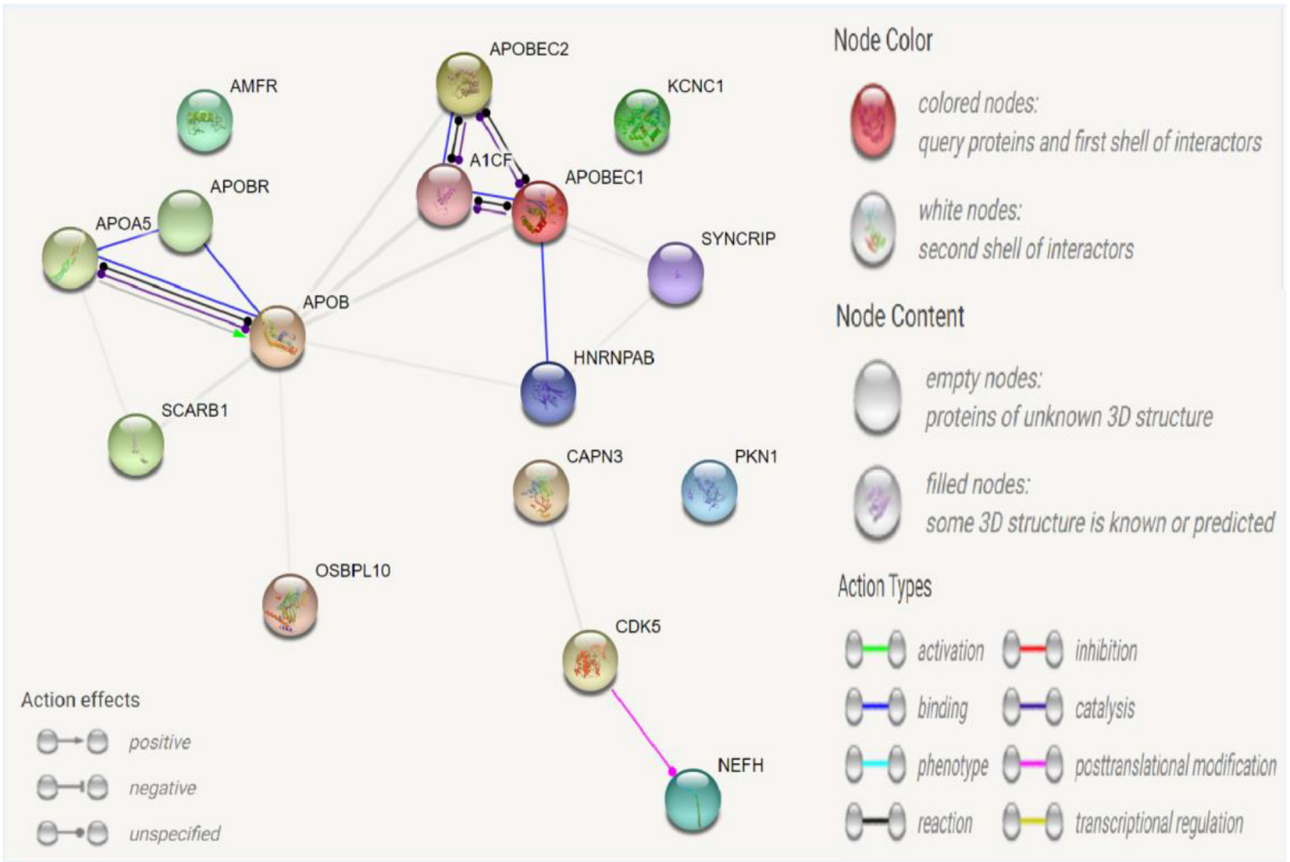

FIGURE 2 | Network for *KCNC1, CAPN3, NEFH, APOB,* and their interacted genes. Network nodes represent proteins. Splice isoforms or post-translational modifications are collapsed, i.e., each node represents all the proteins produced by a single, protein-coding gene locus. Edges represent protein-protein associations: associations are meant to be specific and meaningful, i.e., proteins jointly contribute to a shared function; this does not necessarily mean they are physically binding each other.

mutation has a negative effect on the Kv3.1 channel by producing electrophysiological abnormalities, resulting in the expression of the corresponding neuron (39). The clinical manifestations reported in previous studies were similar to those of the patient of this study.

CAPN3 encodes a muscle-specific member of the calcium-activated neutral protease family. Mutations in the *CAPN 3* gene are associated with the pathogenesis of limb muscular dystrophy type 2A (*LGMD2A*) and limb-girdle muscular dystrophy II. In many patients with myopathy, dozens of different *CANP3* gene mutations have been detected. The main clinical manifestations are progressive symmetrical muscle atrophy and proximal limb muscle weakness (40). A novel homozygous missense mutation of the *CAPN3* gene (c.1699G > A) was detected in a Saudi Arabian family (41). Studies have suggested that a pair of calpain protein lesions carry the mutations c.146G>A and c.329G>A in the CANP3 gene, and the clinical manifestation is LGMD2A (limb muscular dystrophy type 2A). The mutation site of the former is located in the short N-terminal domain 1 of the calpain-3 protein, which encodes a regulatory propeptide rich in cysteinase (42), whereas the mutation of the latter encodes the IIa domain of the calpain-3 protein, which forms a catalytic crack related to self-degradation together with the IIb domain (40). *CAPN3* mutation can be considered a powerful genetic factor leading to LGMD2A disease. Previous studies have found that HSD17B10 C.526G>A leads to problems of kinetic damage and complex formation (43). According to the ACMG guidelines, the variation is suspected to be pathogenic. In this study, a novel variant C.526G > A (p. Val176Met) was identified that has not previously been reported in patients. This variant is a heterozygous mutation that the patient inherited from his father, although both patient's parents had no related clinical manifestations. Similar manifestations seem to exist in this patient, such as unsteady walking and ease of falling.

NEFH is the pathogenic gene of Charcot-Marie-Tooth 2 (CMT2), and the hereditary model is autosomal dominant inheritance. Charcot-Marie-Tooth disease is a disease of the peripheral nervous system that is characterized by progressive muscle weakness and muscle atrophy. The clinical manifestation of *CMT2* is axonal degeneration without myelinated lesions, and the nervous transmission rate is normal or slightly decreased. *CMT2* can lead to progressive distal muscle weakness and atrophy, which is partly consistent with the clinical manifestations observed

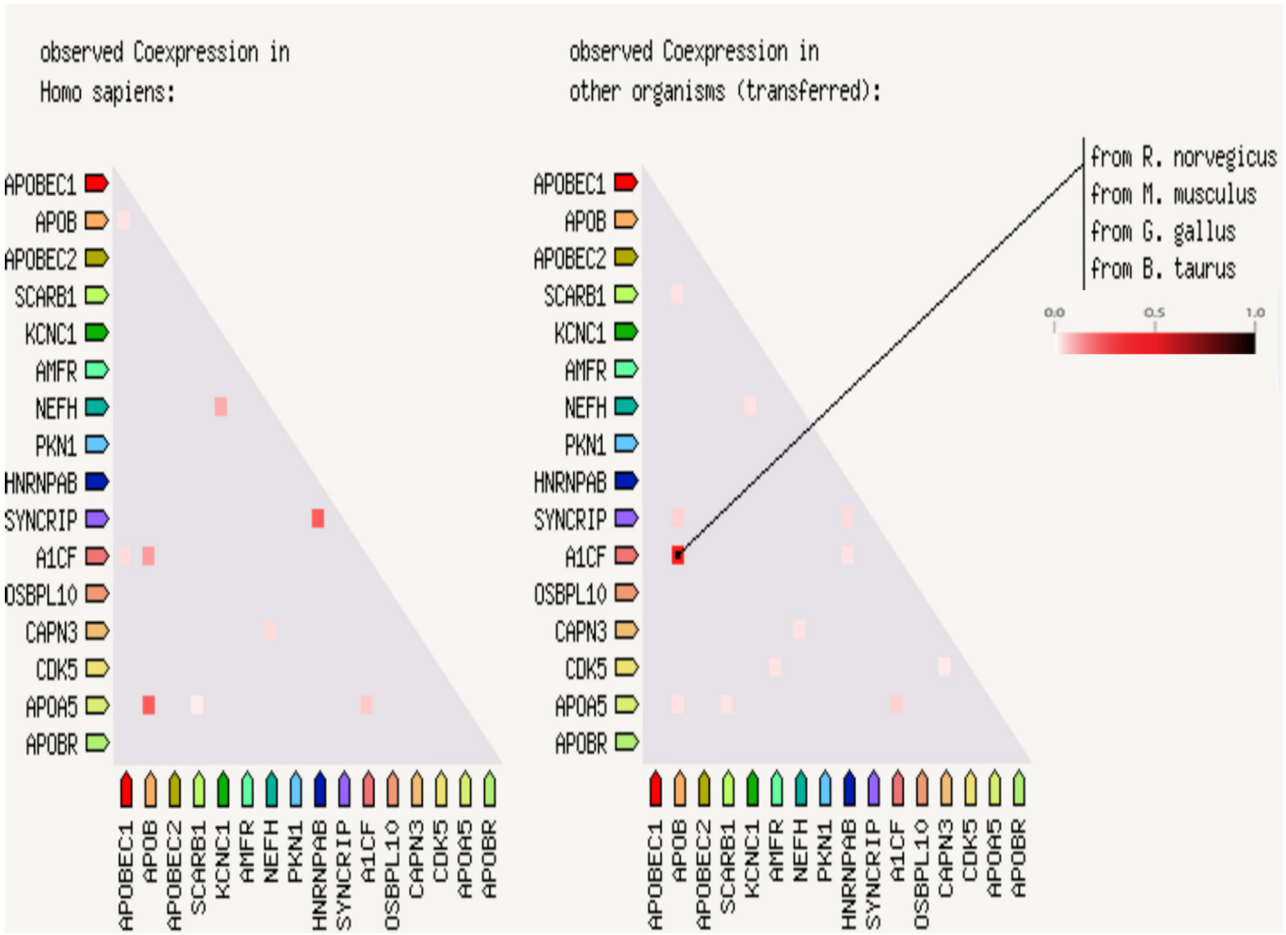

FIGURE 3 | Coexpression scores based on RNA expression patterns and protein co-regulation. In the triangle-matrices above, the intensity of color indicates the level of confidence that two proteins are functionally associated, given the overall expression data in the Homo sapiences and other organisms.

TABLE 2 | Clinical phenotype of patients with mutation site of c.959G>A.

Gender (male, female)	50.0% male
	50.0% female (12:12)
Initial symptom	
MS	52.2% (12/23)
GTCS	17.4% (4/23)
Trembling	30.4% (7/23)
Ataxic	8.7% (2/23)
FS	4.3% (1/23)
Seizure types	
GTCS	91.3% (21/23)
FS	4.3% (1/23)
MS	95.7% (22/23)
GTCS, MS	87.0% (20/23)
Ataxia	100.0% (24/24)
Mental retardation	63.6% (14/22)

MS, myoclonic seizure; FS, Focal seizure; GTCS, generalized tonic clonic seizure.

in this study. Whole-exome sequencing revealed a mutation (NEFH c.2595delC, p. Lys866Argfs∗51). There have been no reports on the pathogenicity of this mutation. It has been reported that in the CMT family, *NEFH* mutations interfere with neurofilament assembly by protein sequestration and cause neurotoxicity (44, 45). In the present study, Sanger sequencing confirmed that the variation in *NEFH* was inherited from the mother. The patient had clinical manifestations, such as unstable gait, but the parents had no relevant clinical manifestations.

APOB apolipoprotein E (apo E) is a 34 kDa glycosylation and excretion protein, and APOB is a major protein constituent of chylomicrons (apo B-48), LDL (apo B-100), and VLDL (apo B-100). *APOB* is associated with familial hypercholesterol type 1 and autosomal dominant hypercholesterolemia type B. An *APOB* mutation (c.10579C>T, p. Arg3527Trp) was detected by unexpected detection and reported as a pathogenic mutation based on ACMG guidelines. The respective patient was found to have an *APOE* mutation (p. Leu167del), which was the cause of dominant inheritance of familial hypercholesterolemia (20, 46).

Epilepsy is a heterogeneous disease characterized by abnormal signal transduction of neurotransmitters and abnormal ion channels. The etiology of epilepsy is complex, and many studies

TABLE 3 | The clinical features and gene test result of 24 patients with mutation site of c.959G>A.

Number	Gender	Age at onset	Initial symptom	Seizure types	Ataxia	Mental retardation	Gene mutation site	Amino acid variation	Age, outcome	References
1	F	10y	MS, GTCS	MS, GTCS	Yes	No	c.959G>A	P.Arg320His	13y; Unsteady walking	(34)
2	F	11y	MS, FS	MS, FS	Yes	Yes	c.959G>A	P.Arg320His	12y; Unsteady walking	(34, 35)
3	M	12y	MS	MS, GTCS	Yes	Yes	c.959G>A	P.Arg320His	38y; He was in a wheelchair at the age of 27	(33, 36)
4	M	6y	MS	MS, GTCS	Yes	Yes	c.959G>A	P.Arg320His	34y; He was in a wheelchair at the age of 17	(33, 36)
5	M	<5y	Ataxic	MS, GTCS	Yes	No	c.959G>A	P.Arg320His	40y; He was in a wheelchair at the age of 16	(33, 36)
6	F	10y	MS	MS, GTCS	Yes	Yes	c.959G>A	P.Arg320His	36y; He was in a wheelchair at the age of 15	(33, 36)
7	M	9y	Trembling, MS	MS, GTCS	Yes	No	c.959G>A	P.Arg320His	24y; Unsteady walking	(33, 36)
8	F	7y	Trembling	MS, GTCS	Yes	No	c.959G>A	P.Arg320His	22y; He was in a wheelchair at the age of 14	(33, 36)
9	F	10y	MS	MS, GTCS	Yes	No	c.959G>A	P.Arg320His	19y; He was in a wheelchair at the age of 17	(33, 36)
10	F	12y	MS	MS, GTCS	Yes	Yes	c.959G>A	P.Arg320His	24y; He can walk at the age of 17	(33, 36)
11	F	9y	MS	MS, GTCS	Yes	Yes	c.959G>A	P.Arg320His	15y; He was in a wheelchair at the age of 13	(33, 36)
12	F	9y	MS	MS, GTCS	Yes	Yes	c.959G>A	P.Arg320His	25y; He was in a wheelchair at the age of 19	(33, 36)
13	F	10y	Trembling	MS, GTCS	Yes	No	c.959G>A	P.Arg320His	42y; Unsteady walking	(33, 36)
14	F	13y	MS	MS, GTCS	Yes	Yes	c.959G>A	P.Arg320His	37y; Unsteady walking	(33, 36)
15	M	12y	Ataxic	MS, GTCS	Yes	Yes	c.959G>A	P.Arg320His	19y; Unsteady walking	(33, 36)
16	F	14y	GTCS	GTCS	Yes	No	c.959G>A	P.Arg320His	16y; Unsteady walking	(33, 36)

(Continued)

TABLE 3 | Continued

Number	Gender	Age at onset	Initial symptom	Seizure types	Ataxia	Mental retardation	Gene mutation site	Amino acid variation	Age, outcome	References
17	M	10y	MS	MS, GTCS	Yes	Yes	c.959G>A	P.Arg320His	18y; Unsteady walking	(33, 36)
18	M	NA	NA	NA	Yes	NA	c.959G>A	P.Arg320His	NA	(33, 36)
19	M	8y	Trembling, MS	MS	Yes	No	c.959G>A	P.Arg320His	18y; Unsteady walking	(36)
20	M	12y	GTCS	MS, GTCS	Yes	Yes	c.959G>A	P.Arg320His	17y;	(36)
21	F	15y	Trembling, MS	MS, GTCS	Yes	Yes	c.959G>A	P.Arg320His	40y; Unsteady walking	(36)
22	M	9y	Trembling, MS	MS, GTCS	Yes	Yes	c.959G>A	P.Arg320His	63y; Die of pneumonia and respiratory failure	(36)
23	M	9y	Trembling	MS, GTCS	Yes	Yes	c.959G>A	P.Arg320His	12y; Hypophrenia, Ataxic	(32)
24	M	7y	GTCS	MS, GTCS	Yes	NA	c.959G>A	p.Arg320His	10y; Myoclonics	(32)

NA, not available; MS, myoclonic seizure; FS, Focal seizure; GTCS, generalized tonic clonic seizure.

have shown that genetic factors are the main cause of epilepsy. The clinical manifestations of epilepsy are phenotypically heterogeneous; that is, a gene associated with epilepsy may have different clinical characteristics. In this study, three genes, *KCNC1, CAPN3,* and *NEFH*, were found to be genetically mutated. The former is a *de novo* mutation, and the latter two heterozygous mutations were inherited from the proband's father and mother. *CANP3* and *NEFH* are suspected pathogenic genes closely related to the clinical manifestations of patients. The STRING database (http://string-db.org) provides a critical assessment and integration of protein–protein interactions, including direct (physical) and indirect (functional) associations, and was used to analyse the evidence for the interaction of *KCNC1, CAPN3, NEFH,* and *APOE*. It seems that the heterogeneity of patient phenotypes results from the interaction of multiple mutated genes. Although our study identified *KCNC1* as the main cause of pathogenic mutations, the role of *NEFH* and *CAPN3* in mutations may be a fortuitous phenomenon. However, we should not ignore the multigene interactions leading to the diversity of epilepsy phenotypes in clinical analysis. Meanwhile, in this case, due to the application of gene sequencing, the disease of the proband was reasonably explained, which laid a foundation for finding a better treatment plan and brought the possibility of healthy growth and development of the next generation for similar families.

With the rapid development of gene sequencing technology, especially the application of whole-exome sequencing technology, the problems of case divergence, gene-site heterogeneity and exon incompleteness in the diagnosis of epilepsy and other diseases have been solved. Whole-exome technology has high sensitivity and accuracy and can be used to identify rare monogenic genetic diseases, which considerably facilitates the study of the etiology of diseases. Whole-exome sequencing technology is used to capture epilepsy-related pathogenic genes and their mutation sites, after which prenatal diagnosis can be performed by Sanger sequencing technology to detect the causes of rare clinical diseases and carry out genetic diagnosis for high-risk groups with a family history of disease. This technology is a reliable means of identifying pathogenic genes and exploring pathogenic mechanisms that can be employed in prenatal diagnosis and genetic counseling to effectively reduce the risk of having children with epilepsy. Thanks to gene sequencing technology, we can diagnose, treat, and follow up patients with genetic abnormalities as the main line. Overall, based on the previous information on gene mutations, we could not make a definite connection on these genes, but analysis of the genotype and phenotype correlation of this case alone does not rule out the possibility.

DATA AVAILABILITY STATEMENT

The datasets presented in this study can be found in online repositories. The names of the repository/repositories and accession number(s) can be found below: SAMN21236071 (https://www.ncbi.nlm.nih.gov/biosample/?term=Epilepsy-FJS-%2001).

ETHICS STATEMENT

The studies involving human participants were reviewed and approved by the IRB at the Third Affiliated Hospital of Guangzhou Medical University (No. 2021-113). The

patients/participants provided their written informed consent to participate in this study.

AUTHOR CONTRIBUTIONS

XY designed the study. WQ, LZ, WD, and SX performed the experiments. HQ and ZJ wrote the paper. All the authors read and approved the final manuscript.

FUNDING

This study was supported by the National Natural Science Foundation of Guangdong Province (Grant No. 2020A0505100062), Clinical Innovation Research Program of Guangzhou Regenerative Medicine and Health Guangdong Laboratory (Grant No. 2018GZR0201002), and 2018 Dr. Start Research Fund of the Third Affiliated Hospital of Guangzhou Medical University (Grant No. 2018B11).

ACKNOWLEDGMENTS

We would like to thank the reviewers for useful comments and the technical support from Ph.D. Li Jia (BGI Genomics, BGI-Shenzhen, Shenzhen, 518083, China).

REFERENCES

1. Szaflarski JP. Epilepsy and neurodegeneration: a bidirectional relationship. *Epilepsy Curr*. (2021) 21:102–4. doi: 10.1177/1535759721989668
2. Scheffer IE, Berkovic S, Capovilla G, Connolly MB, French J, Guilhoto L, et al. ILAE classification of the epilepsies: position paper of the ILAE Commission for Classification and Terminology. *Epilepsia*. (2017) 58:512–21. doi: 10.1111/epi.13709
3. Linehan C, Tellez-Zenteno JF, Burneo JG, Berg AT. Future directions for epidemiology in epilepsy. *Epilepsy Behav*. (2011) 22:112–7. doi: 10.1016/j.yebeh.2011.06.006
4. Fiest KM, Sauro KM, Wiebe S, Patten SB, Kwon CS, Dykeman J, et al. Prevalence and incidence of epilepsy: a systematic review and meta-analysis of international studies. *Neurology*. (2017) 88:296–303. doi: 10.1212/WNL.0000000000003509
5. Oyrer J, Maljevic S, Scheffer IE, Berkovic SF, Petrou S, Reid CA. Ion channels in genetic epilepsy: from genes and mechanisms to disease-targeted therapies. *Pharmacol Rev*. (2018) 70:142–73. doi: 10.1124/pr.117.014456
6. Jacob TC, Moss SJ, Jurd R. GABA(A) receptor trafficking and its role in the dynamic modulation of neuronal inhibition. *Nat Rev Neurosci*. (2008) 9:331–43. doi: 10.1038/nrn2370
7. Rabbani B, Tekin M, Mahdieh N. The promise of whole-exome sequencing in medical genetics. *J Hum Genet*. (2014) 59:5–15. doi: 10.1038/jhg.2013.114
8. Mei D, Parrini E, Marini C, Guerrini R. The impact of next-generation sequencing on the diagnosis and treatment of epilepsy in paediatric patients. *Mol Diagn Ther*. (2017) 21:357–73. doi: 10.1007/s40291-017-0257-0
9. Myers CT, Mefford HC. Genetic investigations of the epileptic encephalopathies: recent advances. *Prog Brain Res*. (2016) 226:35–60. doi: 10.1016/bs.pbr.2016.04.006
10. Cen ZD, Xie F, Lou DN, Lu XJ, Ouyang ZY, Liu L, et al. Fine mapping and whole-exome sequencing of a familial cortical myoclonic tremor with epilepsy family. *Am J Med Genet B Neuropsychiatr Genet*. 168:595–9. doi: 10.1002/ajmg.b.32337
11. Perucca P, Scheffer IE, Harvey AS, James PA, Lunke S, Thorne N, et al. Real-world utility of whole exome sequencing with targeted gene analysis for focal epilepsy. *Epilepsy Res*. (2017) 131:1–8. doi: 10.1016/j.eplepsyres.2017.02.001
12. Human Chromosomes: Principles & Techniques, 2nd edition, by Ram Verma and Arvind Babu, McGraw-Hill, Inc., New York, 1995. 419pp, $55. *Mol Reprod Dev*. (1996). 43:134. doi: 10.1002/mrd.1996.1080430105
13. Wei X, Ju X, Yi X, Zhu Q, Qu N, Liu T, et al. Identification of sequence variants in genetic disease-causing genes using targeted next-generation sequencing. *PLoS ONE*. (2011) 6:e29500. doi: 10.1371/journal.pone.0029500
14. Li H, Durbin R. Fast and accurate short read alignment with Burrows-Wheeler transform. *Bioinformatics*. (2009) 25:1754–60. doi: 10.1093/bioinformatics/btp324
15. Richards S, Aziz N, Bale S, Bick D, Das S, Gastier-Foster J, et al. Standards and guidelines for the interpretation of sequence variants: a joint consensus recommendation of the American College of Medical Genetics and Genomics and the Association for Molecular Pathology. *Genet Med*. (2015) 17:405–24. doi: 10.1038/gim.2015.30
16. Szklarczyk D, Franceschini A, Wyder S, Forslund K, Heller D, Huerta-Cepas J, et al. STRING v10: protein-protein interaction networks, integrated over the tree of life. *Nucleic Acids Res*. (2015) 43:D447–52. doi: 10.1093/nar/gku1003
17. Biesecker LG, Harrison SM. The ACMG/AMP reputable source criteria for the interpretation of sequence variants. *Genet Med*. (2018) 20:1687–8. doi: 10.1038/gim.2018.42
18. Gelb BD, Cave H, Dillon MW, Gripp KW, Lee JA, Mason-Suares H, et al. ClinGen's RASopathy Expert Panel consensus methods for variant interpretation. *Genet Med*. (2018) 20:1334–45. doi: 10.1038/gim.2018.3
19. Zastrow DB, Baudet H, Shen W, Thomas A, Si Y, Weaver MA, et al. Unique aspects of sequence variant interpretation for inborn errors of metabolism (IEM): The ClinGen IEM Working Group and the Phenylalanine Hydroxylase Gene. *Hum Mutat*. (2018) 39:1569–80. doi: 10.1002/humu.23649
20. Pirillo A, Garlaschelli K, Arca M, Averna M, Bertolini S, Calandra S, et al. Spectrum of mutations in Italian patients with familial hypercholesterolemia: new results from the LIPIGEN study. *Atheroscler Suppl*. (2017) 29:17–24. doi: 10.1016/j.atherosclerosissup.2017.07.002
21. Ogiwara I, Nakayama T, Yamagata T, Ohtani H, Mazaki E, Tsuchiya S, et al. A homozygous mutation of voltage-gated sodium channel beta(I) gene SCN1B in a patient with Dravet syndrome. *Epilepsia*. (2012) 53:e200–3. doi: 10.1111/epi.12040
22. Brackenbury WJ, Yuan Y, O'Malley HA, Parent JM, Isom LL. Abnormal neuronal patterning occurs during early postnatal brain development of Scn1b-null mice and precedes hyperexcitability. *Proc Natl Acad Sci USA*. (2013) 110:1089–94. doi: 10.1073/pnas.1208767110
23. Veeramah KR, Johnstone L, Karafet TM, Wolf D, Sprissler R, Salogiannis J, et al. Exome sequencing reveals new causal mutations in children with epileptic encephalopathies. *Epilepsia*. (2013) 54:1270–81. doi: 10.1111/epi.12201
24. Johansen TK, Dickinson BD, Wilson M. The promise and challenges of next-generation genome sequencing for clinical care. *JAMA Intern Med*. (2014) 174:275–80. doi: 10.1001/jamainternmed.2013.12048
25. Rudy B, McBain CJ. Kv3 channels: voltage-gated K+ channels designed for high-frequency repetitive firing. *Trends Neurosci*. (2001) 24:517–26. doi: 10.1016/S0166-2236(00)01892-0
26. Rudy B, Chow A, Lau D, Amarillo Y, Ozaita A, Saganich M, et al. Contributions of Kv3 channels to neuronal excitability. *Ann N Y Acad Sci*. (1999) 868:304–43. doi: 10.1111/j.1749-6632.1999.tb11295.x
27. Figueroa KP, Waters MF, Garibyan V, Bird TD, Gomez CM, Ranum LP, et al. Frequency of KCNC3 DNA variants as causes of spinocerebellar ataxia 13 (SCA13). *PLoS ONE*. (2011) 6:e17811. doi: 10.1371/journal.pone.0017811
28. Rajakulendran S, Roberts J, Koltzenburg M, Hanna MG, Stewart H. Deletion of chromosome 12q21 affecting KCNC2 and ATXN7L3B in a family with neurodevelopmental delay and ataxia. *J Neurol Neurosurg Psychiatry*. (2013) 84:1255–7. doi: 10.1136/jnnp-2012-304555
29. Ho CS, Grange RW, Joho RH. Pleiotropic effects of a disrupted K+ channel gene: reduced body weight, impaired motor skill and muscle

contraction, but no seizures. *Proc Natl Acad Sci USA*. (1997) 94:1533–8. doi: 10.1073/pnas.94.4.1533
30. Joho RH, Ho CS, Marks GA. Increased gamma- and decreased delta-oscillations in a mouse deficient for a potassium channel expressed in fast-spiking interneurons. *J Neurophysiol*. (1999) 82:1855–64. doi: 10.1152/jn.1999.82.4.1855
31. Espinosa F, McMahon A, Chan E, Wang S, Ho CS, Heintz N, et al. Alcohol hypersensitivity, increased locomotion, and spontaneous myoclonus in mice lacking the potassium channels Kv3.1 and Kv3.3. *J Neurosci*. (2001) 21:6657–65. doi: 10.1523/JNEUROSCI.21-17-06657.2001
32. Kim H, Lee S, Choi M, Kim H, Hwang H, Choi J, et al. Familial cases of progressive myoclonic epilepsy caused by maternal somatic mosaicism of a recurrent KCNC1 p.Arg320His mutation. *Brain Dev*. (2018) 40:429–32. doi: 10.1016/j.braindev.2018.01.006
33. Muona M, Berkovic SF, Dibbens LM, Oliver KL, Maljevic S, Bayly MA, et al. A recurrent de novo mutation in KCNC1 causes progressive myoclonus epilepsy. *Nat Genet*. (2015) 47:39–46. doi: 10.1038/ng.3144
34. Jing Z, Yuehua Z, Jiaoyang C, Ying Y, Qi Z, Xiaoling Y, et al. Three cases of progressive myoclonic epilepsy caused by KCNC1 gene mutations and literature review. *Zhonghua Clin Pract Pediatr*. (2019) 34:6–16. doi: 10.3760/cma.j.issn.2095-428X.2019.24.009
35. Zhang J, Zhang YH, Chen JY, Ji TY, Yang ZX, Yang XL, et al. Pathogenic gene variants and clinical phenotype features of 26 children with progressive myoclonic epilepsy. *Zhonghua Er Ke Za Zhi*. (2019) 57:458–64. doi: 10.3760/cma.j.issn.0578-1310.2019.06.011
36. Oliver KL, Franceschetti S, Milligan CJ, Muona M, Mandelstam SA, Canafoglia L, et al. Myoclonus epilepsy and ataxia due to KCNC1 mutation: Analysis of 20 cases and K(+) channel properties. *Ann Neurol*. (2017) 81:677–89. doi: 10.1002/ana.24929
37. Seoh SA, Sigg D, Papazian DM, Bezanilla F. Voltage-sensing residues in the S2 and S4 segments of the Shaker K+ channel. *Neuron*. (1996) 16:1159–67. doi: 10.1016/S0896-6273(00)80142-7
38. Aggarwal SK, MacKinnon R. Contribution of the S4 segment to gating charge in the Shaker K+ channel. *Neuron*. (1996) 16:1169–77. doi: 10.1016/S0896-6273(00)80143-9
39. Moreau A, Gosselin-Badaroudine P, Chahine M. Biophysics, pathophysiology, and pharmacology of ion channel gating pores. *Front Pharmacol*. (2014) 5:53. doi: 10.3389/fphar.2014.00053
40. Duguez S, Bartoli M, Richard I. Calpain 3: a key regulator of the sarcomere? *FEBS J*. (2006) 273:3427–36. doi: 10.1111/j.1742-4658.2006.05351.x
41. Al-Harbi T, Abdulmanaa S, Dridi W. A novel homozygous missens mutation in capn3 gene detected in Saudi Arabian patient with limb-girdle muscular dystrophy type 2A. *J Neurol Sci*. (2015) 357:e235–6. doi: 10.1016/j.jns.2015.08.826
42. Suzuki K, Sorimachi H. A novel aspect of calpain activation. *FEBS Lett*. (1998) 433:1–4. doi: 10.1016/S0014-5793(98)00856-4
43. Oerum S, Roovers M, Leichsenring M, Acquaviva-Bourdain C, Beermann F, Gemperle-Britschgi C, et al. Novel patient missense mutations in the HSD17B10 gene affect dehydrogenase and mitochondrial tRNA modification functions of the encoded protein. *Biochim Biophys Acta Mol Basis Dis*. (2017) 1863:3294–302. doi: 10.1016/j.bbadis.2017.09.002
44. Rebelo AP, Abrams AJ, Cottenie E, Horga A, Gonzalez M, Bis DM, et al. Cryptic amyloidogenic elements in the 3' UTRs of neurofilament genes trigger axonal neuropathy. *Am J Hum Genet*. (2016) 98:597–614. doi: 10.1016/j.ajhg.2016.02.022
45. Jacquier A, Delorme C, Belotti E, Juntas-Morales R, Sole G, Dubourg O, et al. Cryptic amyloidogenic elements in mutant NEFH causing Charcot-Marie-Tooth 2 trigger aggresome formation and neuronal death. *Acta Neuropathol Commun*. (2017) 5:55. doi: 10.1186/s40478-017-0457-1
46. Marduel M, Ouguerram K, Serre V, Bonnefont-Rousselot D, Marques-Pinheiro A, Erik BK, et al. Description of a large family with autosomal dominant hypercholesterolemia associated with the APOE p.Leu167del mutation. *Hum Mutat*. (2013) 34:83–7. doi: 10.1002/humu.22215

Conflict of Interest: The authors declare that the research was conducted in the absence of any commercial or financial relationships that could be construed as a potential conflict of interest.

Publisher's Note: All claims expressed in this article are solely those of the authors and do not necessarily represent those of their affiliated organizations, or those of the publisher, the editors and the reviewers. Any product that may be evaluated in this article, or claim that may be made by its manufacturer, is not guaranteed or endorsed by the publisher.

Copyright © 2022 Qiuju, Jianlong, Qi, Zhifa, Ding, Xiaofang and Yingjun. This is an open-access article distributed under the terms of the Creative Commons Attribution License (CC BY). The use, distribution or reproduction in other forums is permitted, provided the original author(s) and the copyright owner(s) are credited and that the original publication in this journal is cited, in accordance with accepted academic practice. No use, distribution or reproduction is permitted which does not comply with these terms.

frontiers in Neurology

ORIGINAL RESEARCH
published: 07 March 2022
doi: 10.3389/fneur.2022.747053

Electrocorticography to Investigate Age-Related Brain Lateralization on Pediatric Motor Inhibition

Chao-Hung Kuo[1,2,3,4], Kaitlyn Casimo[5], Jing Wu[6], Kelly Collins[4,7], Patrick Rice[8], Bo-Wei Chen[1], Shih-Hung Yang[9], Yu-Chun Lo[10], Edward J. Novotny[11,12], Kurt E. Weaver[13,14], You-Yin Chen[1,10]* and Jeffrey G. Ojemann[4,14,15]*

[1] Department of Biomedical Engineering, National Yang Ming Chiao Tung University, Taipei, Taiwan, [2] School of Medicine, National Yang Ming Chiao Tung University, Taipei, Taiwan, [3] Department of Neurosurgery, Neurological Institute, Taipei Veterans General Hospital, Taipei, Taiwan, [4] Department of Neurological Surgery, University of Washington, Seattle, WA, United States, [5] Graduate Program in Neuroscience, Center for Neurotechnology, University of Washington, Seattle, WA, United States, [6] Department of Bioengineering, Center for Neurotechnology, University of Washington, Seattle, WA, United States, [7] Department of Neurological Surgery, Oregon Health & Science University, Portland, OR, United States, [8] Department of Psychology, Institute for Learning and Brain Sciences, University of Washington, Seattle, WA, United States, [9] Department of Mechanical Engineering, National Cheng Kung University, Tainan, Taiwan, [10] The Ph.D. Program for Neural Regenerative Medicine, College of Medical Science and Technology, Taipei Medical University, Taipei, Taiwan, [11] Departments of Neurology and Pediatrics, University of Washington, Seattle, WA, United States, [12] Center for Integrative Brain Research, Seattle Children's Research Institute, Seattle, WA, United States, [13] Department of Radiology, Integrated Brain Imaging Center, University of Washington, Seattle, WA, United States, [14] Center for Neurotechnology, University of Washington, Seattle, WA, United States, [15] Departments of Surgery, Seattle Children's Hospital, Seattle, WA, United States

OPEN ACCESS

Edited by:
Jean-Pierre Sao-Ming Lin, Guy's and St Thomas' NHS Foundation Trust, United Kingdom

Reviewed by:
Maurizio Elia, IRCCS Oasi Maria SS, Italy
Eishi Asano, Children's Hospital of Michigan, United States
Shih Ming Weng, National Taipei University of Nursing and Health Sciences, Taiwan

***Correspondence:**
You-Yin Chen
irradiance@so-net.net.tw
Chao-Hung Kuo
chaohungk@gmail.com

Specialty section:
This article was submitted to Pediatric Neurology, a section of the journal Frontiers in Neurology

Received: *25 July 2021*
Accepted: *24 January 2022*
Published: *07 March 2022*

Citation:
Kuo C-H, Casimo K, Wu J, Collins K, Rice P, Chen B-W, Yang S-H, Lo Y-C, Novotny EJ, Weaver KE, Chen Y-Y and Ojemann JG (2022) Electrocorticography to Investigate Age-Related Brain Lateralization on Pediatric Motor Inhibition. Front. Neurol. 13:747053. doi: 10.3389/fneur.2022.747053

Response inhibition refers to the ability to suppress inappropriate actions that interfere with goal-driven behavior. The inferior frontal gyrus (IFG) is known to be associated with inhibition of a motor response by assuming executive control over motor cortex outputs. This study aimed to evaluate the pediatric development of response inhibition through subdural electrocorticography (ECoG) recording. Subdural ECoG recorded neural activities simultaneously during a Go/No-Go task, which was optimized for children. Different frequency power [theta: 4–8 Hz; beta: 12–40 Hz; high-gamma (HG): 70–200 Hz] was estimated within the IFG and motor cortex. Age-related analysis was computed by each bandpass power ratio between Go and No-Go conditions, and phase-amplitude coupling (PAC) over IFG by using the modulating index metric in two conditions. For all the eight pediatric patients, HG power was more activated in No-Go trials than in Go trials, in either right- or left-side IFG when available. In the IFG region, the power over theta and HG in No-Go conditions was higher than those in Go conditions, with significance over the right side ($p < 0.05$). The age-related lateralization from both sides to the right side was observed from the ratio of HG power and PAC value between the No-Go and Go trials. In the pediatric population, the role of motor inhibition was observed in both IFG, with age-related lateralization to the right side, which was proved in the previous functional magnetic resonance imaging studies. In this study, the evidence correlation of age and response inhibition was observed directly by the evidence of cortical recordings.

Keywords: electrocorticography, Go/No-Go, high-gamma, inferior frontal gyrus, lateralization, motor inhibition

INTRODUCTION

Motor inhibition refers to the ability to suppress inappropriate or prepotent actions that interfere with goal-driven behavior. Go/No-Go tasks are designed to provide experimental epochs of movement preparation, response execution, and motor inhibition. Consequently, they are widely used to investigate neural responses specifically attributable to motor inhibition (1). Typically, during the task, participants are requested to press a button or otherwise respond to one type of stimuli, such as a set of alphabet letters, a colored dot, or an image (Go stimuli), and withhold or inhibit a response to another type of stimuli, such as a specific single letter, a different color dot, or a contrasting image (No-Go stimuli). Inhibition is a conversion process of motor behavior, reflecting the capacity to selectively withhold voluntary movements (2).

A large accumulation of neuroscientific evidence from functional (fMRI) studies has reported an increase in the concentration of oxygenated hemoglobin during successful No-Go inhibition in the predominantly right-lateralized brain network comprising the orbitofrontal cortex, dorsolateral pre-frontal cortex, supplementary motor areas (SMA)/pre-SMA areas, basal ganglia circuits, and inferior frontal gyrus (IFG) (3–6). The results indicate that motor inhibition is a largely lateralized process within (generally) the right hemisphere, with the right IFG believed to be particularly sensitive to response suppression (7). Within this inhibition network, the right IFG is predicted to serve as an execution center when inhibition is required (8–10).

Following a literature review, a power spectrum analysis based on adults' electroencephalogram (EEG) studies demonstrated that the theta frequency band (4–8 Hz) plays an important role during motor inhibitory control (11–13). Considering the demand for motor inhibition, theta band activity revealed a correlation with right IFG during inhibition tasks (14). The power change between the Go and No-Go conditions were also observed in electrocorticography (ECoG) studies. A previous ECoG study of 16 patients with intracranial electrodes recording for medically refractory epilepsy found significantly increased gamma band activity in the right IFG after No-Go signal cueing (15). Motor inhibition-evoked gamma-band responses during No-Go trials localize to the right IFG (15), which is compatible with the activation of blood oxygenation level-dependent (BOLD) response in functional MRI (fMRI) studies (3, 8). The aforementioned findings, based on EEG and ECoG studies, show that the right IFG has a role in the motor inhibition of adults.

Age-related functional and anatomical neural development has been observed (16). In a meta-study including 2–12-year-old children from 65 EEG studies, the No-Go-related negative amplitude became progressively negative by age, compared with the Go conditions. The results implied that No-Go-related EEG signals as indexing motor inhibition would change with age (17). In the pediatric population, the findings of frontal activation in No-Go conditions were similar to those in adult populations (2, 18, 19), with some notable differences, including an overall greater engagement of more widespread brain networks (19) and left frontal engagement, which was predicted to contribute to motor inhibition in the immature nervous system (20). Yet, to date, the vast majority of electrophysiological investigations of response in inhibition have been based on adult populations; the dominance of right IFG, the contributions of left IFG during motor inhibition, and the connectivity of frontal and other parts of brain regions between Go and No-Go conditions in children have not been explored using ECoG. Because subdural recordings provide the greatest fidelity of gamma-band dynamics, confirmatory recordings using ECoG in pediatric populations during response-inhibition are warranted.

The processing of motor inhibition included not only IFG, but also other parts of the brain, including the pre-SMA, orbitofrontal cortex, dorsolateral pre-frontal cortex, and basal ganglia (3–6). Considering the neural network of motor inhibition, power changes across different parts of the cortex between Go and No-Go conditions were proven to be related to cortical connectivity and response accuracy in tasks (11, 21). Thus, taken all together, phase-amplitude coupling (PAC) is a suitable cross-frequency coupling approach used to evaluate cortical coupling and functional connectivity. For example, in a magnetoencephalography (MEG) study, high-gamma power (HG, 30–70 Hz) was phase-locked to alpha neural oscillation (8–13 Hz) with the human eyes closed within occipital channels (22). Furthermore, in ECoG studies, the phase of canonical low-frequency bands, such as theta (4–8 Hz), has been shown to modulate power in HG band (80–150 Hz) signals (23). The task-related coupling effects were also observed between the phase of low-frequency (0–3.5 Hz) and amplitude of gamma band (28–70 Hz) neural signals (24). Comparing the coupling effect between the ECoG and fMRI signals in the resting state of brain connectivity, PAC mimicked comparable patterns in these two measurements (25). Collectively, it is believed that PAC represents a neural gating mechanism where the presence of significant coupling indicates the phase of a low-frequency oscillator, which serves to briefly facilitate the high-frequency activity of a second, distant cortical region (23, 26).

It has been predicted that PAC may serve as a neurophysiological mechanism underlying the maturation of neural communication (26) and as a driving mechanism for orchestrating function, including motor inhibition (27). However, the degree to which this neural network and physiological mechanism of motor inhibition exist within pediatric populations is unclear. The aim of this study is to investigate the neural activity, extracted from in-dwelling ECoG electrodes, during motor inhibition in the pediatric population, and estimate the degree to which PAC is associated with the maturation of motor inhibition.

MATERIALS AND METHODS

Participants

A total of eight pediatric patients (male:female = 3:5; mean age 9.8 years; range 7–16) underwent neurological surgery at the Seattle Children's Hospital in Seattle, Washington, for the treatment of intractable epilepsy without evidence of anatomical abnormality from the MRI examinations.

TABLE 1 | Demographical and clinical characteristics of pediatric patients implanted ECoG grids.

Patient no.	Age	Gender	Grid location	Side	Handedness	Hand testing	Performance (accuracy, %)
1	7	F	Frontal/Parietal	Right	Right	Right	64.2
2	8	F	Frontal/Parietal	Left	Right	Right	93.9
3	9	M	Frontal/Parietal/Temporal	Left	Right	Both	74.5
4	11	F	Frontal/Parietal/Temporal	Right	Right	Both	95.9
5	11	F	Frontal/Parietal/Temporal	Left	Right	Both	75.0
6	12	M	Frontal/Temporal	Right	Right	Both	92.9
7	15	F	Frontal/Parietal/Temporal	Right	Right	Both	66.3
8	16	M	Frontal/Parietal/Temporal	Left	Right	Right	97.9

Corticographic potentials were acquired from four patients with right hemisphere grids, and four patients with left-sided grids, according to the clinical considerations. Five patients completed Go/No-Go testing for both the hands and the other three patients only performed right-hand testing as shown in **Table 1**. With approval from the Seattle Children's Hospital Institutional Review Board, all patients and guardians provided informed consent, including the use of ECoG recordings and medical records. All patients underwent a two-stage surgery: craniotomy with unilateral subdual grid and strip implantation according to seizure semiology, followed by removal of the electrodes with resection of epileptic foci. Subdural ECoG 8 × 8 grids or 2 × 8 strips (Integra, Princeton, New Jersey, USA) with 4.75-mm diameter platinum electrodes spaced at 10 mm were transiently placed subdurally to localize the epileptic foci according to clinical considerations, and removed after 1 week of ECoG monitoring.

Go/No-Go Task and Signal Recording

The Go/No-Go task was developed in Psychotoolbox-3 with MATLAB software (Mathworks, Natick, Massachusetts, USA) and was optimized for children (28–30). During the task, patients were asked to press a button on the appearance of a Go signal (a lion), and not respond on the appearance of a No-Go signal (a bear). The No-Go vs. Go signals were randomly distributed at the ratio of 1:6 with a total of 49 trials in each experimental run. There was a 1 s jittered intertrial interval as shown in **Figure 1**. Patients were asked to use the right hand during the first run of the task, and the left hand for the 2nd round. However, not all the patients complied. The responses were classified as Go-correct (lion, reaction), Go-wrong (lion, no reaction), No-Go-correct (bear, no reaction), and No-Go-wrong (bear, reaction).

The ECoG signals were recorded at 1.2 kHz by the clinical system with the Xltek® or Natus® Quantum® LTM amplifier (Natus, Pleasanton, California, USA). A portable laptop was utilized for task execution and documenting patients' responses, which were recorded simultaneously with ECoG signals. A digital transistor-transistor logic (TTL) output signal generated through Psychotoolbox-3 time-stamped event boundaries on the ECoG time series data.

Electrocorticography Data Analysis

All the artifact-free ECoG signals were analyzed with MATLAB software (R12, MathWorks, Natick, Massachusetts, USA). The flowchart of ECoG preprocessing was shown in **Figure 2**. Data were rereferenced within the grid by common average and notch filtered for line noise (at 60, 120, and 180 Hz). A spectral density time series was computed for each channel by (HG, 70–200 Hz) bandpass filtering (4th-order zero-phase Butterworth filter) and the absolute values of the Hilbert transform of the filtered signals were estimated. The bandpass filtered time series were binned into response categories and their corresponding HG powers for each trial type within each epoch were calculated from 1 s before to 1 s after the visual cue. The time-series data was then z-normalized to the first second of (i.e., baseline, precue period of the trial) signal.

The coordinates of each electrode were recorded by the intra-operative navigation system and transformed into patient space, which was defined by the preoperative high-resolution T1-weighted MRI volume. The data was further transformed to MNI standard space for the identification of motor and motor areas according to anatomical structure (31). Based on the patients' responses, the results would be Go/Correct, Go/Non-correct, No-Go/Correct, and No-Go/Non-correct. As a screening and selection measure for electrodes over IFG and motor cortex, the maximum value of each trial within an epoch was averaged in Go/Correct and No-Go/Correct conditions. For visualization purposes only, *Z*-score values in the electrodes over the IFG and motor cortex were plotted on the MNI brain and spatially normalized by a Gaussian distribution. Heat (i.e., color) maps were created to reveal HG brain activity in Go/Correct and No-Go/Correct conditions. All the electrodes within the IFG and motor cortex were ranked according to epoch-based normalized-HG activity. For each patient, the most activated electrodes within Go/Correct and No-Go/Correct conditions were identified as motor cortex cortical signal (*Cm*) and IFG cortical signal (*Ci*), respectively, and selected for statistical and cross-frequency coupling analysis.

Broadband power spectra of only *Cm* and *Ci* were further calculated. Raw time series data from *Cm* and *Ci* were bandpass filtered (2–200 Hz, 4th-order zero-phase Butterworth filter); the Morlet wavelet transform was calculated on the bandpass filtered series (32–34) and truncated to each epoch of Go and No-Go conditions from 1 s before to 1 s after the visual cue. For each

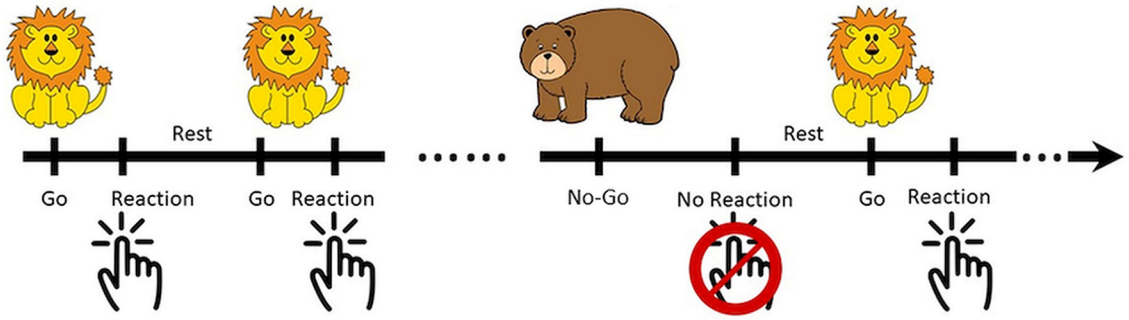

FIGURE 1 | Illustration of the optimized Go/No-Go paradigm (Go vs. No-Go = 1:6) for children. The patients were asked to respond in Go trials (lion) and hold in No-Go trials (bear).

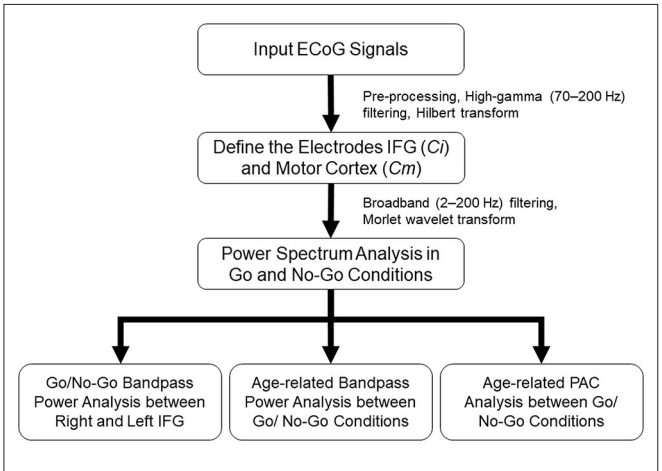

FIGURE 2 | Illustration of the flow chart of data analysis. After preprocessing the ECoG signal, high-gamma (HG) activation was applied to define the most activated electrode to represent inferior frontal gyrus (IFG) (*Ci*) and motor cortex (*Cm*). Broadband pass power spectrum was analyzed between Go and No-Go conditions. Finally, side-related bandpass power changed, as well as age-related bandpass power and phase-amplitude coupling (PAC) between Go and No-Go conditions were further evaluated.

epoch, the calculations of phase and amplitude of the measured ECoG were determined through the Morlet wavelet transform. Amplitude estimates were again *Z*-normalized by the first second of power of each 3 Hz frequency step and averaged across all epochs of Go/Correct and No-Go/Correct conditions. The power change across low-to-high frequencies, from rest (1 s before the visual cue) to reaction (1 s after the visual cue), was estimated in Go/Correct and No-Go/Correct conditions.

Single-band power in right and left-side IFG was analyzed. Pre-processed raw time-series form *Ci* was truncated from 1 s before to 1 s after the visual cue and calculated by the Short-time Fourier transform in each 5 ms window. Power in different frequencies (theta: 4–8 Hz; beta: 12–40 Hz; HG: 70–200 Hz) was filtered and Z-normalized by the same frequency power at rest (1 sec before the visual cue). The peak value in each 5 ms window after the visual cue was chosen. Cross-patient analysis in different frequency bands was compared between right and left IFG.

Age-related analysis was computed using the *Ci* signal in two parts: the power ratio in different frequency bands between Go/Correct and No-Go/Correct, and PAC. The peak values in each 5 ms window after the visual cue were chosen from the normalized power filtered in different frequency bands (theta: 4–8 Hz; beta: 12–40 Hz; HG: 70–200 Hz). The power ratio of each band between No-Go/Correct and Go/Correct was calculated in each patient by the following equation Equation (1):

$$power\ ratio\ =\ \frac{No\ -\ Go/Correct_{ave}}{Go/Correct_{ave}} \tag{1}$$

where $No\text{-}Go/Correct_{ave}$ and $Go/Correct_{ave}$ denote the average power of No-Go/Correct trials and Go/Correct in the 1 s reaction period after the visual cue.

Moreover, PAC was computed by modulation index to determine if there was any change over IFG during Go and No-Go epochs. (23) The PAC value, $z(t)$, was is given by Equation (2).

$$z(t)\ =\ A_{High}(t)e^{i\phi_{Low}(t)} \tag{2}$$

where$A_{High}(t)$ is the normalized high frequency (40–200 Hz) envelope amplitude in the time series; and $i\phi_{Low}(t)$ is the low-frequency (2–20 Hz; stepped every 3 Hz) phase in the time series. The $z(t)$ in 1 s period after visual was then averaged to calculate the ratio between No-Go/Correct and Go/Correct in each different-age patient.

Statistical Analysis

The peak values in each bandpass power between Go and No-Go conditions were illustrated by mean ± 95% CI and *p*-values were calculated by unpaired *t*-test ($p = 0.05$). The Tukey–Kramer test was used to correct multiple comparisons for the unequal sizes between the Go and No-Go conditions. To test for the statistical significance of PAC between motor and IFG areas, a standard permutation test was applied by conducting 1,000 shuffles of each bin of low-frequency phase and high-frequency amplitude. This method generated a null distribution of modulating index and the 95th percentile CIs. Any real-modulating index values calculated between each bin of frequency and amplitude from

Ci revealing greater than null distribution at an alpha level of 0.05 were considered statistically significant. The significance of PAC values of each Go/Correct and No-Go/Correct condition was calculated by a permutation test (significance value = 0.05) (25), and non-significant effects were zero-valued. The results were depicted as the ratio of the average between Go/Correct and No-Go/Correct conditions.

RESULTS

Activation of High-Gamma Band Filtered Signal

High gamma-filtered ECoG power localizes movements from different body parts (35) and fine finger movements (36) across the primary motor cortex. Based on the previous findings, HG power was used to evaluate brain responses over the primary motor cortex and IFG in Go and No-Go conditions (15). For the patients with right-sided grid coverage, activated HG signals over the motor cortex were noted when the contralateral left hand was used in Go conditions (with the exception of one 12-year-old patient with no motor cortex coverage), but no activation when the ipsilateral right hand was used. Independent of which hand was used, right IFG in the No-Go condition exhibited greater HG activation relative to the Go condition (**Figure 3**). Similar high-frequency response profiles in the left IFG were also observed in the patients with left hemisphere grids. HG power over the motor cortex was activated when the contralateral hand was used, as shown in **Figure 4**.

Power Spectrum Over Motor Cortex and IFG

The broadband cortical spectrum (2–200 Hz) was calculated *via* the wavelet transform from the representative electrodes of *Cm* and *Ci*. For the cortical signals from the right *Cm*, increased high-frequency power (70–200 Hz) and decreased low-frequency power (20–40 Hz) were noted after the visual cue, while the contralateral hand was used in Go/Correct conditions. This power change over the motor cortex was consistent with that of a previously published report (37). For the signal over the right *Ci*, the activated power over HG (70–150 Hz), beta (12–40 Hz), and theta (4–8 Hz) were observed when either the right or left hand was used in No-Go/Correct conditions as shown in **Figure 5**. Moreover, the same range of power activation in No-Go/Correct conditions was also noted over the electrode of the left *Ci*, left IFG region (**Figure 6**). In the cross-patient power analysis, the mean values of HG, beta, and theta power in the

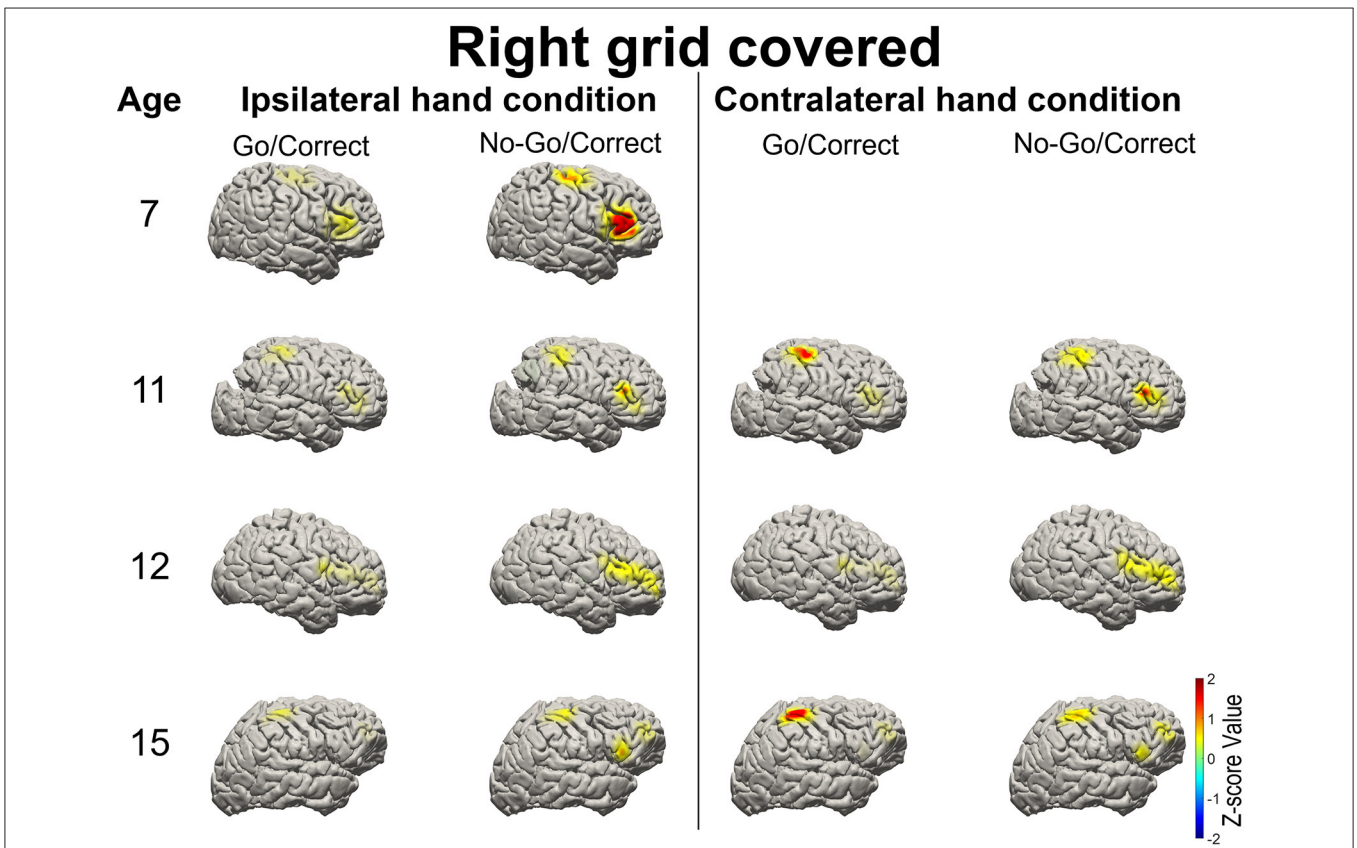

FIGURE 3 | Illustration of the mean high-gamma (HG) activation for the patients aged 7, 11, 12, and 15 years with right side grid coverage. Activation of the right IFG in No-Go/Correct trials is greater than that in Go/Correct trials. HG activation over the sensorimotor cortex was observed in Go/Correct trials when the contralateral hand was used (in this case the left hand).

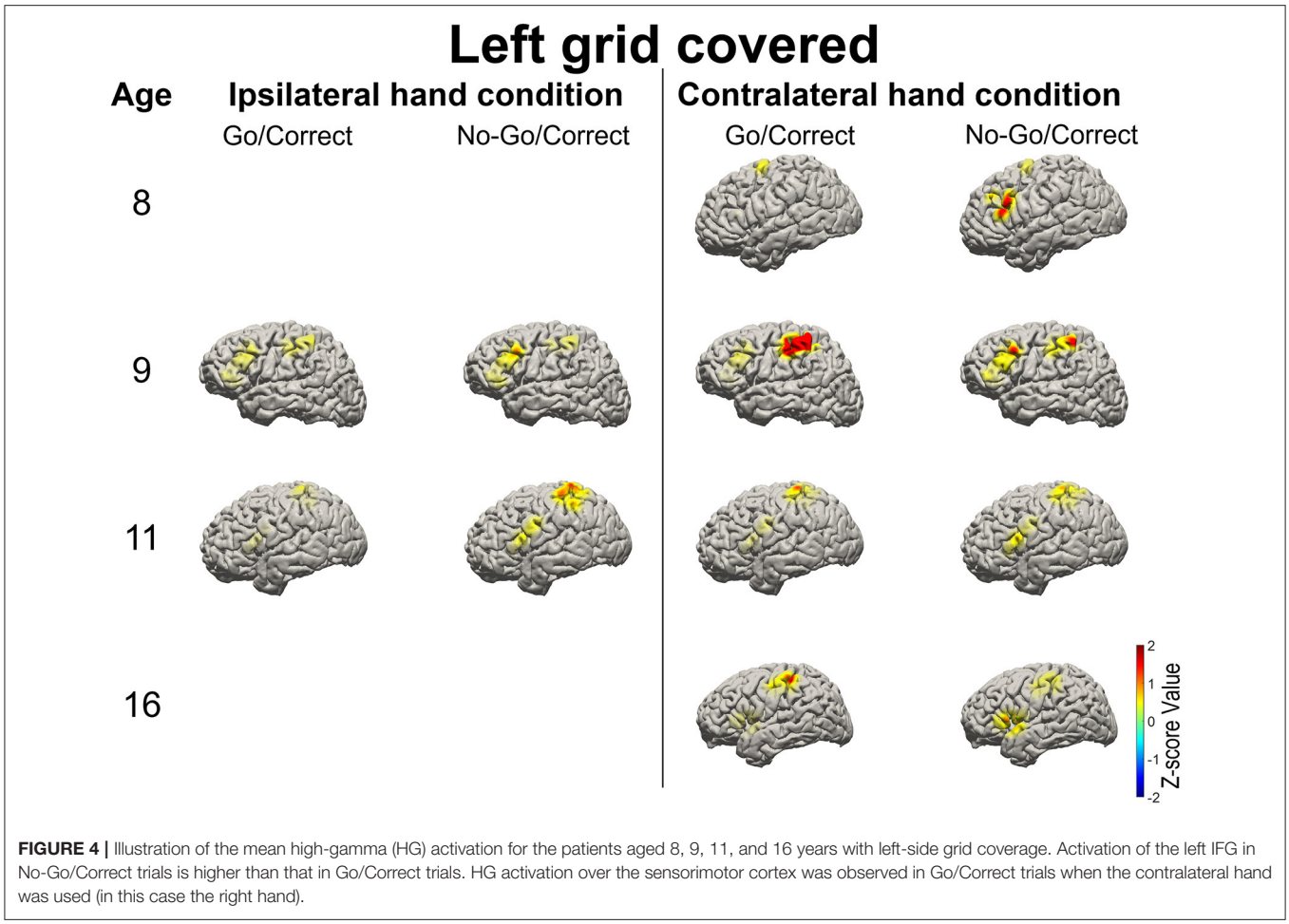

FIGURE 4 | Illustration of the mean high-gamma (HG) activation for the patients aged 8, 9, 11, and 16 years with left-side grid coverage. Activation of the left IFG in No-Go/Correct trials is higher than that in Go/Correct trials. HG activation over the sensorimotor cortex was observed in Go/Correct trials when the contralateral hand was used (in this case the right hand).

No-Go/Correct condition over *Ci* were higher than those in the Go/Correct conditions over both sides of the IFG, but statistical significance was only noted in the HG and theta power over the right IFG ($p < 0.05$, with corrected by Tukey-Kramer test) as shown in **Figure 7**.

Age-Related ECoG Power and PAC Analysis

In each patient, the theta, beta, and HG band power ratios over the right IFG between No-Go/Correct and Go/Correct conditions were calculated. The bandpass powers among different frequency in the No-Go/Correct conditions were higher than those in the Go/Correct conditions, which mean the ratios were over 1. For the patients with grid-covered right IFG, the ratio of theta, beta, and HG frequency bands showed obvious change by age. However, with grid-covered left IFG, there was a decreasing trend of power ratio in HG by ages, and also an increasing trend in theta, but no age-related pattern was observed in the power ratio of the beta frequency band as shown in **Figure 8**.

The PAC values over IFG (*Ci*) were computed separately for the Go/Correct and No-Go/Correct conditions. Most of the PAC values after the permutation test were non-significant (i.e., set to zero). For the right IFG, the PAC value in the No-Go/Correct conditions was higher than that in the Go/Correct conditions. Although a similar pattern was observed in the younger patients for left IFG, the ratio progressively decreased with age as shown in **Figure 9**.

DISCUSSION

In this study, we investigated movement inhibition in the eight pediatric patients who received transient subdural grid implantation for localizing epileptic foci. Our observations highlight two things. First, HG activation in No-Go conditions was higher than that in the Go condition over both the left and right side IFGs. The PAC values in the No-Go condition, calculated between low-frequency (2–40 Hz) phase and high-frequency amplitude (70–200 Hz) from IFG, were higher than those in Go conditions, and we also observed in both left and right cortices. This indicates that activation of IFG in the No-Go condition may modulate the cortical activities to inhibit movements. Second, in the left IFG, the HG and PAC ratio decreased, while the theta ratio increased, with increasing age. In the previous literature, maturational patterns of EEG activity in the resting state revealed that theta-band power decreased

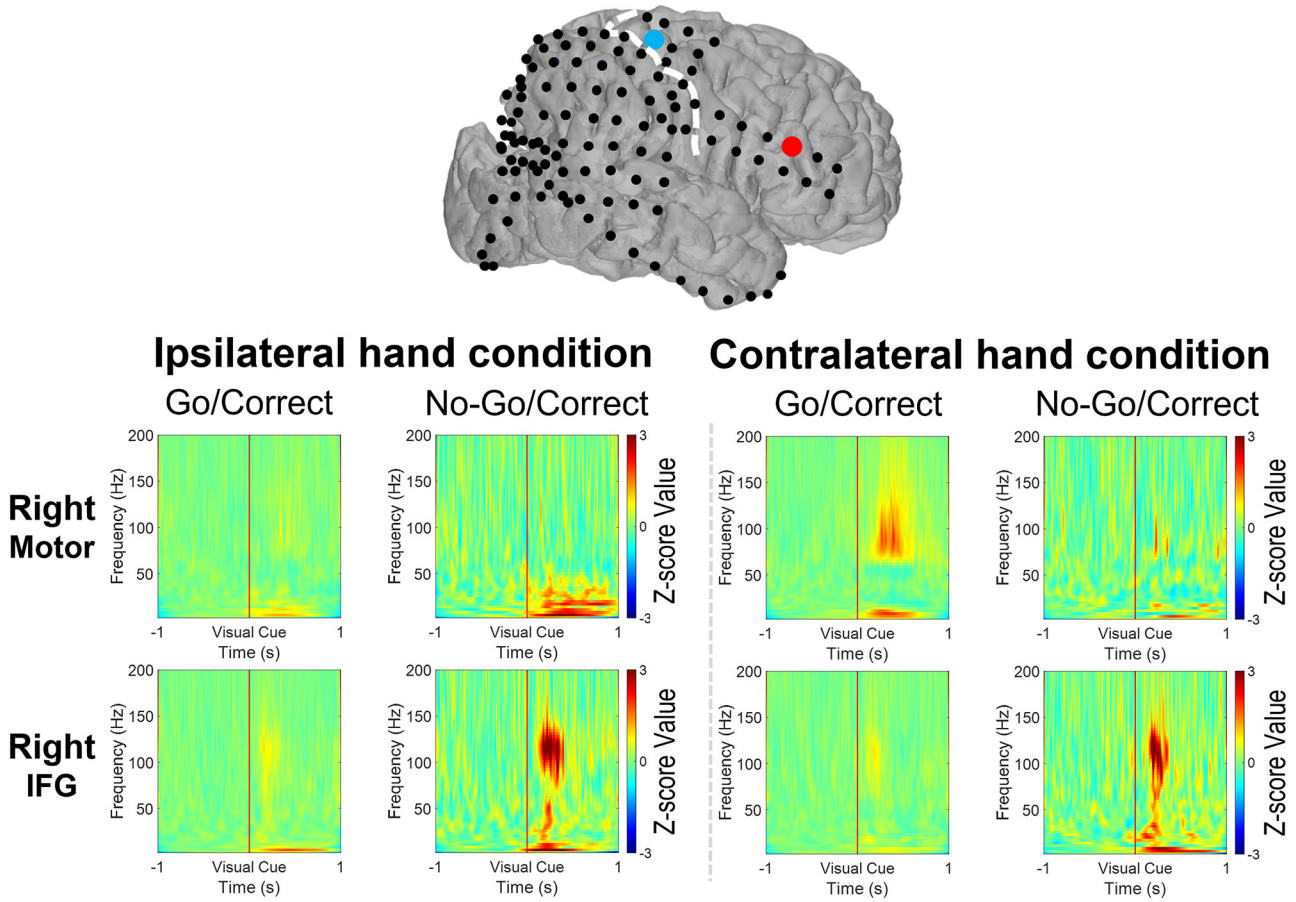

FIGURE 5 | The broadband spectral changes revealed the power change over the motor cortex (the blue dot) and the IFG (the right dot) from 1-second before to 1-second after the visual cues (Go or No-Go) by the 11-year-old with a right-side grid implanted. When the left hand was used, the power within the high-gamma band (HG, 70–200 Hz) increased with the decreased beta band (12–40 Hz) over the motor cortex after visual cues in the Go/Correct trials. Increased HG, beta, and theta (4–8 Hz) power was noted when both the right and left hands were used in No-Go/Correct trials.

while the alpha-band power increased with age (38). The theta-band activity was replaced by the alpha-band first in the occipital regions and progressed later to frontal regions by ages (39). Many studies suggested changes in the white matter (WM) volume was thought to reflect the process of increased myelination, whereas myelination increases the speed of nerve impulse propagation across the brain's region-specific neurocircuitry, especially in the prefrontal cortex, up until 24 years old (40). Thus, growth-related changes in WM might lead decreasing in resting-state theta-band activity with development. In this study, we used the baseline-normalized event-related spectral perturbation (ERSP) (41) to determine the activation of ECoG data under the No-Go trial. There was an increasing power ratio of theta oscillation with stronger theta activity in No-Go trials as lower resting-state theta activity (baseline) by age. The observed age-dependent relationship between theta activity and inhibitory control at the neurophysiological and behavioral level may relate to biophysical properties of theta oscillations and their role in coordinating information processing in a network in the maturation process (42, 43). Critically, relative to adult populations, our results support the hypothesis that the center of motor inhibition in the pediatric populations is not limited to the right IFG, but rather is a product of bilateral contributions from the IFG (20).

The process of motor inhibition is generally assumed to be a multiple step, functional process, mapping onto multiple regions of the cortex (7). In an fMRI study, 26 healthy volunteers (mean age: 23.4 years old) were asked to continuously tap a button with their right index finger, stopping the movement following occasional visual cues, in order to compare the brain activation between the voluntary and forced inhibition of ongoing actions. The results revealed that during the period of inhibition there were greater activations over the SMA, middle cingulate cortex, bilateral insula, and inferior parietal cortex in addition to the right IFG (44). In another fMRI study of 26 healthy subjects, BOLD signals were measured in a Go/No-Go task. Greater activation over the right IFG and pre-SMA regions were noted in No-Go conditions than in Go conditions (45). A 15-participant study (mean age = 27.5 years old) compared different degrees

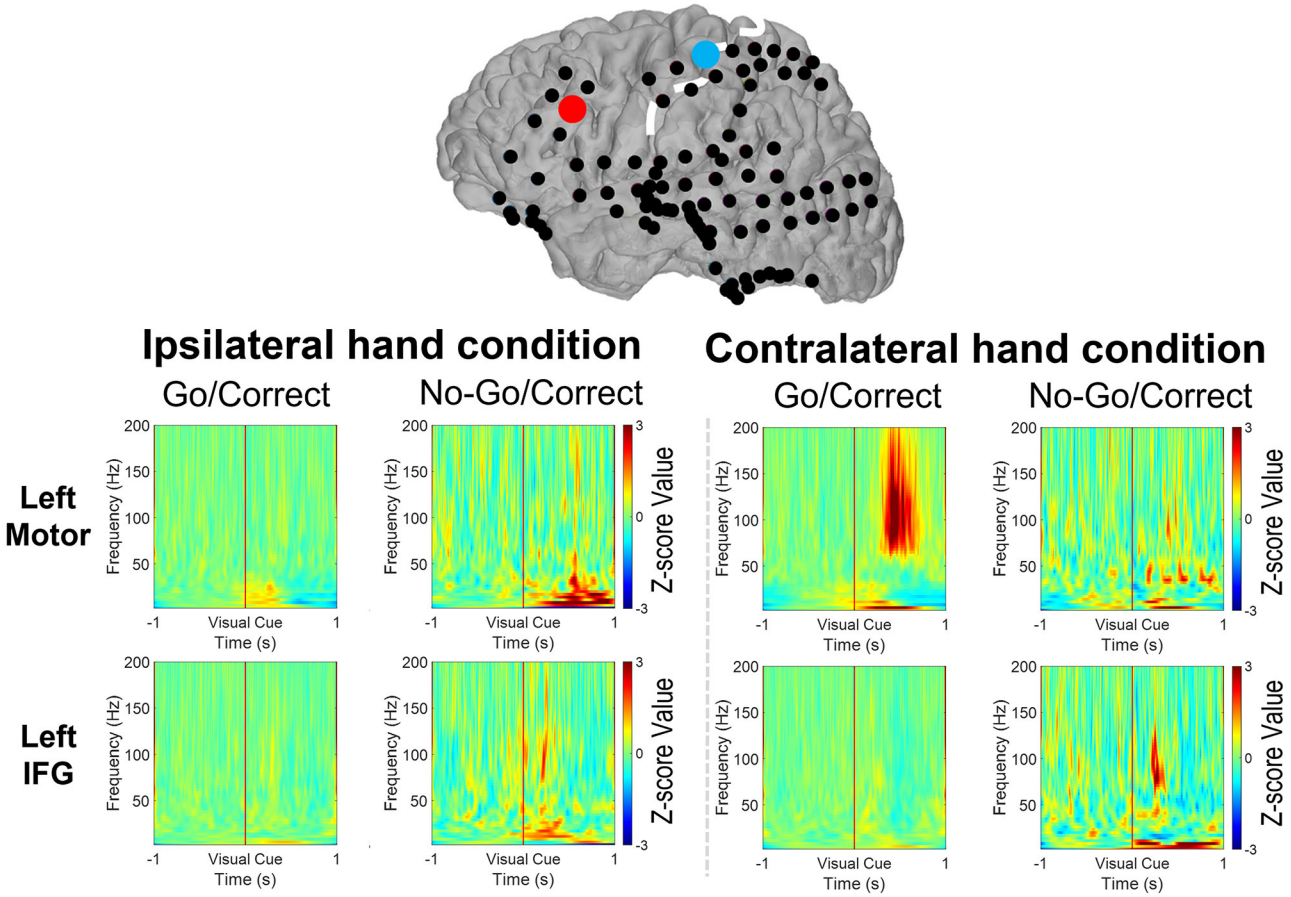

FIGURE 6 | The spectrum revealed the power change over the motor cortex (the blue dot) and the IFG (the right dot) from 1 s before to 1 s after the visual cues (Go or No-Go) by a 9-year-old boy with a left-side grid implanted. When the right hand was used, the power of the high-gamma band (HG, 70–200 Hz) increased with a decreased beta band (12–40 Hz) over the motor cortex after visual cues in Go/Correct trials. Increased HG and theta (4–8 Hz) power were noted when both the right and left hands were used in No-Go/Correct trials.

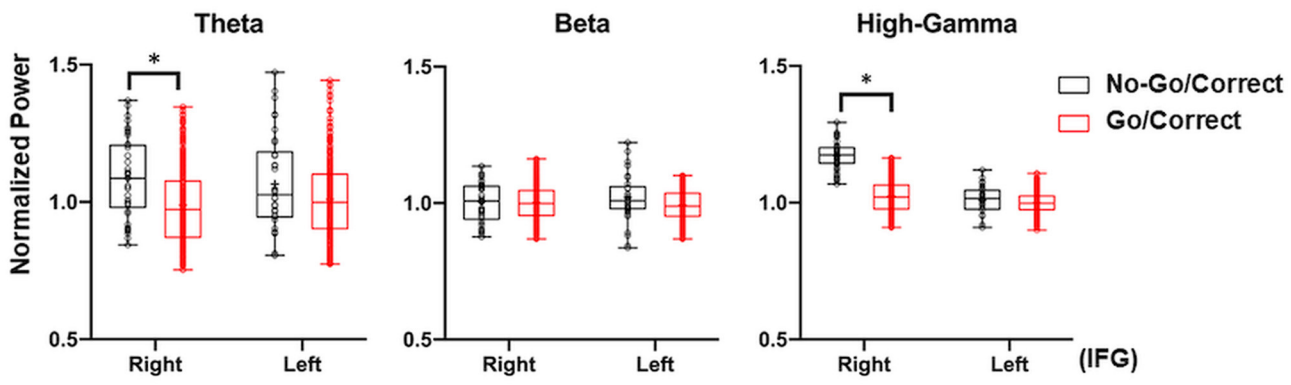

FIGURE 7 | Illustration of the right and left IFG with cross-patient power analysis in Go/Correct and No-Go/Correct conditions. The normalized power in theta (4–8 Hz), beta (12–40 Hz), and high-gamma (HG, 80–200 Hz) were calculated by mean value, interquartile range (box plot), and maximal/minimal (error bar). In No-Go/Correct conditions, the power of theta, beta, and HG were higher than those in Go/Correct condition, with statistical significance in theta and HG power over the right IFG (marked by an asterisk, $p < 0.05$, corrected by the Tukey–Kramer Test).

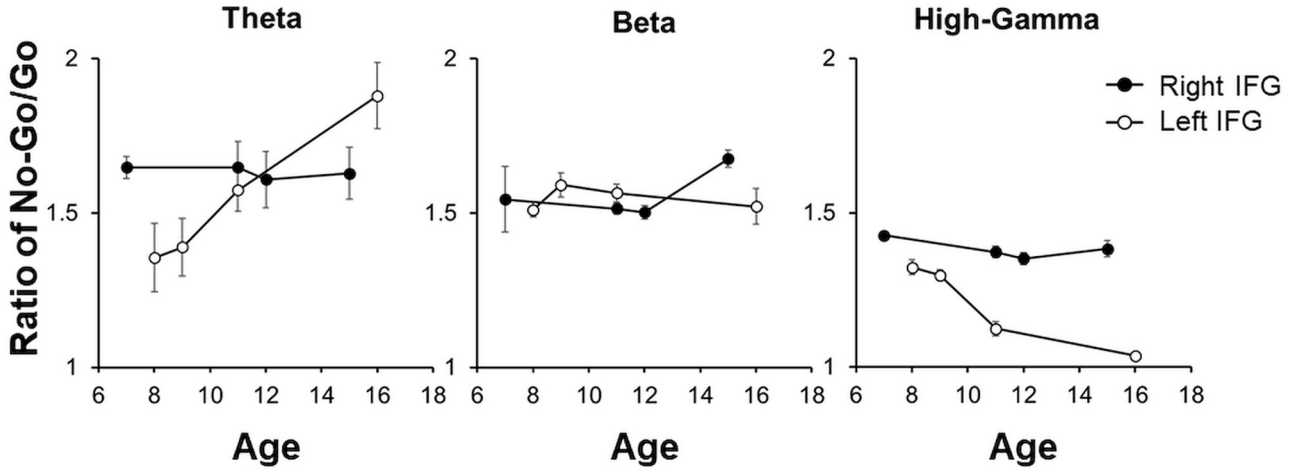

FIGURE 8 | The power ratios between No-Go/Correct and Go/Correct in theta, beta, and HG were illustrated by mean ± 95% CI in each patient. For the patients with the right IFG coverage, there was no obvious change by age. For the left IFG, there was a decreasing trend in HG by age as well as an increasing trend in theta, but no obvious pattern was noted in the ratio of beta.

of difficulty of the stop signal task and found that the right IFG and adjacent anterior insula had more activation during more difficult tasks (46). Additional insight regarding the role of the left IFG in Go/No-Go task execution was demonstrated in a 22-participant fMRI study. The study included two variants of the Go/No-Go ratio: a high frequency of Go cues (Go: No-Go = 3: 1), and a high frequency of No-Go cues (Go: No-Go = 1: 3). The results revealed that the left IFG and a dorsal portion of the pre-SMA were more reactive to No-Go cues compared with Go cues, whether the frequency of No-Go cues was high or low (47). Together, these studies indicate that the right IFG participates in a network that orchestrates the process of motor inhibition. The findings of this study support the conclusion that in addition to the right IFG, which is well-established as being involved in motor inhibition in adults, the left IFG also plays a role in motor inhibition within the maturing brain (20).

Considering the whole neural network for movement inhibition, the change of neural activations over extended regions of the cortex, such as motor, premotor, and pre-SMA regions, would also be observed between Go and No-Go conditions. In a stop-event-related study of 12 adult epileptic patients, event-related spectral power was measured by intracranial ECoG to identity the movement-related spectral change over the sensorimotor cortex. The early increased *mu* band (10–20 Hz) reflected a transient state of motor inhibition over the precentral gyri (48). In another Go/No-Go task, the middle frontal gyrus (MFG) demonstrated transiently increased HG power during stop signals, and the increased HG over MFG was stronger for unsuccessful stop conditions compared to successful stop conditions, which implied the role of MFG in behavioral monitoring (49). The processing of motor inhibition not only included the frontal region, but also the pre-SMA, orbitofrontal cortex, dorsolateral pre-frontal cortex, and basal ganglia (3–6).

Modulating effects between different brain regions, including the IFG, anterior insula, pre-SMA, and sensorimotor cortex, with interaction with basal ganglia, were demonstrated in a neural network study of movement inhibition (47). The movement context was modulated by the neural activity of the basal ganglia, anterior cingulate cortex, and frontal cortex (50, 51). In an fMRI study, response-related amplitudes were calculated *via* logistic regression analysis. Covariance was applied to evaluate the coupling effects between two regions. The results revealed the coupling between the fronto-parietal regions and right IFG increased in successful stop signal tasks compared with that of unsuccessful stop signal tasks, suggesting that the right IFG had more neural interaction during movement inhibition (52). The role of the left IFG in movement inhibition was also evaluated by correlation in another fMRI study by a Go/No-Go task. In No-Go trials, the left IFG revealed positive connectivity with the dorsal portion of the pre-SMA, but negative connectivity with regions responding to Go cues (left sensorimotor cortex) (47). In a clinical case report, the fMRI data analysis in the Go/No-Go task revealed left IFG compensated the original right IFG function after brain injury, which may be the reactivation of the original left IFG function (53). These findings are congruent with the results of our study, which revealed that both the right and left IFG serve to modulate focal activity with the motor cortex during No-Go conditions.

Age-related neural development has been widely discussed, including changes in cortical thickness (16), cortical structure (54), the number of synapse formations (55), and functional activity (54). For example, visual acuity has been correlated to the structure and thickness of the visual cortex (16). Most neural development, such as the sensorimotor cortex, matures symmetrically over both sides (56). However, the language function lateralizes to the dominant cortex with age (57). Utilizing structural MRI, lateralization was strongly correlated

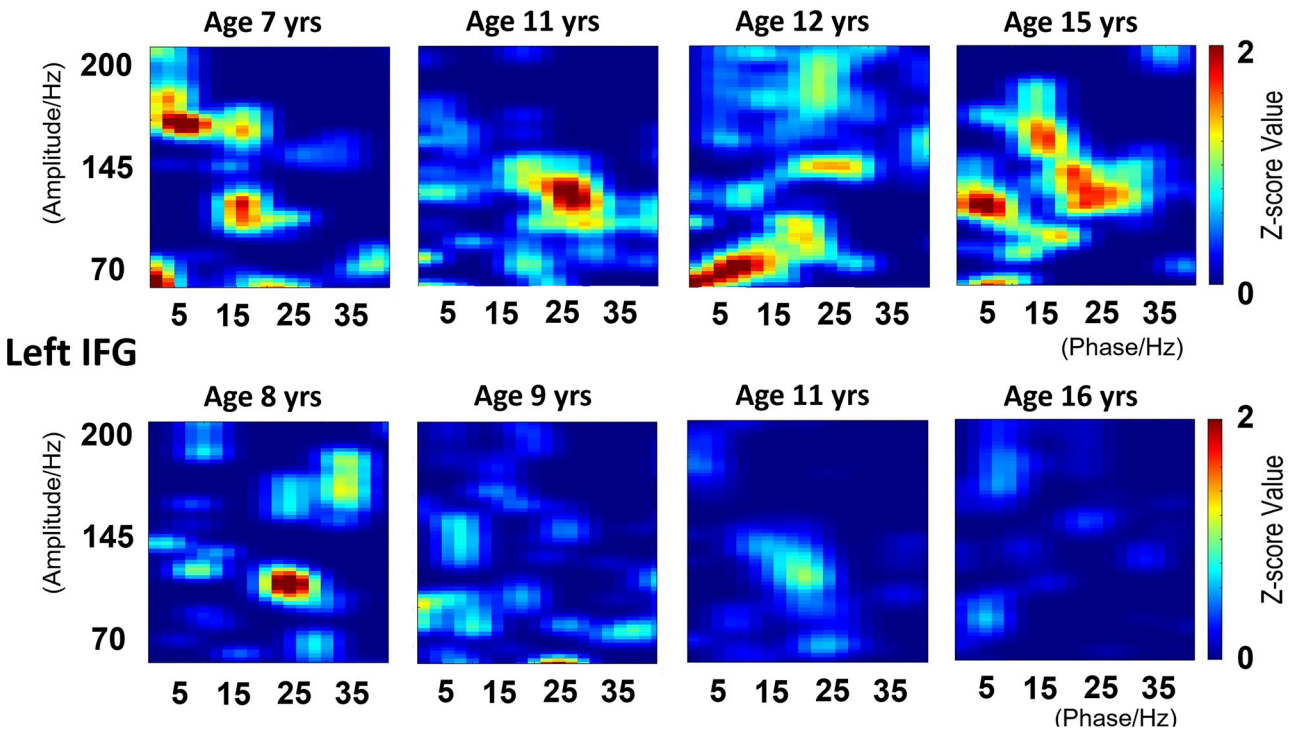

FIGURE 9 | The phase-amplitude coupling (PAC) values were calculated by modulating the index between low-frequency phase (2–40 Hz) and high frequency amplitude (70–200 Hz) in Go/Correct and No-Go/Correct conditions. The illustration revealed the calculated ratio between Go/Correct and No-Go/Correct conditions in right and left-side IFGs. For the right IFG, the PAC value in No-Go/Correct conditions is higher than that in Go/Correct conditions, which means the ratio is over 1, and consistent between the low-frequency phase (5–25 Hz) and high frequency amplitude (100–150 Hz). For left IFG, a similar pattern was observed in younger patients, but the ratio decreased with age.

with volume and thickness over the left IFG (58). For the function of motor inhibition, the presented studies show that right IFG plays an important role (2, 7, 8, 15), but some reports have revealed equal contribution by bilateral IFG (20). In an MRI study, decreasing WM tracts over right IFG was observed in the patients with Attention Deficit Hyperactivity Disorder, compared with the normal population. For the motor inhibition, the results identified the pathogenesis of WM tracts over IFG potentially related to deficient inhibitory control (59). Our study indicated that both IFG played a role in motor inhibition in the pediatric population, but with age, lateralization to the right IFG becomes dominant.

There were some limitations in this study. The brain activity recorded by the ECoG signal was limited by the location of grids and strips, and coverage of the regions of interest was determined entirely by the clinical need. In the future, more cases are needed to investigate the correlation between age and motor inhibition, which may reveal the developmental pattern from bilateral IFG involvement in children to solely right IFG involvement in adults.

CONCLUSION

In our pediatric patients, both the right and left IFG had roles in motor inhibition. The power ratio between the No-Go and Go conditions revealed age-related lateralization from the bilateral-to-right side IFG. The PAC modulation over IFG was more synchronized in No-Go trials than in Go trials. The correlation of age computed by the PAC ratio between two conditions further supported age-related right side IFG lateralization.

DATA AVAILABILITY STATEMENT

The datasets generated for this study are available on request to the corresponding author.

ETHICS STATEMENT

The studies involving human participants were reviewed and approved by Seattle Children's Hospital Institutional Review

Board. Written informed consent to participate in this study was provided by the participants' legal guardian/next of kin.

AUTHOR CONTRIBUTIONS

C-HK, KCa, JW, PR, KW, and JO designed the study. C-HK, KCa, JW, KCo, and JO participated in data collection. EN and JO provided the data resource. C-HK, KCa, B-WC, S-HY, Y-CL, and Y-YC analyzed the data. C-HK, KCa, KCo, Y-YC, Y-CL, KW, and JO wrote and reviewed the manuscript. All the authors reviewed and approved the final version of the manuscript.

FUNDING

We are grateful for support from the Ministry of Science and Technology of Taiwan under Contract numbers of MOST 110-2321-B-010-006, 109-2811-E-010−502, 109-2221-E-010-004-MY2, and 108-2321-B-010-008-MY2. We also are grateful for support from the Higher Education Sprout Project of the National Chiao Tung University and Headquarters of University Advancement at the National Cheng Kung University, Ministry of Education (MOE), Taiwan.

REFERENCES

1. Fujiyama H, Tandonnet C, Summers JJ. Age-related differences in corticospinal excitability during a Go/NoGo task. *Psychophysiology.* (2011) 48:1448–55. doi: 10.1111/j.1469-8986.2011.01201.x
2. Smith JL, Jamadar S, Provost AL, Michie PT. Motor and non-motor inhibition in the Go/NoGo task: an ERP and fMRI study. *Int J Psychophysiol.* (2013) 87:244–53. doi: 10.1016/j.ijpsycho.2012.07.185
3. Steele VR, Aharoni E, Munro GE, Calhoun VD, Nyalakanti P, Stevens MC, et al. A large scale (N=102) functional neuroimaging study of response inhibition in a Go/NoGo task. *Behav Brain Res.* (2013) 256:529–36. doi: 10.1016/j.bbr.2013.06.001
4. Hampshire A, Chamberlain SR, Monti MM, Duncan J, Owen AM. The role of the right inferior frontal gyrus: inhibition and attentional control. *Neuroimage.* (2010) 50:1313–9. doi: 10.1016/j.neuroimage.2009.12.109
5. Hart H, Radua J, Nakao T, Mataix-Cols D, Rubia K. Meta-analysis of functional magnetic resonance imaging studies of inhibition and attention in attention-deficit/hyperactivity disorder: exploring task-specific, stimulant medication, and age effects. *JAMA Psychiatry.* (2013) 70:185–98. doi: 10.1001/jamapsychiatry.2013.277
6. Simmonds DJ, Pekar JJ, Mostofsky SH. Meta-analysis of Go/No-go tasks demonstrating that fMRI activation associated with response inhibition is task-dependent. *Neuropsychologia.* (2008) 46:224–32. doi: 10.1016/j.neuropsychologia.2007.07.015
7. Aron AR, Robbins TW, Poldrack RA. Inhibition and the right inferior frontal cortex: one decade on. *Trends Cogn Sci.* (2014) 18:177–85. doi: 10.1016/j.tics.2013.12.003
8. Aron AR, Fletcher PC, Bullmore ET, Sahakian BJ, Robbins TW. Stop-signal inhibition disrupted by damage to right inferior frontal gyrus in humans. *Nat Neurosci.* (2003) 6:115–6. doi: 10.1038/nn1003
9. Ridderinkhof KR, Ullsperger M, Crone EA, Nieuwenhuis S. The role of the medial frontal cortex in cognitive control. *Science.* (2004) 306:443–7. doi: 10.1126/science.1100301
10. Rubia K, Russell T, Overmeyer S, Brammer MJ, Bullmore ET, Sharma T, et al. Mapping motor inhibition: conjunctive brain activations across different versions of go/no-go and stop tasks. *Neuroimage.* (2001) 13:250–61. doi: 10.1006/nimg.2000.0685
11. Brier MR, Ferree TC, Maguire MJ, Moore P, Spence J, Tillman GD, et al. Frontal theta and alpha power and coherence changes are modulated by semantic complexity in Go/NoGo tasks. *Int J Psychophysiol.* (2010) 78:215–24. doi: 10.1016/j.ijpsycho.2010.07.011
12. Funderud I, Lindgren M, Lovstad M, Endestad T, Voytek B, Knight RT, et al. Differential Go/NoGo activity in both contingent negative variation and spectral power. *PLoS ONE.* (2012) 7:e48504. doi: 10.1371/journal.pone.0048504
13. Harmony T, Alba A, Marroquin JL, Gonzalez-Frankenberger B. Time-frequency-topographic analysis of induced power and synchrony of EEG signals during a Go/No-Go task. *Int J Psychophysiol.* (2009) 71:9–16. doi: 10.1016/j.ijpsycho.2008.07.020
14. Adelhofer N, Beste C. Pre-trial theta band activity in the ventromedial prefrontal cortex correlates with inhibition-related theta band activity in the right inferior frontal cortex. *Neuroimage.* (2020) 219:117052. doi: 10.1016/j.neuroimage.2020.117052
15. Bartoli E, Aron AR, Tandon N. Topography and timing of activity in right inferior frontal cortex and anterior insula for stopping movement. *Hum Brain Mapp.* (2018) 39:189–203. doi: 10.1002/hbm.23835
16. Shaw P, Kabani NJ, Lerch JP, Eckstrand K, Lenroot R, Gogtay N, et al. Neurodevelopmental trajectories of the human cerebral cortex. *J Neurosci.* (2008) 28:3586–94. doi: 10.1523/JNEUROSCI.5309-07.2008
17. Hoyniak C. Changes in the NoGo N2 event-related potential component across childhood: a systematic review and meta-analysis. *Dev Neuropsychol.* (2017) 42:1–24. doi: 10.1080/87565641.2016.1247162
18. Albares M, Lio G, Criaud M, Anton JL, Desmurget M, Boulinguez P. The dorsal medial frontal cortex mediates automatic motor inhibition in uncertain contexts: evidence from combined fMRI and EEG studies. *Hum Brain Mapp.* (2014) 35:5517–31. doi: 10.1002/hbm.22567
19. Jonkman LM, Sniedt FL, Kemner C. Source localization of the Nogo-N2: a developmental study. *Clin Neurophysiol.* (2007) 118:1069–77. doi: 10.1016/j.clinph.2007.01.017
20. Abdul Rahman A, Carroll DJ, Espy KA, Wiebe SA. Neural correlates of response inhibition in early childhood: evidence from a Go/No-Go task. *Dev Neuropsychol.* (2017) 42:336–50. doi: 10.1080/87565641.2017.1355917
21. Liu L, Rosjat N, Popovych S, Wang BA, Yeldesbay A, Toth TI, et al. Age-related changes in oscillatory power affect motor action. *PLoS ONE.* (2017) 12:e0187911. doi: 10.1371/journal.pone.0187911
22. Osipova D, Hermes D, Jensen O. Gamma power is phase-locked to posterior alpha activity. *PLoS ONE.* (2008) 3:e3990. doi: 10.1371/journal.pone.0003990
23. Canolty RT, Edwards E, Dalal SS, Soltani M, Nagarajan SS, Kirsch HE, et al. High gamma power is phase-locked to theta oscillations in human neocortex. *Science.* (2006) 313:1626–8. doi: 10.1126/science.1128115
24. Bruns A, Eckhorn R. Task-related coupling from high- to low-frequency signals among visual cortical areas in human subdural recordings. *Int J Psychophysiol.* (2004) 51:97–116. doi: 10.1016/j.ijpsycho.2003.07.001
25. Weaver KE, Wander JD, Ko AL, Casimo K, Grabowski TJ, Ojemann JG, et al. Directional patterns of cross frequency phase and amplitude coupling within the resting state mimic patterns of fMRI functional connectivity. *Neuroimage.* (2016) 128:238–51. doi: 10.1016/j.neuroimage.2015.12.043
26. Voytek B, Knight RT. Dynamic network communication as a unifying neural basis for cognition, development, aging, and disease. *Biol Psychiatry.* (2015) 77:1089–97. doi: 10.1016/j.biopsych.2015.04.016
27. Durschmid S, Quandt F, Kramer UM, Hinrichs H, Heinze HJ, Schulz R, et al. Oscillatory dynamics track motor performance improvement in human cortex. *PLoS ONE.* (2014) 9:e89576. doi: 10.1371/journal.pone.0089576
28. Brainard DH. The psychophysics toolbox. *Spat Vis.* (1997) 10:433–6. doi: 10.1163/156856897X00357
29. Kleiner M, Brainard D, Pelli D, Ingling A, Murray R, Broussard C. What's new in psychtoolbox-3. *Perception.* (2007) 36:1–16. doi: 10.1068/v070821
30. Pelli DG. The VideoToolbox software for visual psychophysics: transforming numbers into movies. *Spat Vis.* (1997) 10:437–42. doi: 10.1163/156856897X00366
31. Poliachik SL, Poliakov AV, Jansen LA, McDaniel SS, Wray CD, Kuratani J, et al. Tissue localization during resective epilepsy surgery. *Neurosurg Focus.* (2013) 34:E8. doi: 10.3171/2013.3.FOCUS1360

32. Jmail N, Zaghdoud M, Hadriche A, Frikha T, Ben Amar C, Bénar C. Integration of stationary wavelet transform on a dynamic partial reconfiguration for recognition of pre-ictal gamma oscillations. *Heliyon.* (2018) 4:e00530. doi: 10.1016/j.heliyon.2018.e00530
33. Wang J, Wang J, Xing GG, Li X, Wan Y. Enhanced gamma oscillatory activity in rats with chronic inflammatory pain. *Front Neurosci.* (2016) 10:489. doi: 10.3389/fnins.2016.00489
34. Zhou Y, Sheremet A, Qin Y, Kennedy JP, DiCola NM, Burke SN, et al. Methodological considerations on the use of different spectral decomposition algorithms to study hippocampal rhythms. *eNeuro.* (2019) 6:ENEURO.0142-19.2019. doi: 10.1523/ENEURO.0142-19.2019
35. Blakely TM, Olson JD, Miller KJ, Rao RP, Ojemann JG. Neural correlates of learning in an electrocorticographic motor-imagery brain-computer interface. *Brain Comput Interfaces.* (2014) 1:147–57. doi: 10.1080/2326263X.2014.954183
36. Kuo CH, Blakely TM, Wander JD, Sarma D, Wu J, Casimo K, et al. Context-dependent relationship in high-resolution micro-ECoG studies during finger movements. *J Neurosurg.* (2019) 132:1358–66. doi: 10.3171/2019.1.JNS181840
37. Miller KJ, Leuthardt EC, Schalk G, Rao RP, Anderson NR, Moran DW, et al. Spectral changes in cortical surface potentials during motor movement. *J Neurosci.* (2007) 27:2424–32. doi: 10.1523/JNEUROSCI.3886-06.2007
38. Cellier D, Riddle J, Petersen I, Hwang K. The development of theta and alpha neural oscillations from ages 3 to 24 years. *Dev Cogn Neurosci.* (2021) 50:100969. doi: 10.1016/j.dcn.2021.100969
39. Segalowitz SJ, Santesso DL, Jetha MK. Electrophysiological changes during adolescence: a review. *Brain Cogn.* (2010) 72:86–100. doi: 10.1016/j.bandc.2009.10.003
40. Arain M, Haque M, Johal L, Mathur P, Nel W, Rais A, et al. Maturation of the adolescent brain. *Neuropsychiatr Dis Treat.* (2013) 9:449–61. doi: 10.2147/NDT.S39776
41. Grandchamp R, Delorme A. Single-trial normalization for event-related spectral decomposition reduces sensitivity to noisy trials. *Front Psychol.* (2011) 2:236. doi: 10.3389/fpsyg.2011.00236
42. Pscherer C, Bluschke A, Muckschel M, Beste C. The interplay of resting and inhibitory control-related theta-band activity depends on age. *Hum Brain Mapp.* (2021) 42:3845–57. doi: 10.1002/hbm.25469
43. Pscherer C, Muckschel M, Summerer L, Bluschke A, Beste C. On the relevance of EEG resting theta activity for the neurophysiological dynamics underlying motor inhibitory control. *Hum Brain Mapp.* (2019) 40:4253–65. doi: 10.1002/hbm.24699
44. Omata K, Ito S, Takata Y, Ouchi Y. Similar neural correlates of planning and execution to inhibit continuing actions. *Front Neurosci.* (2018) 12:951. doi: 10.3389/fnins.2018.00951
45. Gavazzi G, Orsolini S, Rossi A, Bianchi A, Bartolini E, Nicolai E, et al. Alexithymic trait is associated with right IFG and pre-SMA activation in non-emotional response inhibition in healthy subjects. *Neurosci Lett.* (2017) 658:150–4. doi: 10.1016/j.neulet.2017.08.031
46. Hughes ME, Johnston PJ, Fulham WR, Budd TW, Michie PT. Stop-signal task difficulty and the right inferior frontal gyrus. *Behav Brain Res.* (2013) 256:205–13. doi: 10.1016/j.bbr.2013.08.026
47. Meffert H, Hwang S, Nolan ZT, Chen G, Blair JR. Segregating attention from response control when performing a motor inhibition task: segregating attention from response control. *Neuroimage.* (2016) 126:27–38. doi: 10.1016/j.neuroimage.2015.11.029
48. Klopp J, Marinkovic K, Clarke J, Chauvel P, Nenov V, Halgren E. Timing and localization of movement-related spectral changes in the human peri-Rolandic cortex: intracranial recordings. *Neuroimage.* (2001) 14:391–405. doi: 10.1006/nimg.2001.0828
49. Fonken YM, Rieger JW, Tzvi E, Crone NE, Chang E, Parvizi J, et al. Frontal and motor cortex contributions to response inhibition: evidence from electrocorticography. *J Neurophysiol.* (2016) 115:2224–36. doi: 10.1152/jn.00708.2015
50. Le TM, Zhang S, Zhornitsky S, Wang W, Li CR. Neural correlates of reward-directed action and inhibition of action. *Cortex.* (2020) 123:42–56. doi: 10.1016/j.cortex.2019.10.007
51. Marmor O, Rappel P, Valsky D, Bick AS, Arkadir D, Linetsky E, et al. Movement context modulates neuronal activity in motor and limbic-associative domains of the human parkinsonian subthalamic nucleus. *Neurobiol Dis.* (2020) 136:104716. doi: 10.1016/j.nbd.2019.104716
52. Padmala S, Pessoa L. Moment-to-moment fluctuations in fMRI amplitude and interregion coupling are predictive of inhibitory performance. *Cogn Affect Behav Neurosci.* (2010) 10:279–97. doi: 10.3758/CABN.10.2.279
53. Gavazzi G, Lenge M, Bartolini E, Bianchi A, Agovi H, Mugnai F, et al. Left inferior frontal cortex can compensate the inhibitory functions of right inferior frontal cortex and pre-supplementary motor area. *J Neuropsychol.* (2019) 13:503–8. doi: 10.1111/jnp.12170
54. Durston S, Casey BJ. What have we learned about cognitive development from neuroimaging? *Neuropsychologia.* (2006) 44:2149–57. doi: 10.1016/j.neuropsychologia.2005.10.010
55. Huttenlocher PR, de Courten C. The development of synapses in striate cortex of man. *Hum Neurobiol.* (1987) 6:1–9.
56. Karmali F, Whitman GT, Lewis RF. Bayesian optimal adaptation explains age-related human sensorimotor changes. *J Neurophysiol.* (2018) 119:509–20. doi: 10.1152/jn.00710.2017
57. Travis KE, Curran MM, Torres C, Leonard MK, Brown TT, Dale AM, et al. Age-related changes in tissue signal properties within cortical areas important for word understanding in 12- to 19-month-old infants. *Cereb Cortex.* (2014) 24:1948–55. doi: 10.1093/cercor/bht052
58. Scheppele M, Evans JL, Brown TT. Patterns of structural lateralization in cortical language areas of older adolescents. *Laterality.* (2019) 24:450–81. doi: 10.1080/1357650X.2018.1543312
59. Tremblay LK, Hammill C, Ameis SH, Bhaijiwala M, Mabbott DJ, Anagnostou E, et al. Tracking inhibitory control in youth with ADHD: a multi-modal neuroimaging approach. *Front Psychiatry.* (2020) 11:831. doi: 10.3389/fpsyt.2020.00831

Conflict of Interest: The authors declare that the research was conducted in the absence of any commercial or financial relationships that could be construed as a potential conflict of interest.

Publisher's Note: All claims expressed in this article are solely those of the authors and do not necessarily represent those of their affiliated organizations, or those of the publisher, the editors and the reviewers. Any product that may be evaluated in this article, or claim that may be made by its manufacturer, is not guaranteed or endorsed by the publisher.

Copyright © 2022 Kuo, Casimo, Wu, Collins, Rice, Chen, Yang, Lo, Novotny, Weaver, Chen and Ojemann. This is an open-access article distributed under the terms of the Creative Commons Attribution License (CC BY). The use, distribution or reproduction in other forums is permitted, provided the original author(s) and the copyright owner(s) are credited and that the original publication in this journal is cited, in accordance with accepted academic practice. No use, distribution or reproduction is permitted which does not comply with these terms.

Advantages of publishing in Frontiers

OPEN ACCESS
Articles are free to read for greatest visibility and readership

FAST PUBLICATION
Around 90 days from submission to decision

HIGH QUALITY PEER-REVIEW
Rigorous, collaborative, and constructive peer-review

TRANSPARENT PEER-REVIEW
Editors and reviewers acknowledged by name on published articles

Frontiers
Avenue du Tribunal-Fédéral 34
1005 Lausanne | Switzerland

Visit us: www.frontiersin.org
Contact us: frontiersin.org/about/contact

REPRODUCIBILITY OF RESEARCH
Support open data and methods to enhance research reproducibility

DIGITAL PUBLISHING
Articles designed for optimal readership across devices

FOLLOW US
@frontiersin

IMPACT METRICS
Advanced article metrics track visibility across digital media

EXTENSIVE PROMOTION
Marketing and promotion of impactful research

LOOP RESEARCH NETWORK
Our network increases your article's readership